Feasibility of Improving Risk Stratification in the Inherited Cardiac Conditions

Ji-Jian Chow

Imperial College London

National Heart and Lung Institute

A PhD thesis

28th June 2022

Declaration of Originality

All work in this thesis is either original material produced by the author, or appropriately referenced. Any material produced by the author which has been presented or published prior to the release of this document is also appropriately referenced.

Copyright Declaration

Acknowledgements

The Declaration of Originality on the previous page may be true but does not do justice to the team of people who made the work in this thesis possible. These acknowledgements are an attempt to put that right.

I'd like to extend special thanks to my senior supervisors, Professor Prapa Kanagaratnam and Dr Amanda Varnava. Together they have immeasurably driven my personal and professional development in both research and the clinical arena.

Prapa introduced me to more aspects of the research world than I even knew existed and encouraged me through moments which at the time seemed like scientific brick walls. His vision for the project brings people, organizations and funding together in a uniquely successful way. Mostly I'm grateful for his insight into problem solving strategy, and his pragmatic way of thinking about electrophysiology.

Amanda's weekly chats greatly expanded my knowledge of the inherited cardiac conditions, and her unique approach to centralizing care across a whole region of west London made patient recruitment and data collection possible. Her advice went beyond the academic and clinical, and I thank her especially for the times she reminded me that stepping back from work could be as productive as pushing on blindly.

The Daniel Bagshaw Trust, a family charity, funded me through the research years and made all this possible. Many of Dan's Trustees are affected in some way by inherited cardiac conditions. It's impossible to state in words what this means to a young researcher – the human voices that scientific nomenclature cannot simply summarize.

Dr Kevin Leong, my project predecessor and co-supervisor to Prapa and Amanda was seemingly an infinite source of knowledge and new ideas to kickstart the developments in this thesis. Many of the ideas in it stemmed from scribbles made on scrap paper between clinical cases or after work. Kevin was always there to keep me going with a smile.

Professor Darrel Francis, and his supervisees Drs Matthew Shun-Shin and James Howard were indispensable in my journey from code-naïve to novice software developer. They always had time to discuss the intricacies of programming with me and share their considerable experience. Drs Ahran Arnold and Nadine Ali provided vital feedback as end users of my finished software.

Dr Cheng Yao and Mr Ian Little of Medtronic patiently taught me everything I know about using CardioINSIGHT™ and were instrumental in securing both information and insightful conversation time with the mathematicians developing the inverse solution.

To all the consultants, cardiac research fellows, clinical registrars, physiologists, nurses and allied health professionals from many divisions: your encouragement, teaching, hard work and above all friendship was appreciated every second - I'm just sorry I couldn't name all of you here.

To all the patients and healthy volunteers who took part, without ever asking for anything in return. Taking part in research might be the greatest act of medical charity; for that I am ever grateful to you.

To my partner Dr Antonia Whitaker, for her endless patience whilst this PhD dealt out late nights by the dozen and hours of tapping away at the computer. Toni was always willing to listen to my ramblings (no matter how boring) and helped me stay in context not just with the science, but life in general. She was the essential voice from another medical specialty – giving me insight into what really matters to doctors outside our tiny niche in research.

To my parents Chow Whye-Seng and Ong Swi-Neo, always supportive as they have been since my first memories. Thank you for bringing me up to persevere and inspiring me to always work for the community, in whatever little way I could. To my sister, Dr Li-Yan Chow, who as well as being a fantastic scientific sounding board could always lighten the mood with some amusing quip from our distant childhood.

Some specific thanks are needed for individual chapters. In chapter 3, Drs Momina Yazdani and Hani Huzaien spent many an hour with me making the Brugada database truly comprehensive across sites between Imperial College Healthcare and University Hospital Wales. Prof. Zaheer Yousef and Dr Peter O'Callaghan provided many Welsh patients for our validation of the Sieira score, as well as insight into the landscape of Brugada risk management. In chapter 4, Dr Shun-Shin introduced me to many of the statistical concepts involved. In chapter 6, Prof. Francis and Dr Howard inspired me to start machine learning, and once started, showed me how to escape the pitfalls. In chapters 4, 7 and 8 I thank Drs. Julian Ormerod, Sam Mohiddin, Oliver Guttmann and Profs. Pier Lambiase, Perry Elliott and Elijah Behr for introducing me to those rare survivors of sudden cardiac arrest without whom this study would have been impossible.

Abstract

Fatal ventricular arrhythmias can occur in patients with Hypertrophic Cardiomyopathy, Brugada Syndrome and rarely in patients with normal cardiac investigations. Despite very different pathogeneses, we hypothesised that a common electrophysiological substrate precipitates these arrhythmias and could be used as a marker for risk stratification.

In Chapter 3 of this thesis, we found that fewer than half the cardiac arrest survivors with Brugada Syndrome would have been offered prophylactic defibrillators based on current risk scoring, highlighting the need for better risk stratification. Our group previously used a commercially available 252-electrode vest which constructs ventricular electrograms onto a CT image of the heart to show exercise related differences in high-risk patients. In Chapter 4, we applied this method to Brugada patients, but could not reproduce prior results. Further investigation revealed periodic changes in activation patterns after exercise that could explain this discrepancy. An alternative matrix approach was developed to overcome this problem. Exercise induced conduction heterogeneity differentiated Brugada patients from unaffected controls, but not those surviving cardiac arrest. However, if considered alongside spontaneous type 1 ECG and syncope, inducible conduction heterogeneity markedly improved identification of Brugada cardiac arrest survivors. In Chapter 5 the method was shown to differentiate idiopathic ventricular fibrillation patients from those fully recovered from acute ischaemic cardiac arrest, implying a permanent electrophysiological abnormality. In Chapter 8, we showed prolonged mean local activation times and activation-recovery intervals in hypertrophic cardiomyopathy cardiac arrest survivors compared to those without previous ventricular arrhythmia. These metrics were combined into both logistic regression and support vector machine models to strongly differentiate the groups.

We concluded that electrophysiological changes could identify cardiac arrest survivors in various cardiac conditions, but a single factor common pathway was not established. Prospective studies are required to determine if using these parameters could enhance current risk stratification for sudden death.

Contents

List of figures

List of tables

Publications from this thesis

Papers accepted

Chow JJ, Leong KMW, Yazdani M, Huzaien H, Jones S, Koa-Wing M, Lefroy D, Lim PB, Linton N, Ng FS, Qureshi N, Whinnett ZI, Peters NS, O'Callaghan P, Yousef Z, Kanagaratnam P, Varnava A. A Multicenter External Validation of a Score Model to Predict Risk of Events in Patients With Brugada Syndrome. Am J Cardiol. 2021;00:1-7. DOI: 10.1016/j.amjcard.2021.08.035

Chow JJ, Kaza N, Varnava A. The Brugada Type 1 Electrocardiogram and Ventricular Tachycardia With High-Dose Amitriptyline. JACC Case Reports. 2021 Jan; 3(1):156-161. DOI: 10.1016/j.jaccas.2020.11.016

Chow JJ. Computer programming for clinicians: five steps to your new favourite skill. Part 2. Heart. 2020 Nov;106(22):1777. doi: 10.1136/heartjnl-2020-317808. Epub 2020 Aug 27. PMID: 32855197.

Chow JJ. Computer programming for clinicians: five steps to your new favourite skill. Part 1. Heart. 2020 Nov;106(21):1700-1701. doi: 10.1136/heartjnl-2020-317344. Epub 2020 Jul 14. PMID: 32665360.

Abstracts

Chow JJ, Leong KMW, Koa-Wing M, Lefroy D, Lim PB, Linton N, Ng FS, Qureshi N, Whinnett ZI, Peters NS, Varnava A, Kanagaratnam P. Amalgamating Electrophysiological Parameters May Better Define The Multi-factorial Pro-arrhythmic Substrate In Hypertrophic Cardiomyopathy That Causes Risk Of Ventricular Fibrillation. Heart Rhythm Supplement May 2020; D-AB11-06.

Chow JJ, Leong KMW, Koa-Wing M, Lefroy D, Lim PB, Linton N, Ng FS, Qureshi N, Whinnett ZI, Peters NS, Varnava A, Kanagaratnam P. Periodic Alterations Of Ventricular Activation Patterns Are Triggered By Exercise In Patients With Inherited Cardiac Conditions. Heart Rhythm Supplement May 2020; D-PO4-221.

Chow JJ, Leong KMW, Ormerod J, Koa-Wing M, Lefroy D, Lim PB, Linton N, Ng FS, Qureshi N, Whinnett ZI, Peters NS, Kanagaratnam P, Varnava A. Activation Patterns Are Disrupted In Concealed Brugada Syndrome Patients Compared To Controls When Exposed To Exercise: A Potential Diagnostic Tool? JICE Supplement April 2020; 07-17.

Chow JJ, Leong KMW, Koa-Wing M, Lefroy D, Lim PB, Linton N, Ng FS, Qureshi N, Whinnett ZI, Peters NS, Varnava A, Kanagaratnam P. Electrographic Imaging Non-Invasively Unmasks Patchy Conduction And Repolarisation Slowing In Hypertrophic Cardiomyopathy Despite Inability To Image The Septum. JICE Supplement April 2020; 28-11.

Chow JJ, Leong KMW, Ormerod J, Jones S, Koa-Wing M, Lefroy D, Lim PB, Linton N, Ng FS, Qureshi N, Whinnett ZI, Peters NS, Kanagaratnam P, Varnava A. Dynamicity of the ST segment as a risk marker for ventricular arrhythmia in Brugada syndrome. European Journal of Arrhythmia &

Electrophysiology. 2019;5(Suppl. 1):abstr114

Leong KMW, Ng FS, Jones S, **Chow JJ**, et al. Prevalence of spontaneous type I ECG pattern, syncope, and other risk markers in sudden cardiac arrest survivors with Brugada syndrome. Pacing Clin Electrophysiol. 2019;42:257–264.

Chow JJ, Yazdani M, Leong KMW, Jones S, Koa-Wing M, Lefroy D, Lim PB, Linton N, Ng FS, Qureshi N, Whinnett ZI, Peters NS, Kanagaratnam P, Varnava A. Validation Of The Sieira Score For Risk Stratification In Brugada Syndrome. JICE Supplement June 2019; 07-13.

Chow JJ, Leong KMW, Shun-Shin MS, Koa-Wing M, Lefroy D, Lim PB, Linton N, Ng FS, Qureshi N, Whinnett ZI, Peters NS, Varnava A, Kanagaratnam P. Ventricular Conduction Stability Is A Novel Non-Invasive Measure Of Arrhythmic Substrate Which Is Reduced In Idiopathic Ventricular Fibrillation Survivors. Heart Rhythm Supplement May 2019; SP02-190.

Under review

Chow JJ, Leong KMW, Shun-Shin MS, Jones S, Ormerod J, Koa-Wing M, Lefroy D, Lim PB, Linton N, Ng FS, Qureshi N, Whinnett ZI, Peters NS, Francis DP, Varnava A, Kanagaratnam P. The Ventricular Conduction Stability (V-CoS) non-invasively identifies an arrhythmic substrate in survivors of idiopathic ventricular fibrillation or tachycardia.

Chapter 1: Introduction

1.1 Lethal arrhythmia: Ancients to the modern era

Where and when the 'first' documentation of arrhythmia was made appears to have as many different answers as there are historians writing about it. Estimates range from thousands to hundreds of years before the common era (BCE). Citations arising from Babylonian and Chinese texts from around 2600 BCE describe sudden death from a still heart and a fast pulse to ventilation rate ratio in illness (Karagueuzian 2004). Detailed descriptions of pulse taking were made across ancient China, India, Egypt and Greece between 600 and 400 BCE (Ghasemzadeh and Zafari 2011). Various features of pulse rate and character were noted to correspond to the wellbeing of patients. Pulse taking formed a large bulk of early medicine, but the origin of the pulsation at the heart was not definitively described until Harvey in the 16th century of the common era (CE).

The involvement of electricity in sudden death was first noted by Benjamin Franklin's (United States of America) observation of lightning strikes in the 1750s. Twenty years later, Peter Abildgaard (Denmark) noted that a shock could render a bird 'lifeless', before 'reviving' it with another shock – possibly the first ever defibrillation. Abildgaard even noted that his chicken recovered well enough to lay an egg (Karagueuzian 2004).

Measuring bio-electricity was pioneered by Luigi Galvani (Italy) in 1791, using an unusual contraption on a skinned frog leg as a transducer – notably used by Rudolf Koelliker (Switzerland) as late as 1856 to record the frog heart's epicardial impulse (Fye 1999). Koelliker noted that the leg transducer twitched before cardiac systole – a sign that the mechanical activity was triggered by the electrical current. The first mechanical 'galvanometer' was produced by Hans Orsted (Denmark) in 1820, and the first intact human heart measurements were made by Augustus Waller (United Kingdom) in 1887 at St Mary's Hospital, London. Willem Einthoven (the Netherlands) refined this into a practical electrocardiogram (ECG) machine in 1895.

Rapid advancements in both recording and understanding cardiac electricity through the 20th and early 21st centuries bring us to our level of knowledge today, but sudden cardiac death (SCD) remains a major challenge to the modern physician. SCD accounts for a fifth of deaths in the more economically developed world. The World Health Organisation defines SCD as unexpected death within one hour of symptom onset or within 24 hours of having been last seen well. No cause is

identified in up to a third of victims under the age of 35 (Paratz, Rowsell et al. 2020). The underlying heart rhythm is generally ventricular tachycardia or fibrillation (Zipes and Wellens 1998).

1.2 Pro-arrhythmic conditions and sudden death

Coronary artery disease is the leading cause of sudden cardiac death; alongside ischaemic cardiomyopathy this forms up to 50-75% of sudden deaths (Hayashi, Shimizu et al. 2015). Effective strategies are available for quantifying and reducing the risk of sudden death from coronary artery disease in current guidelines (Priori, Blomstrom-Lundqvist et al. 2015; Al-Khatib Sana, Stevenson William et al. 2018). Of the remaining 25-50% of sudden deaths, the inherited cardiomyopathy and arrhythmia syndromes dominate.

Cardiomyopathies

Hypertrophic cardiomyopathy (HCM) is the commonest inherited cardiac condition, affecting 1 in 500 adults, and the commonest inherited structural syndrome (Maron, Gardin et al. 1995). HCM is caused by mutations in genes that encode components of the cardiac muscle, most commonly the sarcomeric myosin and troponin coding genes, and more rarely also genes responsible for the Z-disc boundaries between sarcomeres and calcium handling. Inheritance is autosomal dominant. (Marsiglia and Pereira 2014) The diagnostic criteria include ventricular hypertrophy greater than 15mm in isolation or 13mm in conjunction with supporting features from family history, symptom evaluation, ECG abnormalities, laboratory testing and cardiac imaging (Authors/Task Force, Elliott et al. 2014). Secondary causes of ventricular hypertrophy must be ruled out. Sudden cardiac death is a feature, affecting between 1-2% of the known HCM population per year (O'Mahony, Elliott et al. 2013).

Channelopathies

The commonest inherited arrhythmia syndrome without a protective drug treatment is Brugada syndrome, affecting 1 in 2000 adults (Vutthikraivit, Rattanawong et al. 2018). This condition features coved-ST elevation in the right precordial leads, autosomal dominant inheritance and an association with sudden cardiac death (Brugada and Brugada 1992). Brugada syndrome and the other channelopathies may be under-diagnosed in sudden cardiac death victims as there are no structural abnormalities detectable by currently used clinical and histopathological tests. Patients surviving sudden cardiac arrest can be tested for channelopathies using challenge testing (ajmaline provocation or exercise) alongside detailed electrophysiological assessment (signal averaged ECG,

high-precordial lead ECG, 12-lead 24 hour ECG recording) (Visser, van der Heijden Jeroen et al. 2016).

If all known cardiac conditions are ruled out, the cardiac arrest survivor is said to have suffered idiopathic ventricular fibrillation or tachycardia. Idiopathic ventricular fibrillation is diagnosed when a battery of commonly used clinical tests fail to demonstrate an underlying condition that may have provoked the arrhythmia (Viskin and Belhassen 1990). This group shrinks as new conditions are identified, implying that in the future some of these cases may be reclassified under a new diagnosis. The idiopathic VF group is therefore inherently heterogenous, and by the nature of the presentation, currently impossible to predict before a potentially lethal outcome.

1.3 Modern management of the pro-arrhythmic patient

Various medical or invasive treatments can be considered for many pro-arrhythmic conditions, but in HCM, Brugada syndrome and idiopathic VF none are considered to be curative (Priori, Blomstrom-Lundqvist et al. 2015; Al-Khatib Sana, Stevenson William et al. 2018). The mainstay of risk management is the implantable cardioverter-defibrillator (ICD). First approved for implantation in 1985, at the time of the most recent survey some 85,000 devices were implanted yearly in Europe alone (Raatikainen, Arnar et al. 2015).

ICDs are effective at terminating ventricular arrhythmia and/or reducing mortality in multiple pathologies (Ozaydin, Moazzami et al. 2015; Shun-Shin, Zheng et al. 2017; Wang, Xie et al. 2017; Dereci, Yap et al. 2019). However, complications can occur at comparable rates to the frequency of potentially lethal arrhythmia (Wang, Xie et al. 2017; Dereci, Yap et al. 2019). Patients may suffer inappropriate shocks, device infection, erosion, chronic pain and other long-lasting causes of morbidity or mortality. For this reason, accurate risk stratification is needed to increase the number of high-risk patients undergoing ICD implantation and reduce the number of patients receiving ICDs they do not go on to use.

1.3.1 Risk stratification in Hypertrophic Cardiomyopathy

Implantation of ICDs in HCM cardiac arrest survivors is uncontroversial. Optimal risk stratification for primary prevention devices is a topic of intense debate.

Single risk factors

Over the years many associations with sudden death in HCM have been described and used to estimate risk in the primary prevention candidate. The first was family history, starting with an

addendum to the original 8-case series that defined HCM, describing the sudden death of a brother to one of the original cases (Teare 1958). An early cohort of 119 patients followed up at the Hammersmith Hospital (UK) published in 1973 established the association of family history with sudden death (Hardarson, Curiel et al. 1973).

The early work of William McKenna and colleagues established several risk factors for sudden death: ventricular tachycardia (McKenna, England et al. 1981), diagnosis at a young age (McKenna, Deanfield et al. 1981), and obstructive features on echocardiography (Doi, McKenna et al. 1980). Larger cohorts with longer follow up went on to confirm and quantify the effects of these risk factors.

Patients under 30 with non-sustained VT were found to be at four times the risk of sudden death, compared with HCM patients without NSVT, and this was found to be a binary relationship, with no effect of increasing duration or longer runs of arrhythmia (Monserrat, Elliott et al. 2003). Left ventricular wall thickness, syncope, abnormal blood pressure response, late Gadolinium enhancement, genetic features and left atrial size have all been associated with sudden death in the intervening years (Elliott, Poloniecki et al. 2000; Varnava, Elliott et al. 2001; O'Mahony, Jichi et al. 2014; Weng, Yao et al. 2016).

High risk genes have been described, notably Troponin T mutations in patients with milder hypertrophy (Watkins, McKenna et al. 1995). Whilst known, the variation in genotype-phenotype correlation between individuals, even in the same family means that these features are currently not recommended for risk stratification for sudden death (O'Mahony, Elliott et al. 2013).

Despite the associations, the positive predictive value of most single risk factors is only 10-30% (Saumarez, Pytkowski et al. 2008; Sen-Chowdhry and McKenna 2008). The highest positive predictive value of a single risk factor is paced ventricular electrogram fractionation, at 38% (Saumarez, Pytkowski et al. 2008). This invasive electrophysiologic measure uses programmed ventricular stimulation to determine if aberrant conduction is present, manifesting as fractionated paced electrograms. However, the risks of an invasive procedure combined with the dynamic nature of the arrhythmia substrate (which may explain poor reproducibility of other electrophysiological studies) led to limited adoption of this method.

In summary, single risk factors lack sensitivity and specificity to be used in isolation. Multiple variable, or multivariate strategies offer a potential solution.

Multiple variable strategies

Two main approaches to multivariate risk stratification in HCM exist: the European Society of Cardiology (ESC) guidance, and the American College of Cardiology Foundation/American Heart Association guidance (ACCF/AHA) (American College of Cardiology Foundation/American Heart Association Task Force on, American Association for Thoracic et al. 2011; Authors/Task Force, Elliott et al. 2014).

First published in 2003 and fully revised in 2011, the ACCF/AHA guidelines recommend offering a patient an ICD if they have a family history of sudden death in a first degree relative with hypertrophic cardiomyopathy, or under 50 years old without a diagnosis, left ventricular hypertrophy ≥30mm or recent unexplained syncope. If these features are absent, either non-sustained ventricular tachycardia or an abnormal blood pressure response to exercise are considered. These are combined with 'sudden death risk modifiers' such as left ventricular outflow tract obstruction, late Gadolinium enhancement on cardiac magnetic resonance imaging (CMRI), left ventricular aneurysm or malignant genotypes to guide implantation. In 2020, an LV ejection fraction <50% was added as an indication for ICD therapy.

Defined in 2014, the ESC guidelines recommend the use of a multivariate risk calculator to estimate the 5-year risk of sudden cardiac death. The patient's age, maximum left ventricular wall thickness, left atrial size, left ventricular outflow tract gradient, family history of sudden death, non-sustained ventricular tachycardia and unexplained syncope are considered. This calculation is made on the basis of a retrospective study of 3675 patients, of which 198 suffered a potentially lethal arrhythmia in a 5.7 year average follow up. A Cox proportional hazards model was developed and validated internally by bootstrapping. An estimate of 6%/5-year risk was deemed sufficient to mandate ICD implantation, with an intermediate recommendation between 4-6%/5-year and a recommendation not to implant in those with 4%/5-year risk (O'Mahony, Jichi et al. 2014).

Following the publication of these guidelines, a retrospective analysis of 1629 adult patients with Hypertrophic Cardiomyopathy was released, comparing the recommendations made by the ESC risk calculator against actual outcomes (Maron, Casey et al. 2015). Of the 35 patients suffering sudden cardiac arrest, only 4 (11%) were classified in the high-risk, ICD mandatory group, and more than half were misclassified as low risk, ICD not recommended. A similar proportion of the 46 patients who received an appropriate ICD therapy during the average follow up of 8.1 years were misclassified as low risk. The authors concluded that the ESC guidance was unreliable.

An independent comparison of the ACCF/AHA and the ESC strategies was performed in 288 patients with HCM, 14 of whom had survived potentially lethal arrhythmia (Leong, Chow et al. 2018). In the 14 survivors, the ACCF/AHA would have recommended 43% to have defibrillators, compared to 7% using the ESC guidance. In contrast, from those not experiencing potentially lethal arrhythmia, the ESC correctly classified 82% of patients as low risk, compared to the 57% of patients using the ACCF/AHA score.

A balance of risk clearly has to be struck – once a model has been constructed, a score can be weighted for greater sensitivity or specificity. In the original publication of the ESC score the authors calculated that in their dataset, following their own rule of mandatory implantation at 6%/5-year risk up to half of those experiencing potentially lethal arrhythmia may have been left without an ICD. This figure improved to 29% with the less stringent criterion of 4%/5-year risk (O'Mahony, Jichi et al. 2014).

1.3.2 Risk stratification in Brugada syndrome

Single risk factors

Risk stratification in Brugada syndrome is complicated by the transience of the Type 1 Brugada ECG pattern. The Type 1 ECG pattern can be elicited using sodium channel blockade by flecainide or ajmaline; the presence of either spontaneous or drug-induced Type 1 ECG is diagnostic by current guidelines (Priori, Wilde et al. 2013). Conversely, some argue that the Brugada ECG pattern alone in asymptomatic patients should not be considered the full syndrome, owing to the low rate of sudden cardiac arrest in this group (Honarbakhsh, Providencia et al. 2018). Another alternative view promotes associated symptoms – syncope or sleep apnea – or family history as instrumental to the diagnosis (Antzelevitch, Yan et al. 2016). Use of historic databases are complicated by variance in previous guidelines and the increase in family screening over time, meaning that the study groups used to define high arrhythmic risk may have significant differences with modern populations.

Aside from the Type 1 ECG pattern, early repolarization, the aVR sign, S-wave in lead I and fragmented QRS have been proposed as risk markers for sudden death (Honarbakhsh, Providencia et al. 2018). An inferolateral early repolarization pattern and fractionated QRS was shown to independently confer risk with odds ratios 2.87 and 5.31 respectively in a multivariate analysis of 246 consecutive Brugada patients in Japan (Tokioka, Kusano et al. 2014). Within the same study, syncope had an odds ratio of 28.57. S-waves with a duration of more than 40 milliseconds in lead I were assessed in 276 patients with a spontaneous Type 1 Brugada pattern and found to confer a

hazard ratio of 39.1 for sudden death in a 48 month follow up if present (Calo, Giustetto et al. 2016). The aVR sign was assessed in only 24 Brugada patients, 13 of whom were already symptomatic (Babai Bigi, Aslani et al. 2007). The small, heterogenous cohort sizes of the original papers, and inconsistent inclusion in larger studies contributed to these markers not being incorporated into current risk stratification.

The largest registry of Brugada patients collated information from France, Italy, the Netherlands and Germany (FINGER), reporting 1029 individuals with Brugada syndrome (Probst, Veltmann et al. 2010). Over a 2.6 year follow up, the investigators recorded 51 instances of potentially lethal arrhythmia – 44 of these resulted in ICD therapy, 7 in sudden death. The yearly cardiac event rates were 7% in those with previous aborted cardiac arrest, 2% in those with previous syncope and 0.5% in asymptomatic individuals. Presence of a spontaneous Type 1 ECG was also found to confer increased risk of potentially lethal arrhythmia. Also investigated but found to be insignificant predictors of risk were programmed ventricular stimulation, SCN5a mutation status, male gender and a family history of sudden death. Particular note should be given to the poor independent predictive value of genetic and family history when other risk factors are considered: underlining the poor genotype-phenotype correlation and dynamicity of arrhythmia. A spontaneous Type 1 ECG and unexplained (likely arrhythmic) syncope remain the key determinants of an ICD recommendation in the guidelines (Priori, Blomstrom-Lundqvist et al. 2015; Al-Khatib Sana, Stevenson William et al. 2018).

Programmed ventricular stimulation for the inducibility of ventricular arrhythmia has been studied several times with varying results (Probst, Veltmann et al. 2010; Priori, Gasparini et al. 2012; Calo, Giustetto et al. 2016; Sieira, Conte et al. 2017; Asada, Morita et al. 2020). There is no current consensus on the optimal protocol to use for stimulation, with options ranging from two stimulation sites, 2-3 extrastimuli and a minimum coupling interval of 180-200 milliseconds. Current guidelines make a IIb recommendation that programmed ventricular stimulation may be used to assist decision making, meaning it holds less weight than spontaneous Type 1 ECG and previous syncope.

Multiple variable strategies

Like for HCM, Brugada syndrome specialists have also sought to create a multivariate risk strategy from a database of 400 patients (Sieira, Conte et al. 2017). Univariate analysis found that previous aborted cardiac arrest, spontaneous type 1 ECG, early familial sudden death, inducible ventricular fibrillation or compromising tachycardia by programmed stimulation, previous syncope or evidence of a diseased sinus node were predictors of potentially lethal arrhythmia. Over an average 6.6 year

follow up, 34 patients had either cardiac arrest or appropriate therapy by a primary prevention ICD. The authors then performed a multivariate model of risk and weighted the risk factors into a score by rounding the regression coefficients. Internal validation was very promising, with a C-statistic of 0.81. The investigators reported a sensitivity of 79.4% and a specificity of 72.2% for a threshold of two points at 5 years. This score has yet to be externally validated.

1.3.3 Risk stratification in idiopathic ventricular fibrillation

Patients without an identifiable cause of documented ventricular fibrillation are generally assumed to be at risk of future lethal arrhythmia. A third of patients had a recurrence of ventricular arrhythmia during an average 5 year follow up in the latest meta-analysis (Ozaydin, Moazzami et al. 2015). Due to the inherent normality of most clinic investigations and the high rate of recurrence, detailed risk stratification strategies have been eschewed in favour of widespread implantation (Priori, Blomstrom-Lundqvist et al. 2015; Al-Khatib Sana, Stevenson William et al. 2018). 11 studies from 1998 to 2012 failed on aggregate to predict ventricular arrhythmia recurrence using programmed ventricular stimulation (Ozaydin, Moazzami et al. 2015).

1.4 Ventricular arrhythmogenesis

The conditions examined so far are heterogenous – with lethal arrhythmia being the only common link. Ventricular fibrillation and tachycardia links these conditions as a final common pathway to sudden death, despite their heterogeny. Likewise, all the conditions mentioned demonstrate some unpredictability of the occurrence or recurrence of potentially lethal arrhythmia. A closer look at the arrhythmogenic processes leading to this final common pathway could provide opportunities to improve risk stratification in the inherited cardiac conditions.

Arrhythmogenesis is thought of as an interaction between triggers, substrate and modulating factors (Coronel, Baartscheer et al. 2001). Figure 1.1 illustrates the link between these factors in the 'Triangle of Coumel' (Coumel 1987). In this section these contributory components will be discussed in turn.

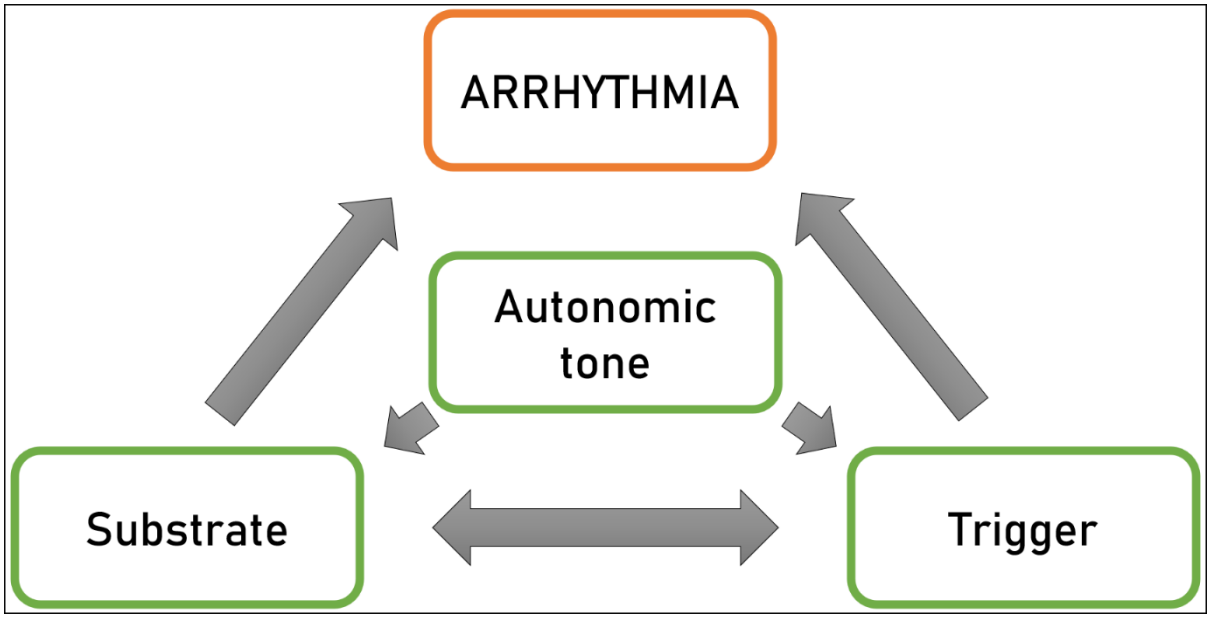

Figure 1.1: Coumel's triangle. Arrhythmogenesis can be thought of as an interaction between triggers, substrates and modulating factors. Understanding this may enhance our ability to predict arrhythmia.

1.4.1 Triggers: the ventricular ectopic

A ventricular ectopic is a premature depolarization generated within ventricular myocardial cells or conduction tissue distal to the bifurcation of the bundle of His. They are often seen as broad-complex beats on the surface electrocardiogram (ECG): an example body surface recording from this study is shown in Figure 1.2.

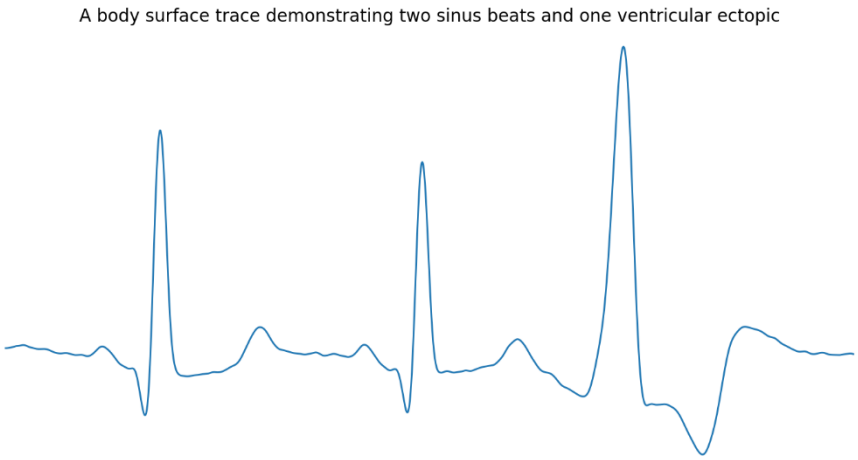

Figure 1.2: A body surface trace demonstrating two sinus beats followed by a ventricular ectopic. Image produced from the body surface signals from a patient in this study.

Pathophysiology

There are 3 accepted mechanisms for the generation of ventricular ectopic depolarizations:

1. Enhanced automaticity
2. Triggered activity
3. Re-entry

Enhanced automaticity

Many cardiac cells can depolarize without external influence – this is known as normal automaticity (Hoffman and Cranefield 1964). This occurs due to a 'funny' current, so named because it is activated by hyperpolarization than depolarization. It is a slow inward flux of potassium and sodium ions across the cardiac cell membrane during diastole (Brown, Difrancesco et al. 1979). Ions cross hyperpolarization activated, cyclic nucleotide dependent channels (HCN); these are sensitive to cyclic adenosine monophosphate (cAMP), in turn conferring sensitivity to beta adrenergic and muscarinic acetylcholine agents (Robinson and Siegelbaum 2003). Other currents have been noted to contribute to automaticity, most notably the sodium-calcium exchanger current (I_{NCX}) (Lakatta and DiFrancesco 2009), which is also modulated by catecholamines (Gao, Rasmussen et al. 2013).

Upon crossing a threshold membrane voltage there is a rapid sodium influx through the voltage gated sodium channel Nav1.5, encoded by the SCN5a gene. This results in cell depolarization. The velocity of the action potential and therefore impulse propagation is related to this rapid sodium influx (MacLeod, Marston et al. 2015). Calcium enters through the L-type calcium channel and stimulates the ryanodine receptor, which facilitates excitation-contraction coupling (Eisner, Caldwell et al. 2017).

<u>Parasystole</u>

Cells of the sinoatrial node (SAN) have the highest rate of automaticity in the normal heart, leading to its dominance in determining heart rate (Baruscotti, Bucchi et al. 2005). Most subsidiary pacemakers will be depolarized at a higher rate by the dominant signal of the SAN. However, if these subsidiary pacemakers are shielded from a depolarization by an area of slow conduction, they may activate of their own accord. This produces parasystolic ectopy (Pick 1953).

<u>Depolarization induced automaticity</u>

Whilst cells with subsidiary pacemaker potential depolarize spontaneously in normal physiologic conditions, many myocardial cells can develop automaticity from changes in their immediate

environment. This occurs when membrane potentials are brought close to the threshold transmembrane voltage (Carmeliet 1984; Yu, Chang et al. 1993). This is called 'depolarization induced automaticity' and is modulated largely by the L-type voltage-gated Ca channel (Katzung 1975; Ypey, van Meerwijk et al. 2013).

These conditions can occur when extracellular potassium is higher than usual (including the high rates of cell death in myocardial ischaemia), reduction in the number or function of I_{K1} channels, or the electrotonic influence of neighbouring cells (Antzelevitch and Burashnikov 2011).

Triggered activity

Following depolarization of a cardiac myocyte, two types of 'afterdepolarization' can occur – the early afterdepolarization (EAD) and the delayed afterdepolarization (DAD). EADs occur during the main action potential plateau or during phase 3 repolarization, whereas DADs occur following full repolarization of the previous action potential (Wit and Rosen 1986).

Like enhanced automaticity, afterdepolarizations are also modulated by beta-adrenergic agonists due to the influence of cAMP and protein kinase A on voltage-gated ion channels (Xie, Grandi et al. 2013). In contrast to depolarization induced automaticity, afterdepolarizations follow a cardiac action potential rather than stemming from a sub-threshold depolarizing influence in the cellular environment.

Early afterdepolarizations

Repolarization of the myocyte occurs in multiple phases. In the phase 1 notch, I_{to}, the transient outward K current rapidly and briefly activates, which quickly but partially repolarizes the cell – the action potential notch. In phase 2, further potassium outflow helps to repolarize the cell via I_{kr} (rapid) and I_{ks} (slow). The balance of I_{ca} and I_{kr} + I_{ks} leads to a plateau. In phase 3 the potassium currents continue whilst calcium flux stops, and the cell repolarizes faster. This is partially slowed by I_{NCX} which produces a slow net inward sodium current to expel calcium. Full repolarization is achieved by I_{k1} (MacLeod, Marston et al. 2015).

Any current which can overcome the net outward current produced by these potassium channels can cause an EAD. Both the L-type Ca channel and I_{NCX} are capable due to positive feedback in depolarized states (Weiss, Garfinkel et al. 2010). If $I_{Ca,L}$ and I_{NCX} predominate over I_{kr} and I_{ks}, repolarization is terminated and an EAD is produced at the cellular level.

EADs are important in congenital and acquired long QT syndromes (Shimizu, Ohe et al. 1991; Yan, Wu et al. 2001), heart failure (Li, Lau et al. 2002) and Torsade de pointes (Wu, Wu et al. 2002).

Delayed afterdepolarizations

Delayed afterdepolarizations occur after full repolarization (phase 4 of the action potential) (Fink, Noble et al. 2011). They are believed to be caused by calcium flux between the sarcoplasmic reticulum and cytoplasm (Marban, Robinson et al. 1986).

DADs are important in ischaemia (Said, Becerra et al. 2008), heart failure (Verkerk, Veldkamp et al. 2001), diabetic heart models (Nordin, Gilat et al. 1985), right ventricular outflow tract VT (Calvo, Jongbloed et al. 2013), and healthy tissues exposed to any one of sustained tachycardia (Stambler, Fenelon et al. 2003), hypokalaemia (Miura, Ishide et al. 1993), elevated sympathetic tone (Chen, Chiang et al. 1994) or digitalis toxicity (Xie, Cunningham et al. 1995).

Several of these conditions are linked to intracellular calcium overload (Vassalle and Lin 2004; Garcia-Dorado, Ruiz-Meana et al. 2012; Marks 2013). It is believed that calcium release from sarcoplasmic reticulum activates the I_{NCX} which then leads to depolarization of the cell membrane (Fink, Noble et al. 2011). This in turn leads to activation of Nav1.5 sodium channel once the threshold is passed.

Re-entry – a disorder of impulse conduction

Alterations in impulse conduction can lead to the action potential propagating in a closed loop. Border zones of heterogenous heart tissues are associated with generation of focal ectopic activity in several animal studies (Kaplinsky, Yahini et al. 1972; Boineau and Cox 1973; Arutunyan, Swift et al. 2002). These forms of arrhythmia highlight potential overlap between trigger and substrate – sometimes only divided by scale. The limits of differentiating between true focal (arising from a single cell or contiguous mass of cells) and micro re-entry are defined by the resolution and dimensionality of mapping technology (Ideker, Rogers et al. 2009).

Delayed propagation of the action potential from a sinus beat through varying levels of conduction block can lead to the initiation of a ventricular ectopic, especially in models of ischaemia (Pogwizd and Corr 1987). Intramural re-entry is important in this context, and epicardial or endocardial mapping alone can cause the misinterpretation of these ectopics as non-reentrant. Electrical remnants of the sinus beat delayed by slow conduction reach sections of myocardium which are once again ready to depolarize. The reactivation of this tissue generates a ventricular ectopic. An in-silico study using high-fidelity patient derived data has also demonstrated micro re-entry as a probable mechanism for borderzone arrhythmogenesis (Oliveira, Alonso et al. 2018).

Reflection

This is a special form of re-entry caused by a conduction block in a long fibre. The inward and outward path of propagation are shared. Whilst the area of conduction block may be unable to support an action potential, longitudinal current flow through it can be sufficient to depolarize the distal fibre, reversing the current flow. If the conduction delay is sufficiently long, the proximal fibre may become excitable again and depolarize under the influence of current flow through the region of block. This impulse is now ectopic. This can occur in acute ischaemia, chronic infarct and areas of localized extracellular hyperkalaemia (Janse and D'Alnoncourt 1987).

From cellular depolarization to ventricular ectopic

To become a ventricular ectopic at the tissue level, cellular premature depolarizations must propagate. Normally repolarizing cells in the immediate vicinity can oppose this through electrotonic effects via well coupled gap junctions. A critical mass has to be achieved – thought to be a group of nearly a million cardiomyocytes in simulations (Xie, Sato et al. 2010). Modelling simulation of poor gap junction coupling, fibrosis, reduced repolarization reserve and heart failure electrical remodeling conditions decreases this critical mass significantly, giving an indication as to why we see more ventricular ectopy in such conditions.

Clinical relevance

Ventricular ectopics are common in normal hearts. In the most thorough study to date 101 subjects with a normal physical examination, electrocardiogram (ECG), echocardiogram, maximal exercise tolerance test (ETT), left and right heart catheterization with coronary angiography underwent 24 hour continuous ECG (Holter monitoring) (Kostis, McCrone et al. 1981). 39% of subjects had at least one ventricular ectopic in a 24 hour period, but only 4% had more than 100.

Large cohort studies appear to suggest that ventricular ectopics may confer a higher risk of sudden cardiac death. The Multiple Risk Factor Intervention Trial (MRFIT) studied 15,637 apparently healthy white men aged 35-57 over 7.5 years (Abdalla, Prineas et al. 1987). During 2 minute ECG recording, 4.4% of participants were found to have ventricular ectopics. An four-fold increase in risk was found for patients with ‘complex’ ventricular ectopy (polymorphic, bigeminous, repetitive or R-on-T) for sudden cardiac death. The Framingham Heart study recorded 1 hour continuous ECG in 6,033 men and women, finding complex ventricular ectopy in 12% of apparently healthy subjects. An two-fold increased risk for sudden death was also demonstrated in men over a maximum 6 year follow up (Bikkina, Larson et al. 1992). These large studies have been criticized for incomplete exclusion of structural heart disease – bringing into question their definition of ‘apparently healthy’ (Ng 2006).

MRFIT excluded only patients with a previous history of myocardial infarction or diabetes. Framingham employed a two-year follow up with patient history, physical examination and 12 lead ECG.

Other studies of apparently healthy individuals provide a contrasting view that without other signs of cardiac disease, ventricular ectopics may be benign during rest or exercise. A study of 1,160 adult subjects undergoing maximal ETT found that 6.9% developed frequent or repetitive ectopic activity. During a follow up period of 5.6 years this did not confer additional risk for cardiac events including angina pectoris, non-fatal myocardial infarction, cardiac syncope or sudden cardiac death (Janette Busby, Shefrin et al. 1989). Ventricular ectopy at rest on routine ECG was further examined in 1,214 volunteers aged 35-69 over 10 years – no predictive value of manifest ectopy was demonstrated (Fisher F and Tyroler Herman 1973). Ninety-eight older subjects aged 60-85 years who were examined with 24 hour continuous ECG similarly could not be stratified into high- and low- cardiac risk groups by manifest ectopy after 10 years of follow up (Fleg and Kennedy 1992).

The role of ventricular ectopy in prognosticating those with overt cardiac disease is less controversial. In 533 patients surviving 10 days post myocardial infarction, the occurrence of more than 10 ventricular ectopics per hour was an independent risk factor for sudden death in a 24 month follow up (Mukharji, Rude et al. 1984). In 933 patients were studied with 6 hour continuous ECG following myocardial infarction, complex ventricular ectopy was found to have a greater association with sudden and non-sudden cardiac death in an average 36 month follow up (Moss, Davis et al. 1979). Prior to the turn of the 21st century, the consensus view was that ventricular ectopy was most relevant to those with concurrent structural heart disease.

Yet we know that in some patients with apparently normal hearts, ventricular ectopy may be the trigger for a fatal arrhythmia. A clear demonstration of this came in 2002, when ectopy was shown to be a treatable cause of ventricular fibrillation in the structurally normal heart (Haissaguerre, Shah et al. 2002). Figure 1.3 shows a trace from an implantable defibrillator in a patient from this study in which ventricular ectopy initiates rapid ventricular arrhythmia.

Figure 1.3: Endocardial recording from an implantable cardioverter defibrillator. The device was implanted for secondary prevention in this patient with a structurally normal heart, who took part in this study. Closely coupled ectopy recurs in a triplet pattern. Following the vertical dashed line, the ventricles begin to fibrillate. This arrhythmia was likely triggered by the closely coupled ectopics.

Haïssaguerre et al. investigated 16 survivors of cardiac arrest in the context of apparently normal hearts. All had normal physical examination, electrocardiogram, exercise testing, coronary angiography and echocardiography. Coronary spasm was ruled out by ergonovine challenge or documentation of an isoelectric ST segment prior to ventricular fibrillation. Class IA and IC drug challenge excluded a long QT or Brugada syndrome. Six underwent endomyocardial biopsy – the results were unremarkable. Ventricular ectopics were seen to initiate ventricular arrhythmia in these patients and were targeted by mapping the earliest endocardial electrogram relative to onset of the ectopic QRS complex. Radiofrequency ablation of these sites resulted in a significant reduction in ectopic beats and no recurrence of ventricular fibrillation or syncope in a follow up of 32 months.

Since this study, more patients have been successfully treated by these means, establishing it as an option for patients suffering recurrent ventricular arrhythmia (Haïssaguerre, Shoda et al. 2002; Knecht, Sacher et al. 2009) – although there has been no move towards viewing this as fully curative in the current consensus (Priori, Blomstrom-Lundqvist et al. 2015; Al-Khatib Sana, Stevenson William et al. 2018).

1.4.2 The substrate for ventricular arrhythmia

An arrhythmogenic substrate is a set of conditions that are conducive to arrhythmia induction. Well-known examples include the dual atrioventricular (AV) node physiology believed to underlie AV

nodal re-entrant tachycardia, or accessory pathways in AV reentrant tachycardia. A substrate can be static, such as an established myocardial infarction scar; or dynamic, such as areas of ischemia during ST-elevation myocardial infarction, which can disappear with early revascularization.

Perhaps the earliest and best characterized substrates are those of the ischaemic and infarcted heart. The circus movement of electrical activity during ventricular tachycardia (VT) had been demonstrated in 1913 (Mines 1913), but not until 1983 was the nature of the substrate detailed in humans: a mixture of viable myocardial cells and fibrotic tissue (Fenoglio, Pham et al. 1983). Further characterization noted 'zigzag' motion of electrical activity and poor electrical coupling of cells in such regions, leading to localized slow conduction – the preconditions for ventricular arrhythmia (de Bakker, van Capelle et al. 1993). Although ischaemic VT was subsequently mapped and targeted for ablation, haemodynamic instability meant this approach was not suitable for all patients (Proietti, Roux et al. 2016). Substrate mapping in sinus rhythm was first performed in the mid-1980s, finding fractionated, split and late electrograms in areas surrounding earliest activation during mapping in VT (Kienzle, Miller et al. 1984). Ischaemic cardiomyopathy was differentiable from non-ischaemic cardiomyopathy in humans by the detection of abnormal electrograms (Cassidy, Vassallo et al. 1986), and histological scar was demonstrated in areas where low-voltage or prolonged electrograms were detected in porcine models, with late potentials detected in peri-scar areas (Wrobleski, Houghtaling et al. 2003). Based on these findings, substrate based ablation of VT circuits became a possibility, but despite two decades of development, recurrence rates at 1 year remain high (Josephson and Anter 2015).

Ischaemic cardiomyopathy has histologically identifiable substrate, a property not shared with functional causes of ventricular arrhythmia, such as idiopathic ventricular fibrillation or Brugada syndrome. These functional syndrome substrates are less well characterized and rarely treated by ablation compared to ischaemic cardiomyopathy.

The substrate for Brugada Syndrome

The exact nature of the Brugada substrate is still debated, but there is consensus that the abnormality occurs in the right ventricular outflow tract (Pieroni, Notarstefano et al. 2018). Two main theories were postulated: from canine wedge preparations, the 'repolarization hypothesis'; from human mapping and electrophysiological studies, the 'depolarization hypothesis'. These theories compete, but may not be mutually exclusive (Wilde, Postema et al. 2010). The competing theories are described in Figure 1.4.

Conduction delay in humans can explain many features of Brugada syndrome. Loss of function mutations in SCN5a, a gene encoding the Nav1.5 sodium channel, contribute to a reduction in the fast sodium current required for depolarization. Sodium channel blockers unmask the pathognomic Type 1 Brugada ECG whilst causing concurrent conduction slowing in the atria and ventricles. Recorded late ventricular potentials coupled with biopsy and histopathological evidence of fibrosis, myocarditis or apoptosis suggest that the disease reflects disordered conduction through diseased myocardial tissue (Wilde, Postema et al. 2010).

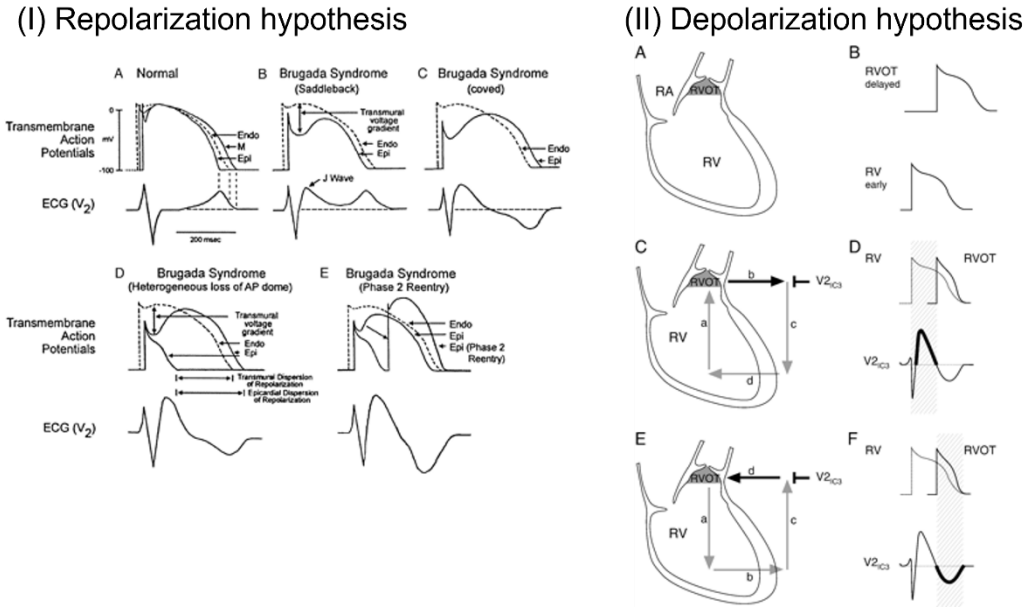

Figure 1.4: Competing theories of Brugada syndrome pathogenesis. (I) The repolarization hypothesis states that stronger outward potassium currents in the epicardium lead to both J wave elevation due to reduced depolarizing force (Panels IB and ID) and T wave inversion (Panels IC-E) by either prolonged epicardial action potential or Phase 2 re-entry. (II) The depolarization hypothesis states that delayed action potential in the right ventricular outflow (RVOT) relative to the right ventricle (RV) (IIA-B) leads to current flow from RV to RVOT during the J point. This flow towards the high RV ECG lead causes ST elevation (IIC-D). During whole heart repolarization, the delayed RVOT action potential causes current to flow toward the RV, leading to a negative T wave. Figure adapted from (Meregalli, Wilde et al. 2005)

Proponents of the repolarization hypothesis contend that no animal or in vitro model compatible with the depolarization hypothesis has been produced to date. In contrast, canine wedge models can demonstrate the characteristic ST elevation, transmural dispersion of repolarization and subsequent Phase 2 reentrant extrasystoles which lead to ventricular tachycardia and fibrillation (Yan and Antzelevitch 1999). Monophasic action potential recordings from patients exhibiting a spontaneous type 1 Brugada ECG demonstrate epi- to endocardial differences in repolarization without evident conduction delay (Kurita, Shimizu et al. 2002).

Whilst the debate is unlikely to be settled soon, clinicians have already started investigating therapy directed at the right ventricular outflow tract (RVOT). Early case series indicated that in a subset of patients, premature complexes from the RVOT could be detected and targeted by radiofrequency ablation (Haïssaguerre, Extramiana et al. 2003). Patients not exhibiting clear triggers continued to pose a problem, however. The first attempt at substrate modification in sinus rhythm used radiofrequency ablation in the RVOT in 9 Brugada syndrome patients with recurrent and inducible ventricular fibrillation or tachycardia (Nademanee, Veerakul et al. 2011). Low voltage, prolonged electrograms with evidence of fractionation were found clustered in the anterior aspect of the RVOT epicardium. 7 patients were rendered non-inducible and the Brugada ECG was suppressed in 8; a 20-month average follow up recorded no further recurrent ventricular arrhythmia.

Further work introduced sodium channel blocker administration as a strategy for clarifying the substrate during mapping (Brugada, Pappone et al. 2015). Administration of flecainide was observed to increase the area of the epicardium exhibiting low voltage electrograms. Once again, the Type 1 ECG could be suppressed by ablation, and recurrence of ventricular arrhythmia in the ablation group was low. By the time of writing, there are a few hundred cases of Brugada syndrome ablation in the literature, but similar to ischaemic ventricular arrhythmia, there is not sufficient evidence to consider the procedure fully curative in the guidelines, not least because outcomes following ablation may vary (Priori, Blomstrom-Lundqvist et al. 2015; Veerakul and Nademanee 2016; Al-Khatib Sana, Stevenson William et al. 2018).

The substrate for idiopathic ventricular fibrillation

The idea of a single substrate for idiopathic ventricular fibrillation may be problematic. Prior to 1992 Brugada syndrome fell under this diagnostic umbrella whilst it is very much a condition in its own now. As a grouping term for as-yet unidentified conditions, the idiopathic VF group is inherently heterogenous. Nonetheless, the previously mentioned work eliminating Purkinje ectopic triggers suggests that detailed electrophysiological analysis may play a role in future treatment (Haïssaguerre, Shoda et al. 2002).

Haïssaguerre et al. followed up their initial work by examining the evidence for a mappable substrate during sinus rhythm in 24 idiopathic VF survivors (Haïssaguerre, Hocini et al. 2018). Non-invasive body surface recordings were taken during the induction of ventricular fibrillation and epicardial fibrillatory electrograms reconstructed using a previously developed inverse solution (Rudy and Lindsay 2015). Phase mapping was used to identify ‘driver regions’ during fibrillation – areas thought to be critical to the maintenance of VF. Subsequent invasive mapping found co-

location of abnormal electrograms with these regions in 76%, suggestive of myocardial structural alterations. In patients without regions of abnormal electrograms, the previously described Purkinje triggers were found. Ablation resulted in arrhythmia suppression for 15 of 18 patients in an average 11 month follow up.

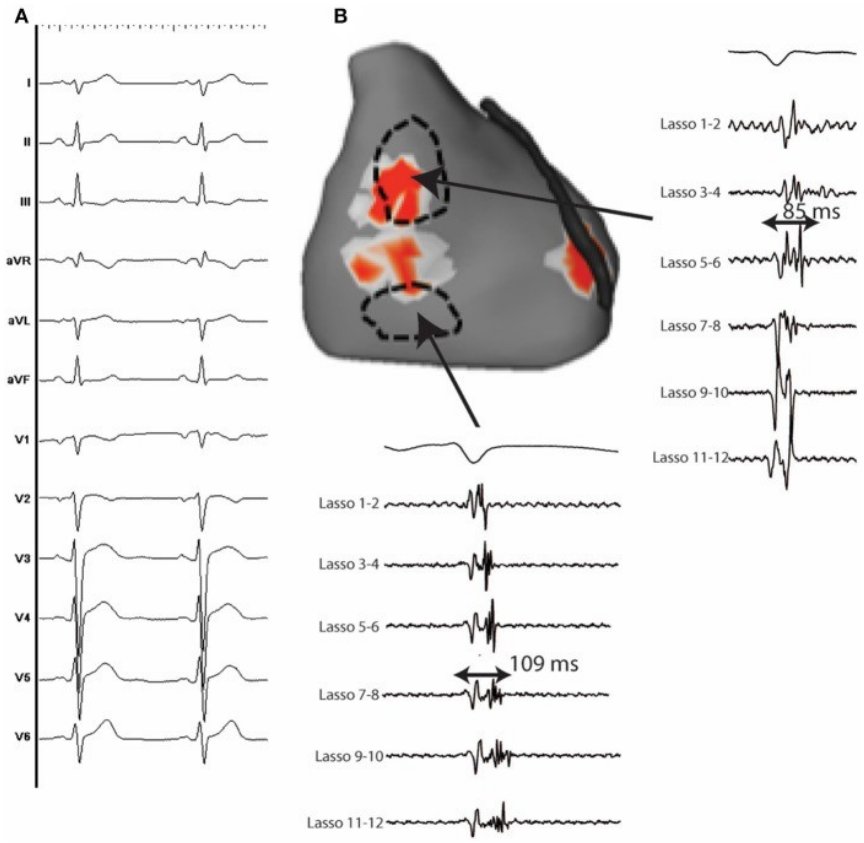

Figure 1.5: (A) The 12 lead ECG of a patient with idiopathic ventricular fibrillation. (B) Non-invasive mapping of ventricular fibrillation (VF) 'driver regions' thought to be critical to VF maintenance – labelled in red. Invasive mapping of the areas in the dashed ovals demonstrated prolonged and fractionated electrograms thought to be the substrate for ventricular fibrillation in this patient. Adapted from (Haïssaguerre, Hocini et al. 2018)

Reports of idiopathic VF ablation remain rare, but early experimentation describing the existence of triggering ectopics or regions of abnormal electrograms believed to represent structural abnormality share a similarity with the findings in Brugada syndrome mentioned in the previous section. This raises the question of whether diverse conditions may indeed share a common pathway to fatal ventricular arrhythmia.

The substrate for Hypertrophic Cardiomyopathy

Although a structural syndrome, the substrate of HCM has been sparsely mapped. From the first histopathological description by Donald Teare, myocyte disarray and fibrosis were noted and

associated with the palpitations and sudden deaths befalling his initial 8 study subjects (Teare 1958) (Figure 1.6-I). Programmed ventricular stimulation is not favoured for risk stratification of HCM, but a study of 179 patients with HCM showed that fractionation of the paced electrogram could predict potentially lethal arrhythmia over a 4 year follow up (Saumarez, Pytkowski et al. 2008) (Figure 1.6-II).

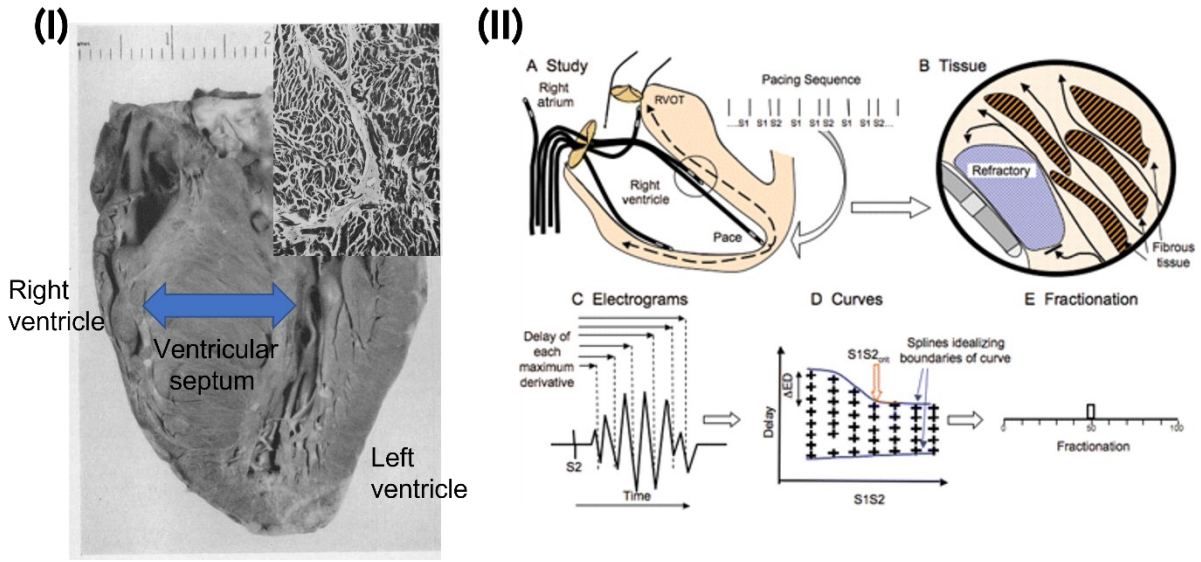

Figure 1.6: (I) Main picture – the ventricular septum is selectively enlarged in this hypertrophic heart. Inset – tissue from the affected areas shows myocyte disarray, in contrast to the normal linear arrangement of cardiac muscle. (II) Principles of paced electrogram fractionation. Pacing and detection of electrical impulses from distant endocardial sites produces electrograms (A). In tissue with fibrotic disruption, electrical impulses are slow and tortuous (B). Electrograms can have their fractionation assessed and quantified (C-E). Adaptations from (Teare 1958) and (Saumarez, Pytkowski et al. 2008)

Two explanted HCM hearts have been studied in the context of a wider cohort of Langendorff perfused hearts, in which activation delay and fractionation could be demonstrated in the HCM hearts. However, in contrast to the chronically infarcted hearts in the study, sustained ventricular tachycardia and zig-zag slow conduction could not be demonstrated, despite present fibrosis (Janse and De Bakker 2001). Catheter ablation for arrhythmia in HCM is only reported in patients with ventricular tachycardia secondary to left ventricular aneurysm. In this study of 15 patients, low voltage substrate areas could be seen in the apical aneurysm, and radiofrequency ablation effectively suppressed further arrhythmias (Igarashi, Nogami et al. 2018). It should be noted that apical aneurysms are uncommon in HCM, and these patients form a distinct subgroup from the rest of the at-risk HCM population.

1.5 Newer non-invasive techniques for the evaluation of electrophysiological substrate

Potential arrhythmic substrates can be evaluated histopathologically, electrophysiologically or through cardiac imaging. Histopathology is of limited use in live patients, as removal of cardiac tissue can be dangerous and has a potentially high false negative rate (From, Maleszewski et al. 2011). Fully non-invasive methods have the advantage of being better tolerated by patients and generally safer.

1.5.1 Conventional imaging

Left ventricular ejection fraction, an imaging correlate of arrhythmic risk, is widely used in clinical practice and well recognized by the guidelines (Al-Khatib Sana, Stevenson William et al. 2018). Recent developments in myocardial imaging have made detection and evaluation of the arrhythmic substrate more feasible in recent years (Rijnierse, Allaart et al. 2016). In ischaemic cardiomyopathy, inducibility at programmed ventricular stimulation has been found to be linked to the size of resting perfusion defects found on single photon emission computer tomography (SPECT) (Gradel, Jain et al. 1997). This metric is thought to correlate with established myocardial scar. SPECT has also been shown to be useful in predicting electrophysiologic scar defined by low-voltage areas during invasive mapping, and also the area in which the successful ablation occurred (1cm from the scar border) (Tian, Smith et al. 2012).

In both ischaemic and non-ischaemic indications, cardiac magnetic resonance imaging (CMR) is increasingly important in the evaluation of myocardial scar and therefore potential arrhythmic substrates (Wu 2017). During imaging, areas of late gadolinium enhancement have good co-location with scar both globally in the myocardium and transmurally, and can be used to guide ablation of arrhythmic substrates clinically (Bisbal, Fernández-Armenta et al. 2014). Tissue characterization by T1 mapping has also been shown to be a predictor of ventricular arrhythmia in a wide range of pathologies (Chen, Sohal et al. 2015).

CMR has been investigated for risk stratification in hypertrophic cardiomyopathy. A meta-analysis of 2993 patients found late gadolinium enhancement was associated with sudden cardiac death, all-cause mortality and cardiovascular mortality in an average 3 year follow up (Weng, Yao et al. 2016). For every 10% of the myocardial volume occupied by late gadolinium enhancement, the hazard ratio for sudden cardiac death was found to increase by 1.36. T1 mapping and extracellular volume quantification has also been studied in regard to diagnosis of hypertrophic cardiomyopathy, but at the time of writing has not been used in risk stratification (Swoboda, McDiarmid et al. 2016). Of the

investigated measures, only late gadolinium enhancement has been used clinically for risk stratification of sudden death in HCM, and then only as a supporting piece of evidence (American College of Cardiology Foundation/American Heart Association Task Force on, American Association for Thoracic et al. 2011).

CMR has not been used for the evaluation of the substrate in the structurally normal heart arrhythmias – Brugada syndrome and idiopathic VF.

1.5.2 Electrographic imaging

Electrographic imaging (ECGi) has been previously mentioned in the context of idiopathic ventricular fibrillation (Haïssaguerre, Hocini et al. 2018). ECGi is a tool for reconstructing electrical potentials at the cardiac surface based on electrical signal recording at the body surface and geometric data derived from computerized tomography (CT) of the chest. Initial experiments were made by comparing recorded signals from the epicardia of perfused explanted canine hearts suspended in torso-shaped tanks with recordings made from the surface of these tanks. Live human validation was performed using direct intra-operative recordings during open heart surgery (Rudy and Lindsay 2015). For a known geometry defined by the CT scan, these two sets of recordings can be related by a transfer coefficient matrix. Large result errors can be produced with small input errors, and for this reason ECGi is a heavily regularized process – constraining the possible outputs for a given range of inputs (Rudy and Messinger-Rapport 1988). Nonetheless, in comparisons between directly measured electrograms (EGM) and the ECGi simulations, the correlation coefficients were found to be more than 0.9 for 72% of all epicardial locations (Rudy and Lindsay 2015).

As previously alluded to, ECGi has been used clinically to evaluate activation sequences during arrhythmia; work has also been performed to evaluate arrhythmic substrate during sinus rhythm. The epicardial substrate of Brugada syndrome has been quantified in 25 patients with the syndrome, and differentiated from 6 patients with right bundle branch block (RBBB) for comparison (Zhang, Sacher et al. 2015). 6 of the patients were also tested at higher heart rates from exercise or isoprenaline infusion (a sympathomimetic) to determine effects of rate on the electrophysiology. The investigators found delayed activation and activation recovery interval (ARI – a correlate of action potential duration) lengthening in the right ventricular outflow tract (RVOT) of Brugada syndrome patients but not of controls. Fractionated electrograms were also found in the RVOT of Brugada syndrome patients, not found in controls. During raised heart rate, activation times became comparatively later and ARIs comparatively longer in the RVOT of Brugada syndrome patients. The

authors concluded that ECGi might be used to differentiate Brugada syndrome from benign RBBB, but also noted the findings of delayed activation and steep repolarization gradients, which are known to be arrhythmogenic.

ECGi has been used to evaluate the sinus rhythm substrates of arrhythmogenic right ventricular cardiomyopathy, long-QT syndrome and early repolarization syndrome (Vijayakumar, Silva et al. 2014; Andrews, Srinivasan et al. 2017; Zhang, Hocini et al. 2017).

In 2017 Leong et al. took the approach of studying sudden cardiac arrest survivors to determine if arrhythmic phenotypes could be defined by ECGi (Leong, Ng et al. 2018). 11 sudden cardiac arrest survivors with structurally normal hearts were studied: 4 with Brugada syndrome and 7 with all other cardiology investigations being normal i.e. idiopathic VF. These patients were compared with 10 patients with Brugada syndrome but no history of life-threatening arrhythmia, and 10 control volunteers without an inherited cardiac condition and structurally normal hearts. All subjects underwent ECG imaging during a maximal effort treadmill test. Three electrograms were analysed immediately after peak exercise and at full recovery from each of 15 anatomical segments of the myocardium to provide values of activation/repolarization dispersion and change with exercise. Despite no significant changes in surface ECG markers such as corrected QT dispersion or T-peak to T-end dispersion, significant increases in corrected ARI dispersion could be detected in the sudden cardiac arrest survivors. These were not seen in the normal controls or Brugada patients without a previous history of sudden cardiac arrest. This was the first publication to indicate that the arrhythmic substrate leading to cardiac arrest might be detectable using ECG imaging, and also emphasized the importance of external stressors in unmasking this effect.

Leong et al. went on to show that activation changes were also unmasked by exercise in sudden cardiac arrest survivors (Shun-Shin, Leong et al. 2019). Whilst change in dispersion was shown to be important in the previous example, using the same 31 patients it was shown that the sequence of activation could also be seen to change following a stressor. To this end, the group developed Ventricular Conduction Stability (V-CoS), a rapid and automated method of comparing changes in global activation between two cardiac cycles mapped with ECG imaging. V-CoS is the percentage concordance of activation times (to an accuracy of <10 milliseconds) across the heart between these two cardiac cycles. A score of 100% indicates perfect preservation of the activation sequence between the two cycles; progressively lower scores indicate more activation heterogeneity. The investigators found that exercise testing resulted in significantly lower V-CoS scores immediately following peak exercise in the sudden cardiac arrest survivors, and this effect diminished as patients

returned to full recovery. Tilt testing to stimulate high vagal tone failed to elicit a significant difference. Furthermore, they found their technique to be reproducible between operators for 10 patients, and between tests in one patient who underwent repeat exercise testing.

Critically, Leong et al. showed that surface ECG taken during exercise and recovery appeared identical, but the corresponding ECGi signals could be shown to be different using only a simple concordance measure like V-CoS. Furthermore, spatial distribution of electrophysiological features like delayed conduction or prolonged repolarization may not be appreciated by surface measures, even when hundreds of electrodes (without epicardial reconstruction) are considered (Bear, Huntjens et al. 2018). This may account for the poor risk stratification produced by routinely used surface measures only such as 12 lead or continuous ECG.

ECGi has therefore shown potential in identifying arrhythmic substrates over and above conventional measures and could possibly be used to define a threshold level of risk for sudden cardiac arrest. Numbers of studies (and patients) are small, and no mention of ECGi is made in current risk stratification guidelines (Priori, Blomstrom-Lundqvist et al. 2015; Al-Khatib Sana, Stevenson William et al. 2018).

1.6 Summary

Despite the origins of potentially fatal arrhythmia in the interaction of electrophysiological triggers and myocardial substrates, direct measurements of these factors do not feature in clinical risk stratification for sudden cardiac arrest. Much about the preconditions for arrhythmia are already known on the cellular and tissue level, but modern risk stratification strategies are still frustrated by unacceptably high proportions of patients dying suddenly after being classified as ‘low-risk’.

Some of the discoveries we have touched upon in this introduction give an idea as to why this is the case. For example, ventricular ectopics appear to be very dangerous to some patients with structurally normal hearts, but essentially benign to most of the population. Some patients who have had ventricular fibrillation in the past go on to have it again – but an even greater proportion do not. Patients with Brugada syndrome are thought to have a type 1 ECG because of significant electrical abnormalities in their right ventricular outflow tracts; yet patients spend almost all of their lives in normal sinus rhythm. Programmed ventricular stimulation has been shown to be useful in some, and not useful in others, but more worryingly, the results are not always reproducible (Priori, Gasparini et al. 2012).

Such findings reinforce the idea of the dynamic arrhythmic substrate. Invasive mapping is highly detailed but places the patient in a non-physiological environment. From the findings of adrenergic sensitivity in the ionic currents of the cardiomyocyte to the exercise induced changes demonstrated using ECG imaging during a treadmill test, it seems likely that non-invasive mapping of dynamic substrates will be useful in future risk stratification. Early experiments by Leong et al. have shown promising results differentiating sudden cardiac arrest survivors from controls.

For a tool to be useful in risk stratification, it must pass several criteria:

1. It should identify those at elevated risk of sudden death - sensitivity.
2. It should also exclude those not at elevated risk of sudden death - specificity.
3. It should be reproducible.
4. It should have a low inherent cost to the patient, whether through discomfort or the risk of complications.

With these concepts in mind, the aim of this thesis is to evaluate ECG imaging in the context of modern risk stratification, to further understand whether it is feasible to improve risk stratification in the inherited cardiac conditions.

1.7 Hypotheses

1.7.1 Main

The electrophysiological substrate for life threatening arrhythmia is quantifiable by non-invasive ECG imaging.

1.7.2 Sub-hypotheses

1. State of the art risk stratification for Brugada syndrome adequately differentiates patients suffering life threatening arrhythmia (Chapter 3).
2. V-CoS is a reproducible measure of exercise induced conduction abnormalities in structurally normal hearts, including in survivors of idiopathic VF (Chapter 4 and 5).
3. Ischaemic cardiac arrest survivors with reversed substrate i.e. full revascularization and recovery of ventricular function have preserved ventricular conduction in response to exercise (Chapter 5).
4. Improvements in reproducibility of ECGi measures can be gained by automation of signal processing (Chapter 6).

5. Automated ECGi measurements can successfully differentiate patients with Brugada syndrome and Hypertrophic Cardiomyopathy from normal controls (Chapters 7 and 8).
6. Automated ECGi measurements can successfully differentiate patients with HCM at both high and low risk of future arrhythmia (Chapter 8).

1.8 Scope of the thesis

Chapter 2 details the cohort who volunteered for this study, as well as the technologies and protocols used in this thesis. Recruitment criteria, CardioInsight ECGi and exercise testing are covered in this chapter.

Chapter 3 is a collaboration between our centre and University Hospital of Wales: 192 consecutive Brugada syndrome patients with sufficient data for analysis were stratified for risk of sudden death by a the Sieira et al. (2017) state of the art algorithm. We found that prior to their sentinel event, the cardiac arrest survivors would have been largely classified in the low-risk group, underlining the need for improvements in risk stratification.

Chapter 4 evaluates the reproducibility of our group's Ventricular Conduction Stability score at the most granular level yet. The reproducibility of each step in the multi-stage methodology is assessed and shows that understanding natural beat-to-beat variability is key in assigning a representative score to a patient. Automated methods are suggested to improve consistency.

Using the lessons in improving reproducibility, Chapter 5 considers patients with structurally normal hearts. Survivors of idiopathic ventricular fibrillation are compared to a range of controls. As well as truly normal hearts, we study patients who survived ischaemic VF but recovered full ventricular function after revascularization. The idiopathic VF survivors, who have not had a curative procedure, are shown to be distinct from the control groups. The beat-to-beat variability is shown to follow a pattern, which is distinct from artefact attributable to exercise induced noise in a simulation study.

Chapter 6 investigates further methods for improving ECGi reproducibility at a more basic level than V-CoS – the original electrograms and the local activation or repolarization times derived from them. Signal averaging, machine learned feature detection and rule-based programming are used as a multi-pronged approach which we show improves reproducibility as more cardiac cycles are considered in the analysis.

Using these novel methods, Chapters 7 and 8 take a detailed look into epicardial electrophysiology of patients with Brugada syndrome and HCM. They are shown to be distinct from controls, and in

the case of HCM the cardiac arrest survivors are differentiable from patients without a personal history of sustained ventricular arrhythmia. Chapter 8 concludes with an examination of ECGi measures as risk stratifiers in HCM and finds that considering multiple variables whether by regression or more modern machine learning methods can improve segregation of cardiac arrest survivors from those without a personal history of lethal arrhythmia.

Chapter 2: Methods

2.1 Patient recruitment and selection

2.1.1 Setting

Recruitment was carried with the assistance of consultant cardiologists at multiple locations across the UK taking care of patients, some with inherited cardiac conditions (ICC). These patients were recruited directly from clinics or by screening from databases of patients by their care team or nominated representatives thereof. The organizations are:

- Imperial College Healthcare NHS Trust
- Barts Health NHS Trust
- Oxford University Hospitals NHS Trust
- West Hertfordshire NHS Trust
- University Hospital of Wales
- St George's University Hospital
- Cambridge University Hospitals NHS Trust
- Basingstoke Hospital.

2.1.2 Patient definitions

Cardiac arrest survivors and other ventricular arrhythmia

Throughout this thesis, patients of various underlying conditions will be classified into those who have never suffered a potentially life-threatening ventricular arrhythmia and those who have not. This is to provide the strongest possible differentiator between the highest and lowest risk patients in any given cohort. Cardiac arrest survivors from multiple conditions are considered the highest risk patients and are recommended unequivocally for secondary prevention implantable cardioverter defibrillators (ICD) (Priori, Blomstrom-Lundqvist et al. 2015; Al-Khatib Sana, Stevenson William et al. 2018).

The following are definitions of terms which will be used in the thesis:

Sudden cardiac arrest survivor/cardiac arrest survivor

This term is used in the thesis as a contraction of 'Arrhythmic sudden cardiac arrest survivor'. The patient must have had a collapse with documented loss of cardiac output, regardless of underlying condition. Although cardiac arrests can have non-arrhythmic origin, only cardiac arrests with

ventricular fibrillation or tachycardia are considered in this thesis. Where a printed rhythm strip is not available, documentation of sustained ventricular arrhythmia in the context of haemodynamic collapse is accepted. In absence of this explicit declaration, the decision by an advanced life support qualified practitioner or automated external defibrillator to deliver an unsynchronized shock during cardiac arrest is accepted. Any cardiac arrest not fitting these criteria is excluded from the classification.

Appropriate therapy survivor

Patients with primary prevention ICDs may suffer sustained, haemodynamically compromising ventricular arrhythmia. Their ICD may deliver anti-tachycardia pacing or unsynchronized shock to terminate the offending rhythm. Patients are included only if the ICD trace demonstrates ventricular tachycardia above a threshold rate, or ventricular fibrillation prior to the delivery of therapy. The therapy must be considered 'appropriate' by an accredited cardiac physiologist or consultant cardiologist. ICD therapies not fitting these criteria are excluded from the classification.

The programming thresholds can vary from patient to patient, adapted to avoid the preconditions for previously experienced 'inappropriate' therapies against more benign rhythms, but patients start off with settings recommended by a global consensus document published in 2015 (Wilkoff, Fauchier et al. 2016). The slowest tachycardias treated are >185 beats per minute in rate and 6-12 seconds in duration, although settings up to >200 beats per minute should be considered especially in young patients or those with concomitant supraventricular tachycardia.

Sudden cardiac death/arrest equivalent

A combination of cardiac arrest and appropriate therapy survival is considered to be a sudden cardiac death, or sudden cardiac arrest equivalent.

Potentially lethal arrhythmia

The potentially lethal arrhythmias are defined to include ventricular fibrillation and ventricular tachycardia with haemodynamic compromise, or fitting criteria for device therapy. Explicitly excluded are rhythms that may result in inappropriate therapy, including but not restricted to (Wilkoff, Fauchier et al. 2016):

- Sinus tachycardia
- Atrial fibrillation/flutter/tachycardia
- Re-entrant supraventricular tachycardia
- Frequent premature ventricular complexes

- T wave oversensing.

Brugada syndrome

The Brugada syndrome is currently diagnosed by the 2013 HRS/EHRA/APHRS expert consensus statement on the diagnosis and management of patients with inherited arrhythmia conditions (Priori, Wilde et al. 2013). The guideline states:

"1. BrS is diagnosed in patients with ST-segment elevation with type I morphology ≥2 mm in ≥1 lead among the right precordial leads V1, V2 positioned in the 2nd, 3rd, or 4th intercostal space occurring either spontaneously or after provocative drug test with intravenous administration of Class I antiarrhythmic drugs.

2. BrS is diagnosed in patients with type 2 or type 3 ST-segment elevation in ≥1 lead among the right precordial leads V1, V2 positioned in the 2nd, 3rd, or 4th intercostal space when a provocative drug test with intravenous administration of Class I antiarrhythmic drugs induces a type I ECG morphology."

The Type 1 morphology is characterized by an elevated J-point and ST-segment in a coved shape, accompanied by T wave inversion. The spontaneous type 1 ECG is defined as this pattern seen at baseline – without aggravating factors such as fever or drugs (Priori, Wilde et al. 2013). The ability to detect this pattern at baseline is enhanced by the use of 10- or 12-lead 24- or 48-hour continuous ECG.

The ajmaline challenge test

At our centre, the drug challenge of choice for diagnosis of Brugada syndrome is the ajmaline challenge. Ajmaline is a class I antiarrhythmic agent – a sodium channel blocker, like flecainide and procainamide. Flecainide and procainamide are also used in Brugada syndrome diagnostic challenges in other centres. Ajmaline has been shown to be able to produce a Type 1 ECG in an equivalent (Probst, Gourraud et al. 2013) or greater number of patients than flecainide (Wolpert, Echternach et al. 2005) or procainamide (Cheung, Mellor et al. 2019). No significant difference was found in the number or severity of complications for each drug. No study to date has been able to conclude whether this disparity in diagnosis is due to over- or underdiagnosis by another drug as the sodium channel blocker test is the gold standard for diagnosis.

Ajmaline has been shown to produce the Type 1 Brugada ECG pattern in up to 27% of patients with atrioventricular nodal re-entrant tachycardia (AVNRT) and even 5% of controls (Hasdemir, Payzin et

al. 2015). The authors of the paper concluded that there was a high coincidence of AVNRT and concealed Brugada syndrome, but even the 5% figure of controls is significantly higher than the widely accepted known prevalence of 1 in 2000 adults (Vutthikraivit, Rattanawong et al. 2018). Whether these patients, and those without other signs or symptoms of Brugada syndrome actually do have a concealed version of the disease is debated (Viskin, Rosso et al. 2015). Furthermore, ajmaline tests confer an immediate risk of sustained ventricular arrhythmia in 2% of patients, which can be refractory in 0.4% (Conte, Sieira et al. 2013).

For this reason, the eligibility criteria at our centre for ajmaline challenge are restricted to (Varnava 2018):

- Patients surviving ventricular fibrillation (VF)
- Patients experiencing unexplained collapse
- A 1st degree adult relative of a patient with confirmed Brugada syndrome
- 1st degree adult relatives of patients suffering unexplained cardiac arrest
- Patients seen and discussed in ICC clinic in whom Brugada syndrome is suspected.

To mitigate the risk of sustained ventricular arrhythmia, the following adult patients are excluded (Varnava 2018):

- Those with myocardial infarction <3 months ago
- Hypertrophic cardiomyopathy
- Left ventricular hypertrophy >15mm
- Bradycardia <50bpm
- 2nd or 3rd degree AV block
- Prolonged corrected QT
- Pregnant
- QRS prolongation >130ms.

During the test, patients are intensively monitored for safety using continuous 15-lead ECG – the additional leads in the upper right precordium.

The test is performed in the supine position. Anti-arrhythmic drugs (and lamotrigine, an anti-epileptic with sodium channel blocking properties) are stopped 48 hours before the test and patients are requested not to eat or drink for 4 hours before the test. As well as the 15 lead ECG, adhesive defibrillation pads are placed in the antero-apical position on the patient's chest. A cut-off

of 1.3x the duration of the baseline QRS is calculated and noted to be used as a termination criterion for the test. 1mg/kg of ajmaline (up to a maximum of 120mg) is infused intravenously over 5 minutes, stopping either when a termination criterion is reached, or the target dose has been administered. During infusion, the QRS duration is evaluated at least every 30 seconds. After the infusion is stopped, the patient and ECG are continuously monitored for pro-arrhythmic adverse reactions until baseline parameters return.

The termination criteria include (Varnava 2018):

- Full target dose of ajmaline administered
- Type 1 Brugada ECG elicited
- Sinus arrest or 2nd/3rd degree atrioventricular block
- Frequent or complex ventricular ectopy
- Sustained ventricular arrhythmia
- QRS duration prolongation of >130%
- Cardiac arrest

Diagnosis of patients from other centres was required to conform to these standards prior to inclusion into our study.

Brugada relatives

At Hammersmith Hospital, the first degree and sometimes second-degree relatives are screened for Brugada syndrome. This begins initially with a consultation at the ICC clinic. The minimum investigative dataset is a 12 lead ECG, high right precordial leads ECG and echocardiogram. As there is a risk of death associated with the diagnostic ajmaline challenge, the decision to undertake this is the result of a discussion between clinician and patient. Amongst the factors aiding this decision is whether it will have implications for the children of the patient, and whether the patient's symptoms could potentially put them into a high-risk group if Brugada syndrome is diagnosed. Increasingly, patients can undergo 10- or 12-lead continuous ECG for 24 or 48 hours which increases the likelihood of a spontaneous type 1 pattern being seen, avoiding the ajmaline challenge.

For the purposes of our study, we decided to only include relatives as control subjects who were asymptomatic, with normal ECG, echocardiogram and had a negative ajmaline test when the full target dose had been administered. Patients who had the test terminated early due to QRS prolongation or arrhythmia were excluded. In addition, patients were excluded if they had incidental

findings of frequent or complex ventricular ectopy, non-sustained ventricular tachycardia or significant co-morbidities such as advanced coronary artery disease.

In short, these patients were the closest we felt we could get to 'normal' hearts, whilst retaining a benefit to the patient of undergoing our testing regime. We believed this gave optimal balance between the research goal of a normal control group and the clinical goal of only applying tests where patients could stand to benefit.

Hypertrophic cardiomyopathy

Hypertrophic cardiomyopathy (HCM) was diagnosed using the European Society of Cardiology guidelines (Authors/Task Force, Elliott et al. 2014). The definition is directly quoted as follows:

"In an adult, HCM is defined by a wall thickness ≥15 mm in one or more LV myocardial segments—as measured by any imaging technique (echocardiography, cardiac magnetic resonance imaging (CMR) or computed tomography (CT))—that is not explained solely by loading conditions.

Genetic and non-genetic disorders can present with lesser degrees of wall thickening (13–14 mm); in these cases, the diagnosis of HCM requires evaluation of other features including family history, non-cardiac symptoms and signs, electrocardiogram (ECG) abnormalities, laboratory tests and multi-modality cardiac imaging."

Diagnoses for our study were either made by echocardiography performed by an accredited sonographer or cardiac magnetic resonance imaging (MRI) reported by a consultant cardiologist or radiologist. Exclusion of conditions that could produce secondary hypertrophy was carried out by detailed assessment in the inherited cardiac conditions clinic. Patients were screened for signs of persistent and severe hypertension, aortic stenosis, features of Anderson-Fabry disease, amyloidosis, mitochondrial and glycogen storage disorders, Danon disease, LEOPARD/Noonan syndrome and Friedreich's ataxia. In addition, alpha-galactosidase enzymatic testing could be performed to rule out Anderson-Fabry disease.

Idiopathic ventricular fibrillation

Patients surviving out of hospital ventricular fibrillation are brought to a cardiology centre, sometimes via the nearest Accident and Emergency resuscitation unit. In general these patients will have undergone monitoring in the ambulance prior to arrival at the recipient unit, and the first investigations they usually undergo are ECG and coronary angiography to rule out ischaemia, the commonest cause of cardiac arrest (Paratz, Rowsell et al. 2020). Blood tests at the time of cardiac

arrest also indicate whether there were electrolyte or thyroid imbalances, and a review of medications or a toxicological screen is carried out to determine if there were pharmacological triggers.

Outside of the immediate resuscitation phase, patients undergo chest X-ray, continuous ECG, echocardiography, cardiac MRI, drug and exercise challenge testing. In some cases, electrophysiological studies or endomyocardial biopsies are performed. If no cause can be identified for cardiac arrest, the patient fits the criteria for idiopathic ventricular fibrillation. ICDs are implanted in almost all patients with a life expectancy of greater than one year.

These individuals are cared for at the inherited cardiac conditions clinic as most of the tests are directed at diagnosing ICCs, to guide screening of relatives. Patients fitting these criteria were recruited from the clinic for testing.

Ischaemic ventricular fibrillation

Coronary artery disease is the commonest cause of sudden cardiac death (Paratz, Rowsell et al. 2020), occurring due to the disruptive effect of ischaemia on normal electrophysiology. Presenting rhythms are often ventricular fibrillation or haemodynamically compromised ventricular tachycardia, which can be treated by effective cardiac compressions and unsynchronized DC shocks from an external defibrillator. To ensure the reduction of future arrhythmia the ischaemic trigger must be removed (Al-Khatib Sana, Stevenson William et al. 2018). Optimal treatment is the immediate revascularization of the affected coronary territories, usually by percutaneous coronary intervention, although thrombolysis and emergency coronary artery bypass grafting can also be used.

According to current guidance, the risk of further arrhythmia is higher when there are remaining coronary lesions, or the left ventricular function is reduced (Al-Khatib Sana, Stevenson William et al. 2018). Greater reductions in left ventricular function are linked to larger infarcts and increased myocardial scarring (Palazzuoli, Beltrami et al. 2015), scar being the substrate for ventricular arrhythmia (Coronel, Baartscheer et al. 2001). Currently, patients are deemed to have sufficient risk to justify implantation of an ICD when they have a left ventricular ejection fraction (LVEF) below <40%, although the exact figure is dependent on the source of the guidelines.

The American Heart Association/American College of Cardiology/Heart Rhythm Society guidelines (Al-Khatib Sana, Stevenson William et al. 2018) state that primary prevention patients without symptoms require LVEF <30%, those with New York Heart Association (NYHA) symptom score II or III requiring <35%, and those with LVEF <40% requiring inducible ventricular tachyarrhythmia to qualify

for an ICD. Secondary prevention patients require LVEF <35% to qualify for an ICD unless they have inducible ventricular arrhythmia on programmed stimulation. The European Society of Cardiology guidelines from 2015 (Priori, Blomstrom-Lundqvist et al. 2015) recommend evaluation of LVEF 6-12 weeks following infarction; if the patient has LVEF <35% and symptoms greater than NYHA symptom score I they should receive an ICD. If the ventricular arrhythmia has a reversible cause (ischaemia treatable by revascularization), there is no immediate mandate for ICD implantation.

Based on the above guidelines, patients suffering ischaemic ventricular fibrillation who are successfully treated and found to have normal left ventricular function (including no regional wall motion abnormalities detectable on echocardiography) are not offered ICDs. These patients were recruited by screening the local IBM Cognos database of patients presenting in ventricular fibrillation to the cardiac catheter laboratory. Patients with reduced LV function or regional wall motion abnormalities were excluded, as well as those suffering ongoing symptoms, or reduced exercise tolerance.

These patients were selected to provide a control group that had suffered previous ventricular arrhythmia but were no longer thought to be at elevated risk of sudden cardiac arrest.

Benign ventricular ectopy

Ventricular ectopy in the context of a structurally normal heart is thought to be benign in terms of mortality, but significant morbidity can be conferred in terms of symptoms and in a limited number of patients, a high ectopic beat burden may lead to cardiomyopathy (Ng 2006). In the absence of structural heart disease or previous documented tachyarrhythmia, neither the American nor European guidelines suggest ICD implantation for this condition (Priori, Blomstrom-Lundqvist et al. 2015; Al-Khatib Sana, Stevenson William et al. 2018).

Frequent ventricular ectopy can be targeted using traditional mapping using a digital cardiographer, as well as newer 3D mapping techniques (Pruszkowska-Skrzep, Kalarus et al. 2005). Invasive mapping techniques are widely used, but rely on the clinically relevant ectopic beat manifesting during the procedure. In cases where ectopic beats are rare or have triggers not easily replicated in the catheter lab, pre-procedural ECG imaging (ECGi) is a viable adjunct. In a study of 24 patients, all ventricular ectopics were correctly localized compared to intracardiac mapping, and ablation partly guided by ECGi led to medium term success reducing ectopy burden in 22 of 24 patients (Jamil-Copley, Bokan et al. 2014).

For this reason, ECGi assisted ablation of ventricular ectopy is offered at our centre. Patients offered this procedure were screened for entry into our study as a control group. Exclusion criteria include:

- Structural heart disease diagnosed either by echocardiography or cardiac MRI
- Known channelopathy
- Previous documented ventricular fibrillation or haemodynamically unstable ventricular tachycardia.

2.2 Ethical approval

This combined study was composed of the patient volunteers from two ethically approved research studies: "Predicting Risk Using Ecvue: Detection Of Activation Changes During Physiological Stress That Indicate A Critical Substrate For Ventricular Fibrillation" (PREDICT-VF: 14/LO/1318) and "Feasibility Of Improving Risk Stratification In Brugada Syndrome" (FIRST-BrS: 17/LO/1660). Both studies were approved on the local level by the Fulham Research Ethics Committee and on national level by the Health Research Authority, as well as receiving research and development approvals at local centres if database screening was required.

2.3 Summary of volunteer journey

Prior to the detail of the methods, an overview of the process undertaken by our patient volunteers is provided below and summarized in Figure 2.1.

Following recommendation of a patient from clinic or a database, contact details for the patient were obtained by, or under direct supervision of a care team member already authorized to access this patient's data. If this care team member was not already a study investigator, the patient was contacted directly by a study investigator to confirm their willingness to continue communications and receive further information about the study. If this was agreed, the patient volunteer was sent a patient information sheet for review. A Brugada syndrome specific patient information sheet is provided in Appendix A and a general conditions information sheet in Appendix B – there were further individualized documents for other medical conditions and healthy controls.

Volunteers were allowed unlimited time to review the documentation before deciding if they would proceed with the study. Additionally, contact details were provided for the volunteers to call or email the study investigators at any time with questions and concerns about their testing. In cases

where a clinical decision was required, the referring clinician was involved in the discussion with patient and study team.

The study visit consisted of a half-day at the Hammersmith Hospital. Volunteers were consented for the study procedures either on the day or prior to the study visit; this was documented in writing. An example consent form is provided in Appendix C.

At this point volunteers were prepared and fitted with the electrocardiographic imaging (ECGi) equipment. Recordings were taken throughout a maximal Bruce protocol exercise test and then into 10 minutes of supine recovery. Following full recovery, the volunteers underwent low dose computerized tomography (CT) of the chest. A 3D anatomical mesh was derived from the CT images and used in the reconstruction of electrograms using the ECGi workstation. Following the reconstruction, individual volunteer Ventricular Conduction Stability (V-CoS) scores were calculated from 10 consecutive peak exercise and 10 consecutive full recovery cardiac cycles to determine absolute scores and variability.

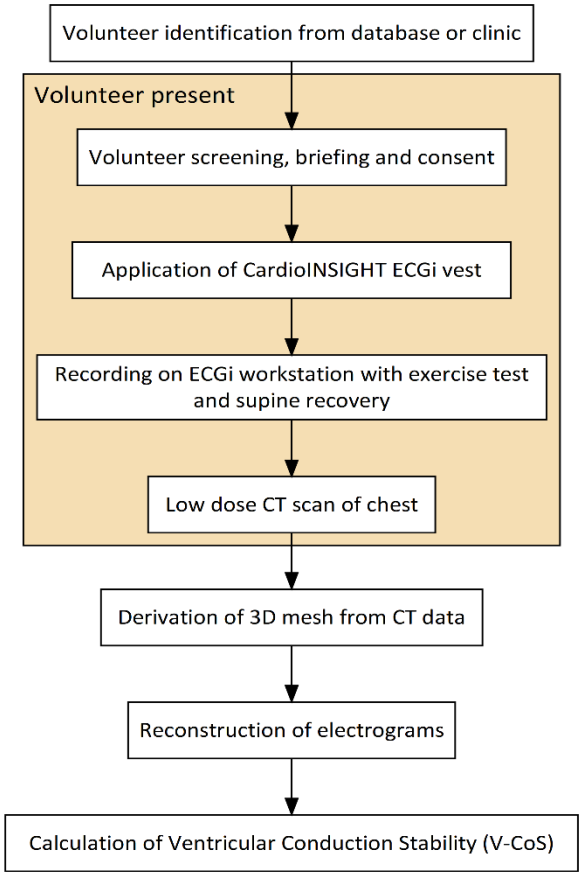

Figure 2.1: Summary of the patient volunteer's journey in the study

2.4 Electrocardiographic imaging

2.4.1 Selection of an ECGi system

Electrocardiographic imaging is the 3D reconstruction of myocardial electrical properties from body surface electrical recordings and cross-sectional imaging. At the time of writing there are three systems available for mapping, two of which were available for our use at the conception of this project.

The latest system uses a 12-lead ECG combined with an MRI derived volumetric mesh of the heart; it is termed Cardiac Isochrone Positioning System (CIPS-ECGi). The technique was first reported in 2013 (van Dam, Tung et al. 2013) as a collaboration between University Medical Center Nijmegen (the Netherlands) and University of California Los Angeles (USA), and was CE marked in 2018. In contrast to the other two systems, CIPS-ECGi uses an 'Equivalent Double Layer' (EDL) model to perform visualization. At the forefront of the depolarizing wave, a dipole layer is present – the separation between positively and negatively charged elements. The nature of this source can be determined by the external signals it produces and allows determination of the point at which depolarization reaches both the endo- and epicardium (although intramural elements cannot be resolved) (Huiskamp and Van Oosterom 1988). The body geometry is constructed from cardiac MRI (van Dam, Oostendorp et al. 2009). This version is not used in clinical practice at present and was not available to us at the conception of the project.

Various ECGi systems stemming from the original Rudy design exist, mostly used in research, with one for commercial applications. The research systems are widely spread over the world, but are not available as a stand-alone device to most end-users. CE marks are awarded to individual pieces of equipment in the system such as the BioSemi digital recording system (Amsterdam, the Netherlands), the electrode strips manually arranged on the patient torso, or the MRI scanner used at the point of care. Relatively few centres worldwide perform the inverse solution – which can be highly customized from project to project, but by the same token vary in methods between papers coming even from similar authors (Vijayakumar, Silva et al. 2014; Zhang, Sacher et al. 2015; Andrews, Srinivasan et al. 2017; Zhang, Hocini et al. 2017). These systems work based on the relationship between epicardial potentials and body surface potentials expressed through a linear system of equations (Ramanathan, Ghanem et al. 2004). Reversing the resultant transfer matrix with regularization allows the reconstruction of epicardial potentials from the known body surface potentials from the recorder.

The only commercially available ECGi system available at the beginning of this project was the CardioINSIGHT™ system (Minneapolis, USA). Acquired from start-up company ECVUE in 2015, the CardioINSIGHT™ system is part of the family of original Rudy design. This system is available for clinical use worldwide. A computer workstation unit is provided which performs the inverse solution with input from the end-user. Single-use vests of 252 electrodes are used to collect the body surface potentials used in the calculation. The geometry is derived from a low-dose CT scan of the chest (1.5 milliSieverts) without contrast. Table 2.1 summarizes the currently available solutions.

Table 2.1: Currently available ECG imaging solutions.

	CIPS-ECGi	CardioINSIGHT	Research systems
Model surfaces	Endocardial Epicardial	Epicardial	Epicardial
Imaging	MRI	CT	MRI
Body surface electrodes	9	252	64-256
Regulatory approval	Yes (CE mark 2018)	Yes (CE mark 2011)	CE mark via constituent parts: BioSemi recording system, MRI machine

The CardioINSIGHT™ system was selected because it was commercially available in a standard format to multiple users worldwide. We felt that using an existing clinically deployed product would give the most realistic assessment of the feasibility of ECGi to improve risk stratification in the ICC.

2.4.2 Practical usage of the CardioINSIGHT ECGi system

Version

We primarily used the v3.1 CardioINSIGHT workstation to record and analyse our cases. If any studies were performed using the other versions delivered to our centre (v1.1 and v3.5), these were transferred to the v3.1 workstation before final analysis to improve standardization.

Components of the system

Figure 2.2 summarizes the components and connectivity of each component in the CardioINSIGHT system. Power is supplied via a transformer and transmitted to a desktop computer, monitor and

mapping amplifier. This workstation is housed on a portable trolley. The sensor arrays are connected to the mapping amplifier by custom serial buses and signal cables, before the data is relayed by ethernet cable to the computer workstation for processing and display. A mouse and keyboard are connected to the workstation for operator interfacing.

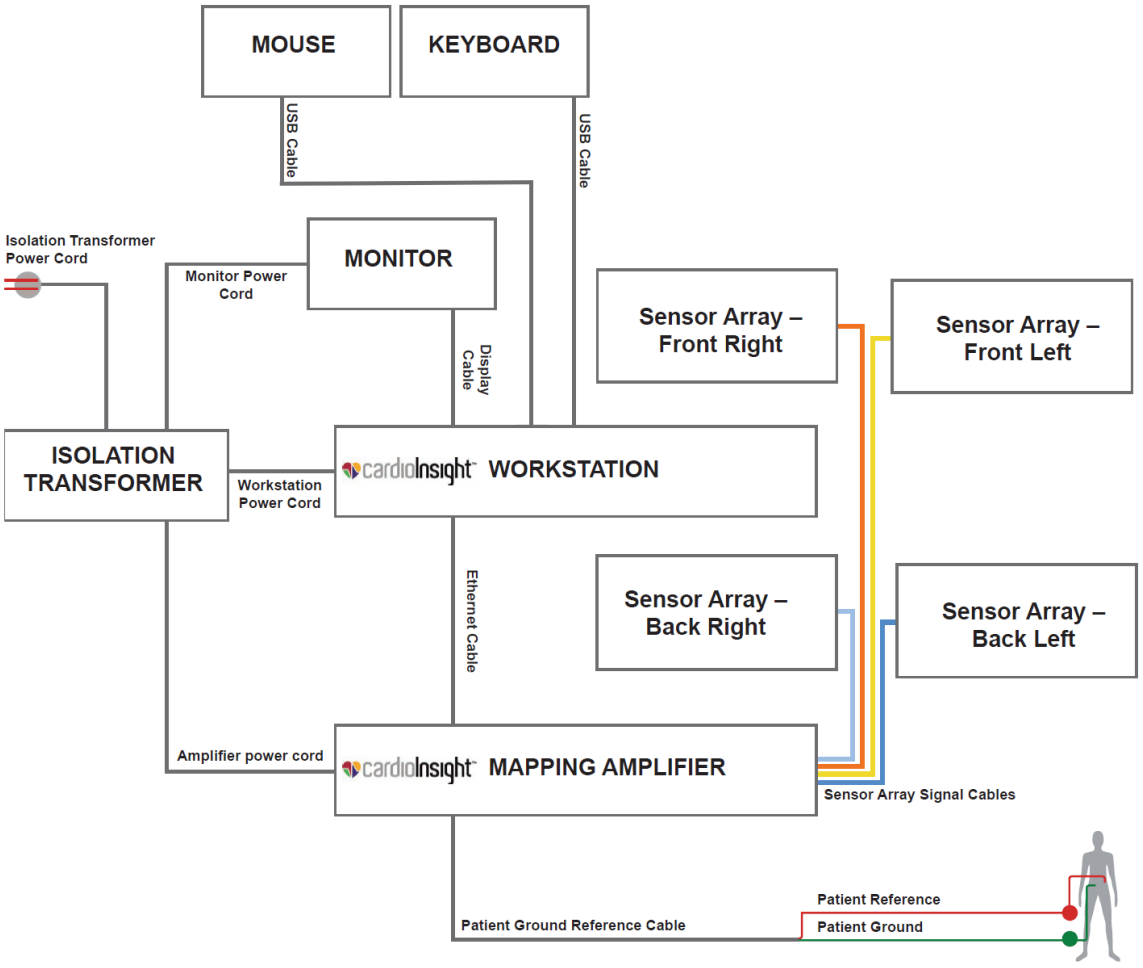

Figure 2.2: Systems diagram of CardioINSIGHT™ components. Modified by the author of this thesis from a figure in the CardioINSIGHT™ manual with kind permission of Medtronic, USA. Original documentation lists extra components and mouse/keyboard connections via USB to the monitor, not present in our setup.

Sensor array – applying the 'vest'

Body surface potentials are recorded by a custom-made 252-electrode vest pre-impregnated with transducing gel and a mild skin adhesive (Figure 2.3). Each panel is connected to the mapping amplifier by a custom serial bus and signal cable.

Optimization of contact is essential for a good recording. Prior to application, the correct size must be selected according to a sizing chart provided with the workstation (Appendix D, which is kindly contributed by Medtronic, USA). Currently only sizes 2 and 3 are imported to the United Kingdom, a limitation for some of our smaller and larger volunteers.

Volunteers underwent torso hair removal, and a mild cleaning soap was applied using paper towels before being thoroughly cleaned off with dry paper towels. The vest was applied in the standing rather than supine position to optimise consistent contact during the exercise test, contradictory to the recommendation in the official manual. Although the most relevant recordings are taking during supine recovery, the stability of the vest during the treadmill test was judged to be important due to the potential for large portions of the vest to become detached at higher running intensities.

Frontal arrays were placed with the sternum as the horizontal reference and the left clavicle as the vertical reference. Electrodes 66 and 67 were aligned with the left clavicle, whilst the medial edges of the two frontal arrays met in the midline (Figure 2.3). The rear array was placed with the nape of the neck as the vertical reference and the spine as the horizontal reference. The midline of the rear array was taken to be the line of electrodes containing electrode 192.

To improve vest stability, Transpore™ hypoallergenic medical tape (3M, Minnesota, USA) was used to secure sensor vest arrays to each other and also to the skin of the patient.

Figure 2.3: Marketing image of CardioINSIGHT™ sensor vest, reproduced by kind permission of Medtronic, USA. This image shows the front two arrays clearly. A back panel is also included in the package. The panels connect to the amplifier via four custom serial buses.

Performing an ECGi recording

Prior to recording, the workstation is powered on, including the mapping amplifier. A medical-grade filtered mains power socket was used for all recordings in this study.

The sensor vest arrays are individually linked to the mapping amplifier by their individual bus connections and cables. In addition, a set of reference electrodes are needed, which are placed 5-10cm either side of the midline on the volunteer's abdomen below the vest. Ambu® BlueSensor R electrodes (Copenhagen, DK) were preferred, although in some cases Ambu® WhiteSensor 4xxx series electrodes were used dependent on stock in the hospital department. These are also connected to the mapping amplifier by a custom cable.

Patient identifiers were inputted to the workstation which remained in a secure National Health Service (NHS) hospital throughout the study.

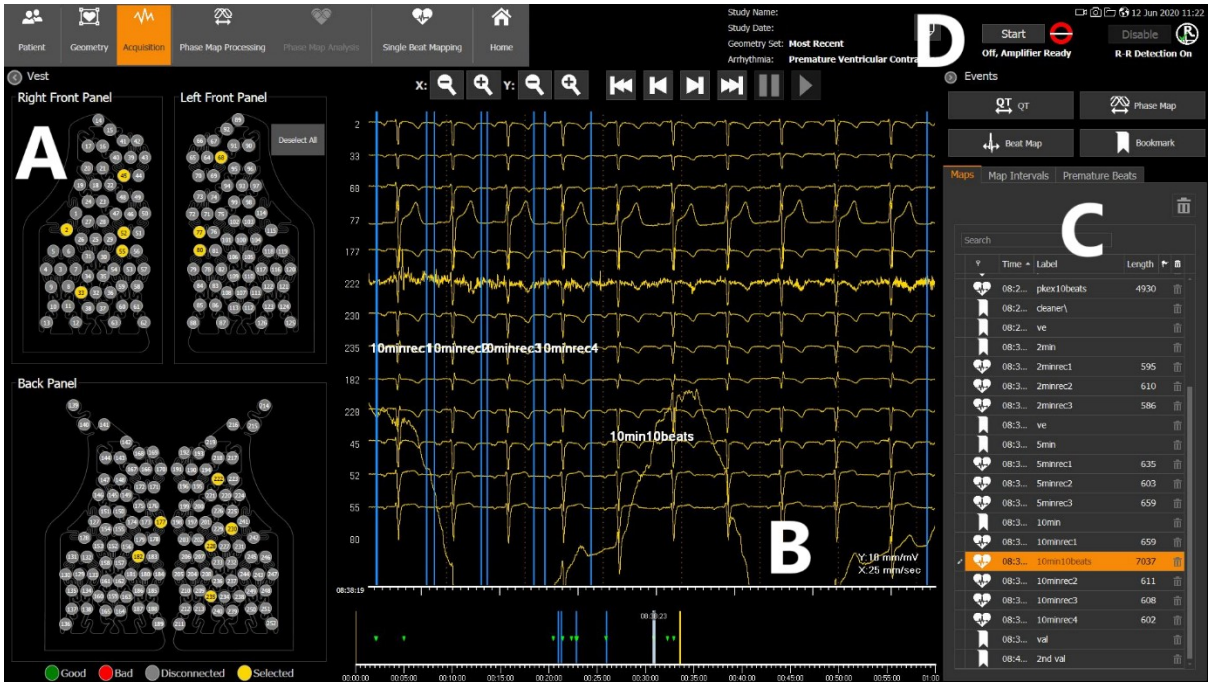

Figure 2.4: Image of ECG acquisition screen in CardioINSIGHT™. Panel A is the sensor array status, Panel B is the signal review screen, Panel C holds bookmarks and beats for evaluation and button D 'Start' controls the recording.

Figure 2.4 demonstrates the recording screen used for signal acquisition. In panel A, contact is evaluated by the workstation based on CardioINSIGHT's proprietary 'Automatic Bad Channel Detection' (ABCD) algorithm. Electrode colour denotes signal status as indicated by the key at the bottom of panel A. Optimization of vest placement by applying pressure or additional tape for improved adhesion is performed at this point. Inspection of the recorded signals can be performed in panel B, whilst bookmarks and heart beats can be marked in panel C. The recording is started and stopped by button D.

Bookmarks are highly useful for marking areas for future processing in subsequent sections of this Methods chapter, such as the point of peak exertion, the minutes following this and any ectopic beats or arrhythmias that may occur.

Performing the CT scan

As per company recommendations, CardioINSIGHT CT scan protocols met the following requirements:

- 250 milliamperage second
- 120 peak kilovoltage (80kV minimum requirement)
- 0.6 mm slice thickness (3mm minimum requirement)

- 1.5 recon increment (overlap)
- 64 slice minimum

All scans were undertaken on a Siemens SOMATOM Definition AS CT scanner.

Volunteers underwent repeat identity confirmation and declaration of non-pregnancy as per radiology department protocols. Field of view was defined as from the lower mandible to the inferior edge of the vest, which was marked out by a metal paperclip to assist identification on initial scan. Volunteers were scanned in the supine position, with arms down by their sides, and slightly spaced from the torso to ensure that automatic segmentation of the arms did not remove electrodes from the vest. Ideal positioning is demonstrated by the photograph in Figure 2.5. An estimated 1.5 milliSieverts is received by each volunteer during this scan. No radiopaque contrast is required.

Figure 2.5: Optimal body positioning of a volunteer for the computerized tomograph. Photograph taken by thesis author on request of the pictured volunteer, and kindly provided for use by that volunteer.

Following the CT scan, approximately 300 images axial images are saved for use in segmentation.

Constructing the 3D mesh

Whilst the segmentation method and its variants have not been studied in depth, the following method is inspired by a combination of their experience and that of operators they have worked

with throughout Europe. Based on clinical experience with the system at our centre, our study method is a modification and standardization of those who used the system before us.

CT scan images are transferred to the CardioINSIGHT workstation where they are processed by proprietary segmentation software (CISH). The result is an OpenGL compatible anatomic mesh of between 1000-3000 points for use with the inverse solution. Automatic segmentation is available but fails inconsistently between subjects in our anecdotal experience. For standardization reasons a predominantly manual segmentation approach was used for all volunteers in this study.

Couch and torso segmentation was allowed to progress automatically as failure had not occurred to date in our anecdotal experience. At this point CISH suggests the position of the electrodes which are checked by the operator. Missing electrodes are added, and suggestions which do not correspond to a true electrode are removed. The numbering of the electrodes is checked over the surface of the vest (Figure 2.6).

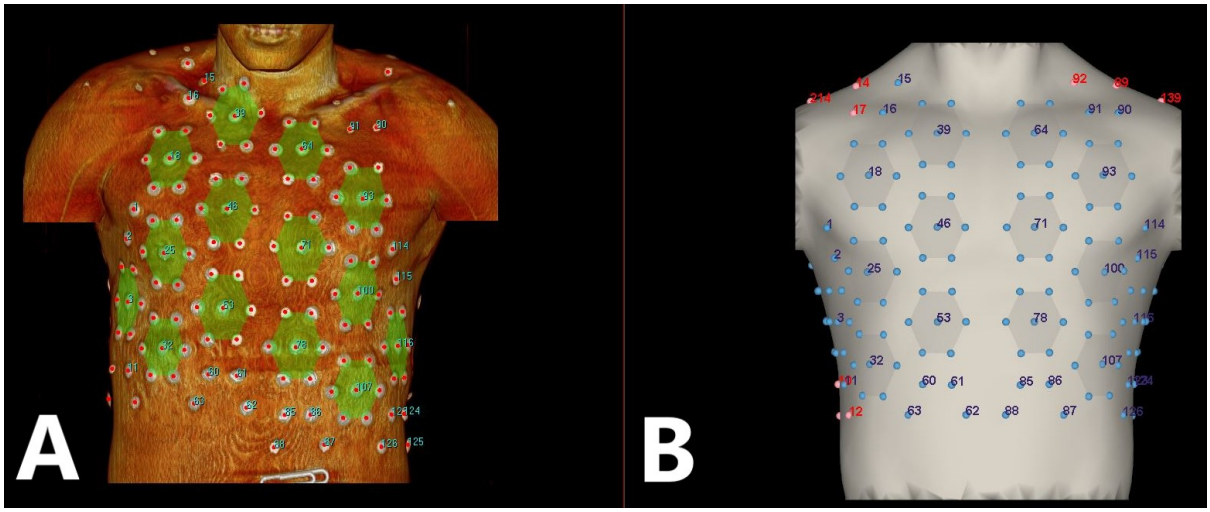

Figure 2.6: CISH segmentation of the electrodes. Panel A demonstrates the 3D reconstruction of the CT scan with annotations for electrodes, whilst Panel B demonstrates all the expected electrodes from a vest.

For processing of ventricular maps, we required the shape of the ventricles, 2D positions of the tricuspid and mitral valves for electrogram exclusion, and a midline septum marker for which we used the left anterior descending coronary artery as a surrogate. Moving through the CT images from cranial to caudal, the branching of the pulmonary trunk is identified. Using a 'volume-of-interest' marking tool, a 2D section of the pulmonary trunk is drawn at this level (Figure 2.7), before continuing caudally. Serial 2D sections are drawn on the axial images, down the right ventricular outflow tract and incorporating the left ventricular summit when it appears. From this point, the

ventricles are drawn together, down to the apex of the heart. Approximately ten 2D sections were drawn from pulmonary trunk to apex, although this number could vary depending on individual volunteer anatomy. Using a similar approach, the aorta and left ventricular outflow tract were designated in 2D sections from the level of the pulmonary trunk branching down to the merging area with the already drawn left ventricle. Due to the epicardial only nature of the system, the ventricular septum is not segmented separately. CISH automatically interpolates between the user defined 2D sections to build the ventricular mesh (Figure 2.8).

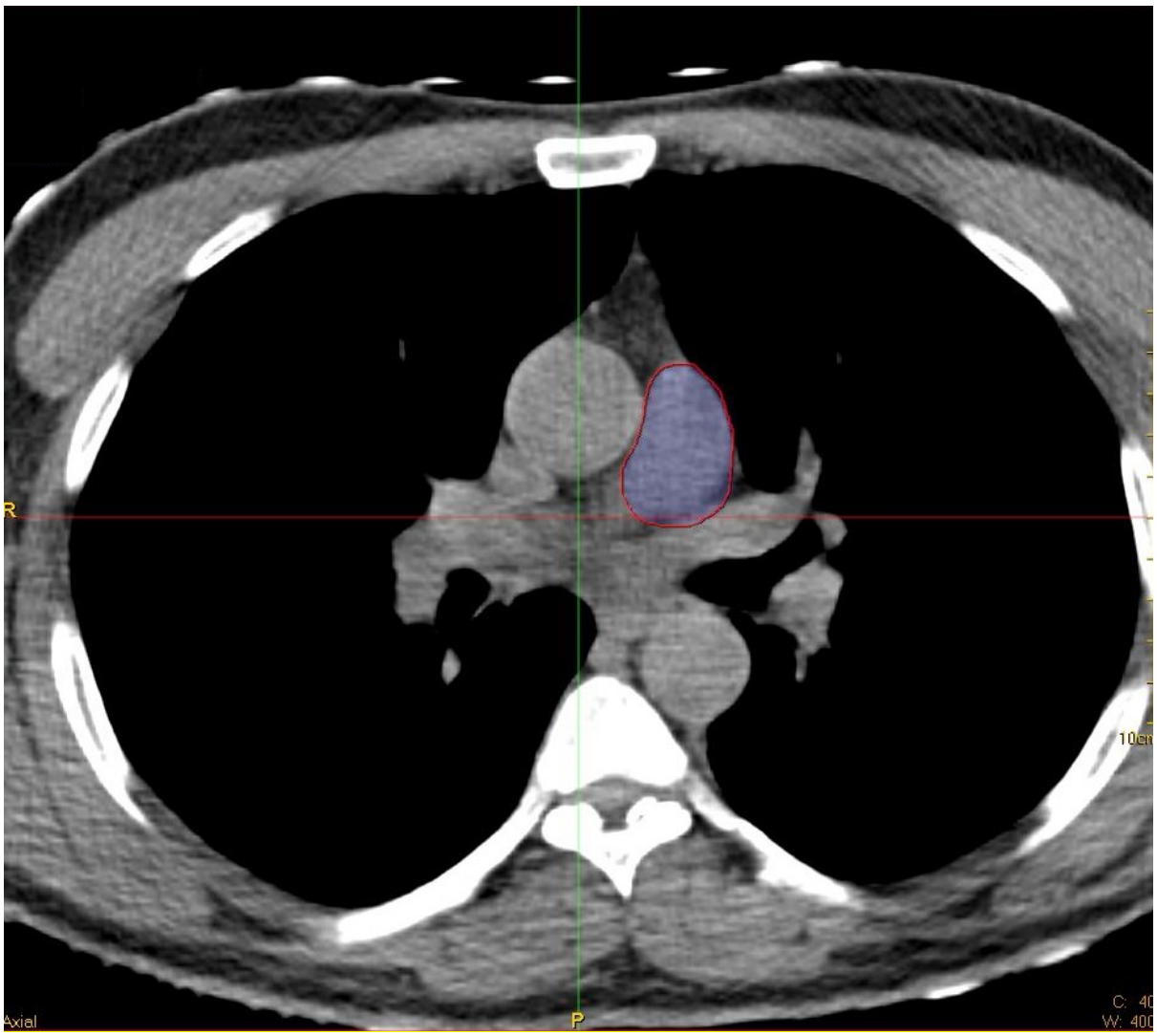

Figure 2.7: Two-dimensional section of the pulmonary trunk selected by the user. A series of these two-dimensional sections through the heart are interpolated to form the final mesh.

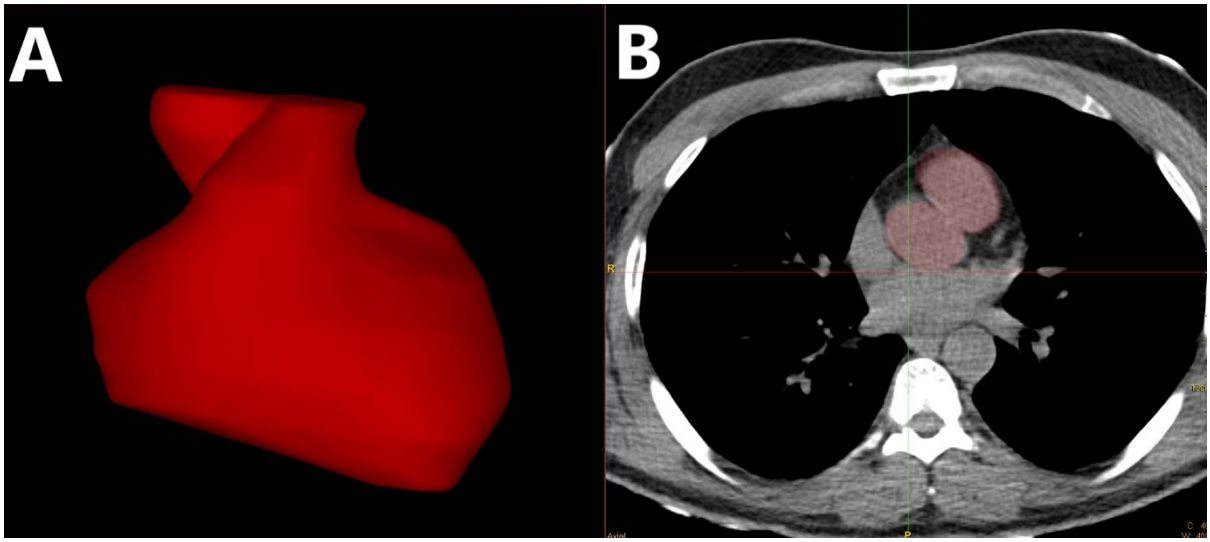

Figure 2.8: Manual segmentation of the ventricles and great vessels. Panel A shows the mesh before manual trimming of hard edges and spikes. Panel B demonstrates axial CT images with red highlighted sections that have been manually incorporated into the mesh shown in Panel A.

Hard steps and spikes can often form during the interpolation of the 2D sections. These are manually removed for two theoretical reasons: (I) sharp spikes and steps are not usually a feature of cardiac anatomy; (II) presence of hard edges and singularities may distort the distribution of activation and repolarization times across the cardiac surface (Figure 2.9).

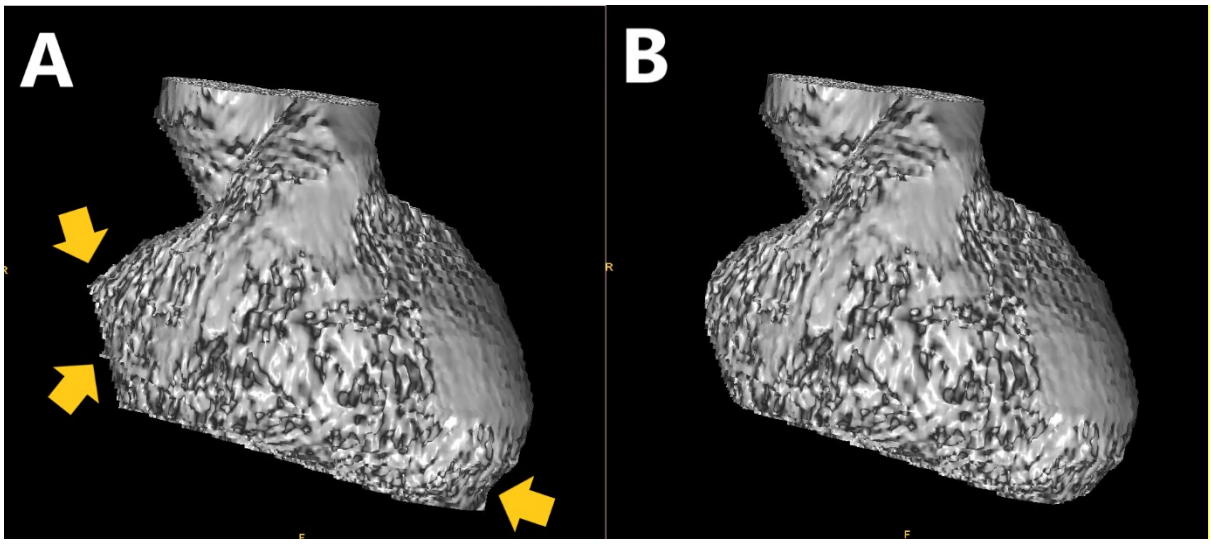

Figure 2.9: Panel A demonstrates steps and spikes in the mesh, indicated by the arrows. Panel B demonstrates the mesh once these have been manually removed.

Following successful construction of the ventricular mesh, areas corresponding to the tricuspid and mitral valves are painted onto the annular surfaces by cross referencing the already created mesh

with the axial images (Figure 2.10). The great vessels are trimmed down to avoid erroneous assignment of electrograms to non-electrically active tissue, but with enough length left on to assist in localisation of electrograms when the final maps are reviewed. Finally, the left anterior descending artery is drawn by connecting points on the axial images starting at the ostium (cranial). If the LAD is not clearly seen in the more caudal slices, the approximate apex of the heart is used as the final reference point (Figure 2.11).

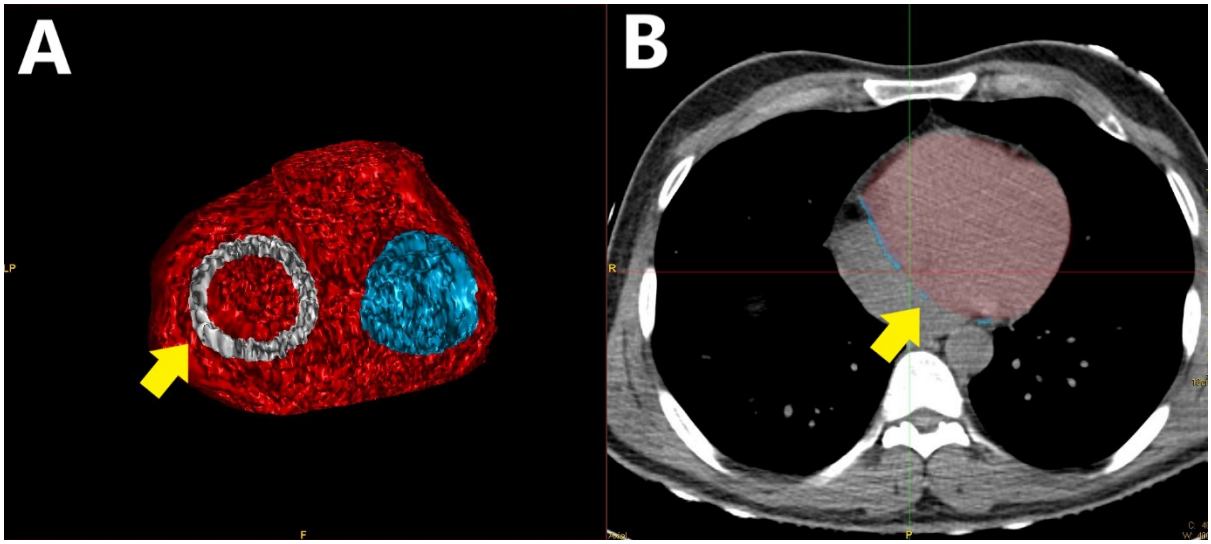

Figure 2.10: Adding the valves onto the 3D mesh of the ventricles. Valve shapes are 'painted' onto the ventricular mesh in Panel A; the arrow denotes the current valve being painted, whilst the blue circle immediately to the right of the screen is a completed valve. The area painted in Panel A appears automatically as a blue selection in Panel B, where the position can be cross-referenced to the axial images, prompting the user to adjust the selection if necessary; the arrow denotes the current valve being painted, whereas the blue line to the top left of the arrow is a completed valve.

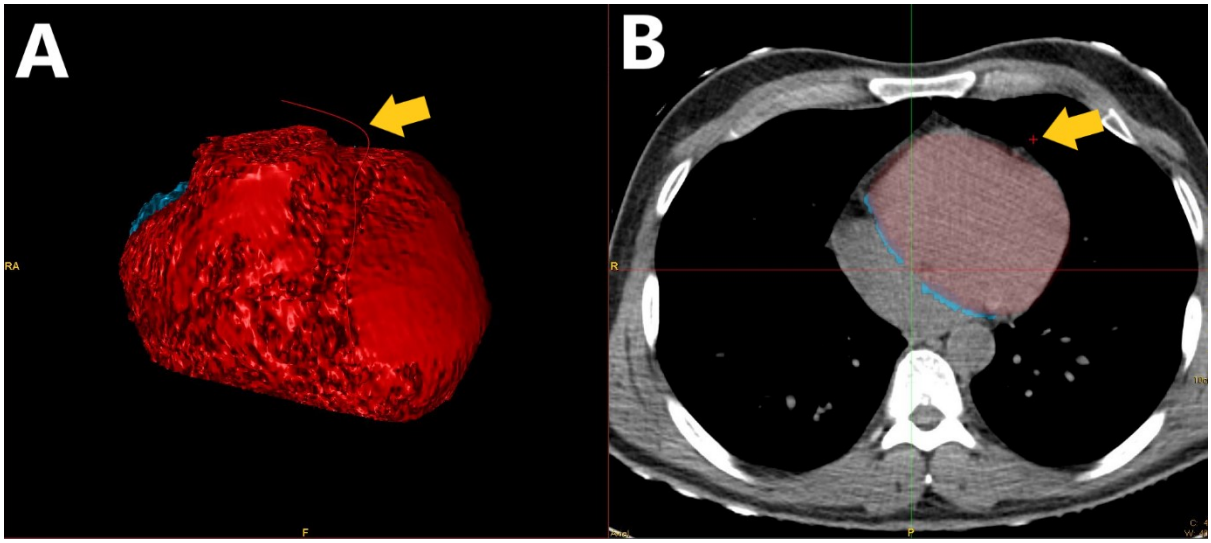

Figure 2.11: Addition of the left anterior descending coronary artery to the mesh. Points outside the mesh close to the path of the left anterior descending coronary artery are marked in axial slices with a cross (indicated by arrow). In Panel A, the results of the selection in Panel B can be seen in 3D space; the red line path is indicated by the arrow.

The ventricular mesh is saved by CISH for use with the main CardioINSIGHT™ programme, which uses the geometric information in the inverse solution.

Performing the inverse solution

The steps in performing the inverse solution on CardioINSIGHT™ can be summarized as:

1. Selecting the beat, or beats
2. Deselection of noisy body surface signals and re-selection of clean body surface signals erroneously deselected by the automated 'ABCD' system (see 'Performing an ECGi recording')
3. Initiating inverse solution.

Steps 1 and 2 are user driven, with the aim of providing the largest amount of clean data to the inverse solution in step 3 to ensure accurate reconstructed electrograms. There are no current objective criteria for electrogram deselection, decisions being subjective to expert opinion and the individual operator. Two main points must be considered during selection:

1. Electrogram parameters are measured in the first differential of the voltage-time graph, so signals with steep artefactual deflections must be excluded
2. Heavy filtering in post-processing can change electrogram characteristics (Bear, Dogrusoz et al. 2018), so signals with large amplitude deviations of any frequency should be strongly

considered for exclusion. The density of electrograms produced and the negative effects of filtering on accuracy compared to ground truth is also the reason why noisy body surface signal deselection is preferred over heavy signal processing.

Beat(s) selection is undertaken as close to the timepoint of interest as possible – for example peak exertion, full recovery, et cetera. If large amounts of artefact are present, subsequent beat(s) may be selected in place of the exact beat of interest. The allowable delay before selection depends on the nature of the beat of interest – for example the effects of exercise may be present minutes following peak exertion (Cole, Blackstone et al. 1999), but a single ectopic beat cannot be substituted by subsequent sinus beats. An example of body surface signals fitting the artefact descriptions above is demonstrated in Figure 2.12.

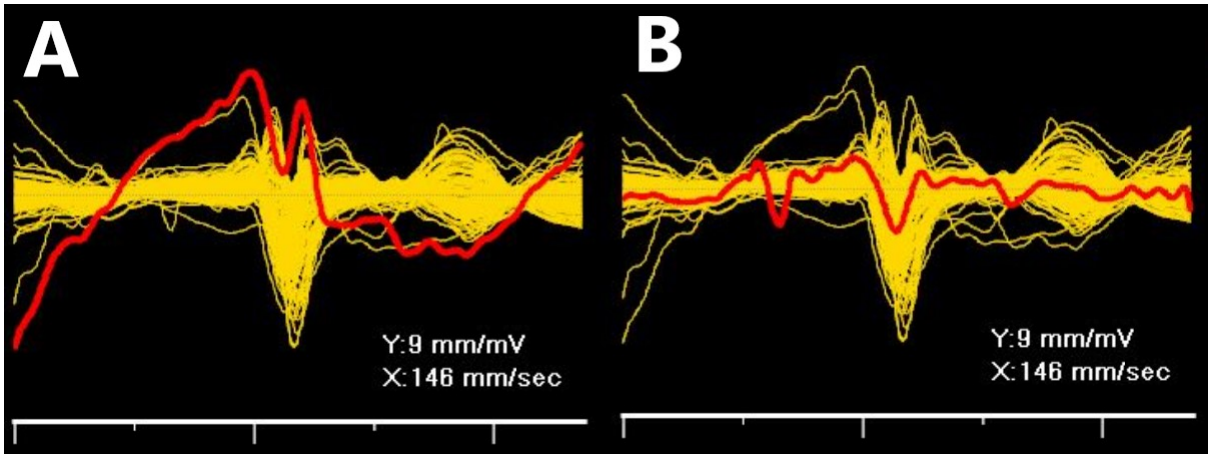

Figure 2.12: Body surface signals removed from processing due to high levels of artefact. Panel A demonstrates high amplitude baseline shift, whilst Panel B demonstrates high frequency noise.

Once the body surface signals suitable for use have been selected, the inverse solution is performed by the CardioINSIGHT™ workstation and saved onto the hard drive.

Extracting reconstructed data for post-processing

The required files can be extracted from the hard drive of the CardioINSIGHT™ workstation for further post-processing in our custom written software. The following files were saved under a file system recording the pseudonymized study number of the volunteer and the type of beat being saved:

- Body surface signal file (.ECGDATA extensions)
- Reconstructed epicardial potentials file (.POTENTIAL extensions)
- Ventricular mesh (.HEART, .TORSO, .VALVE and .LANDMARK extensions)

These pseudonymized data were then transferred to a research computer for further processing.

2.5 Exercise testing to supine rest

Methods of physiological assessment during exercise have been known since the 1700s (Beltz, Gibson et al. 2016). Robert Bruce (Washington, USA) invented the most commonly used standardized protocol in 1963 (Bruce, Blackmon et al. 1963). To ensure standardization between subjects and tests we opted to use this Bruce protocol for all exercise tests. The steps are listed in Table 2.2 (Vilcant and Zeltser 2020).

Table 2.2: Bruce protocol table, adapted from Vilcant et al. (2020) (Vilcant and Zeltser 2020)

Stage	Minutes	Gradient (%)	Pace (min/km)
1	3	10	22:13
2	3	12	15:00
3	3	14	10:55
4	3	16	8:49
5	3	18	7:30
6	3	20	6:44
7	3	22	6:11

Equivalent testing regimes exist for various types of exercise such as the running treadmill, bicycle and hand-crank ergometer (Mitropoulos, Gumber et al. 2017). To maximize physiological stress, we opted for upright treadmill testing as it is the modality shown to cause the greatest heart rate response (Abiodun, Balogun et al. 2015; Mitropoulos, Gumber et al. 2017). This was chosen over and above bike stress testing to elicit the strongest response. ECGi measurements are uniquely sensitive to movement in the torso and bike stress was felt to have insufficient benefits in ECG noise reduction to offset the reduction in maximal heart rate response as described in previous literature.

During ECGi recording, volunteers undertook the Bruce protocol to maximal exertion. Exercise testing was supervised by at least one Advanced Life Support qualified professional (certification by the Resuscitation Council UK).

Rate limiting cardiac medications were paused 48 hours prior to the test. Volunteers were encouraged to report symptoms if present at any point during the test as an indication for termination. Volunteers were allowed to exercise 1 minute after reaching target heart rate, or to

maximal exertion. Volunteers were required to reach at least 85% of predicted maximum heart rate using the formula $200 - Age$ to qualify for the study.

The following termination criteria were used:

- Onset of central chest pain, breathlessness out of keeping with the grade of exercise, pre-syncope, or palpitations
- Muscular fatigue/symptoms limiting continued exercise on treadmill
- Repetitive ventricular ectopy (e.g. bigeminy, trigeminy) or ventricular rhythms lasting >5 consecutive beats at any rate
- Any evidence of ST elevation or depression
- Volunteer preference.

These criteria were deliberately stricter than for the general population guidelines (Gibbons Raymond, Balady Gary et al. 1997) because:

- Our cohort could be considered higher risk than the general population for cardiac events
- ECG monitoring could be compromised by the placement of the ECGi recording vest
- Due to the operator monitoring the ECGi machine at the same time as the exercise machine, fewer blood pressure measurements could be made easily. To mitigate, patients underwent an individualized risk assessment by the responsible consultant prior to participation in the study.

Immediately following test termination, the volunteer was guided back to a couch to lie supine for 10 minutes. The majority of ECGi measurements were made in this period from peak exercise to full recovery. Baseline periods were defined as post exercise to reduce the chance that the vest electrodes had moved between comparison cardiac cycles, potentially causing differences in the ECGi reconstruction. The Ventricular Conduction Stability metric (further described in 2.6.1) is highly sensitive to small changes in cardiac conduction and therefore all measures to reduce inadvertent errors in electrogram reconstruction must be avoided. This comes at the expense of the post-exercise recovery period not being a 'true baseline' period, although the pre-exercise period may also not be a true baseline measurement as the patient is in an unfamiliar environment and has the mental anticipation of the upcoming exercise test which may alter autonomic tone.

2.6 Calculation of Ventricular Conduction Stability related metrics

Files pertaining to the cardiac cycles of interest were saved to a file system catalogued to a pseudonymized database, used by our custom software for retrieval of specific cardiac cycles from specific volunteers.

2.6.1 Ventricular conduction stability (V-CoS) calculation

First described in 2019 (Shun-Shin, Leong et al. 2019), V-CoS is briefly described as the percentage concordance in local activation times across the ventricles when two cardiac cycles are compared. The threshold for discordance is 10 milliseconds, and in general, the measurement is used to compare a reference cardiac cycle (for example at full recovery) with a test cardiac cycle (for example at maximum stress, or in this case peak exercise). Lower V-CoS scores indicate more discordance in activation patterns across the ventricles. The authors hypothesized that this inducible heterogeneity could form the basis for an arrhythmic substrate.

V-CoS is currently written in Python 3.x and is delivered using a Qt for Python (PyQT5) graphical user interface (GUI). Electrograms from the test and reference beats are paired based on their known locations in the epicardial geometry files. As a further failsafe for correct matching, cross-correlation was employed to check the matching in morphology between paired electrograms. Smoothing is performed by a Savitzky-Golay filter (Savitzky and Golay 1964) prior to further calculation. Local activation time (LAT) was calculated for each electrogram by determining the steepest negative slope in the electrogram QRS complex, i.e. $argmax(-\frac{dV}{dt})$.

The local activation times in each electrogram pair are subtracted. V-CoS is the percentage of these pair differences which is <10 milliseconds.

To assist in visualisation, a fiducial point was formed around the median pair difference by subtracting this median time from all pairs across the epicardium. Differences shorter than the median (negative times) were encoded blue and differences longer than the median were encoded red with increasing intensity. The pair differences were then plotted in two dimensions using a McBryde-Thomas flat polar quartic projection (Snyder 1997) using the left anterior descending coronary artery as the prime meridian. Three-dimensional representations were generated by projecting the results onto the known geometry. Figure 2.13 is a reproduction of data from one of the original patients tested by the V-CoS software, demonstrating the comparison of two activation maps to form a V-CoS map.

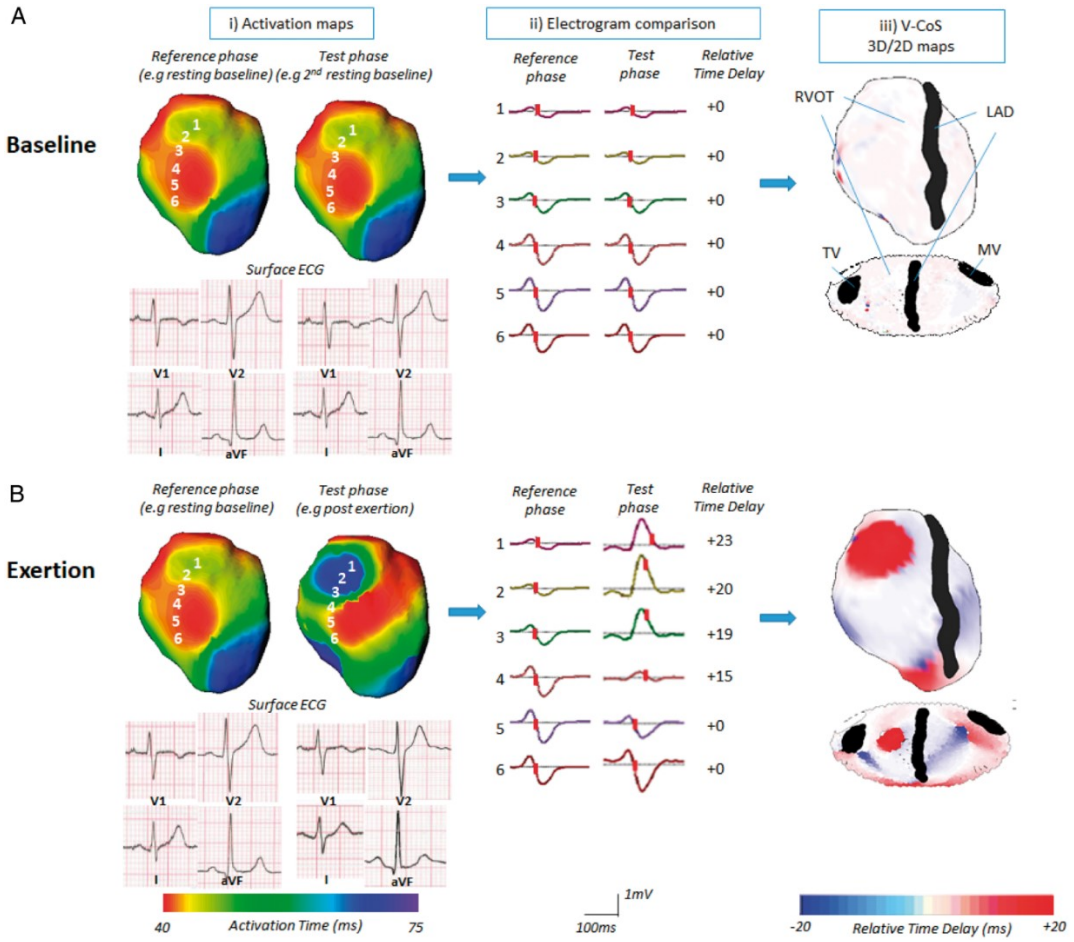

Figure 2.13: Reproduction of figure from original V-CoS manuscript, kindly contributed by Dr Kevin Leong (Shun-Shin, Leong et al. 2019). Panel A demonstrates the comparison of two cardiac cycles from the full recovery phase of exercise testing. Activation maps visually appear similar, as do the surface ECG traces. Comparison of electrograms finds little significant difference which leads to a blank V-CoS map and V-CoS score close to 100%. Panel B demonstrates clear differences in activation maps with much more subtle changes in the surface ECG. Comparison of electrogram pairs here finds significant relative time delay which can be visualised on the V-CoS maps, corresponding to a V-CoS score of <90% in this case.

2.6.2 Practical usage of the V-CoS software

Figure 2.14 summarizes the steps needed to calculate a V-CoS score for a patient. Most of the steps enclosed in the 'ECGi software' box have been detailed in previous sections. In this section we will examine the steps required by the V-CoS software itself.

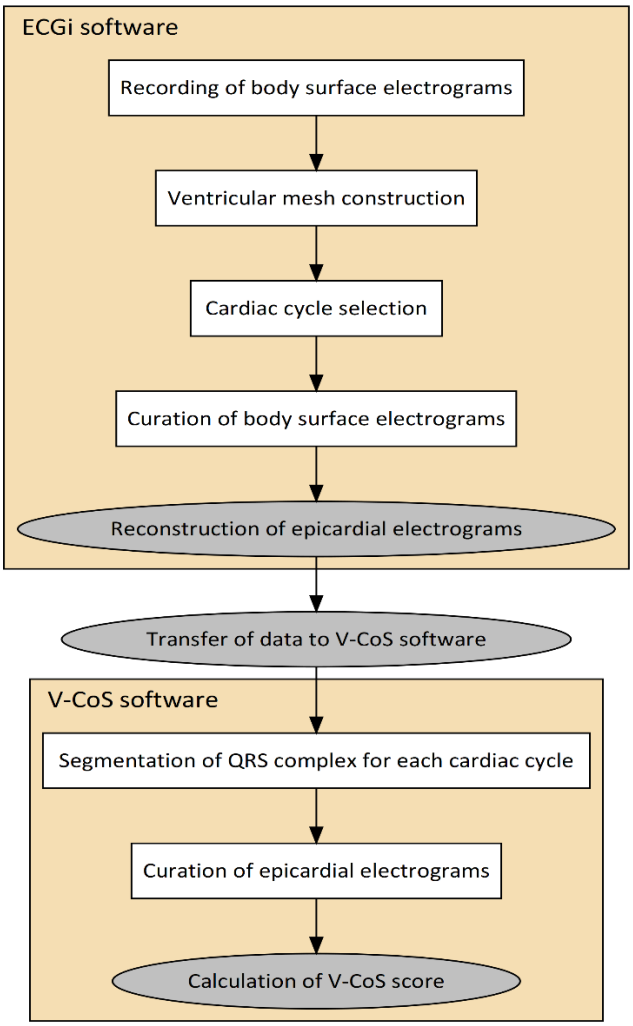

Figure 2.14: Process for calculating a V-CoS score for a patient. Stages in white square boxes are user-driven, whilst stages in oval grey boxes are either fully automated or not driven by subjective user actions. ECGi = ECG imaging; V-CoS = Ventricular conduction stability.

Segmentation of the QRS complex

Figure 2.15 demonstrates the region of interest which is defined by the user to enclose the whole QRS complex upon a graph of the body surface traces to provide a time reference. As the measurement being made is of the steepest negative slope in the electrogram QRS, the region is sized widely enough to include the likely locations of this point, but tightly enough to exclude sharp deflections in the baseline recording not relevant to the QRS complex.

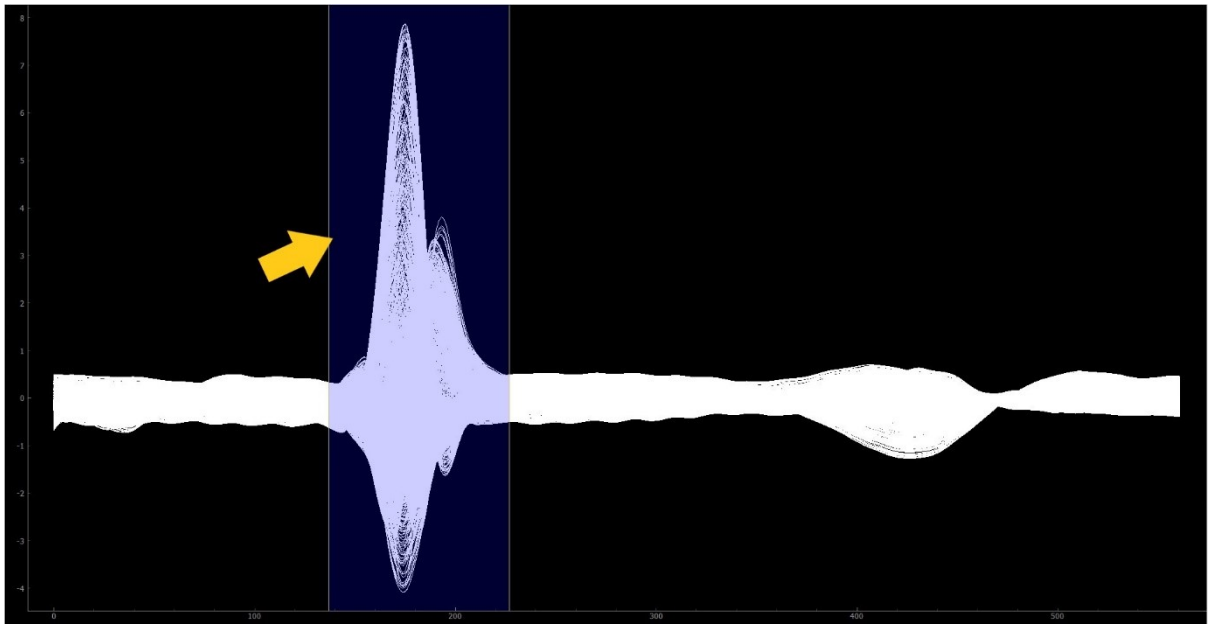

Figure 2.15: V-CoS user interface, Qt for Python (PyQT5). A graph displaying all body surface electrograms is shown to the user, who moves the region of interest (indicated by arrow) until the QRS complex is contained within. This region of interest allows the software to only include steep negative deflections relevant to the QRS complex.

Curation of epicardial electrograms

Despite curation of the body surface electrograms in the ECGi software, some epicardial electrograms are still reconstructed with high frequency or high amplitude noise that can lead to misleading measurements of activation time (similar to Figure 2.12). For this reason, a second round of electrogram curation takes place within the V-CoS software. Figure 2.16 demonstrates the V-CoS user interface following QRS region of interest selection for both cardiac cycles in the comparison.

The software suggests a confidence in the electrogram pair based on the similarity of the test electrogram to the reference electrogram, but ultimately the decision to include or exclude a pair is down to the user.

Following these user decisions, the V-CoS score can be calculated automatically by the software.

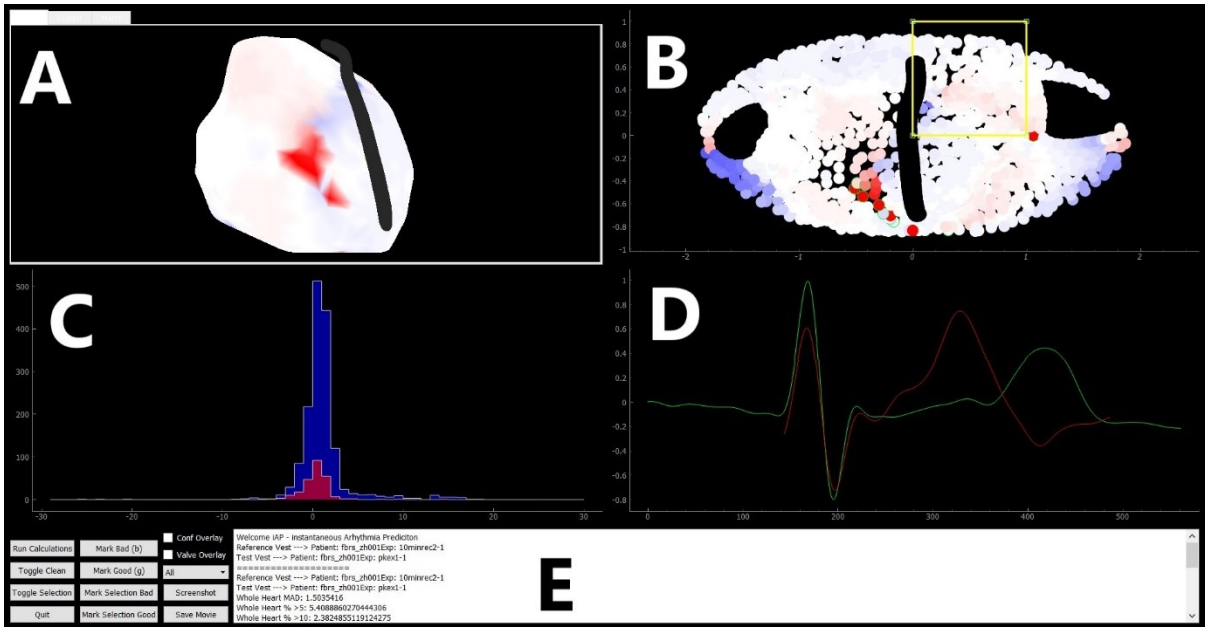

Figure 2.16: V-CoS user interface for calculation of final results. Panel A demonstrates the 3D mesh of the ventricles with the V-CoS map projected onto it. Panel B contains the flattened mesh and results, as well as the ability for the user to select electrograms for inspection in Panel D and mark them as 'Good' for acceptable quality or 'Bad' for high amplitude or frequency noise using the buttons on the far left of Panel E. The yellow box in Panel B allows group selection of several electrogram pairs at once. 'Bad' electrogram locations are denoted in Panel B by a green ring around the location. Panel C is a histogram depicting spread of electrogram pair differences in local activation time. In Panel D the 'test' electrogram in red is at peak exercise, whereas the 'reference' electrogram in green is at 10 minutes of supine recovery. The electrograms are considered here to be of acceptable quality and have been accepted for analysis.

2.6.3 Assessment of variability in Ventricular Conduction Stability

In the original paper describing V-CoS, scores for a small number of cardiac cycle pairs were reproduced well (Shun-Shin, Leong et al. 2019). To determine the true variability of V-CoS scores, we assessed ten consecutive cardiac cycles from immediately after peak exertion and ten consecutive cycles from 10 minutes of supine recovery (referred to as 'peak exercise' and 'full recovery' for brevity). By pairing each beat, 100 V-CoS scores could be calculated per patient.

This required setting the QRS region of interest for each cardiac cycle examined. Figure 2.17 demonstrates the construction of a 10-by-10 beat V-CoS comparison matrix to visualize the results. The mean of all 100 scores can be taken as the summary result for each patient, which we opted to use as the primary measure of activation heterogeneity and arrhythmic substrate.

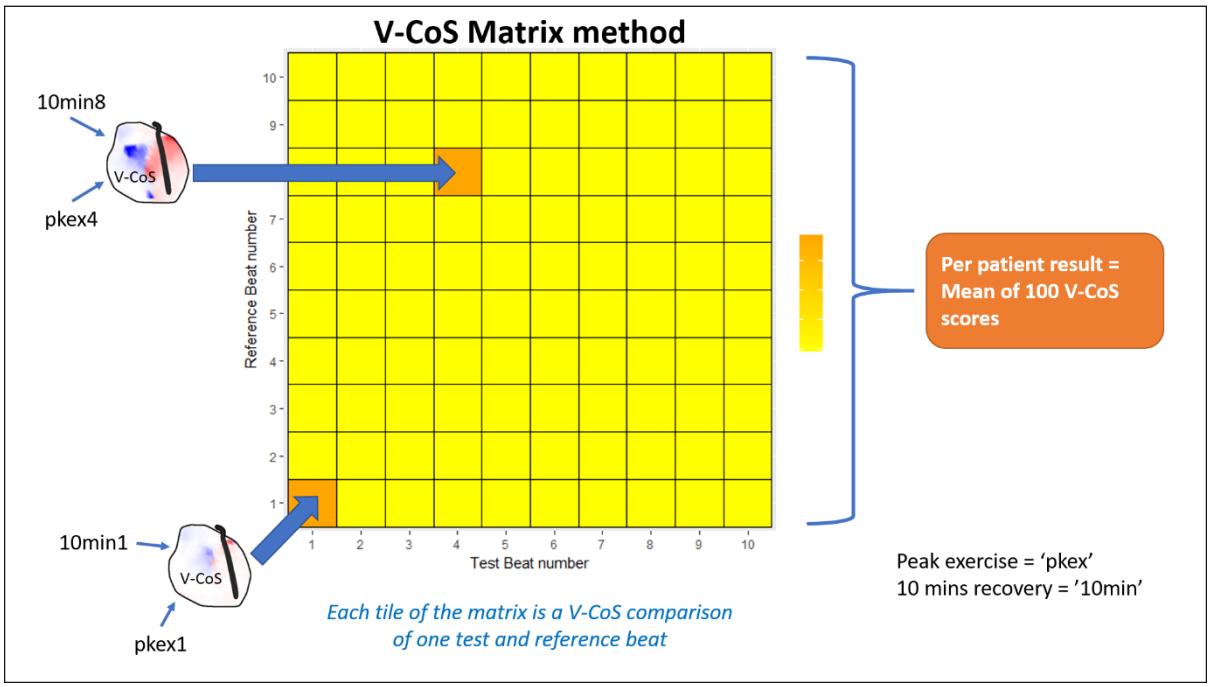

Figure 2.17: The V-CoS matrix method. 10 consecutive cardiac cycles from peak exercise and 10 consecutive cardiac cycles from full recovery are placed in a comparison matrix where each of the 100 tiles is a V-CoS score. The scores can be visualized numerically or by colour coding. The per-patient summary result is the mean of all 100 V-CoS scores in the matrix.

2.7 Conclusion

This methodology was used to recruit and test over 130 volunteers. It was designed to assess the feasibility of using the known techniques in ECG imaging for risk stratification. The results from this analysis are presented in chapters 4 and 5. During this work, further methods were developed to assess the data recorded from the volunteers. This is covered from Chapter 6 onwards.

Chapter 3: Evaluation of the Sieira multivariate risk model for sudden death in Brugada syndrome

3.1 Introduction

The challenge of risk stratification for sudden death in Brugada syndrome is heightened by the similar rates of either implantable device complications or appropriate therapies for potentially life-threatening arrhythmia (Sacher, Probst et al. 2013; Conte, Sieira et al. 2015; Hernandez-Ojeda, Arbelo et al. 2017). Using medium term prospective data and retrospective analysis of registry data, multiple risk factors had been previously proposed, but more recent work casts doubt upon their effectiveness in stratifying primary prevention candidates (Raju, Papadakis et al. 2011; Leong, Ng et al. 2019).

Multivariate risk scoring is being explored in multiple conditions to improve stratification of patient care (Delise, Allocca et al. 2011; O'Mahony, Jichi et al. 2014; Cadrin-Tourigny, Bosman et al. 2019). Most recently for Brugada syndrome, a 400-patient single-centre cohort was retrospectively examined by Sieira and colleagues to identify risk factors for sudden death (Sieira, Conte et al. 2017). Six risk factors were identified, and a multivariate model was constructed to predict sudden death or appropriate implantable cardioverter defibrillator (ICD) therapy. The authors also validated this score in a separate cohort of 150 patients, for which an impressive C-index of 0.81 was reported.

If this validation were representative of worldwide performance, this would be a highly effective tool in risk stratifying sudden death in Brugada syndrome. Our objective was to perform the first independent evaluation of the Sieira model in two UK tertiary centres caring for Brugada syndrome patients.

3.2 Methods

Ethical approval was given by the Fulham Research Ethics Committee and the Heart Research Authority for the data collection under references 14/LO/1318 and 17/LO/1660. All processing

outside a National Health Service (NHS) setting or by persons not in the direct care team was performed using de-identified data.

Patient recruitment

Between 2004 and 2019, databases of consecutive patients diagnosed with Brugada syndrome at Imperial College Healthcare NHS Trust and University Hospital of Wales. Patients could only receive a Brugada syndrome diagnosis if a Type 1 ECG pattern was recorded either spontaneously or by drug challenge. At both centres, ajmaline was used as the challenge agent. The diagnostic criteria were particularly chosen to match that of the Sieira cohort in order to represent the score model in similar conditions (Sieira, Conte et al. 2017). Patients with more than 2 missing items of information needed to complete the score were excluded. From a total of 206 consecutive patients, 192 remained in the analysis with an average follow up of 5.1 ± 2.8 years.

Collection of data

Table 3.1: Points conferred by multiple risk factors in a score model for sudden death risk in Brugada syndrome. Designed by Sieira and colleagues (2017) (Sieira, Conte et al. 2017)

Risk factor	**Score points conferred**
Spontaneous Type 1 ECG pattern	1
Early familial sudden death	1
Inducibility at electrophysiological study	2
Syncope	2
Sinus node dysfunction	3
Sudden cardiac death	4

The Sieira score is an additive score of multiple risk factors which are detailed, along with respective points in Table 3.1.

In patients presenting with sudden cardiac arrest (SCA), history of syncope or early familiar sudden death were only considered if this occurred prior to the presenting event. Care was taken to recruit and score patients in the same fashion as in the Sieira model cohort.

A spontaneous Type 1 ECG pattern was defined as coved ST elevation ≥2mm in ≥1 lead from V1-3, matching the Sieira cohort definition. Spontaneous type 1 ECG was defined as the Brugada pattern in absence of a sodium channel blocker. Concealed Brugada syndrome diagnoses were made using

up to 1mg/kg bodyweight of ajmaline, administered with continuous monitoring using 15-lead ECG (standard configuration with additional leads in the 2nd, 3rd and 4th intercostal spaces above and including V1-2). To be included, patients must have had evidence of a Type 1 Brugada ECG pattern either spontaneously or on drug challenge. Patients with only Type 2 and 3 Brugada ECG patterns were excluded.

Early familial sudden death was defined as occurring in a first degree relative under the age of 35 years. Electrophysiological studies (EPS) included programmed ventricular stimulation; the EPS was said to be positive if haemodynamically unstable, sustained ventricular arrhythmia was induced by up to 3 extrastimuli with a minimum coupling interval of 200 milliseconds at the right ventricular apex. Drivetrains were performed at 600 milliseconds, down to a minimum of 400 milliseconds if the baseline sinus rate was too high for capture.

Syncope was considered likely arrhythmic if brief, traumatic, without prodrome or triggers. Vasovagal syncope was ruled out using detailed history taking or tilt-testing if appropriate. Sinus node dysfunction was defined when a patient had any one of:

- Symptomatic sinus bradycardia
- Sinus arrest
- Paroxysmal supraventricular tachycardia alternating with periods of bradycardia or asystole
- Failure to achieve 85% of age-predicted maximum heart rate on exercise (using the 220 – Age formula)
- Sinus node recovery time ≥1500 milliseconds or corrected sinus node recovery time ≥550 milliseconds.
- Sinus node recovery time/sinus cycle length ratio ≥160%
- Sinoatrial conduction time ≥125 milliseconds.

Assessment of Sieira score uptake in the United Kingdom

To determine the impact of the Sieira score publication in the United Kingdom (UK), a survey was carried out at the annual Heart Rhythm Congress (Birmingham, UK) 2018, organized by the Arrhythmia Alliance. A questionnaire (provided in Appendix E) was filled out by 13 electrophysiology specialists from 10 different UK centres caring for patients with Brugada syndrome.

Statistical analysis

Data were analysed in R version 3.4.2 using a custom script. Graphs were created using the ggplot2 library. Differences between the Imperial and University Hospital of Wales cohorts were tested by Welch's two-sided T-test. Differences between our pooled cohort and the Sieira et al (2017) cohort were tested by one-sided T-test against mean values in the Sieira paper. Categorical variables for other risk markers were compared using the $\chi 2$ test.

3.3 Results

One hundred and twenty-four patients met full inclusion criteria from Imperial College Healthcare and 68 from University Hospital of Wales (UHW). These groups were significantly different in rates of spontaneous type 1 ECG (16.1 vs 5.9%, $p = 0.02$), but were similar in all other characteristics (Table 3.2). Notably, rates of aborted SCD and Sieira model scores were not significantly different.

*Table 3.2: Comparison of patient characteristics between patients seen at Imperial (n = 124) and University Hospital of Wales (UHW, n = 68). Abbreviations: Family history of sudden cardiac death, FH SCD; Electrophysiological study, EPS; Sudden cardiac death, SCD; Type 1 Brugada ECG, T1 ECG. *EPS percentage calculated as proportion of those undergoing test. **Appropriate ICD therapy calculated as proportion of sudden cardiac arrests terminated by an in-situ device.*

	Imperial	**UHW**	**p-value**
Age (years)	48.1	45.5	0.26
Proportion male (%)	59.7	55.9	0.61
FH SCD (%)	46.0	41.2	0.52
FH SCD <35 yrs (%)	18.5	25.0	0.31
Syncope (%)	31.5	35.3	0.59
Sinus node dysfunction (%)	3.2	5.9	0.42
EPS inducible (%)*	21.3	25.0	0.83
Proband status (%)	60.5	48.5	0.11
Previous aborted SCD (%)	9.7	14.7	0.32
Appropriate ICD therapy (%)**	8.3	10.0	0.89
ICD implantation (%)	35.5	35.3	0.98
Spontaneous T1 ECG (%)	16.1	5.9	0.02
Sieira score (points)	1.73	1.83	0.73

Compared to the 550 patients reported in Sieira et al (2017), our cohort had similar calculated Sieira risk scores (1.56 vs 1.77, p = 0.12). Gender, rates of sinus node dysfunction and ICD implantation were also similar. Our cohort was significantly older, with more sudden death under the age of 35 in the family, more EPS inducibility, more probands, but fewer spontaneous type 1 Brugada patterns on ECG. Over follow-up patients had an average 5.26 ±3.93 ECGs inspected for spontaneous type 1 pattern. More of our cohort were symptomatic – either with syncope or aborted SCD; 22 patients survived sudden cardiac arrest or received appropriate ICD therapy. A full comparison is made in Table 3.3.

*Table 3.3: Comparison of patient characteristics between Sieira et al (2017) (n = 550) and this study (n = 192). Abbreviations: Family history of sudden cardiac death, FH SCD; Electrophysiological study, EPS; Sudden cardiac death, SCD; Type 1 Brugada ECG, T1 ECG. *EPS percentage calculated as proportion of those undergoing test.*

	Sieira et al (2017) (Sieira, Conte et al. 2017)	This study	p-value
Age (years)	42.4	47.1	<0.01
Proportion male (%)	65.1	58.3	0.06
FH SCD (%)	47.6	44.2	0.35
FH SCD <35 yrs (%)	9.1	20.8	<0.01
Syncope (%)	26.0	32.8	0.05
Sinus node dysfunction (%)	2.2	4.1	0.17
EPS inducible (%)*	19.6	21.6	0.65
Proband status (%)	33.6	56.8	<0.01
Previous aborted SCD (%)	5.5	11.4	0.01
ICD implantation (%)	41.8	35.4	0.06
Spontaneous T1 ECG (%)	28.5	12.5	<0.01
Sieira score (points)	1.56	1.77	0.12

Risk stratification of our cohort with the Sieira score resulted in large numbers of false positives and false negatives. The resultant sensitivity was 22.7% (95%CI = 7.82-45.4%), and specificity 57.7% (95%CI = 49.6-65.2%). This is displayed graphically in Figure 3.1. C-statistic was 0.58.

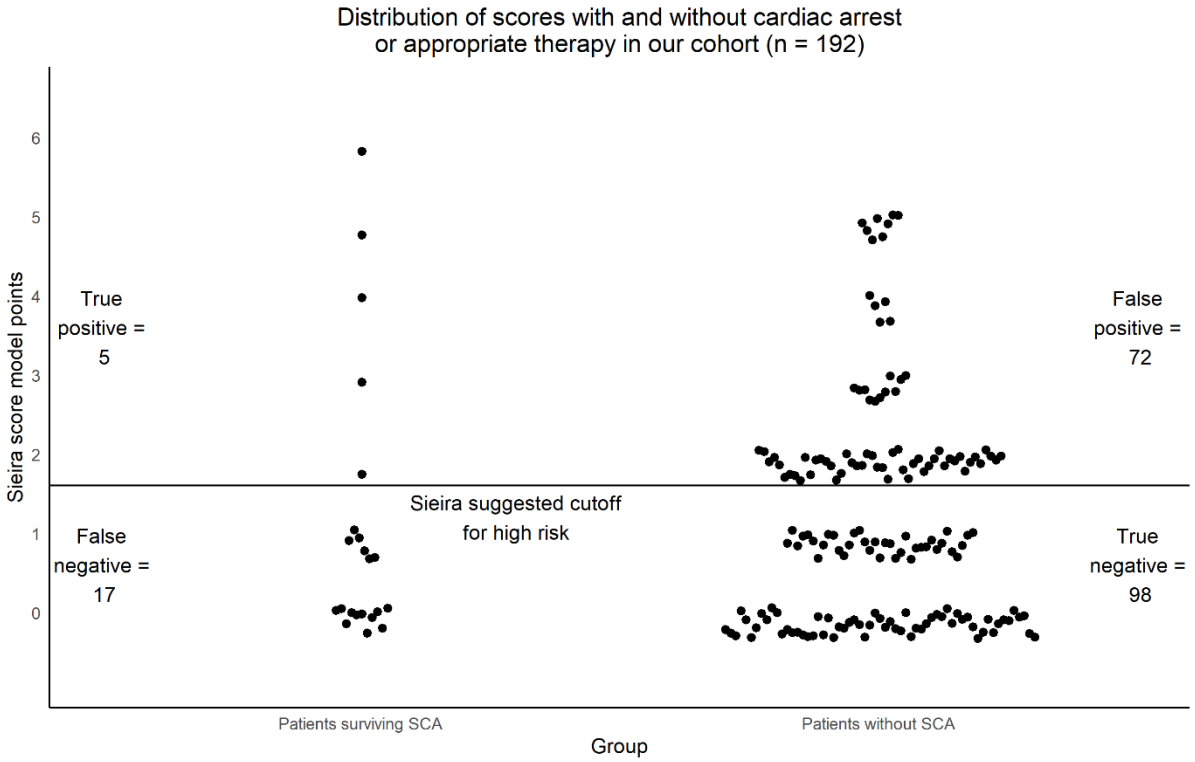

Figure 3.1: Sieira model scores for patients with and without personal history of sudden cardiac arrest (SCA).

Table 3.4: Performance comparison of the Sieira score model in the training cohort and our validation cohort.

Measure	Sieira et al (2017) (Sieira, Conte et al. 2017)	This study
Sensitivity	79.4%	22.7%
Specificity	72.2%	57.6%
C-index	0.82	0.58

Although the score model does not mandate that patients must have an invasive EPS, an EPS only cohort was assessed against the score (n = 88). This produced similar results: sensitivity was 25.0% (95%CI = 0.63-80.6%) and specificity 58.3% (95%CI = 47.0-69.0%) This is displayed graphically in Figure 3.2. C-statistic was 0.56. Positive predictive value was 6.5% and negative predictive value 86.1%. Balanced accuracy was 40.2%.

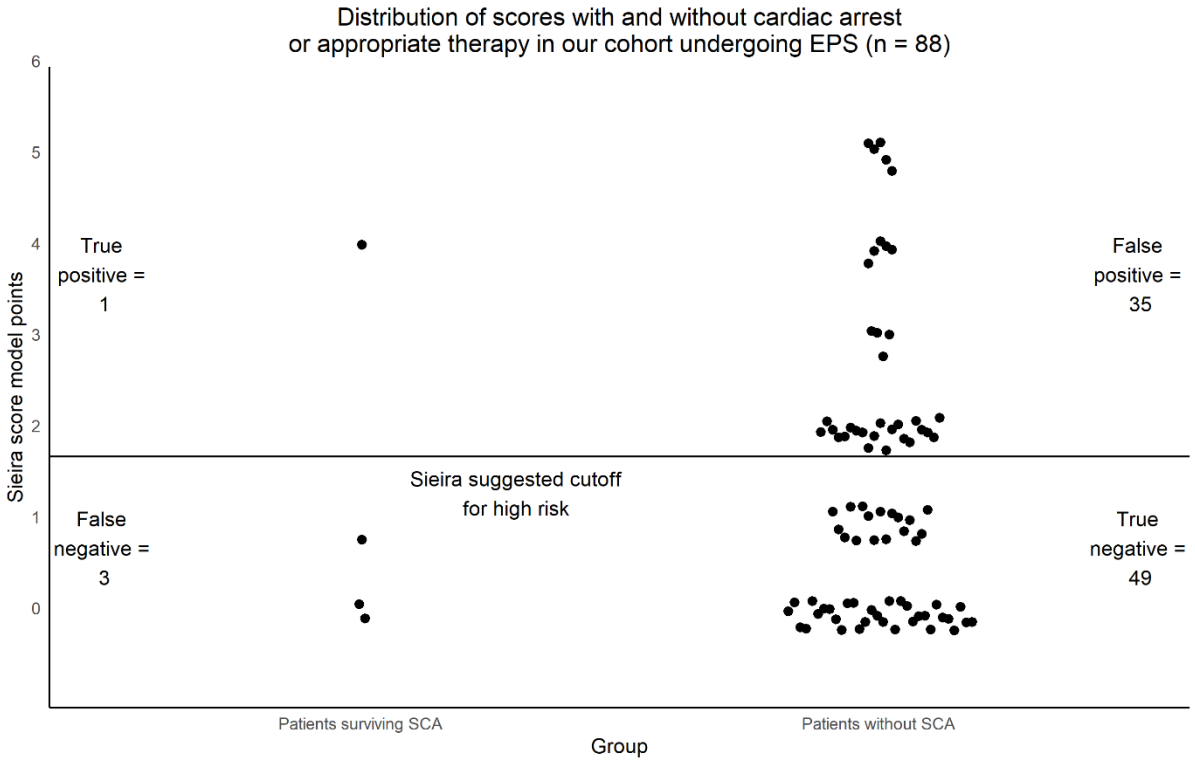

Figure 3.2: Sieira model scores for patients with and without personal history of sudden cardiac arrest (SCA) who had undergone electrophysiological study (EPS).

Characteristics of our sudden cardiac arrest and appropriate therapy survivors are displayed in Table 3.5 (n = 22).

*Table 3.5: Characteristics of sudden cardiac arrest (SCA) and appropriate therapy survivors from our cohort. Abbreviations: point, pt. *Sieira scores are reported from the time of cardiac arrest as described in Methods.*

Sex	**Age**	**ECG type**	**Family history**	**EPS**	**Syncope**	**SND**	**Endpoint**	**Sieira score**
Male	62	Concealed	No	Not performed	No	No	SCD	0
Male	57	Concealed	No	Not performed	No	No	SCD	0
Male	57	Concealed	No	Not performed	No	No	SCD	0
Male	60	Concealed	No	Not performed	No	No	SCD	0
Male	30	Concealed	No	Not performed	No	No	SCD	0
Male	59	Concealed	No	Negative	No	No	SCD	0
Male	46	Concealed	No	Negative	No	No	SCD	0
Male	34	Concealed	No	Not performed	No	No	SCD	0
Male	27	Concealed	No	Not performed	No	No	SCD	0
Male	54	Concealed	No	Not performed	No	No	SCD	0
Male	53	Concealed	No	Not performed	No	No	SCD	0
Female	42	Concealed	Yes (1 pt)	Not performed	No	No	SCD	1
Male	53	Concealed	Yes (1 pt)	Not performed	No	No	SCD	1
Male	55	Concealed	Yes (1 pt)	Not performed	No	No	SCD	1

Male	33	Spontaneous (1 pt)	No	Not performed	No	No	SCD	1
Female	45	Concealed	Yes (1 pt)	Not performed	No	No	SCD	1
Female	32	Concealed	No	Not performed	Yes (2 pts)	No	SCD	2
Male	39	Concealed	No	Not performed	No	Yes (3 pts)	SCD	3
Male	42	Concealed	No	Positive (2 pts)	Yes (2 pts)	No	SCD	4
Male	26	Spontaneous (1 pt)	No	Not performed	Yes (2 pts)	Yes (3 pts)	SCD	6
Male	31	Spontaneous (1 pt)	No	Negative	No	No	Device therapy	1
Male	54	Concealed	No	Not performed	Yes (2 pts)	Yes (3 pts)	Device therapy	5

There were four patients with appropriate defibrillator therapy, two with secondary prevention devices and two with primary prevention devices. In all patients the detected rhythm was ventricular fibrillation; between 3.6 and 7.5 seconds passed before administration of a successful shock.

Furthermore, data was collected on a significant S wave in lead I (≥0.1mV and/or ≥40ms) (Calo, Giustetto et al. 2016) and signal averaged ECG late potentials (Ikeda, Sakurada et al. 2001). S-waves were assessed in 182 patients across both cohorts, but the sign was not significantly more present in the cardiac arrest and appropriate therapy group ($p = 0.65$). Signal averaged ECG was performed in 78 of the Imperial College Healthcare cohort; presence of late potentials was not significantly higher in the sudden cardiac arrest and appropriate therapy group ($p = 0.44$).

Finally, the results of the UK electrophysiology (EP) specialist survey were analysed. All specialists were aware of the Sieira score. 2 out of 13 (15%) interviewed were currently using it in practice. Estimated rates of invasive electrophysiological study were generally low, with most specialists offering this to 0-10% of their patients. This is summarised in Figure 3.3, with the actual rates of

electrophysiological study displayed for UHW, Imperial and Sieira et al (2017) – 10, 65 and 91% respectively.

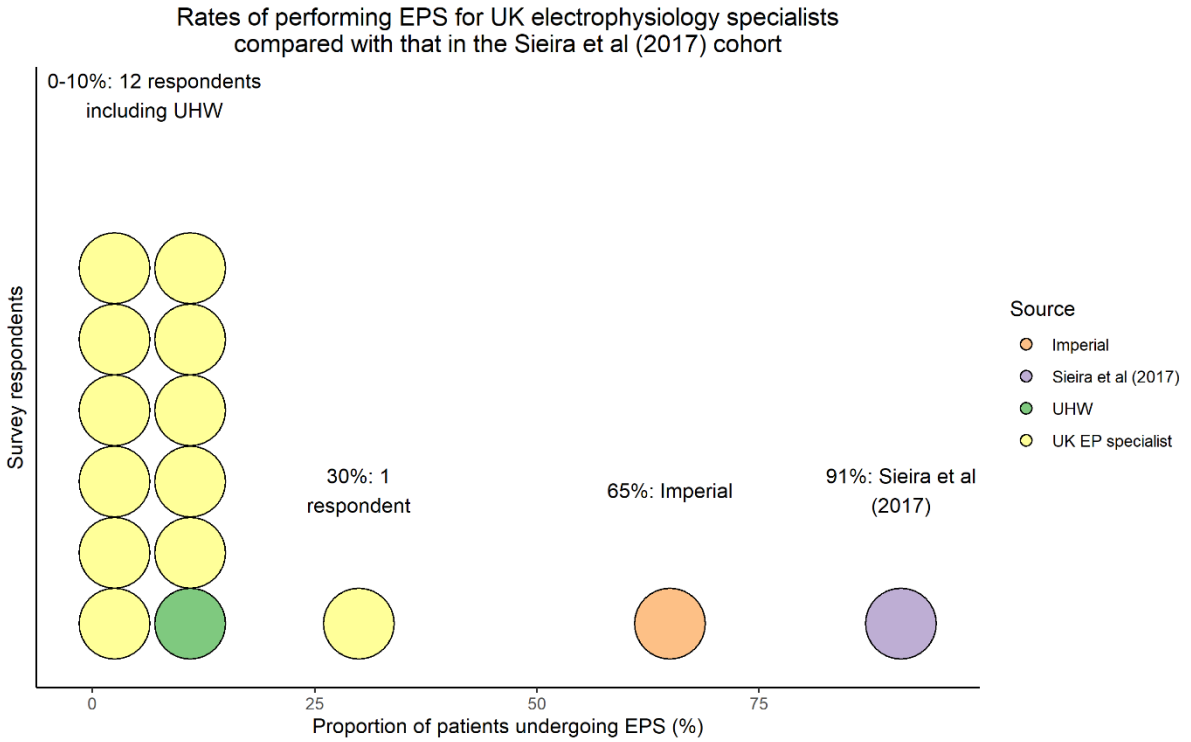

Figure 3.3: Proportion of patients undergoing electrophysiological study (EPS) under the care of 13 electrophysiology (EP) specialists in 10 UK centres according to survey estimate. Actual figures reported for University Hospital of Wales (UHW), Imperial and Sieira et al.

3.4 Discussion

The performance of the Sieira risk score was evaluated in 192 Brugada patients; we found the model to have poor sensitivity and specificity for sudden death events. Cardiac arrest survivors were considered with data around the time of their cardiac arrest to ascertain whether this score model would have adequately protected them before their event. Compared with the internal validation of the Sieira et al (2017) score model, our results are less optimistic about modern Brugada risk stratification. Our strategy of cumulative scoring would bias scores towards better sensitivity; despite this more than half of patients who survived a sudden cardiac arrest or appropriate ICD therapy would have been left unprotected by the recommendations of the Sieira score model. Our validation cohort sensitivity, specificity and C-index were lower than that reported for Sieira et al (2017) in both the full cohort and the selected cohort who had all undergone electrophysiological study.

Regarding patient selection, our cohort has some significant demographic differences with the Sieira cohort, including age, young familial sudden death and spontaneous type 1 ECG (Table 3.2). This is despite identical eligibility criteria. Different population risk profiles may explain some of the discrepancy in score performance over both cohorts. However, the average Sieira risk scores between cohorts were not significantly different. Sieira's own training cohort and validation cohorts also had significant demographic differences without a degradation in score performance (Sieira, Conte et al. 2017). Regardless, for a score to be clinically useful in the wider world, applicability to a range of different Brugada populations would be a necessity.

There are several possible barriers to performance. The Sieira score is highly dependent on the invasive electrophysiological study, with a total of 5 possible points arising from this investigation alone (2 for arrhythmia inducibility, 3 for discovery of sinus node dysfunction). During our survey of UK EP specialists, the use of EPS was mentioned multiple times as a barrier to usage. Our survey suggests that far fewer UK patients are exposed to invasive EP examinations and the associated risks. Whilst the Sieira score does not mandate that all investigations must be carried out – 9% of their patients did not have EPS – we also performed calculations in the subset of our patients who had invasive electrophysiological data. Sensitivity and specificity in this group remained low.

Validation sample size can be a challenge in a rare condition where endpoints are also uncommon. One metric is measuring validation set size comparing it to the original training set. Our total validation set size is 42.6% the size of the Sieira training cohort, with our EPS group accounting for just under half of that figure. Amongst comparable published external evaluations of the Hypertrophic Cardiomyopathy (HCM) SCD-Risk calculator, the mean relative size of the validation set is 25.5%, making our study large relative to a training set also limited by disease prevalence (Wang, Zhang et al. 2019). Nonetheless, the absolute small size of our 88-strong EPS group should be taken into account for this evaluation; however, given the results of the UK EP specialist survey this can be considered the 'real-world' usage of the Sieira score. The centre at which the score was first developed would be considered an outlier by UK standards of offering invasive EP studies. EPS gains only a IIb recommendation in recent guidelines (Al-Khatib Sana, Stevenson William et al. 2018). The non-mandatory nature of the EPS in the Sieira score can be a strength – it may be used early in patients with clear high risk without exposing them to excess risk of an invasive procedure. However, it may also limit overall score performance in many centres in the UK and perhaps worldwide.

Score design can be considered in the context of other current risk stratification models. As mentioned previously, this model is one of a handful of recent attempts to accurately delineate risk

using a multiple variable score. This is the first external validation of the Sieira score; the HCM-Risk calculator has been evaluated externally several times (Maron, Casey et al. 2015; Leong, Chow et al. 2018; Wang, Zhang et al. 2019). In multiple studies the HCM-Risk score creates a significant number of false negatives – much like the Sieira score model. The Arrhythmogenic Right Ventricular Cardiomyopathy (ARVC) Risk score has also been evaluated once, with an underestimation of ventricular arrhythmia occurrence noted in certain disease subtypes (Cadrin-Tourigny, Bosman et al. 2019; Casella, Gasperetti et al. 2020).

For missing data, Sieira et al (2017) used only cases with near complete data, in contrast to the HCM-Risk and ARVC-Risk scores which imputed missing values. The 'near complete cases' strategy has the advantage of only using real data in calculations, at the cost of reducing the number of cases in the training cohort and the risk of bias if data were missing in a non-random fashion (Jakobsen, Gluud et al. 2017). In addition, the tactic of rounding univariate regression coefficients used in the Sieira model results in a score that is simpler to calculate but lacks the robustness of multivariate analysis used in the HCM- and ARVC-Risk scores.

Whilst the HCM-Risk score used both validation set approach and bootstrapping to check their model, Sieira et al (2017) used validation set approach only whilst ARVC-Risk used bootstrapping only. The bootstrapping technique used by the HCM and ARVC-Risk models only tests data from the original dataset but can demonstrate internal validity of the model (James 2013). The validation set approach is easily implemented but reduces the amount of data that can be used to train the model – potentially making it less powerful (James 2013). Sieira's validation set consisted of pre-selected patients not used to develop the model – this method assesses whether the model can be generalised to new, plausibly related populations but does not describe reproducibility of model development (Steyerberg and Vergouwe 2014). In the case of the Sieira model, the significant differences between the training and validation cohorts are an advantage as their model performs well in non-identical groups. Validation set approaches (or more advanced cross-validation methods) and bootstrapping can be performed together to assist in developing accurate risk stratification (Steyerberg and Vergouwe 2014).

All three scores examined a combined endpoint of sudden death and appropriate ICD therapy; the Sieira score model and ARVC-Risk score both have mostly ICD therapies as endpoints. Table 3.6 compares the 3 studies in more detail.

Table 3.6: Selected comparison between scoring strategies in 3 risk stratification calculators

	Sieira score model (Sieira, Conte et al. 2017)	**HCM-Risk (O'Mahony, Jichi et al. 2014)**	**ARVC-Risk (Cadrin-Tourigny, Bosman et al. 2019)**
Cohort size (n)	400	3675	528
Follow up (years)	6.6	5.7	4.8
Event rate (%/yr)	1.4	1.0	5.6
Missing data strategy	Near-complete cases	78% complete data Other data imputed using Rubin's rules	73% complete data Other data imputed using Rubin's rules
Validation strategy	'Validation set approach' (n = 150)	200 bootstrapped samples and 'validation set approach'	200 bootstrapped samples
Outcome criteria	Sudden cardiac death Appropriate ICD intervention.	Sudden death <1hr of symptoms starting OR witnessed OR nocturnal without symptoms Appropriate ICD intervention.	Sudden cardiac arrest/death Spontaneous sustained Ventricular tachycardia >30s >100bpm Ventricular fibrillation Appropriate ICD intervention.
Actual outcomes recorded	89% appropriate ICD therapy 11% sudden death/aborted sudden death	60% sudden death 27% appropriate ICD therapy 13% aborted sudden death	70% appropriate ICD therapy 24% ventricular tachycardia 4% aborted sudden death 2% sudden death

End user input strategy	Summation following multiplication by rounded co-efficients	Exponent formula using un-rounded co-efficients	Exponent formula using un-rounded co-efficients
End user output strategy	Single score cutoff with recommendation	5-year risk output with recommendation	1-, 2- and 5-year risk outputs without recommendation

The observation that most of the Sieira score model endpoints were appropriate ICD therapies (89%) rather than sudden deaths or VF arrests may go some way to explaining why there are slightly higher scores in our patients with ICD therapy versus sudden death survivors. Thus, the Sieira score model may predict ICD events better than sudden deaths.

The statistical strategy behind the Sieira score model is largely robust, and it is not the only risk score to have underperformed at the external validation stage. Questions remain over why this might be; there are several potential explanations.

Firstly, the Sieira score model cohort was drawn from a single centre experience, which may not be generalisable to other centres, let alone other countries and ethnicities.

Secondly, high scoring variables were often based on few patients (sinus node disease: 3 points for 2% of the cohort, sudden death: 4 points for 5%) meaning that small changes in training data could have caused large changes in final score point allocation. This draws on an inherent issue in risk stratification calculations when endpoints or risk markers are rare. Furthermore, the 50 paediatric cases in the study are overrepresented in sinus node disease, casting doubt over whether this can be generalised to adult populations.

The Sieira cohort dates from 1992 to 2013, four years prior to the publication of the article. There are significant differences in spontaneous Type 1 ECG, syncope, proband status and EPS inducibility between the patient groups described from 1992-2005 and 2005-2013 (Sieira, Conte et al. 2017). Patient characteristics were notably different depending on how recently a patient was recruited, and our group (2004-2019) is even more recent. The UHW cohort is the most recent (83% diagnosed after 2010) and most of the patients have been diagnosed by family screening and drug provocation challenge, the likely reason behind the low prevalence of spontaneous type 1 ECG in this centre. The trend of cohorts to have fewer spontaneous type 1 ECGs can be seen over the last 20 years, with numbers dropping from 71.4% in 2003 (Brugada, Brugada et al. 2003), 55.5% in 2009 (Priori,

Gasparini et al. 2012), 45.4% in 2010 (Probst, Veltmann et al. 2010) steadily to the figures reported from both the Sieira and our cohorts (28.5 and 12.5% respectively) (Sieira, Conte et al. 2017). Variation in cohort characteristics may explain performance differences in risk scores and has implications for future patients evaluated in this way.

Other features of the condition previously postulated as risk markers such as significant S waves and late potentials on signal averaged ECG were poorly associated with sudden death in this study. Fractionation of QRS has been previously been shown not to be a significant risk factor in our high risk Brugada cohort (Leong, Ng et al. 2019). In line with previous analyses, spontaneous Type 1 patterns and syncope can be absent from many patients suffering sudden cardiac arrest (Raju, Papadakis et al. 2011; Leong, Ng et al. 2019). Our data reinforces the messages of these earlier studies. Underperformance of risk markers may be due to the changing characteristics of cohorts over time.

3.4.1 Limitations

Some considerations must be given to our study population. The cohort was drawn from two mainly White British populations in London and Cardiff. The extent to which our results could be generalised to other ethnicities and countries is debatable. To improve our analysis of sensitivity, we considered sudden death survivors at the point of their cardiac arrest evaluation. Whilst this allowed us to estimate which of our cardiac arrest survivors would have been offered an ICD, it is impossible to say whether this would have happened in a real-world scenario without a large prospective validation. We considered cardiac arrest patients who had not suffered syncope prior to their sentinel event to be asymptomatic. Our argument is that sustained arrhythmia needing CPR and aborted arrhythmia causing syncope with spontaneous resolution are different clinical presentations – in the latter scenario, the patients are ideally risk stratified whilst in the former, they die or are uncontroversially offered an ICD. However, an opposing argument is that the arrhythmic duration and mode of termination is irrelevant – in this case, our method may introduce bias against the Sieira method.

3.5 Conclusion

The Sieira score model was based on a large, single centre experience of Brugada syndrome. This score was limited by low sensitivity and specificity in our cohort. Inherent problems such as the low overall prevalence of sudden death in Brugada syndrome and certain risk markers such as sinus node

disease will likely limit any attempts at risk stratification using a similar strategic approach. Changing cohort characteristics over time add to the difficulty of building a predictive model.

Patients and clinicians must be well counselled on the performance of modern risk stratification before deciding on ICD implantation. Risk stratification in Brugada syndrome continues to be a challenge.

Chapter 4: Reproducibility testing of ventricular conduction stability and assessment of the arrhythmic substrate in Brugada syndrome

4.1 Reproducibility of Ventricular Conduction Stability

4.1.1 Introduction

Rate adaptation of activation is a property of the myocardium that may be deranged in the presence of abnormal cardiac tissue (Franz, Schaefer et al. 1983). Patients with cardiomyopathies and channelopathies have abnormal cardiac tissue, so their hearts lose normal rate adaptation. Change in conduction velocities and therefore local activation patterns are some of the detectable manifestations of this pathology in invasive or in-vitro studies (Nagase, Kusano et al. 2002; Leoni, Gavillet et al. 2010; Brugada, Pappone et al. 2015). In intact patients, this can be demonstrated using electrocardiographic imaging (ECGi) recordings during exercise treadmill testing (Zhang, Sacher et al. 2015; Shun-Shin, Leong et al. 2019).

Leong et al. developed Ventricular Conduction Stability (V-CoS) to quantify this derangement: the percentage concordance in local activation times for entire ventricular surfaces between a test and reference cardiac cycle. It is further discussed in Chapter 2: Methods. Briefly, scores close to 100% indicate a high degree of similarity between the two cardiac cycles. Scores lower than this indicate progressively more stress-induced heterogeneity between the cardiac cycles – a property than Leong et al. theorized might differentiate survivors of cardiac arrest from those previously unaffected by potentially lethal arrhythmia.

This tool could be useful for diagnosing and risk stratifying patients with rate-related conduction derangements. However, if it is to succeed in the clinical environment, it must be highly reproducible in all stages of processing.

Encouraging reproducibility analyses were performed (Shun-Shin, Leong et al. 2019), demonstrating that in a sample of 10 patients, inter-operator variability in the V-CoS software was low (mean difference 0.62% V-CoS; Bland-Altman 95% limits -1.2 to 2.4). Repeat CT segmentation and repeat ECGi reconstructions were not analysed in the original paper. Furthermore, in two patients, 10 beat standard deviation of V-CoS was 1.6% V-CoS at peak exercise in a single cardiac arrest survivor, and 1.0% V-CoS in a single control. One patient repeated the exercise test, demonstrating Bland-Altman 95% limits of -1.8 to 0.4% V-CoS. Figure 4.1 is a reproduction of the original reproducibility testing results.

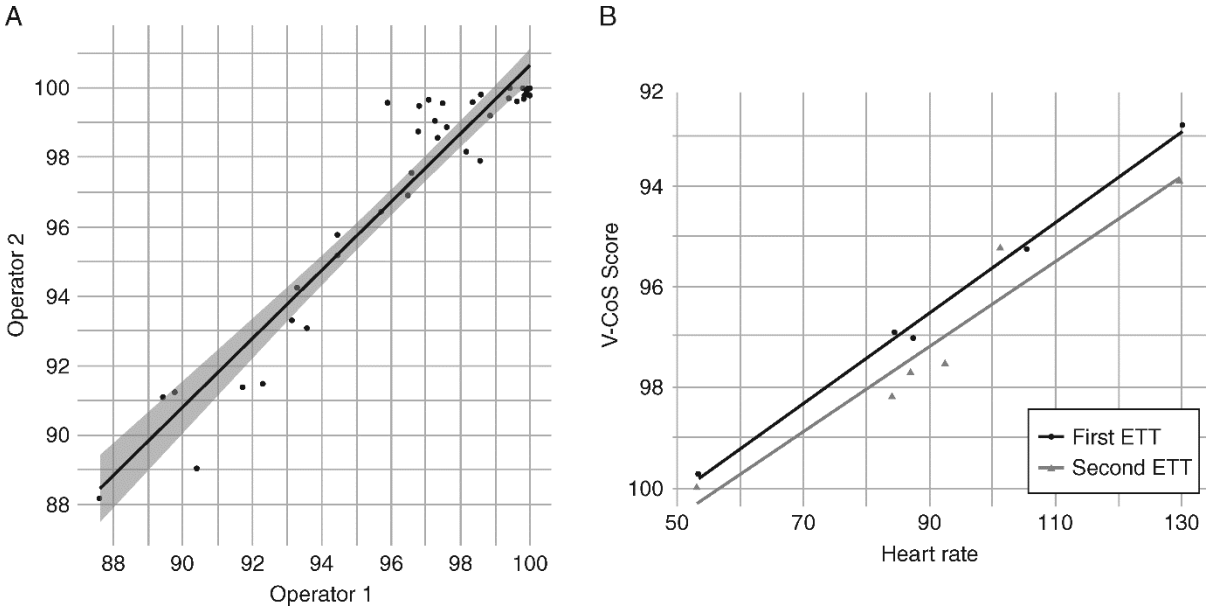

Figure 4.1: Original reproducibility studies into Ventricular Conduction Stability (V-CoS) reproduced with kind permission of Dr Kevin Leong (Shun-Shin, Leong et al. 2019). Inter-operator and inter-test variability were low in this study. Exercise test, ETT.

Ventricular conduction stability calculation is a multi-stage process which must be consistent if it is to succeed as a clinical tool. Using patients from Leong et al.'s original group, we aimed to determine overall reproducibility and the sources of any potential variation. Our hypothesis was that V-CoS would be reproducible across all stages of calculation.

4.1.2 Methods

The V-CoS workflow is discussed in detail in Chapter 2. Figure 4.2 is a summary of chapter 2 to assist interpretation of these methods. In order to isolate the stages for reproducibility during V-CoS processing, the workflow was divided for testing.

CT scans were not repeated due to ethical concerns over radiation re-exposure. CardioINSIGHT vests were not re-applied due to prohibitive cost. Two operators took part:

- Operator 1: Dr Kevin Leong (V-CoS creator)
- Operator 2: Dr Ji-Jian Chow (thesis author)

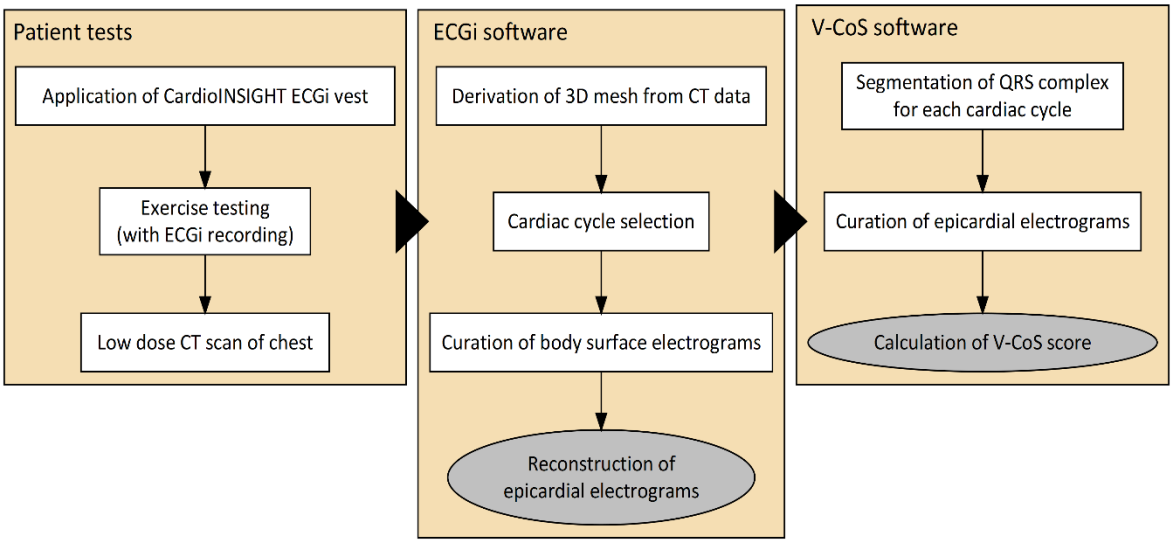

Figure 4.2: A summary of the ventricular conduction stability (V-CoS) workflow. Fully automated steps are marked by grey ovals; all other steps include some user decision making. Electrocardiographic imaging, ECGi; Computerized tomograph, CT; Three dimensional, 3D.

Assessment of V-CoS software reproducibility

In a repeat of the experiments carried out by Leong et al., Operator 2 was blinded to the identities, background condition and final V-CoS scores of the same 10 participants from the original paper (Shun-Shin, Leong et al. 2019). 3 beats were analysed per patient.

CardioINSIGHT electrogram and geometry files were obtained from Operator 1's data repository for analysis, identical to those used for the processing in the original paper. The repeated steps were segmentation of the QRS complex and curation of epicardial electrogram. The original software calculated the V-CoS from this information.

This test was carried out once before Operator 2 received training in interpreting epicardial electrograms, and once following training. Training was carried out personally by Operator 1 reviewing and providing feedback on electrogram selections made by Operator 2 and was provided on an ad-hoc basis over a period of 4 months.

Assessment of ECGi software reproducibility

10 patients with Brugada syndrome and a variety of final V-CoS scores were chosen for repeat reconstruction of epicardial electrograms from recordings and 3D ventricular meshes previously recorded by Operator 1.

In 7 of these patients, we were able to guarantee the same cardiac cycles were selected because these CardioINSIGHT archives contained cycle selection information. In 3 patients this information was unavailable, so best effort was made to match the cycle length and visual morphology based on both bookmarks in the CardioINSIGHT archive and previously extracted electrogram files from Operator 1's data repository.

In the 3 patients where same cardiac cycle selection was not assured, CardioINSIGHT reprocessing was performed personally by Operator 1 to provide control values. Following extraction of electrogram and location files, V-CoS scores were calculated using the custom software.

Assessment of 3D mesh reproducibility

4 patients attending for testing had CT scans segmented by Medtronic staff external to our study. Operator 2 performed repeat segmentations to produce alternative epicardial meshes. V-CoS scores were calculated using the methods above for both epicardial models over multiple beats per patient.

Assessment of exercise test reproducibility

17 patients volunteered for and successfully completed a second exercise test: 8 patients with hypertrophic cardiomyopathy, 3 Brugada VF survivors, 3 unaffected Brugada relatives, 2 patients surviving idiopathic VF and 1 patient surviving ischaemic VF.

Exercise tests were conducted at least 40 minutes apart to ensure adequate recovery. The CT scan of the chest was undertaken in between tests. Large adjustments to the vest were not made, but re-application of tape securing electrode position was permitted.

The earliest consecutive 10 cardiac cycles without visually significant artefact or noise was selected following peak exercise. A second run of 10 consecutive cardiac cycles was selected following 10 minutes of recovery. The first beat of both runs were compared using V-CoS to judge the reproducibility of a single beat between exercise tests. Secondly, to assess the ability of summary statistics to improve reproducibility, the minimum and mean of all 100 V-CoS scores was compared between exercise tests.

CT scans and 3D ventricular meshes were identical but cardiac cycle selection, ECGi and V-CoS processing were performed with identical technique by the same operator. To eliminate the opportunity for bias at the V-CoS stage, the automated electrogram deselection choices were left un-edited.

Statistical analysis

Bland-Altman analysis and Pearson's correlation were used as measures of reproducibility. As the effect sizes from the original paper ranged from 3.1 to 5.0% V-CoS (Shun-Shin, Leong et al. 2019), a proposed *a priori* maximal acceptable difference of ±2% V-CoS is plotted on each of the graphs (Giavarina 2015). The number of patients falling in- and outside of this acceptability range is compared using Fisher's exact test. Differences between methods are tested using the paired T-test in identical cardiac cycles and the unpaired T-test in non-identical cardiac cycles.

4.1.3 Results

Assessment of V-CoS software reproducibility

Prior to training in electrogram interpretation, Pearson's R between operators was 0.89 ($p > 0.001$), and the Bland-Altman 95% confidence intervals were between -2.74 and 3.41% V-CoS (Figure 4.3 upper panel). Following training, Pearson's R between operators was 0.96 ($p > 0.001$) with Bland-Altman 95% confidence intervals between -2.06 and 1.54% V-CoS (Figure 4.3 lower panel). The improvement due to training was significant but small ($p = 0.008$, 95% confidence intervals 0.14 to 0.91% V-CoS).

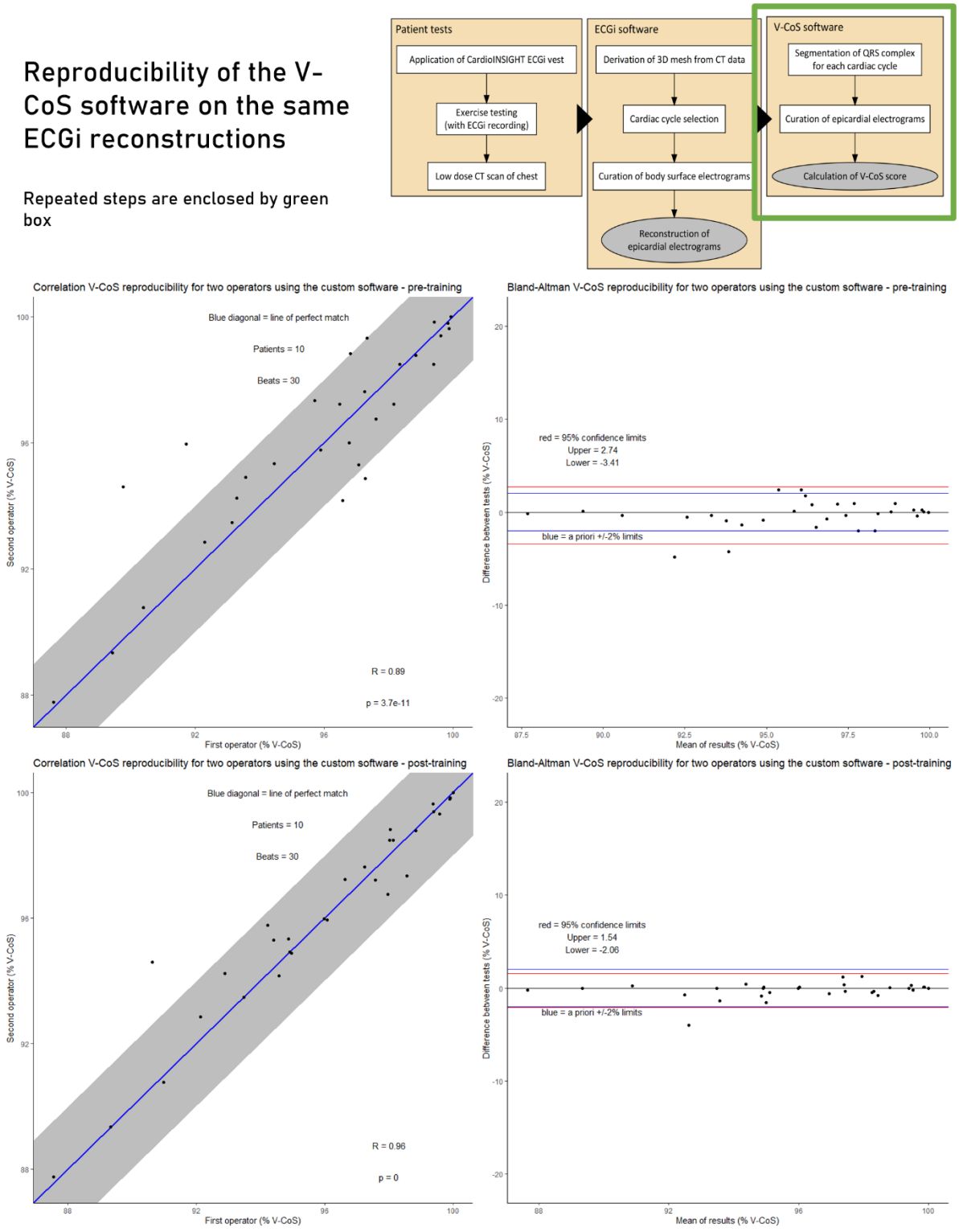

Figure 4.3: Correlation and Bland-Altman graphs for reproducibility of the Ventricular Conduction stability (V-CoS) software used by two operators for 30 cardiac cycles from 10 patients prior to (upper panel) and following (lower panel) electrogram interpretation training.

Assessment of ECGi software reproducibility

When cardiac cycles were processed on CardioINSIGHT™ by two operators, Pearson's R for V-CoS was 0.72 ($p > 0.001$). Bland-Altman 95% confidence intervals were -6.33 to 4.65% V-CoS (Figure 4.4). In 7 patients, the cardiac cycles chosen were identical. For this subgroup, Pearson's R was 0.96 ($p > 0.001$). Bland-Altman 95% confidence intervals were -1.58 to 1.72% V-CoS (Figure 4.5 upper panel). In the remaining 3 patients, the cardiac cycles originally processed by Leong et al. were uncertain – attempts were made to match using correlation of cycle length and morphology. In this subgroup. Pearson's R was 0.43 ($p = 0.23$) and Bland-Altman 95% confidence intervals were -12.23 to 6.22% V-CoS (Figure 4.5 lower panel). The difference in reproducibility was significant ($p = 0.007$ by unpaired T-Test).

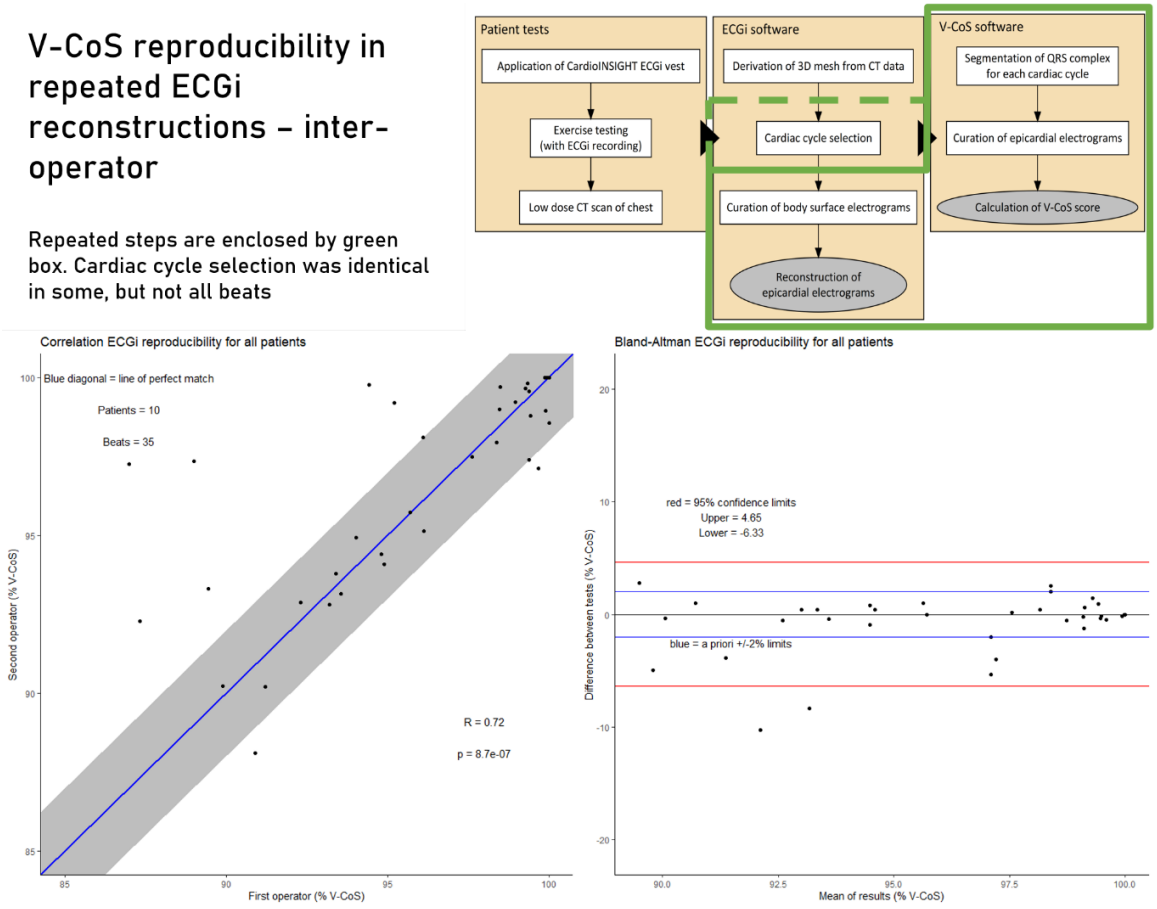

Figure 4.4: Correlation and Bland-Altman graphs for reproducibility of the ECGi software used by two separate operators, using the V-CoS score as the measurement endpoint. Ventricular conduction stability, V-CoS; Electrocardiographic imaging, ECGi.

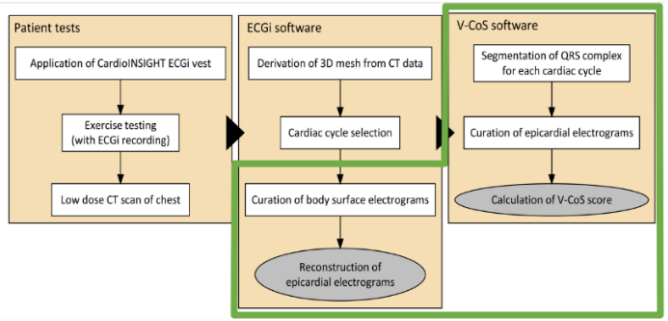

Effect of cardiac cycle selection on V-CoS reproducibility – inter-operator

Repeated steps are enclosed by green box

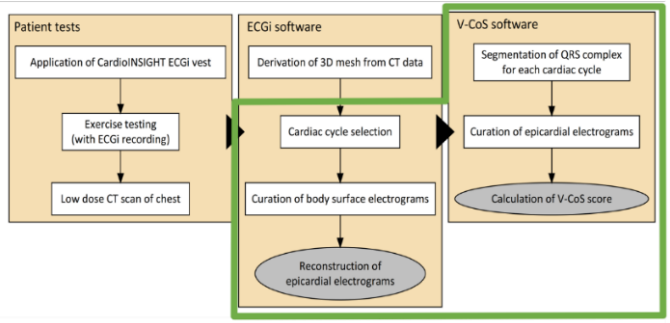

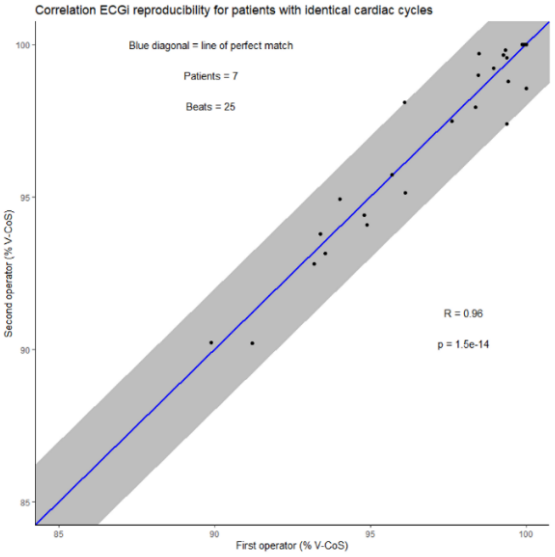

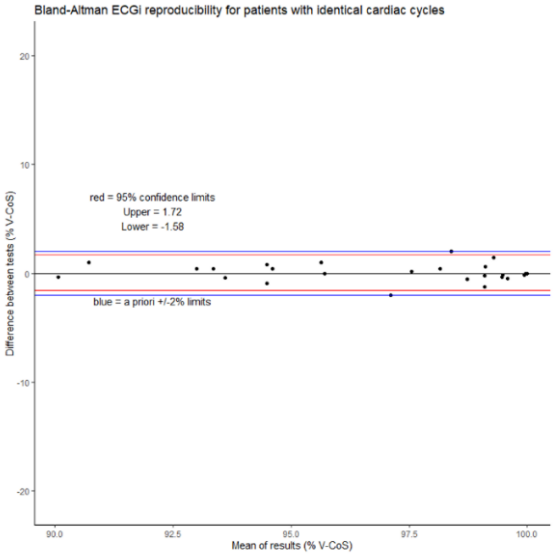

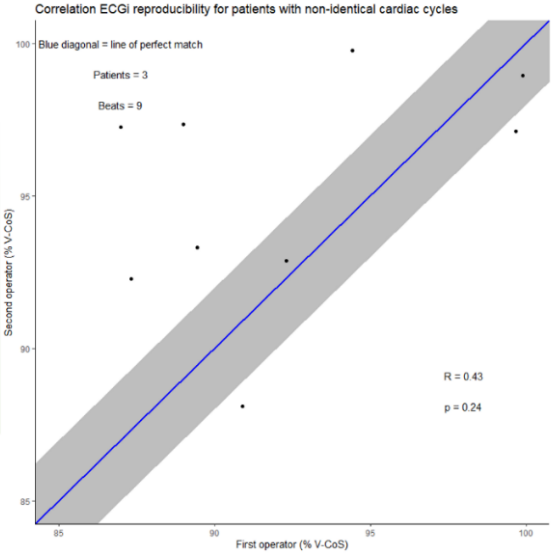

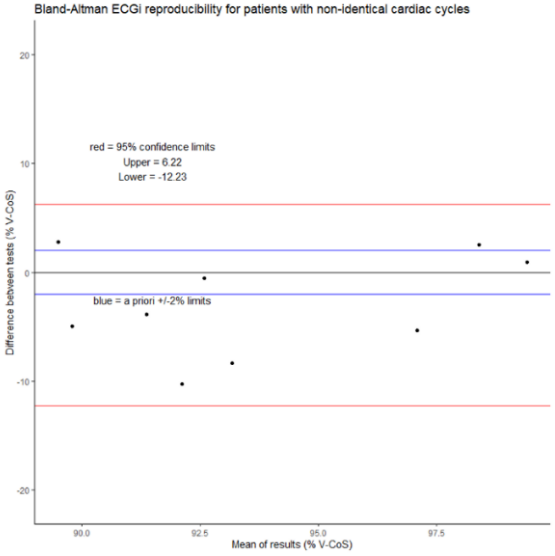

Figure 4.5: (previous page) Inter-operator reproducibility analysis for two operators using the ECGi software to process identical and likely non-identical cardiac cycles, using V-CoS as the measurement endpoint. For cardiac cycles that were assuredly identical, inter-operator reproducibility was good (upper panel). For cardiac cycles which were likely to be non-identical, but best matched for cycle length and morphology, inter-operator reproducibility was poor. Ventricular conduction stability, V-CoS; Electrocardiographic imaging, ECGi

It was surmised that these beats were likely non-identical. To assess identical-beat reproducibility in this group, Operator 1 personally reprocessed these samples; the values were compared to the Operator 1's historical measurements and Operator 2's measurements. Comparing Operator 1's current and historical measurements, intra-operator Pearson's R was 0.14 ($p = 0.71$) and Bland-Altman 95% confidence intervals were -12.99 to 9.16% V-CoS (Figure 4.6 upper panel). When compared to Operator 2, inter-operator Pearson's R on now identical cardiac cycles was 0.92 ($p > 0.001$) with Bland-Altman 95% confidence intervals of -3.73 to 2.32% V-CoS (Figure 4.6 lower panel). This was significantly better ($p = 0.017$, paired T-test).

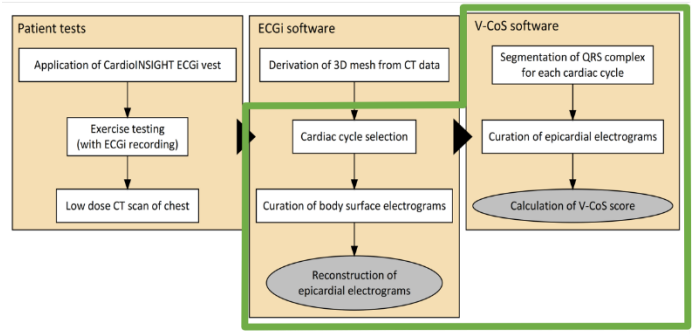

Effect of cardiac cycle selection on V-CoS reproducibility – intra-operator

Repeated steps are enclosed by green box

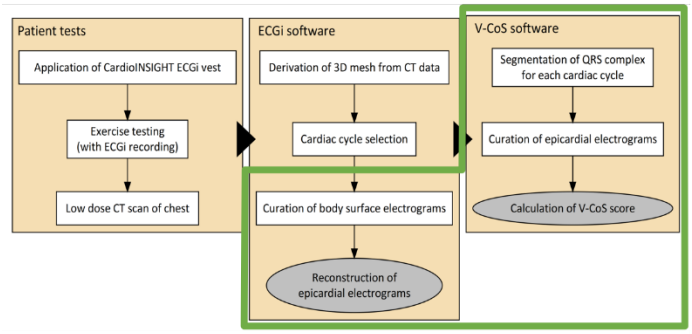

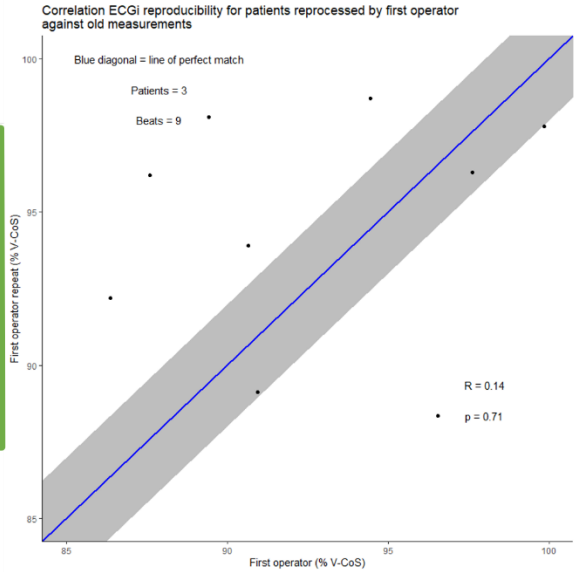

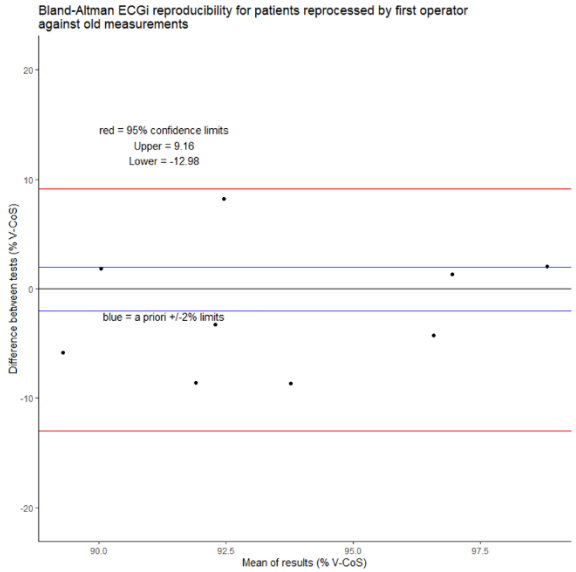

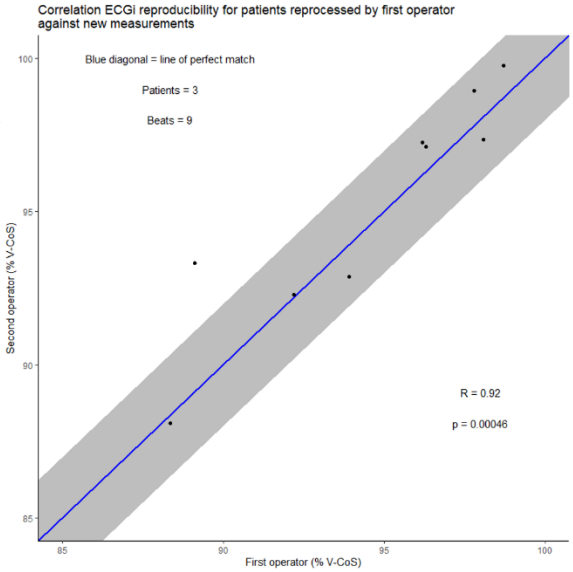

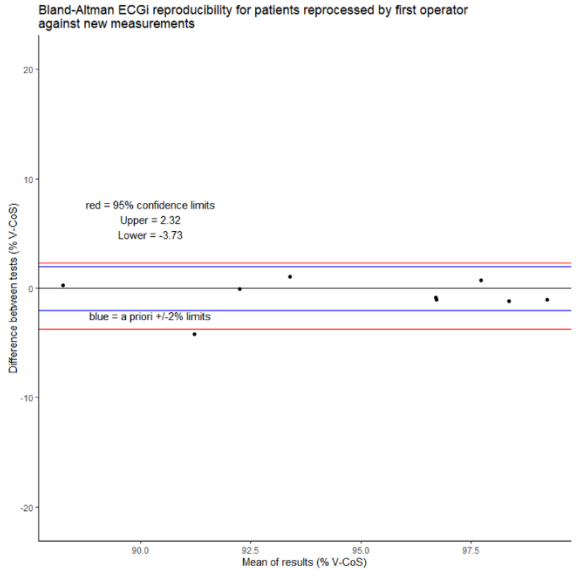

Figure 4.6: (previous page) Correlation and Bland-Altman analysis of ECGi software reproducibility using V-CoS as the measurement endpoint. Upper panel: intra-operator variability when cardiac cycles were unlikely to be identical, despite best matching of cycle length and morphology. Lower panel: inter-operator variability on the same patients where the cardiac cycles were assured to be identical. The improvement in reproducibility implies that this is primarily an issue with beat-to-beat variability rather than inter-operator or patient-specific variables. Ventricular conduction stability, V-CoS; Electrocardiographic imaging, ECGi.

Assessment of 3D mesh reproducibility

Upon repeat segmentation of the ventricles from computerized tomography by two different operators, reproducibility by Pearson's R was 0.97 ($p > 0.001$). Bland-Altman 95% confidence intervals were -1.55 to 1.91% V-CoS (Figure 4.7).

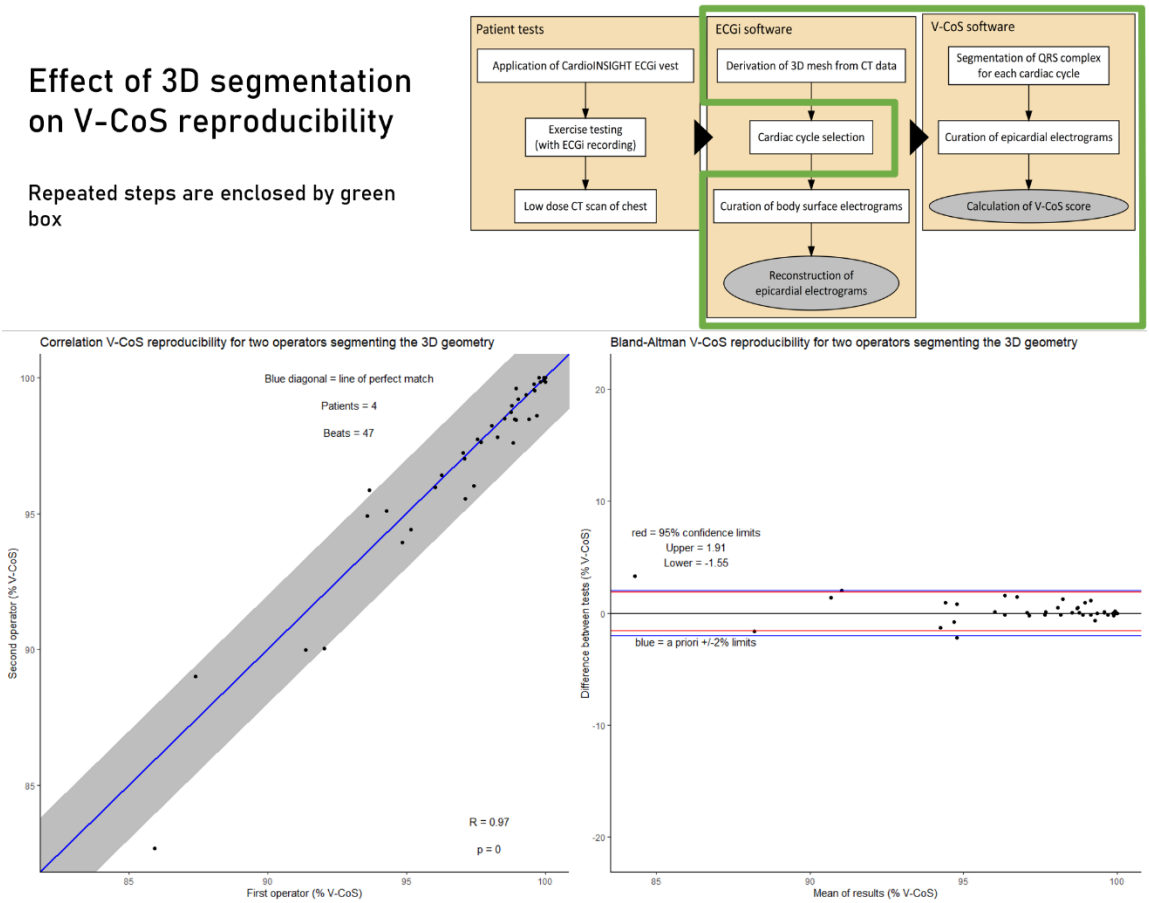

Figure 4.7: Correlation and Bland-Altman analysis of ventricular geometry segmentation reproducibility using V-CoS as the measurement endpoint (two operators). Ventricular conduction stability, V-CoS; Three-dimensional, 3D.

Assessment of exercise test reproducibility

All patients reached >85% of target heart rate in both exercise tests. At the time of sampling, heart rates did not differ significantly when exercise tests were compared (peak exercise: $p = 0.85$; recovery: $p = 0.89$ by paired T-test).

For single V-CoS values taken at equivalent periods of two exercise tests, reproducibility by Pearson's R was 0.60 ($p = 0.011$). Bland-Altman 95% confidence intervals were -8.02 to 8.19% V-CoS (Figure 4.8 top panel).

Assessment of the mean and minimum of 100 scores formed by a 10-by-10 comparison matrix of consecutive rest and consecutive exercise beats was carried out to determine if summary statistics could improve this reproducibility.

For the matrix mean, reproducibility by Pearson's R was 0.81 ($p > 0.001$), with Bland-Altman 95% confidence intervals of -11.49 to 7.42% V-CoS (Figure 4.8 middle panel). For the matrix minimum, reproducibility by Pearson's R was 0.63 ($p = 0.007$), with Bland-Altman 95% confidence intervals of -17.78 to 12.71% V-CoS (Figure 4.8 bottom panel). The matrix mean was significantly better than the matrix minimum (mean absolute difference 2.15% V-CoS, $p = 0.005$ by paired T-test) but was not significantly better in this sample than the single-value V-CoS (mean absolute difference 0.25% V-CoS, $p = 0.85$). Using the *a priori* acceptable tolerance rule of ±2% V-CoS, 12/17 of the matrix mean V-CoS values were acceptably reproducible compared to only 7/17 of the single-value V-CoS. This however did not reach statistical significance ($p = 0.16$ by Fisher's exact test).

Effect of summary statistics on V-CoS reproducibility – inter-test

Repeated steps are enclosed by green box

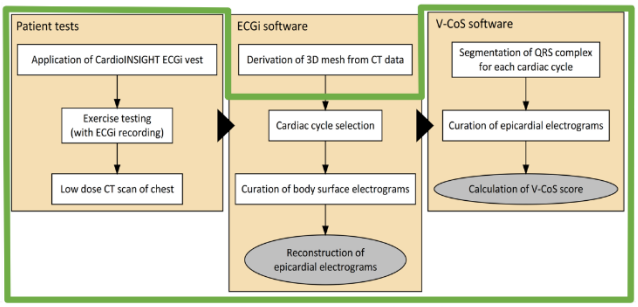

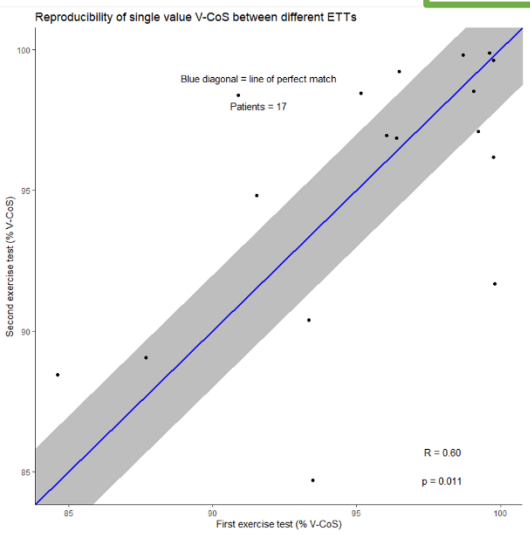

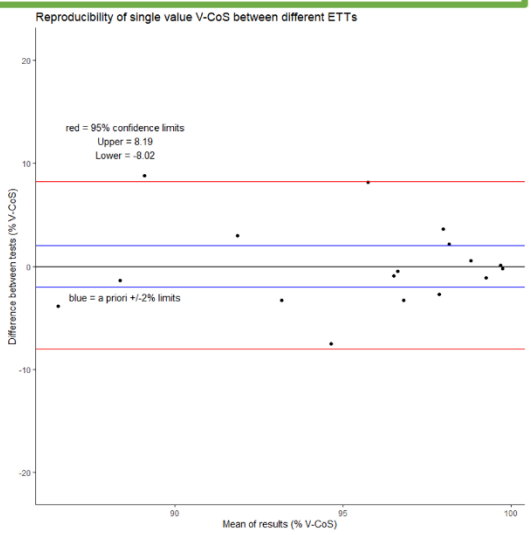

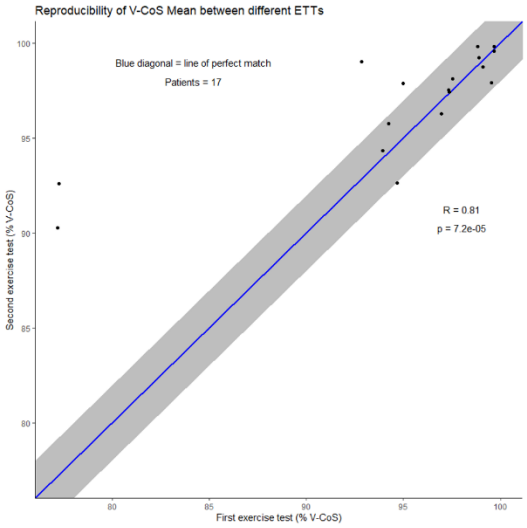

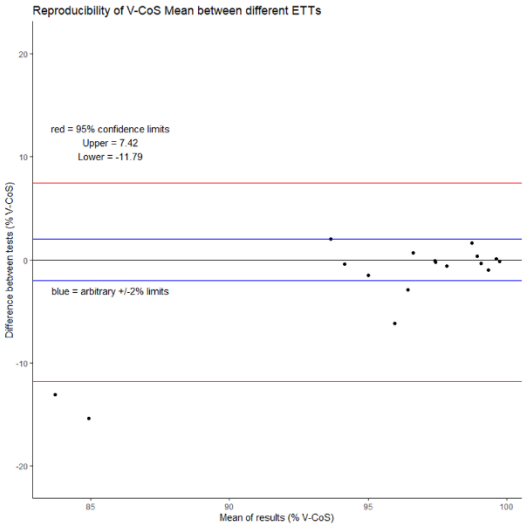

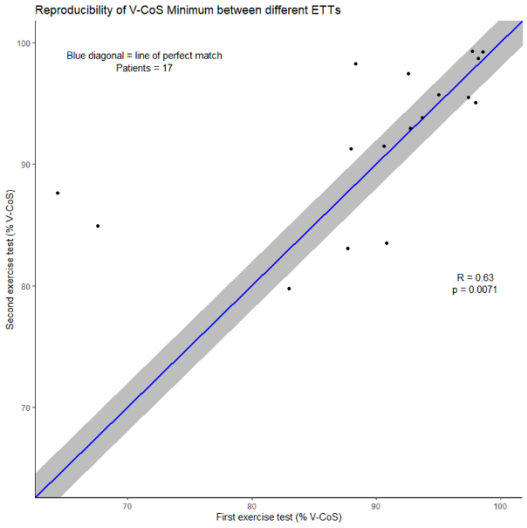

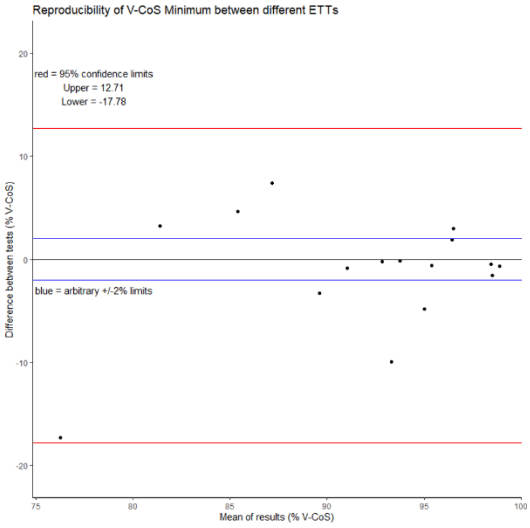

Figure 4.8: (previous page) Correlation and Bland-Altman reproducibility plots between measurements taken during separate exercise tests. Single-value comparisons (top panel) show a poor reproducibility which is marginally improved by the use of the mean from 100 calculated scores (middle panel), but not from the use of the minimum of these 100 scores (bottom panel). Ventricular conduction stability, V-CoS; Exercise tolerance test, ETT.

4.1.4 Discussion

In this study we have examined the reproducibility of the various steps in the calculation of a V-CoS score. Figure 4.9 provides a summary of the best Pearson correlation results of each stage.

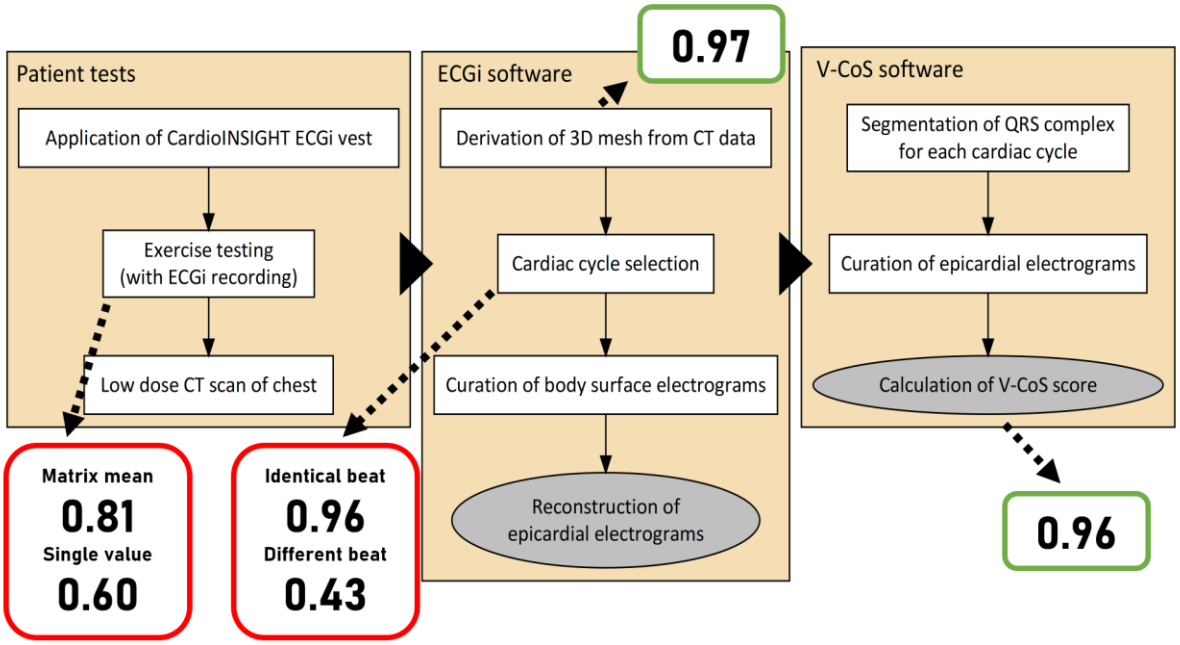

Figure 4.9: Summary of reproducibility findings for each stage of the Ventricular Conduction Stability (V-CoS) process. Figures in rounded boxes are Pearson's R values. Whilst ventricular segmentation and the end calculation of a score was highly reproducible (R = 0.97, 0.96 respectively), significant beat-to-beat and test-to-test variability was discovered. Summary statistics like the mean of multiple calculations only led to a moderate increase in reproducibility. Electrocardiographic imaging, ECGi; Computerized tomograph, CT; Three-dimensional, 3D.

Assessment of V-CoS software reproducibility

Reproducibility in the V-CoS software itself was good. This is similar to the result that had been shown in the original manuscript (Shun-Shin, Leong et al. 2019). The V-CoS software has two main variables which the user may alter: (I) the window of interest denoting the QRS complex; (II) the electrograms which are deemed high in artefact or electrical noise to the extent that a measurement of true activation time may be compromised. Determination of the QRS duration (and hence the time boundaries of the complex) is a commonly performed task in clinical medicine; both operators examined were clinical cardiology trainees with between 6 to 8 years working experience following

medical school at the time of testing. It is likely that the selected QRS complexes would have been quite similar between operators, but the window of interest position is not stored by the CardioINSIGHT software so we do not have this information from Leong et al.'s original dataset to confirm.

Determination of a noisy epicardial electrogram is a less commonly performed task across early-stage cardiology trainees and may be less reproducible in those not experienced in interpretation. Evidence supporting this statement is the training effect seen following several months of expert feedback on selection – there was a significant ($p = 0.008$) improvement in reproducibility. It is possible that the 'training effect' is a biasing effect of having seen these traces before – despite re-blinding it is certainly possible that the pattern recognition for noisy electrograms was simply repeated by rote learning rather than development of objective criteria in the mind of the operator. This is compounded by the lack of explicit guidelines as to the appearance of noise versus true electrogram features such as fractionation. The optimal test of reproducibility may be recruiting an operator with prior epicardial electrogram experience who had not seen the dataset before.

Despite this, even pre-training the Pearson correlation was 0.89, with 26/30 beats falling into the *a priori* acceptable range of ±2% V-CoS. The automated designation of poorly cross-correlated signals as artefactual is likely to be a factor in the good reproducibility of this stage – as described in the original methodology (Shun-Shin, Leong et al. 2019).

Assessment of segmentation and ECGi software reproducibility

Segmentation reproducibility was also good: Pearson correlation was 0.97 with associated narrow Bland-Altman 95% confidence intervals falling within the *a priori* acceptable range of ±2% V-CoS. All segmentation techniques in the group had been taught by the same Europe-based team of trainers from the device company (Medtronic, Minneapolis USA), which may have contributed to the good reproducibility. It is unclear whether other research or clinical groups trained by Medtronic teams from other geographic areas would be reproducible with our data. This is not a problem for the purposes of this research study but may be a concern if the same guideline results are used worldwide for risk stratification of sudden death.

Results from the ECGi software itself were more mixed, with reproducibility results ranging from Pearson's R of 0.43 to 0.96. It should be noted that imperfect reproducibility in the V-CoS software stage would also have contributed to the R-values and Bland-Altman confidence intervals quoted in these results, although prior results in this experiment suggest that this effect should be minimal.

The context in which this reproducibility work was carried out provides some insight into the structure of the results. Prior data had suggested that 10-beat variability in V-CoS was minimal – certainly less than the *a priori* acceptable range of ±2% V-CoS (Shun-Shin, Leong et al. 2019). In 7 patient files, exact beat labels had been stored in the ECGi archive, assuring identical cardiac cycle choice and resulting in tight reproducibility (R = 0.96). In the remaining 3 patients tested, this was not the case. Downstream files processed by the V-CoS software had been saved, allowing us to examine the morphology and approximate cycle lengths of the beats tested. Bookmarks in the ECGi archive indicated the approximate time period from which these beats had been extracted, but the exact beat analysed by Leong et al. could have feasibly been any one of up to 30 or 40 beats. If beat-to-beat reproducibility was truly minimal, the selection of an exact beat would be unlikely to adversely affect performance. However, reproducibility was poor for these patients (R = 0.43). Whether this was due to operator error, patient characteristics or another factor was unclear.

To examine the hypothesis that operator techniques were non-identical, Operator 1 reprocessed the data from these patients 2 years after he had made his original measurements. Intra-operator reproducibility was poor (R = 0.14). This result was surprising, as for 7 other patients, tens of beats and for all previous reproducibility work, even inter-operator reproducibility far surpassed this value. To examine the hypothesis that beat choice was the key factor, Operator 1's new calculations were compared with Operator 2's, assuring that the same beats were selected on the ECGi software – resulting in good reproducibility (R = 0.92).

Out of all the decisions made during the processing performed on the ECGi software itself, it appeared that selection of the 'correct' cardiac cycle was the key determinant of reproducibility. The concept of a 'correct' cardiac cycle is problematic – why should one beat in a short consecutive period of sinus rhythm be more representative of arrhythmogenic risk than the next one? Furthermore, how should the 'correct' beat be chosen?

In order to understand the degree of variability and in the hope that summary statistics from several calculations could help to mitigate the beat selection problem, 10-by-10 comparison matrices of consecutive exercise and consecutive rest beats were analysed. This testing structure was used to examine the reproducibility of exercise tests.

Assessment of exercise test reproducibility

Single value results from different exercise tests were poorly reproducible (R = 0.60). Although this was at odds with the single patient presented by Leong et al., we had previously shown that nearly

neighbouring beats in the same exercise test could have poorly correlated V-CoS scores, so this finding was not surprising. Summary statistics of 100 scores from a matrix of 10 consecutive exercise and 10 consecutive rest beats were tried as a method of improving reproducibility. The minimum score of the matrix was also poorly reproducible (R = 0.60), but the mean score of the matrix provided a modest gain in reproducibility (R = 0.81).

To judge which summary statistic is best, a consideration of the research aim is needed. Initiation of arrhythmia may only need a single event to trigger a potentially lethal event, such as an R-on-T unsynchronized shock or commotio cordis in an otherwise normal heart. If the aim of this research were to prove that arrhythmogenic substrates exist in our population, the matrix minimum could be the best measure. However, of the many millions of cardiac cycles experienced by patients with inherited cardiac conditions, very few result in any arrhythmia at all. To be clinically relevant for the question of defibrillator implantation, an idea of the cumulative risk over time is needed. For this reason, the matrix mean may be more useful, as it summarizes the level of activation heterogeneity where all cardiac cycles could be potentially arrhythmogenic. The better reproducibility in this small group also favours the use of the matrix mean.

However, inter-test correlation of R = 0.81 is still far less reproducible than some of the later stages of processing. Closer analysis of the differences between the test indicates that on average, the results for the first test were lower by 2.18 ± 4.9% V-CoS (95% confidence intervals -4.7 to 0.33% V-CoS), even though heart rates at the time of sampling were not significantly different (p = 0.85, 0.89 for exercise and rest respectively). As the confidence interval of the mean difference crosses zero, this discrepancy is not significant. However, all four individuals outside the *a priori* maximal acceptable difference of ±2% V-CoS had a higher result on the second test. This group was comprised of 3 patients with hypertrophic cardiomyopathy and 1 with Brugada syndrome. The patient with Brugada syndrome and one of the patients with hypertrophic cardiomyopathy were cardiac arrest survivors.

Even in this subset of patients, the heart rate at the sampling time was not significantly different (p = 0.35, p = 0.96 for recovery and peak exercise respectively by paired T-test). It is possible that there is an attenuation of activation heterogeneity in patients who are effectively ‘warmed up’ by the first exercise test. Fatigue is another possible factor, but the time between tests would have been significantly longer than the work intervals of the tests themselves. However, the number of patients tested in this experiment is unlikely to be large enough to draw anything more than speculative conclusions on this topic. An informative comparison would be patients who were tested on multiple

days, with the ethical drawback of multiple exposures to ionizing radiation and the financial drawback of multiple vest usage.

The moderate reproducibility of second exercise test is of clinical concern – if a patient obtains a particular risk score on a particular day, should this result be taken as representative? This phenomenon can be seen in other types of electrophysiological testing. In 1992 a cohort of 64 patients with coronary artery disease underwent repeat invasive programmed ventricular stimulation on separate days to check efficacy of drug therapy. If sustained ventricular tachycardia were induced, the drugs were considered ineffective; if no induction, the drugs were considered effective. Drug efficacy was re-confirmed in only 77% of cases (Ferrick, Luce et al. 1992). In 1995, a cohort of 60 patients without coronary artery disease underwent the same protocol, resulting in re-confirmation of drug efficacy in only 78% of cases (Ferrick, Maher et al. 1995). In the Brugada syndrome, 111 patients from the PRELUDE study underwent identical repeat programmed ventricular stimulation, resulting in reproducibility for only 34% of patients (Priori, Gasparini et al. 2012).

The interactions needed for arrhythmogenesis are clearly dynamic, and so the detectable levels of activation heterogeneity that we have hypothesised lead to arrhythmia may well be similarly changeable. Further testing would be required to identify methods of standardizing the intensity of the stress test needed to produce a V-CoS score.

4.1.5 Conclusion

Whilst sensitivity and specificity are the headline figures reported around clinical testing, reproducibility is also critically important for delivering information to clinicians and patients they can be confident in. Although certain stages of the ventricular conduction stability process are highly reproducible, there is also significant beat-to-beat variability as well as differences between repeat exercise tests. Summary statistics derived from large numbers of calculations may mitigate differences between neighbouring cardiac cycles, but like many other electrophysiological tests, V-CoS has shown significant variability when repeat testing is performed. For ECGi measures to be feasibly used in sudden death risk stratification, further improvements will have to be made to ensure test score reliability as well as sensitivity and specificity.

4.2 Performance of Ventricular Conduction Stability in Brugada syndrome

4.2.1 Introduction

Epicardial conduction abnormalities are a known feature of Brugada syndrome (Nagase, Kusano et al. 2002; Rolf, Bruns et al. 2003) linked to future risk of lethal ventricular arrhythmia (Ikeda, Sakurada et al. 2001), which can be ablated to suppress the pathognomonic ECG and reduce arrhythmic events (Brugada, Pappone et al. 2015). In contrast to invasive techniques, these abnormalities can be demonstrated safely, comfortably and in the presence of realistic physiological stressors using non-invasive electrographic imaging (ECGi) (Zhang, Sacher et al. 2015). Exercise is a stressor known to induce detectable changes in Brugada electrophysiology (Amin Ahmad, de Groot Elisabeth et al. 2009; Zhang, Sacher et al. 2015; Shun-Shin, Leong et al. 2019).

Ventricular conduction stability (V-CoS) has been shown to differentiate a small mixed cohort of cardiac arrest survivors from controls without a personal history of potentially lethal arrhythmia (Shun-Shin, Leong et al. 2019). In the first part of this Chapter, the original V-CoS method suffered significant beat-to-beat variability, and summary statistics of multiple analyses were shown to improve consistency. Volunteers with no evidence of cardiac disease nor history of arrhythmia (benign or malignant) have not been tested by V-CoS, and ECGi's diagnostic utility in concealed Brugada syndrome is unknown.

We sought to test the hypothesis that normal subjects would show preserved activation sequences in response to exercise, and mean V-CoS could safely quantify rate-related conduction abnormalities useful in diagnosing concealed Brugada syndrome patients or identifying those patients with a high risk of future cardiac arrest.

4.2.2 Methods

Patient selection

Fifty-two patients were selected from our cohort.

1. 21 survivors of ventricular fibrillation or sustained ventricular tachycardia and haemodynamic compromise with Brugada syndrome ('BrS VF').
2. 20 patients with Brugada syndrome without previous ventricular fibrillation or sustained ventricular tachycardia ('BrS')
3. 11 asymptomatic relatives of patients with Brugada syndrome, proven not to have the same condition by a negative Ajmaline challenge reaching dose endpoint of 1mg/kg (up to 120mg total dose).

Patients with any of the following exclusion criteria were not selected:

- Inability to provide consent
- Inability to perform exercise test
- Inability to cease anti-arrhythmic drugs prior to test
- Pregnancy or inability to rule out by last menstrual period or highly effective contraceptive
- Abnormal echocardiographic findings.

Exercise ECGi testing and epicardial reconstruction

Each volunteer underwent the following procedures as detailed in Chapter 2:

- Drug cessation if necessary
- Torso preparation and vest application
- Maximal Bruce protocol exercise testing
- Supine recovery for a minimum 10 minutes or to return of resting pulse rate
- Low dose-CT scan of chest
- Epicardial reconstruction of electrograms.

When selecting body surface signals from immediate post-exercise and 10 minutes of recovery, care was made to ensure the same array of electrodes were used in cardiac cycles compared to each other. In effect, if any surface electrode recorded too much artefact to be analysed in either exercise or recovery, it was excluded from analysis altogether.

Cardiac cycle selection

In the original study, reproducibility of the same cardiac cycles was tested in 10 individuals with varying V-CoS scores, whilst reproducibility between different cardiac cycles was tested in only one. The V-CoS Matrix method described in Chapter 2 was used to allow us to understand the effect of selecting different cardiac cycles, and any patterns in this variation.

Statistical analysis

Summary patient V-CoS scores were the mean of all V-CoS scores in a matrix. The Wilcoxon-2 sample (also known as Mann-Whitney U test) was performed to compare any two groups. Comparisons between 3 groups were performed using the Kruskal-Wallis test.

To understand the effect of V-CoS on risk stratification, a Receiver Operating Characteristic (ROC) curve was analysed to find an optimal threshold. Discriminant power was analysed in the cardiac arrest survivors against the current IIa recommendation for ICD implantation in patients with both

spontaneous Type 1 ECG and syncope (Priori, Blomstrom-Lundqvist et al. 2015). To understand the utility of V-CoS for diagnosis, a ROC curve was plotted to determine a threshold for classifying concealed Brugada syndrome patients against unaffected relatives.

4.2.3 Results

Patient characteristics

All 52 patients successfully completed the testing protocol, reaching at least 85% of maximum predicted heart rate for age on the treadmill without complications.

Heart rates at the sampling phases immediately post peak exercise and at full recovery were not significantly different between the groups (p = 0.39 at peak phase, p = 0.16 at recovery phase). Gender balance, age and proportions of both spontaneous Type 1 ECG and unheralded syncope were not significantly different between the groups (p = 0.61, 0.93, 0.21 and 0.41 respectively).

These characteristics are summarized in Table 4.1.

*Table 4.1: Characteristics of volunteers undergoing electrocardiographic imaging exercise testing. Peak and recovery phase heart rates were those when signal was clean enough for measurement using the electrocardiographic imaging system. *Spontaneous type 1 ECG was defined as positive if the ECG pattern were seen during the exercise test or any ECG recording from clinic. Brugada syndrome, BrS; Brugada ventricular fibrillation or haemodynamically unstable sustained ventricular tachycardia survivor, BrS VF; Electrocardiogram, ECG.*

Parameter	**BrS VF**	**BrS**	**BrS relative**	**p-value**
Males (proportion)	85.7%	75.0%	72.7%	0.61
Age (years, mean)	46.9	46.1	45.5	0.93
Spontaneous type 1 ECG (proportion)*	23.8%	15.0%	0	0.21
Syncope (proportion)	14.3%	15.0%	0	0.41
Peak phase heart rate (bpm, mean)	145.4	144.1	135.3	0.39
Recovery phase heart rate (bpm, mean)	91.5	91.8	96.1	0.16

Mean V-CoS inter-group comparisons

Unaffected Brugada relatives were significantly differentiated from both BrS VF and BrS groups (p = 0.011 for both). Brugada VF survivors could not be significantly differentiated from patients without previous life-threatening arrhythmia (p = 0.53), even when patients with syncope or spontaneous Type 1 ECG were excluded from the latter group (p=0.61). Mean ±SD V-CoS were 96.1 ±4.8% in the BrS VF group, 97.7% ±1.6% in the BrS group and 98.9 ±0.8% in the BrS relative group (Figure 4.10).

Post-hoc power was calculated at 30.3% to detect the observed difference in V-CoS between BrS VF and BrS groups (Rosner and Glynn 2011). By Welch's two-sample T-Test, the 95% confidence interval for a difference between the groups was between -0.8 and 3.8% V-CoS (p = 0.19).

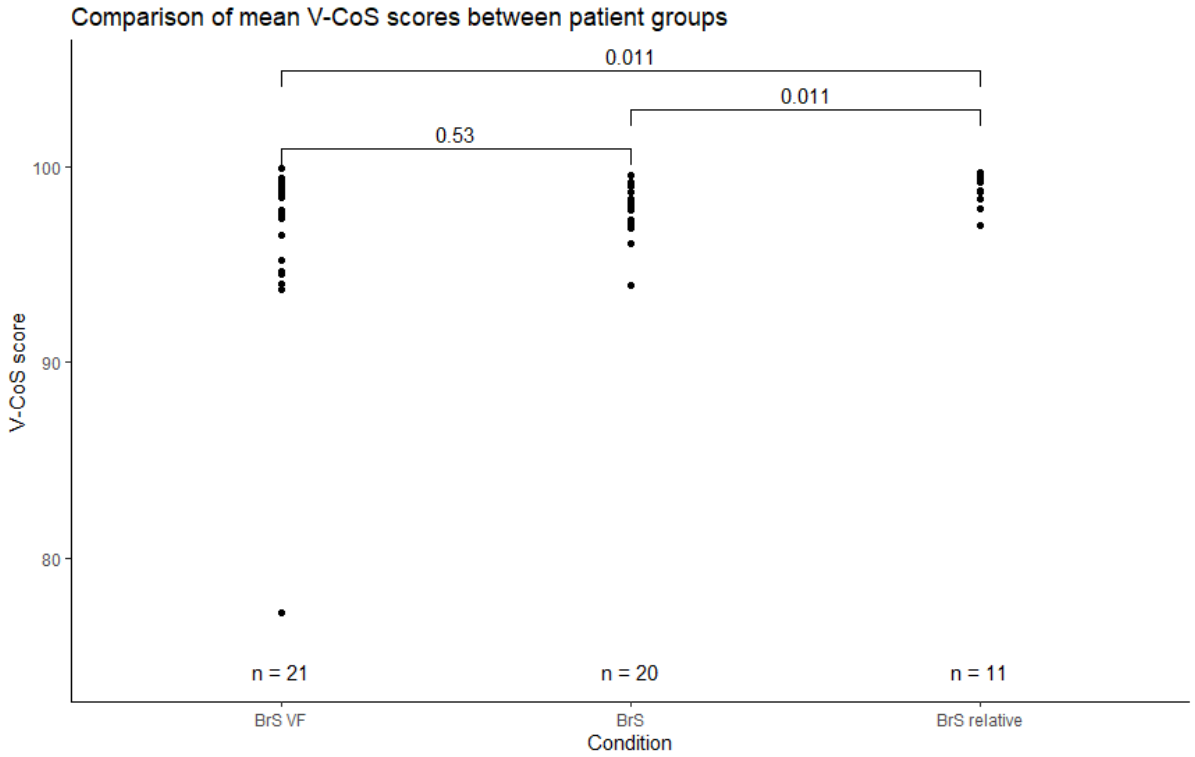

Figure 4.10: Comparison of mean ventricular conduction stability scores between Brugada syndrome patients with and without a personal history of ventricular fibrillation or compromising ventricular tachycardia, and asymptomatic relatives with negative Ajmaline test. Ventricular conduction stability, V-CoS; Brugada syndrome, BrS.

To determine the effect of spontaneous Type 1 ECG patterns on V-CoS, a sub-analysis was performed with concealed Brugada patients and unaffected Brugada relatives (Figure 4.11). V-CoS scores were significantly lower in the concealed Brugada group (mean 97.3% vs 98.9%, p = 0.003).

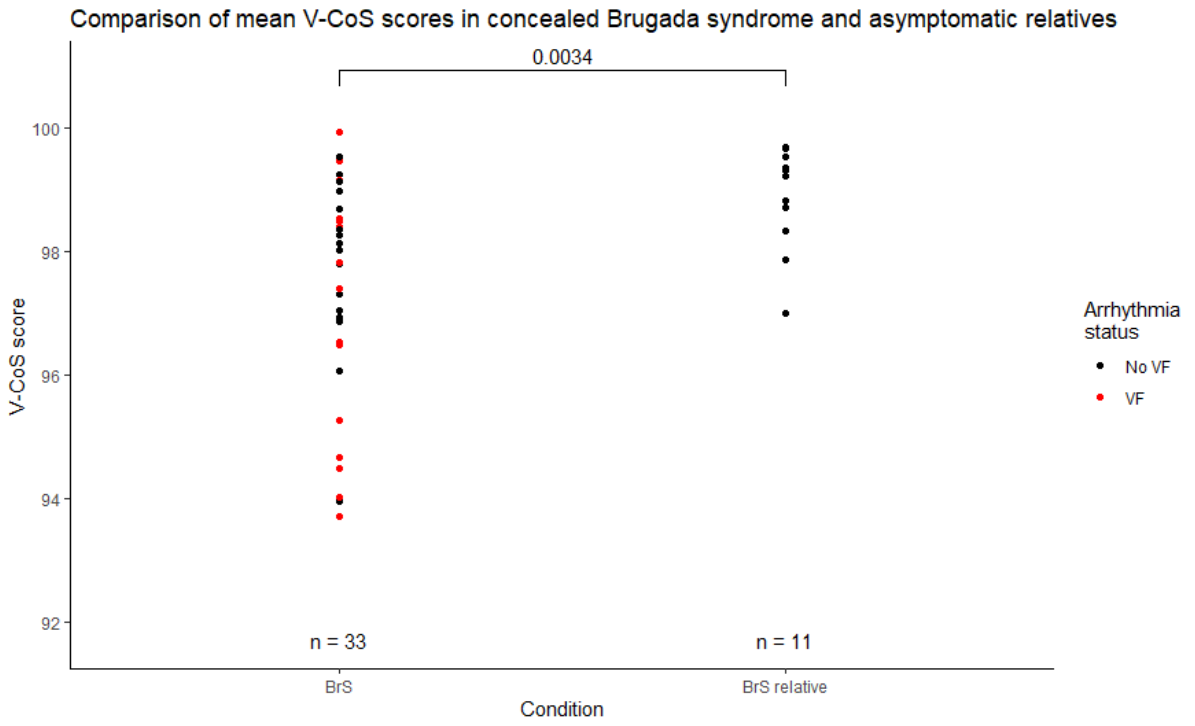

Figure 4.11: Comparison of mean ventricular conduction stability scores between patients with concealed Brugada syndrome (i.e. diagnosed using sodium channel blocker challenge test) and asymptomatic relatives with negative Ajmaline challenge testing. Ventricular conduction stability, V-CoS; Brugada syndrome, BrS.

V-CoS variability

V-CoS matrices were graphically expressed with consecutive peak exercise beats in the horizontal axis and consecutive recovery beats in the vertical axis. Colour scaling was standardized across all patients; V-CoS scores were shaded yellow if 100%, with increasing red intensity to a lower bound of 85%. All scores below 85% were shaded a constant red colour.

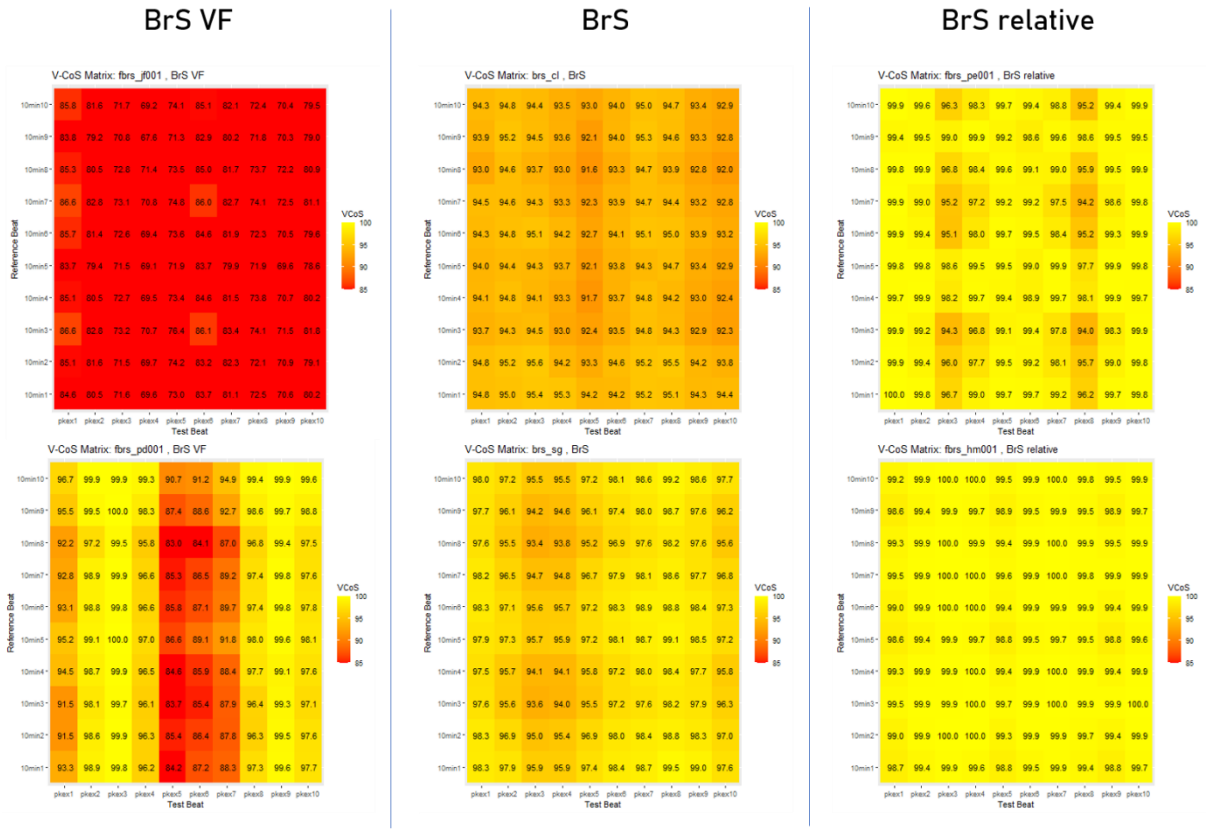

Figure 4.12: Six example V-CoS matrices: two from each condition group. All patients demonstrate some variability in V-CoS scores but this seems to be greater in patients with Brugada syndrome than asymptomatic relatives without Brugada syndrome. Ventricular conduction stability, V-CoS; Brugada syndrome, BrS; Ventricular fibrillation, VF; beats immediately post peak exercise (consecutive beat x), pkex(x); beats from full recovery (consecutive beat x), 10min(x).

Figure 4.12 shows six examples. Brugada syndrome matrices from both groups are more intensely red than the unaffected relatives, in line with the lower mean V-CoS results in the previous section. All groups demonstrate variability, but the magnitude appears to differ between groups. Variability appears to follow a pattern, with certain beats interacting to produce lower V-CoS scores than others.

Taking VF survivor fbrs_pd001 (Figure 4.12, bottom left) as a first example: peak exercise beat 5, 6, and 7 ('pkex5', 'pkex6', 'pkex7') appear to demonstrate the lowest overall V-CoS scores, particularly in their interaction with recovery beat 1 and 8 ('10min1', '10min8'). Similarly, unaffected relative fbrs_pe001 shows drops in V-CoS scores at a regular spacing, with the interactions between peak 3, 8 and recovery 3, 7 producing the lowest results.

The range of individual beat V-CoS comparisons was significantly larger in both groups of Brugada syndrome patients when compared to asymptomatic relatives without the condition. Mean ±SD V-

CoS range was 8.2 ±5.7% for VF survivors (p = 0.001 against relatives), 5.9 ±3.4% for Brugada syndrome without arrhythmia (p = 0.006 against relatives) and 2.9 ±1.6% for relatives. V-CoS range was not significantly different in the two Brugada syndrome groups (p = 0.24). This is graphically expressed in Figure 4.13.

The minimum of V-CoS can also be considered – significant differences were comparable: BrS VF and BrS could not be differentiated (90.6 ±7.3% vs 93.4 ±3.7%, p = 0.23) but BrS relatives could be differentiated from them both (96.8 ±1.6%, p = 0.0007, 0.003 respectively).

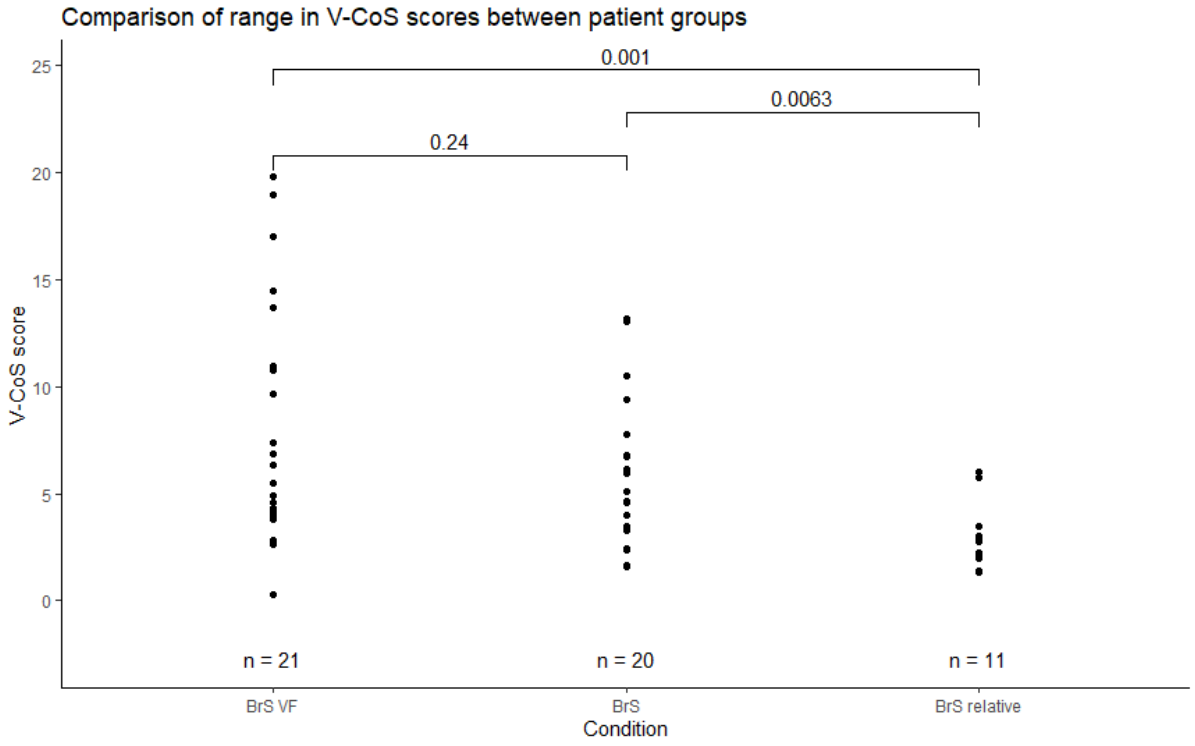

Figure 4.13: Comparison of the range of individual ventricular conduction stability scores between patient groups. Each V-CoS matrix is comprised of 100 individual beat pairings; the range quantifies the variability in these values which is significantly higher in patients with Brugada syndrome than without. Ventricular conduction stability, V-CoS; Brugada syndrome, BrS; Ventricular fibrillation, VF.

Utility of V-CoS for risk stratification

Performing receiver-operating characteristic analysis on this dataset results in an area under the curve of 0.56 (Figure 4.14). Despite the apparent lower p-value of differentiation by V-CoS Range (p = 0.24 vs 0.53), the area under the curve for this test is still only 0.61. Optimal threshold by Youden's method (Youden 1950) was 96.7% V-CoS, which resulted in a specificity of 85.0% and sensitivity of 42.8%. If the test performs clinically as observed in this small study, a low V-CoS score would imply a

high risk to the patient and encourage defibrillator implantation, but a high V-CoS score would not necessarily imply safety.

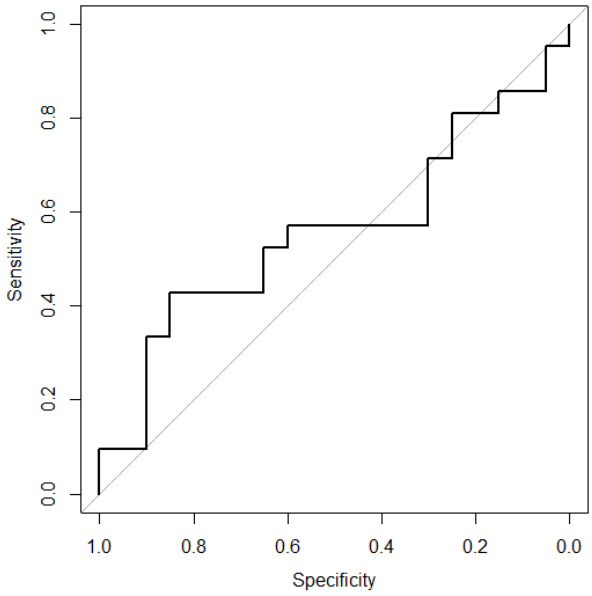

Figure 4.14: Receiver operating characteristic curve for a history of potentially lethal arrhythmia in Brugada syndrome

To understand the benefit of V-CoS as an additional risk factor to current guidelines, we considered which patients from our SCA cohort would have received an ICD recommendation with or without the V-CoS score (Table 4.2). If patients had either Type 1 ECG and syncope or a sub-threshold V-CoS score, a defibrillator was recommended.

Compared with the current IIa recommendation for ICD implantation in those with both spontaneous Type 1 ECG and syncope, considering V-CoS as an additional risk factor would improve the rate of ICD recommendation from 2/21 to 11/21 ($p = 0.034$ by McNemar's Test).

Table 4.2: Cardiac arrest survivors with Brugada syndrome, with V-CoS scores and risk factors. The current guideline recommendation for ICD is in the fourth column and the fifth column makes a recommendation based on a patient having either the two accepted risk factors, or a V-CoS score under the threshold defined by our receiver operating curve analysis. Ventricular conduction stability, V-CoS; Electrocardiogram, ECG.

Patient	V-CoS	Type 1 ECG	Syncope	Guideline IIa recommendation	Recommendation with V-CoS
fbrs_jf001	77.2	Yes	No	No	Yes
brs_dmp	93.7	No	No	No	Yes
brs_sh	94	No	No	No	Yes
fbrs_pe002	94	No	No	No	Yes
brs_dpa	94.5	No	No	No	Yes
fbrs_pd001	94.7	No	No	No	Yes
brs_vd	95.3	No	No	No	Yes
brs_pg	96.5	No	No	No	Yes
fbrs_cw001	96.5	No	No	No	Yes
fbrs_jc002	97.4	No	No	No	No
brs_yb	97.6	Yes	Yes	Yes	Yes
fbrs_az001	97.8	No	No	No	No
brs_mdd	98.4	No	No	No	No
brs_jdw	98.5	No	No	No	No
fbrs_pb001	98.5	No	No	No	No
brs_sk	98.7	Yes	Yes	Yes	Yes
fbrs_cf001	98.9	Yes	No	No	No
fbrs_ab002	99.2	No	Yes	No	No
fbrs_rh001	99.3	Yes	No	No	No
fbrs_ag001	99.5	No	No	No	No
brs_mm	99.9	No	No	No	No

Utility of V-CoS for diagnosis

V-CoS scores in concealed Brugada syndrome patients were compared with asymptomatic, unaffected Brugada relatives. Receiver operating characteristic analysis demonstrated an area under curve of 0.79, which is far superior to V-CoS's performance in differentiating cardiac arrest survivors.

The curve is plotted in Figure 4.17. The optimum threshold by Youden's method was 98.7% V-CoS, resulting in a specificity of 78.7% and a sensitivity of 72.7%.

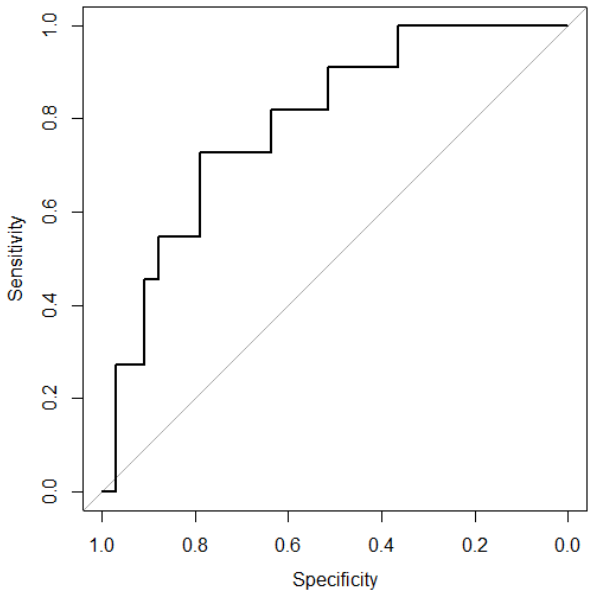

Figure 4.15: Receiver operating characteristic curve for a diagnosis of Brugada syndrome in patients with clinical suspicion of Brugada syndrome and normal baseline ECG.

Comparisons of non-sustained ventricular tachycardia with and without Brugada syndrome

One patient from our Brugada cohort experienced non-sustained ventricular tachycardia (NSVT) in the immediate post-exercise period of testing. For comparison, we draw upon a patient with benign right ventricular outflow tract tachycardia (RVOT-VT) attending for ECGi guided ablation who also experienced non-sustained ventricular tachycardia in the immediate post-exercise period of testing. This control patient was consented under the same ethics approval and contributes to the dataset of Chapter 4: Idiopathic ventricular fibrillation.

Our patient with Brugada syndrome was a 65-year-old male with a normal resting ECG; Brugada syndrome was diagnosed following out-of-hospital cardiac arrest by elicitation of a type 1 ECG pattern by sodium channel blockade. The RVOT-VT patient was a 49-year-old male with palpitations, but no syncope or features of haemodynamic compromise during his ventricular tachycardia. Both patients had normal echocardiography, normal resting ECG, and were free of competing medical conditions. Neither had taken cardiac medications for the 48 hours prior to the test. During non-

sustained tachycardia, neither had syncope, presyncope, hypotension, signs of pulmonary oedema or chest pain.

Sinus beats prior to NSVT were not suitable for mapping due to large amounts of movement artefact. Activation mapping during tachycardia indicated site of earliest epicardial breakout in the right ventricular outflow tract for both patients. Inspection of the early electrogram at this point revealed ST-segment elevation following a QR shaped electrogram in the Brugada syndrome patient, compared to no ST segment elevation following a QS shaped electrogram in the benign RVOT-VT patient. Following termination, this ST segment elevation was present during sinus rhythm in the Brugada patient, gradually reducing back to baseline by 5 minutes post exercise. A second exercise test reproducing matched sinus cycle lengths but no ventricular tachycardia in the Brugada patient failed to elicit ST segment elevation at any point in recovery. Figure 4.18 shows the relevant activation map and electrograms.

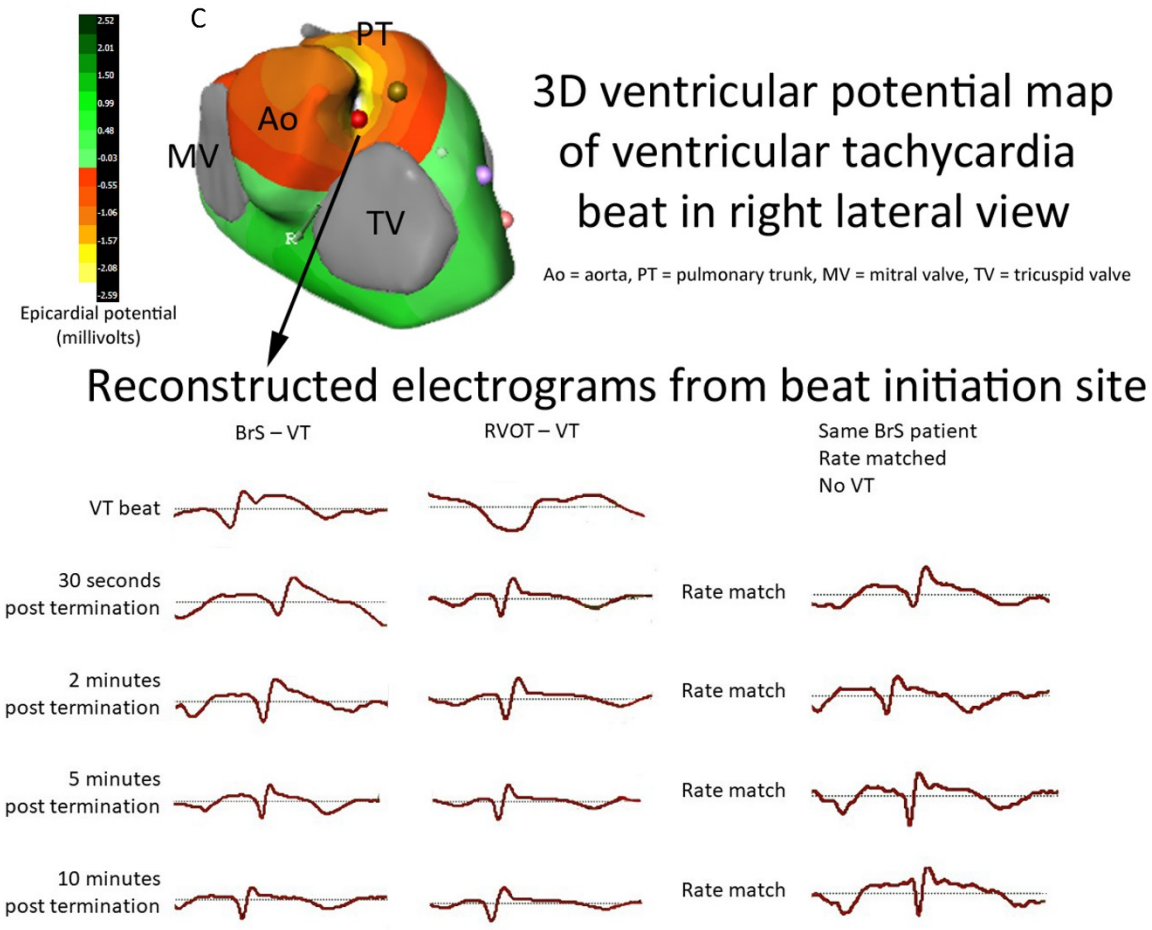

Figure 4.16: Non-sustained ventricular tachycardia (NSVT) originating from the right ventricular outflow tract (RVOT) was associated with coved ST segment elevation in a patient with Brugada syndrome, but not in a patient with benign RVOT-VT. ST elevation was also absent from matched rates in a prior exercise test performed by the Brugada syndrome patient where no NSVT was experienced. This figure is reproduced from a poster presentation by the thesis author, given to the Heart Rhythm Congress of 2019 (Birmingham, UK).

4.2.4 Discussion

A novel ECGi parameter proposed to be linked to risk of sudden death – ventricular conduction stability – was assessed in the largest population of Brugada syndrome patients to date and compared against unaffected relatives. Whilst Brugada syndrome patients could be differentiated from the unaffected relatives by V-CoS, those surviving potentially lethal arrhythmia could not be significantly discriminated from those without a personal history of such arrhythmia. Differentiation of affected patients from unaffected relatives was also possible for patients with concealed Brugada syndrome. A single instance of NSVT in a Brugada patient showed a possible association with ST

segment changes in the right ventricular outflow tract not seen in a control patient with NSVT, suggesting that in concealed Brugada syndrome, manifestation of ST segment elevation is a pre-requisite for arrhythmogenesis.

Rationale for exercise-induced V-CoS in Brugada syndrome

The model of arrhythmogenesis defined by the interaction of trigger and substrate is covered in the introduction to this thesis. It stands to reason that the substrate for arrhythmia may be more easily defined in the presence of an appropriate trigger or stressor. As a concept this is already used in the catheter ablation of epicardial substrates in Brugada syndrome, where sodium channel blockade is used to fully elucidate the mapped targets (Brugada, Pappone et al. 2015; Pappone, Brugada et al. 2017).

Sodium channel blockade as a challenge test is not without risk – 1.8% of patients undergoing the test suffer potentially life threatening sustained ventricular arrhythmia, with 0.4% of patients proving refractory to the first attempt at external defibrillation (Conte, Sieira et al. 2013). Furthermore, the incidence of sustained ventricular arrhythmia in this cohort of 503 patients did not appear to predict future life-threatening cardiac events. This implies that inherently low-risk patients undergoing ajmaline testing may be at unnecessary risk if re-exposed for research purposes. Prior to the commencement of our study, one patient at our centre suffered intractable ventricular fibrillation and did not survive despite optimal post-challenge care including cardiopulmonary bypass. For this reason, we felt that exposure of our research patients to ajmaline testing without clinical indication posed an ethically unacceptable risk.

Fever and restful states characterised by high vagal tone are the widely accepted precipitants of cardiac arrest in patients with Brugada syndrome (Mizusawa and Wilde 2012). The early post-exercise recovery phase can cause increases in ST elevation in up to 57% of patients with Brugada syndrome (Masrur, Memon et al. 2015). In one analysis of 93 patients with Brugada syndrome, ST segment augmentation following exercise was a significant risk marker for future arrhythmia (Makimoto, Nakagawa et al. 2010). The transition from sympathetic to parasympathetic dominance appears to have a role in modifying the Brugada arrhythmic substrate. In the small sample tested for V-CoS feasibility by Leong and colleagues, exercise testing differentiated sudden death survivors where tilt testing failed to produce a result (Shun-Shin, Leong et al. 2019). It could be interpreted that the amount of stress generated by postural change is simply not as great compared to exercise, or that parasympathetic activation affects Brugada syndrome independently of epicardial activation changes.

The data presented here confirms that in a larger population, exercise induced change in activation patterns is quantifiable by V-CoS. The magnitude of change is greater in patients with Brugada syndrome than their unaffected relatives but does not differentiate sudden death survivors from Brugada patients without ventricular arrhythmia.

Utility of V-CoS for risk stratification

The ideal test of V-CoS's utility in risk stratification of sudden death would be a large, prospective study with a long follow up. After 80 months of follow up, Sieira and colleagues found that 8.5% of their patients experienced a sudden death equivalent event (Sieira, Conte et al. 2017). Based on our V-CoS means of 96.1 ±4.8% and 97.7% ±1.6% for Brugada syndrome patients with and without lethal arrhythmia respectively, and an optimistic enrolment ratio of 1:10, more than 850 patients would be needed to achieve 80% power over 5 years or more. At current prices this would equate to a study cost exceeding £1.7 million for test consumables alone if the drop-out rate is zero.

We can draw some limited conclusions from our strategy of examining the survivors of ventricular fibrillation or sustained ventricular tachycardia. Cardiac arrest survival confers a twenty-fold risk increase for future potentially lethal arrhythmia (Sieira, Conte et al. 2017), thus making it the next best testing option to long-term prospective follow up. In our study, V-CoS failed to significantly differentiate cardiac arrest survivors, although the sample size may have been too small to detect a difference. Exclusion of patients with spontaneous Type 1 ECG or syncope from the BrS group without a sudden cardiac arrest history did not change this result.

A common question posed during the review of this data by colleagues was whether the study could be said to have a low post-hoc power. To assist this discussion, the calculation was performed for our results section, finding only 30.3% power. Post-hoc power became popular across multiple biological and social sciences in the late 1980s as a method of determining whether sample sizes were sufficiently large to reject the null hypothesis (Hodges and Schell 1988; Hoenig and Heisey 2001). However, it has been shown that post-hoc power has a 1:1 relationship with p-values – that is, non-significant *observed* p-values always result in low *observed* power (Hoenig and Heisey 2001; Levine and Ensom 2001).

The 95% confidence interval for a difference between the two groups does contain zero (-0.8 to 3.8% V-CoS by Welch's two-sample T-Test), indicating that we cannot rule out that there is no difference between the groups.

Even if there were a significant difference between the groups, a cut-off or range of values denoting high risk status is needed to achieve clinical utility in a single individual. Our ROC analysis demonstrates that discriminant ability is poor for V-CoS alone – the ROC AUC was 0.61, mainly let down by sensitivity – whilst at optimum threshold an 85% specificity could be achieved, the corresponding sensitivity was 42%.

Given the promising specificity, V-CoS could be used as an adjunct to traditional risk stratification. A patient presenting with any of spontaneous Type 1 ECG, syncope or a low V-CoS score could in the future be considered for defibrillator implantation – but further study would be essential to determine the efficacy of this approach in a prospective manner prior to clinical use.

Utility of V-CoS for diagnosis

As mentioned previously, the diagnostic test for Brugada syndrome can be fatal, and lower risk alternatives are desirable. The 12-lead 24- or 48-hour continuous ECG has gained traction as a diagnostic tool but is used more as a 'rule-in' rather than a 'rule-out' test.

Our study demonstrated that even with a normal resting ECG, there were significant differences in V-CoS between the unaffected Brugada relatives and (concealed) Brugada patients. ROC analysis suggested that greater than 70% sensitivity and specificity could be achieved in the diagnosis of Brugada syndrome in those with a normal resting ECG. The area under the curve (0.77) is similar to currently used risk stratification systems (O'Mahony, Jichi et al. 2014). If V-CoS were considered for a 'rule-in' test like the 12-lead continuous ECG, the number of potentially life-threatening sodium channel blocker challenges could be reduced.

During our testing, all patients completed the protocol without complication. Our data suggests that this test should be examined further for potential diagnostic use where concealed Brugada syndrome is suspected.

Variability of V-CoS scores

The introductory study of ventricular conduction stability described excellent reproducibility for identical cardiac cycles in 10 patients and good reproducibility for non-identical cardiac cycles in one patient (Shun-Shin, Leong et al. 2019). Our study took this further by assessing 10 consecutive exercise and 10 consecutive recovery beats against each other in a comparison matrix, generating 100 individual V-CoS calculations.

Our results demonstrate that variability is large and could pose a significant problem to clinical utility. Our V-CoS cut-offs for sudden death risk and diagnosis have been in the range of 97-99%. The range of an individual patient can approach 20% V-CoS, with the mean across all groups being 6.24%. This means that final score could be highly contingent on beat selection.

There does however appear to be a periodicity to the variability which could be exploited to improve reproducibility between beats. We have already done this by taking the mean V-CoS value, which across the group has been shown to produce a smaller range of V-CoS scores than the variability of some single patients. Further study would be needed to determine the optimal number of beats to sample, and the effect this would have on reproducibility.

There are three main factors to balance the number of beats selected for processing. The first and most easily overcome would be processing time. Currently, on a modern high specification laptop (Intel™ Core i7-10510U central processing unit @ 2.3GHz with 16 gigabytes of random-access memory), a single patient's matrix takes in the region of 20-30 minutes to process. This should increase by the square of the number of additional beats considered. The second is a consideration of when the sampling is taken from and how far into recovery the patient is at this point. Considering a very large number of beats would lead to increased bias toward the recovery phase as the patient returns to baseline following exercise. Future studies may go onto consider the change in V-CoS score and other ECGi metrics continuously over a period of several minutes or hours, with a range of stressors that may elicit different responses in different patients. The third factor increases in issue with the number of beats selected: screening signals for accuracy-compromising electrical noise becomes more difficult to perform consistently with larger volumes of data.

Examination of non-sustained ventricular tachycardia in Brugada syndrome

Ventricular arrhythmia in Brugada syndrome has not been panoramically mapped in this manner before. Our case report demonstrates that elements of the Brugada ECG pattern may be present in the peri-arrhythmic sinus rhythm beats, even in patients with a concealed resting ECG.

Catheter ablation is already being performed for patients with Brugada syndrome, but although arrhythmia inducibility is assessed, the characteristics of the arrhythmia are only rarely considered when choosing ablation targets (Haïssaguerre, Extramiana et al. 2003; Pappone, Brugada et al. 2017).

Triggers are studied when there is a consistent mechanism of initiation (Haïssaguerre, Shoda et al. 2002; Haïssaguerre, Extramiana et al. 2003; Hocini, Shah et al. 2015); this is not known to be true for

all Brugada patients. The utility of our finding reinforces prior experience of centres detecting raised Brugada ST segments in exercise states linking to adverse outcomes (Makimoto, Nakagawa et al. 2010; Masrur, Memon et al. 2015). It raises the possibility that detection of Type 1 patterns on ECGi as well as surface ECG could contribute to our idea of risk for an individual Brugada patient.

Limitations

A major limitation of exercise ECGi and the NSVT case is that the pre-arrhythmia beats were too affected by noise for effective mapping by CardioINSIGHT™ ECGi. Characterization of exercise sinus beats or the initiation of tachycardia could give us valuable insights into the mechanism and potential management options for such events. Our small retrospective study makes drawing definitive conclusions about the utility of V-CoS for risk stratification and diagnosis difficult. We have used a summary method proven to be more reproducible (V-CoS Mean), but this may underpower a test with already small effect sizes compared to the minimum of the V-CoS matrix.

4.2.5 Conclusion

Ventricular conduction stability allows the assessment of conduction heterogeneity induced by exercise. It may have some utility in diagnosis of Brugada syndrome in those with normal resting ECG, the test protocol being potentially safer than the gold-standard sodium channel blocker challenge. Although V-CoS alone appears to have little ability to differentiate cardiac arrest survivors from Brugada patients without sustained ventricular arrhythmia, combined assessment with traditional risk markers correctly classifies more cardiac arrest survivors than current guidelines.

Further study into V-CoS would be needed to ascertain prospective performance with or without traditional risk markers before use in a clinical environment. Additionally, the high variability of V-CoS measurements from different-beat selection needs further quantification; if possible, refinements in technique would be desirable to improve reproducibility. Current V-CoS methods require high levels of user interaction which could make analysis of very large numbers of beats difficult.

Chapter 5: Idiopathic ventricular fibrillation and periodic activation changes precipitated by exercise

5.1 Ventricular conduction stability and the arrhythmogenic substrate of idiopathic ventricular fibrillation

5.1.1 Introduction

Idiopathic ventricular fibrillation has, by definition, no known cause. Yet under all models of arrhythmogenesis, there must either be trigger or substrate to lead to this potentially lethal event. Following normal 12-lead electrocardiogram (ECG), continuous Holter ECG, echocardiogram, exercise testing, magnetic resonance imaging, angiography and drug challenge tests our current technology fails to appreciate trigger or substrate in most of these patients.

Some presenting with idiopathic VF may go on to receive a recognized cardiac diagnosis as their phenotype develops during follow-up; there is also an association between the genetics of known inherited cardiac conditions and idiopathic VF survivors even when the clinical phenotype is absent. Despite this, some patients remain without a diagnosis.

In a small subgroup, ECG monitoring in the period around cardiac arrest reveals repetitive premature ventricular beats which can be ablated, reducing the recurrence of arrhythmia (Haïssaguerre, Shoda et al. 2002). Direct contact epicardial mapping has revealed localized structural changes that may correspond to the arrhythmogenic substrate in another small study (Haïssaguerre, Hocini et al. 2018). Identification and characterization of this pathology are key for a better understanding of the generation of lethal arrhythmia, but the interaction with physiological states such as rest and exercise also require examination to fully appreciate methods of reducing future risk. In the Brugada syndrome we understand that certain drugs and fever elevate risk, and in hypertrophic cardiomyopathy, the role of intense exercise is known. This information aids our guidance of patients beyond the cardiac catheter laboratory and into lifestyle management.

Poor characterization of the idiopathic ventricular fibrillation survivor also limits the extent to which relatives can be protected. In Brugada syndrome and hypertrophic cardiomyopathy, family screening is established in the guidelines (Priori, Blomstrom-Lundqvist et al. 2015). Screening recommendations do exist for the relatives of sudden death victims with normal hearts (Behr, Dalageorgou et al. 2008), but for the relatives of sudden death survivors there is no current consensus – the index patient usually undergoes clinical examination instead. If current clinical testing cannot identify the substrate condition for arrhythmia, it is unlikely that these same tests will yield success in the patient's relatives.

For these reasons, understanding the mechanism of idiopathic ventricular fibrillation or identifying new conditions from this heterogenous group would assist management of both patients and families. Electrocardiographic imaging (ECGi) has already shown some promise in mapping localized and re-entrant activity during idiopathic ventricular fibrillation, identifying exercise induced changes in 7 patients surviving idiopathic ventricular fibrillation and repolarization changes at rest in a further 7 patients (Haïssaguerre, Hocini et al. 2018; Shun-Shin, Leong et al. 2019; Blom, Groeneveld et al. 2020).

A notable characteristic of ECGi studies of potentially lethal arrhythmia is that they all take place in survivors of previous cardiac arrest. This maximises the chance of identifying pathology in this rare group but poses the problem of retrospective observation: we cannot be sure that characteristics associated with past ventricular fibrillation should predict future sudden death. It is possible that ECGi changes seen in previous studies are a direct result, rather than predictive of future ventricular fibrillation (Haïssaguerre, Hocini et al. 2018; Shun-Shin, Leong et al. 2019).

Patients surviving ischaemic ventricular fibrillation with full revascularization and return of normal left ventricular function may be the appropriate control group to determine whether ECGi detected substrate in sudden death survivors is likely to be cause or effect. Mortality in patients with preserved left ventricular ejection fraction (>50%) surviving myocardial infarction is 4% in the first year (Perelshtein Brezinov, Klempfner et al. 2017). Approximately half of these deaths are due to sustained ventricular tachycardia or ventricular fibrillation (Uretsky and Sheahan 1997), and the rate falls exponentially following infarction (Solomon, Zelenkofske et al. 2005). Unlike Brugada syndrome and hypertrophic cardiomyopathy, ventricular fibrillation in the context of acute myocardial infarction does not appear to predict future arrhythmic death after the initial dangerous first few months (Volpi, Cavalli et al. 1990). Modern guidelines do not recommend implantable cardioverter defibrillators (ICD) in fully revascularized ischaemic ventricular fibrillation survivors with left

ventricular ejection fraction >40% (Priori, Blomstrom-Lundqvist et al. 2015; Al-Khatib Sana, Stevenson William et al. 2018).

To determine the risk-stratifying potential of ventricular conduction stability, it must be proven that abnormal results are linked with future risk of arrhythmia rather than previous ventricular fibrillation. We aimed to test the hypothesis that idiopathic ventricular fibrillation survivors (with a 31% pooled risk for recurrence (Ozaydin, Moazzami et al. 2015)) would demonstrate lower ventricular conduction stability than fully recovered ischaemic ventricular fibrillation survivors or controls without previous lethal arrhythmia. Our sub-hypothesis was that this effect would be greater in idiopathic ventricular patients with multiple arrhythmic events.

5.1.2 Methods

Patient selection

Thirty-eight patients were selected from our cohort.

1. 17 survivors of idiopathic ventricular fibrillation or haemodynamically compromising ventricular tachycardia ('idiopathic VF')
2. 10 survivors of ventricular fibrillation during ST-elevation myocardial infarction, with full revascularization, normal left ventricular function on echocardiography and return to full exercise capacity and asymptomatic status for >1 year ('IHD VF')
3. 11 patients attending for clinically indicated ablation of benign ventricular ectopy. These patients had normal echocardiography and/or MRI, had no family history of cardiac electrical disease and no symptoms of cardiac ischaemia ('VE').

Patients with any of the following exclusion criteria were not selected:

- Inability to provide consent
- Inability to perform exercise test
- Inability to cease anti-arrhythmic drugs prior to test
- Pregnancy or inability to rule out by last menstrual period or highly effective contraceptive
- Abnormal echocardiographic findings.

Exercise ECGi testing and epicardial reconstruction

Each volunteer underwent the following procedures as detailed in Chapter 2: Methods:

- Drug cessation if necessary
- Torso preparation and vest application

- Maximal Bruce protocol exercise testing
- Supine recovery for a minimum 10 minutes or to return of resting pulse rate
- Low dose-CT scan of chest
- Epicardial reconstruction of electrograms.

When selecting body surface signals from immediate post-exercise and 10 minutes of recovery, care was made to ensure the same array of electrodes were used in cardiac cycles compared to each other. In effect, if any surface electrode recorded too much artefact to be analysed in either exercise or recovery, it was excluded from analysis altogether.

Analysis of surface ECG markers

To examine for body surface recording signs of conduction pathology, QRS durations were measured for the peak exercise and recovery datasets. The vest output rather than conventional 12-lead was used to avoid possible timing issues with the exercise machine output. The positional equivalent of 12-lead ECG V2 was used (electrodes 71-76 on the CardioINSIGHT™ vest), with the first beat from the sample as the representative measurement.

Cardiac cycle selection

Peak exercise and 10 minutes of recovery were bookmarked at the time of testing. The first 10 cardiac cycles considered sufficiently artefact-free for analysis were selected following each of these bookmarks. Effort was made to adhere to bookmark timing as closely as possible, and heart rates were recorded for each of the sampled segments to determine if differences between the test groups existed.

Statistical analysis

The Wilcoxon-2 sample (also known as Mann-Whitney U test) was performed to compare any two groups. Comparisons between 3 groups were performed using the Kruskal-Wallis test.

Repeat statistical analysis was performed using the subgroup of idiopathic VF patients with a history of multiple arrhythmic events.

5.1.3 Results

Patient characteristics

All 38 patients successfully completed the testing protocol, reaching at least 85% of maximum predicted heart rate for age on the treadmill without complications. High detail characterization is available in 5.1.6 Supplementary Material. Cohort characteristics are examined here.

Gender balance was not uniform between groups, with both VF groups having significantly more males than the benign VE group (means 82.4%, 90% and 46.2% respectively, p = 0.034 by Kruskal-Wallis test). The idiopathic VF group were not significantly different from the IHD VF group (p=0.62) but VE patients were more often female than the other groups in pairwise comparisons (p = 0.043 vs idiopathic VF and p = 0.035 vs IHD VF).

Age was also significantly different, lowest in the idiopathic VF group, highest in the IHD VF group with the VE patients in the middle (means 39.1, 58.3 and 42.5 years respectively, p = 0.002 by Kruskal-Wallis test). The idiopathic VF group were not significantly different from the benign VE group (p = 0.63) but IHD VF patients were older than the other groups in pairwise comparisons (p = 0.025 vs benign VE and p = 0.0002 vs idiopathic VF).

Peak phase heart rates were significantly different between the groups, with IHD VF patients showing the lowest sampled heart rates of the three groups (p = 0.025 by Kruskal-Wallis test). This pattern was repeated in the resting phase heart rates (p = 0.024) with IHD VF patients again showing the lowest sampled heart rates.

Due to possibility of age difference confounding this result, sampled heart rates were compared to the patient predicted maximum heart rate by the $220 - Age$ formula. In both peak and recovery phase, there were no significant differences in percentage of predicted maximum heart rate (p = 0.32 and 0.78 by Kruskal-Wallis test). Although the mean heart rates of idiopathic VF patients in the peak sampling phase appeared to be higher than either IHD VF or VE patients (means 83.5%, 73.3% and 75.1% respectively), this was not significant in pairwise tests (p = 0.11 vs IHD VF and p = 0.22 vs VE).

QRS durations were not significantly different across the groups during either phase of data collection (p = 0.53 for exercise and p = 0.07 for recovery). The dataset is summarized in Table 5.1.

Table 5.1: Characteristics of volunteers undergoing electrocardiographic imaging exercise testing. Peak and recovery phase heart rates were those when signal was clean enough for measurement using the electrocardiographic imaging system. Ventricular fibrillation, VF; Ischaemic heart disease, IHD; Ventricular ectopy, VE; beats per minute, bpm; milliseconds, ms.

Parameter	**Idiopathic VF**	**IHD VF**	**VE**	**p-value**
Males (proportion)	82.4%	90%	46.2%	**0.034**
Age (years, mean)	39.1	58.3	42.5	**0.002**

Peak phase heart rate (bpm, mean)	150.6	119.0	132.5	**0.025**
Recovery phase heart rate (bpm, mean)	93.4	81.5	92.2	**0.024**
Peak phase % of predicted maximum heart rate (mean)	83.5%	73.3%	75.1%	0.32
Recovery phase % of predicted maximum heart rate (mean)	51.7%	50.4%	52.2%	0.78
Peak phase QRS duration (ms, mean)	95.1	92.6	91.2	0.53
Recovery phase QRS duration (ms, mean)	110.6	100	106.8	0.07

Mean V-CoS inter-group comparisons

Idiopathic VF survivors were significantly differentiated from both the IHD VF survivors and patients with benign ventricular ectopy (p = 0.023 and 0.0093 respectively). The IHD VF survivors could not be significantly differentiated from the benign VE group (p = 0.39). Mean ±SD V-CoS were 96.3 ±2.9% for idiopathic VF survivors, 98.1 ±1.0% for IHD VF and 98.5 ±1.2% for benign VE patients (Figure 5.1).

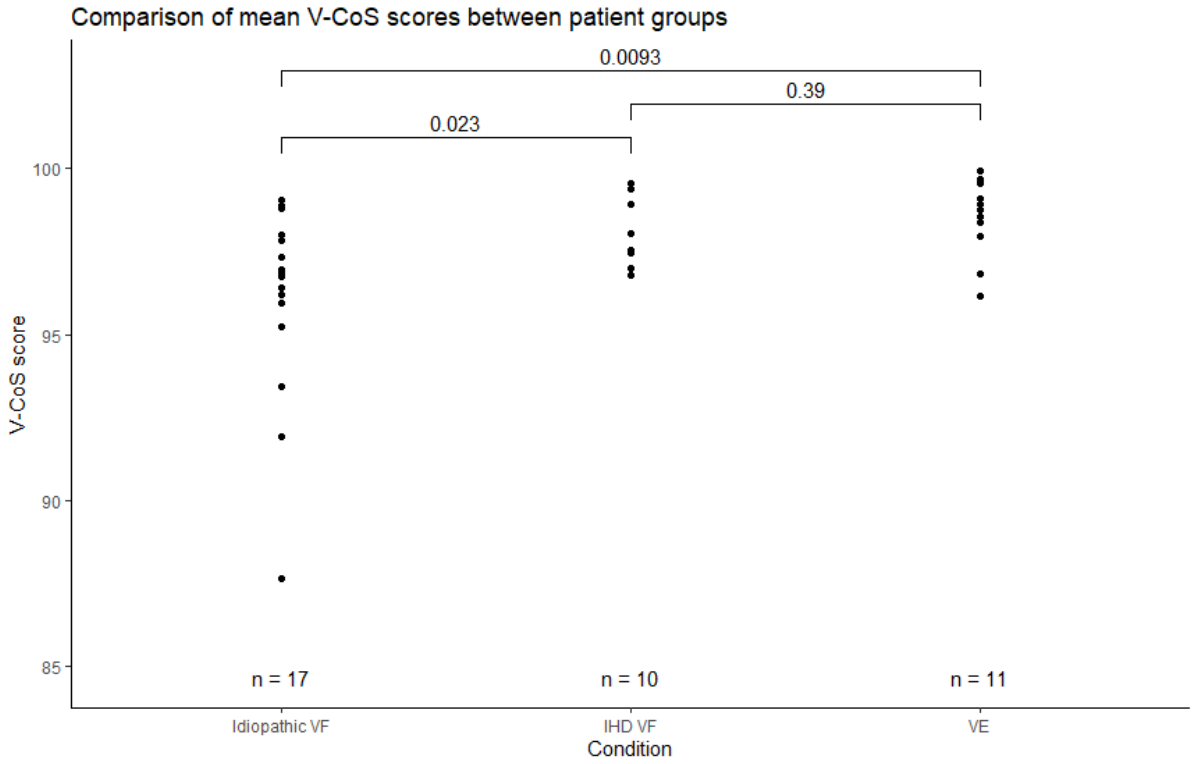

Figure 5.1: Comparison of mean ventricular conduction stability scores between survivors of idiopathic ventricular fibrillation, ischaemic ventricular fibrillation patients with full recovery of left ventricular function and full revascularization and patients attending for the ablation of benign ventricular ectopy. Ventricular conduction stability, V-CoS; Ventricular fibrillation, VF; Ischaemic heart disease, IHD, Ventricular ectopy, VE.

To determine whether a larger effect size could be seen in idiopathic VF patients with multiple arrhythmic events, patients with more than one clinical episode for ventricular fibrillation or appropriate ICD therapy were analyzed against those with a single such episode, with the benign ventricular ectopy group as a control.

Patients with multiple episodes of ventricular arrhythmia (n = 8) were significantly differentiated from the controls with benign ventricular ectopy (p = 0.005). In this sample size they could not be significantly differentiated from the single episode patients (n = 9), who in turn were not significantly differentiated from the benign ventricular ectopy controls (p = 0.17 and 0.11). Mean ±SD V-CoS scores were 94.9 ±3.7% for those with multiple episodes, 97.5 ±1.2% for those with single episodes and 98.5 ±1.2% for the VE group (Figure 5.2).

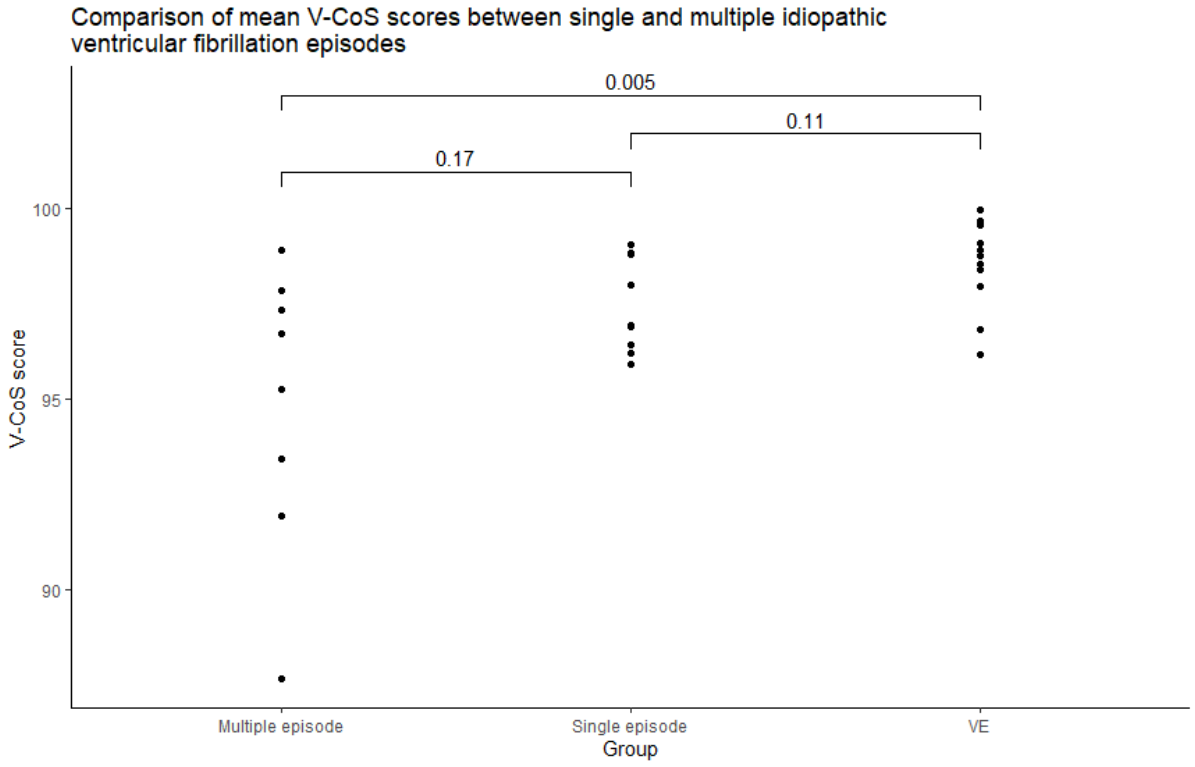

Figure 5.2: Comparison of mean ventricular conduction stability scores between survivors of idiopathic ventricular fibrillation experiencing either multiple or single episodes of ventricular arrhythmia, and the benign ventricular ectopy group as control. Ventricular conduction stability, V-CoS; Ventricular ectopy, VE.

V-CoS variability

V-CoS matrices were graphically expressed with consecutive peak exercise beats in the horizontal axis and consecutive recovery beats in the vertical axis. Colour scaling was standardized across all patients; V-CoS scores were shaded yellow if 100%, with increasing red intensity to a lower bound of 85%. All scores below 85% were shaded a constant red colour.

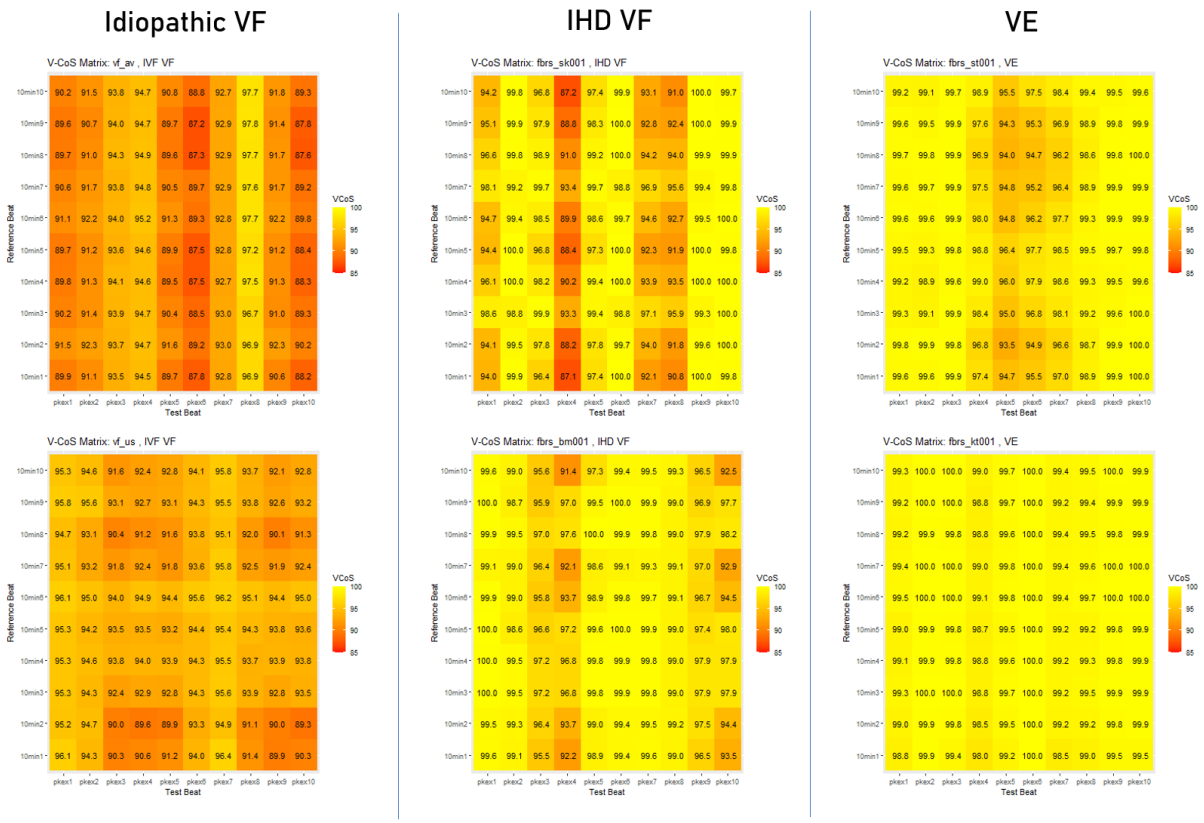

Figure 5.3: Six example V-CoS matrices: two from each condition group. All patients demonstrate some variability in V-CoS scores but this seems to be greater in patients with idiopathic VF than recovered ischaemic VF or benign ventricular ectopy. Ventricular conduction stability, V-CoS; Ventricular fibrillation, VF; Ischaemic heart disease, IHD; Ventricular ectopy, VE; beats immediately post peak exercise (consecutive beat x), pkex(x); beats from full recovery (consecutive beat x), 10min(x).

Figure 5.3 shows six examples. Idiopathic VF matrices are more intensely red than the IHD VF matrices, which are in turn more intensely red than the VE matrices, reflecting the differing means between the groups. All groups demonstrate variability, with the magnitude varying between groups. Variability follows a periodic pattern, with certain beats interacting to produce lower V-CoS scores than others.

Idiopathic VF survivor vf_av (Figure 5.3, top left) has the lowest V-CoS scores from interaction between peak exercise beats 5, 6 and 10 (‘pkex5’, ‘pkex6’, ‘pkex10’) and recovery beats 1, 4 and 8 (‘10min1’, ‘10min4’, ‘10min8’). IHD VF survivor fbrs_bm001 has strong interactions between peak exercise beats 3, 4, 9 and 10, and recovery beats 1, 2, 6, 7 and 10. VE ablation patient fbrs_st001 has repeating ‘islands’ of low V-CoS scores centred around the interaction between peak exercise beat 5 and recovery beats 2 and 8. Even in the matrix of VE ablation patient fbrs_kt001, it is possible to see very subtle periodicity between absolute scores of 97-100% V-CoS.

The range of individual beat V-CoS comparisons was larger in the idiopathic VF survivors than the benign VE patients (p = 0.00047) but not against the IHD VF survivors (p = 0.29). The IHD VF ranges approached significance against the ventricular ectopy patients (p = 0.051). Mean ±SD V-CoS ranges were 8.1 ±3.5% for idiopathic VF survivors, 6.5 ±3.8% for IHD VF survivors and 3.7 ±2.3% for VE ablation patients (Figure 5.4).

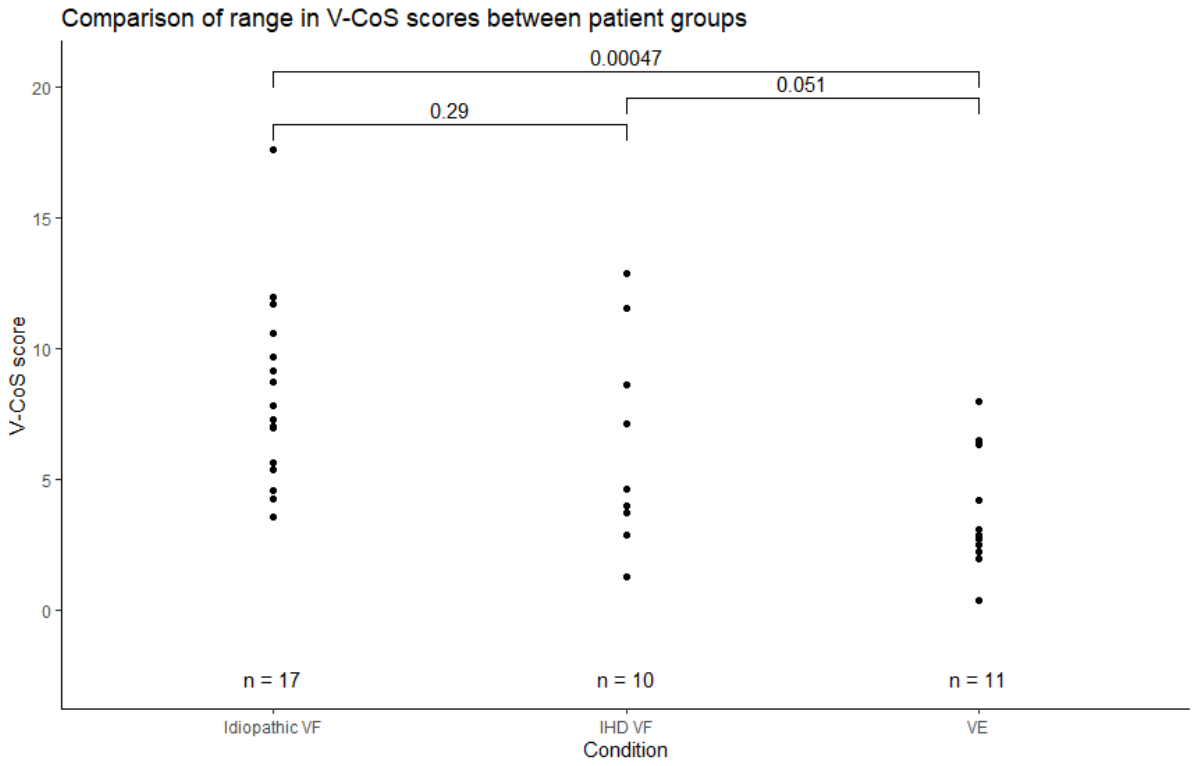

Figure 5.4: Comparison of the range of individual ventricular conduction stability scores between patient groups. Each V-CoS matrix is comprised of 100 individual beat pairings; the range quantifies the variability in these values which is significantly higher in patients surviving ventricular fibrillation than controls. Ventricular conduction stability, V-CoS; Ventricular fibrillation, VF; Ischaemic heart disease, IHD; Ventricular ectopy, VE.

5.1.4 Discussion

In this chapter, ventricular conduction stability was assessed for the ability to differentiate patients surviving idiopathic ventricular fibrillation, ischaemic ventricular fibrillation and those attending for the ablation of benign ventricular ectopy. The idiopathic ventricular fibrillation group had overall lower mean V-CoS scores than the other groups. V-CoS variability between beats was again high, with the idiopathic VF group having significantly greater variability than the VE group, and the IHD VF patients approaching significance over the VE group.

Another arrhythmogenic substrate for idiopathic ventricular fibrillation

Invasive mapping has previously demonstrated one potential substrate for idiopathic ventricular fibrillation, which was then used in targeting radiofrequency ablation directed at reducing arrhythmia episodes (Haïssaguerre, Hocini et al. 2018). Before us, Leong et al. demonstrated changes in the activation recovery intervals during treadmill testing seen on ECGi but not on the surface ECG (Leong, Ng et al. 2018). Most recently, Blom et al. demonstrated steep repolarization time gradients and flattened T waves in the idiopathic VF patients not seen in their single control patient (Blom, Groeneveld et al. 2020). We present another potential substrate: the largest demonstration to date of exercise-induced changes in whole-heart activation as quantified by the V-CoS score.

Different papers finding different electrical properties of the idiopathic VF myocardium is not necessarily conflicting data. The results within our own idiopathic VF group are widely spread, with some patients as high as 99% V-CoS and as low as 87%. This implies that the arrhythmogenic substrate within our group must vary widely between patients. This is an expected result, as the idiopathic VF group could contain multiple undiscovered conditions. In the future, patients with a low V-CoS might be studied in sufficient number to identify common geno- and phenotypes and discover a new condition. Some of these patients may go on to develop a recognized cardiac phenotype. Further work would be needed to achieve this.

Single- versus multiple-event survivor V-CoS scores

Additionally, patients with multiple events seem to form an even lower V-CoS score group than their single-event counterparts. The statistical relationship between multiple- and single-event cardiac arrest survivors does not reach significance, but the differentiation from the control group is more significant in multiple-event survivors. There are two possible conclusions from this information. If we assume that the sub-analysis was appropriately powered to detect a result, we should conclude that patients with only a single episode of idiopathic VF are not significantly different from controls. Ventricular fibrillation is inducible with aggressive programmed stimulation in normal hearts (Avitall, McKinnie et al. 1992). Outside of the cardiac catheter laboratory, harsh stimuli such as commotio cordis and electrocution can initiate ventricular fibrillation in the normal heart (Link 2012; Waldmann, Narayanan et al. 2018). For some survivors of idiopathic VF, it is possible that a rare and previously undetected external stimulus initiates VF, and they will remain arrhythmia free for as long as they do not encounter this trigger again.

However, the sub-analysis is small: a comparison of 8 multiple-event survivors and 9 single-event survivors. It is likely that the sample size is underpowered to detect the difference between single-event survivors and both the control group and multiple-event survivors. If we assume that the sample is underpowered, it becomes possible that V-CoS score describes the extent rather than the binary presence of an arrhythmic substrate. If triggers occur to all randomly, we would expect a patient group with larger arrhythmic substrate to suffer a greater number of arrhythmias. The low mean V-CoS score in the multiple-event group appears to support this idea.

The arrhythmic substrate of ischaemic VF survivors

Ventricular fibrillation is a well-known sequela of myocardial infarction, but arrhythmia susceptibility in patients with acute myocardial infarction is not uniform. Familial sudden death has been shown to be a risk factor in two case-control studies of patients presenting with ST-elevation myocardial infarction (Dekker, Bezzina et al. 2006; Jabbari, Engstrøm et al. 2015). The GEnetic causes of Ventricular Arrhythmias in patients with first ST-elevation Myocardial Infarction (GEVAMI) study enrolled 219 cases of patients suffering STEMI complicated by VF and compared to 441 STEMI survivors without VF. First-degree familial sudden death conferred a higher risk of VF with STEMI (odds ratio 1.80, CI 1.27-2.56, p = 0.001).

In the Arrhythmia Genetics in the Netherlands (AGNES) cohort, 330 cases of patients suffering STEMI complicated by VF were compared to 372 age, gender, and infarct size matched controls. Patients with previous MI, known congenital or structural heart disease, severe comorbidities, electrolyte disturbance, trauma, surgery, or coronary artery bypass grafting within 4 weeks were excluded. Despite familial prevalence of cardiovascular disease being similar in the relatives of case and control groups, the percentage of cases with at least one sudden death in first degree relatives was significantly higher than control (43.1% vs 25.1%). Genome-wide study of an extension of this cohort revealed an association at 21q21 with an odds-ratio of 1.78. This was co-located with the coxsackie-adenovirus receptor gene (CXADR), also implicated in myocarditis and dilated cardiomyopathy (Bezzina, Pazoki et al. 2010). Another study found mutations in SCN5A with acute MI complicated by ventricular fibrillation, but only in a small proportion of cases (Boehringer, Bugert et al. 2014). In summary, whilst the association of familial sudden death with VF in STEMI is known, the mechanism is unclear.

In the present study, we have employed our IHD-VF volunteers as a control group who have significantly greater mean V-CoS scores than idiopathic VF survivors. Clinically, this group are

considered at low risk of future arrhythmia, and the non-significant difference in mean V-CoS against patients with benign VE appears to support this notion.

However, the range in V-CoS scores for an individual IHD-VF survivor is not distinguishable from the idiopathic VF patients, and approaches significance against the benign VE patients. As the sample sizes are small, we cannot rule out low study power, so it remains unclear whether these patients have an underlying electrical substrate which can support VF in conjunction with a trigger such as myocardial infarction. Although echocardiography did not demonstrate the gross abnormalities known to be a risk factor for sudden arrhythmic death, it is possible that the IHD-VF group have substrate abnormalities that would be detected on detailed MRI or histopathology studies.

Variation in V-CoS scores

Wide intra-patient variation was seen in all patient groups, greatest in the idiopathic VF group, then the IHD-VF and then benign VE group. This further supports the use of summary statistics to define the V-CoS value for an individual patient. Significance was only reached between the idiopathic and benign VE groups.

The pattern of periodicity seen in this patient cohort is very similar to that seen in the Brugada cohort in the previous chapter. This, combined with the similar observation of lower mean scores in ventricular fibrillation survivors, has two potential explanations.

First, that survivors of Brugada VF and idiopathic VF have a similar final common pathway toward death, and this is detectable by the V-CoS score. Ventricular fibrillation can initiate when there is spatially heterogenous delay in conduction; this heterogeny would mean that local activation times in different beats would follow different patterns, a change which V-CoS is designed to detect. Periodicity in altered conduction may also have follow-on effects on repolarization, which may be predictive of imminent arrhythmia (Oosterhoff, Tereshchenko et al. 2011). Since periodicity is seen in all groups, it may be a physiological phenomenon which is more marked in those further along the spectrum of arrhythmia vulnerability.

Second, that the periodicity is a result of the experimental method. This is plausible because it is seen in almost all experimental subjects, regardless of pathology, although more marked in the VF survivors. Patterns in the V-CoS matrix appear to reach a nadir every 3-5 beats, giving a frequency at 120-150 beats per minute of 0.3-1 Hz. Further study would be needed to elucidate any sources of noise in the experimental method that could produce this periodicity.

Limitations

Like the limitations of Chapter 4, small group sizes mean that we cannot be confident that there is no difference between two groups where the confidence in the effect size is >0.05. Patients were primarily characterized by echocardiography to reflect current guidelines on arrhythmia risk stratification from both European and American societies. However, from a mechanistic viewpoint, full MRI characterization would have been preferable, and MRI derived metrics of tissue/scar characterization may correlate with our findings. This would be a good opportunity for future study.

5.1.5 Conclusion

Periodic loss of uniform conduction can be induced by exercise and detected by ventricular conduction stability. Less uniformity is seen in patients surviving idiopathic ventricular fibrillation, which may be a substrate for future potentially lethal arrhythmia. This is seen to a lesser extent in survivors of ischaemic ventricular fibrillation who have made a full recovery and patients attending for the ablation of benign ventricular ectopy. Less conduction heterogeneity in recovered ischaemic patients and those with benign ectopy tallies with the observation that future cardiac arrest is uncommon in these groups.

Periodic patterns occur in all pathology groups, but it is currently unclear whether this is a true physiological phenomenon or a product of the experimental technique. Further study is required to determine the answer.

5.1.6 Supplementary Material

Ischaemic VF

Count	10
Age (years)	58.3 ±8.0
Gender M:F	9:1
VF during presentation	10/10
Anginal symptoms in year prior to testing	0/10
ECG at testing	3 normal sinus rhythm 3 residual ST elevation (<1mm) 1 anterior early repolarization 3 residual T wave inversion

MRI	Performed in 1, late Gadolinium enhancement of papillary muscle but no regional motion abnormality
Normal LV function, no regional wall motion abnormalities on echocardiogram	10/10
Infarct location/revascularization	2 LAD 2 Circumflex/OM 2 RCA/PDA 4 triple vessel disease
Mean peak troponin I (ng/L)	15387 ±20919

Brugada relatives

Count	11
Age (years)	45.5 ±11.0
Gender M:F	8:3
ECG at testing	8 normal sinus rhythm 1 RSR' in V1-2 1 early repolarization in V1-2 1 W pattern in V1
Echocardiogram	10 normal 1 bicuspid aortic valve, otherwise normal
MRI	Performed in 1, normal
Coronary assessment	10 normal ETT 1 normal ETT and DSE
Negative Ajmaline challenge	11/11
Family history	4 (aborted) sudden death 4 spontaneous Type 1 ECG 3 concealed Type 1 ECG

Idiopathic VF survivors

Count	14

Age (years)	36.9 ±7.5
Gender M:F	11:3
Presentation rhythm	14 VF
Lifetime events	5 multiple events 9 single event
ICD implanted at time of test	14/14
Normal echocardiography (including LV function)	14/14
Normal ETT/adrenaline challenge	14/14
Normal coronary angiogram/CT CA	14/14
MRI	10 normal 1 mild LV volume increase in context of multiple ectopy 1 subepicardial late Gadolinium enhancement 1 too claustrophobic 1 transient apical hypokinesia post arrest with full resolution on subsequent echo
Monomorphic ectopy identified	5/14
Ajmaline	14/14 negative
ECG	5 normal sinus rhythm 3 T wave abnormalities 3 Early repolarization 2 RBBB 1 frequent ectopy
Index arrhythmia context	3 walking 2 intense exercise 3 at rest but awake 3 during sleep 1 after alcohol 1 practicing yoga 1 not identified
Genetics	5 gene negative

	4 with VUS (AKAP9; KCNH2; TMEM43, MYBPC3) 5 not submitted for testing

Ventricular ectopy ablation

Count	11
Age (years)	44.5 ±14.3
Gender M:F	6:5
ECG (excluding ectopy)	9 normal sinus rhythm 1 RBBB 1 T wave inversion V1-4
Echocardiogram	10 normal 1 mitral valve prolapse, otherwise normal
MRI	3 normal 2 mild LV dysfunction in the context of ectopy without evidence of fibrosis 6 not performed
Ectopy location	8 RVOT 1 LVOT 1 Basal septal LV 1 inferior LV
Ectopy burden	17.2 ±10.2%

5.2 The effect of simulated bio-electrical noise on ventricular conduction stability

5.2.1 Introduction

In both chapter 4 and 5, remarkably similar periodic patterns were seen in the V-CoS matrices of all patients. The magnitude of the changes was greater, and the mean score lower in patients with idiopathic VF than their ischaemic VF and benign VE counterparts, as well as in Brugada syndrome patients over their unaffected relatives.

It is possible that idiopathic VF and Brugada syndrome share a common arrhythmic substrate – both diagnosed in patients with structurally normal hearts and associated with potentially fatal ventricular arrhythmia. The periodic loss of uniform conduction is present to a lesser extent in our control patients. As V-CoS is the percentage concordance of local activation times over the myocardium, loss of uniform conduction implies that the electrogram QRS complex is altered.

The alterations in QRS could be due to intrinsic conduction changes of the diseased myocardium, but it is also plausible that movement artefact from exercise is the cause of these QRS changes. Like many other cardiac signal processing packages, both CardioINSIGHT and the custom software used to calculate V-CoS employ filters to improve signal quality prior to calculations. These filters can, in themselves, cause inaccuracies of measurement (Buendía-Fuentes, Arnau-Vives et al. 2012; Bear, Dogrusoz et al. 2018).

Relatively lower V-CoS scores in the matrices can be visually estimated to occur once every 3-5 cardiac cycles. At heart rates between 120-150 beats per minute this corresponds to a period of between 1-3 seconds. Baseline wander has a frequency of 0.5-0.6Hz, making it a likely candidate for the cause of the periodicity. This baseline wander is also visually more extreme when the patients have recently completed peak exertion, due to increase in ventilatory depth and positional changes as a supine position is attained.

Our aim was to perform a simulation study to help understand whether exercise-induced changes in measured activation times result from true QRS changes, or the interaction between noise and filters in our software. The hypothesis was that changes in V-CoS induced by exercise could not be replicated by periodic noise added to cardiac cycles.

5.2.2 Methods

Patient selection

All 38 patients from the cohort were used to provide data for offline simulation. All underwent Bruce protocol treadmill testing with ECGi recording as detailed in the methods 5.1.2.

Initial measurements

10 consecutive cardiac cycles immediately following peak exercise and 10 consecutive cardiac cycles following 10 minutes of recovery were collected for analysis. V-CoS matrices were calculated for the exercise vs recovery beats, producing 100 exercise-induced V-CoS scores. The recovery beats were then compared to themselves, producing 100 recovery-baseline V-CoS scores.

Simulated measurements

To closely replicate baseline wander, noise was extracted from the exercise traces using a low-pass finite impulse response filter, frequency 1Hz, order 600 and sampling rate 1kHz. ECGi datasets are formed of one electrogram $\frac{Voltage}{Time}$ graph per reconstructed point in the epicardial mesh. For a numeric array of m electrogram traces by n samples, the filter resulted in an identically sized numeric array of m noise traces by n samples.

One-dimensional linear interpolation was used to ensure noise trace arrays had identical length to the recovery trace. Then, each individual noise trace was added onto its counterpart recovery trace. A synthetic electrogram with the QRS properties of recovery but noise characteristics of exercise. These synthetic, patient specific, noise-augmented traces were then compared to the unmodified recovery traces to calculate a final, simulated noise V-CoS matrix.

The process is summarized in Figure 5.5.

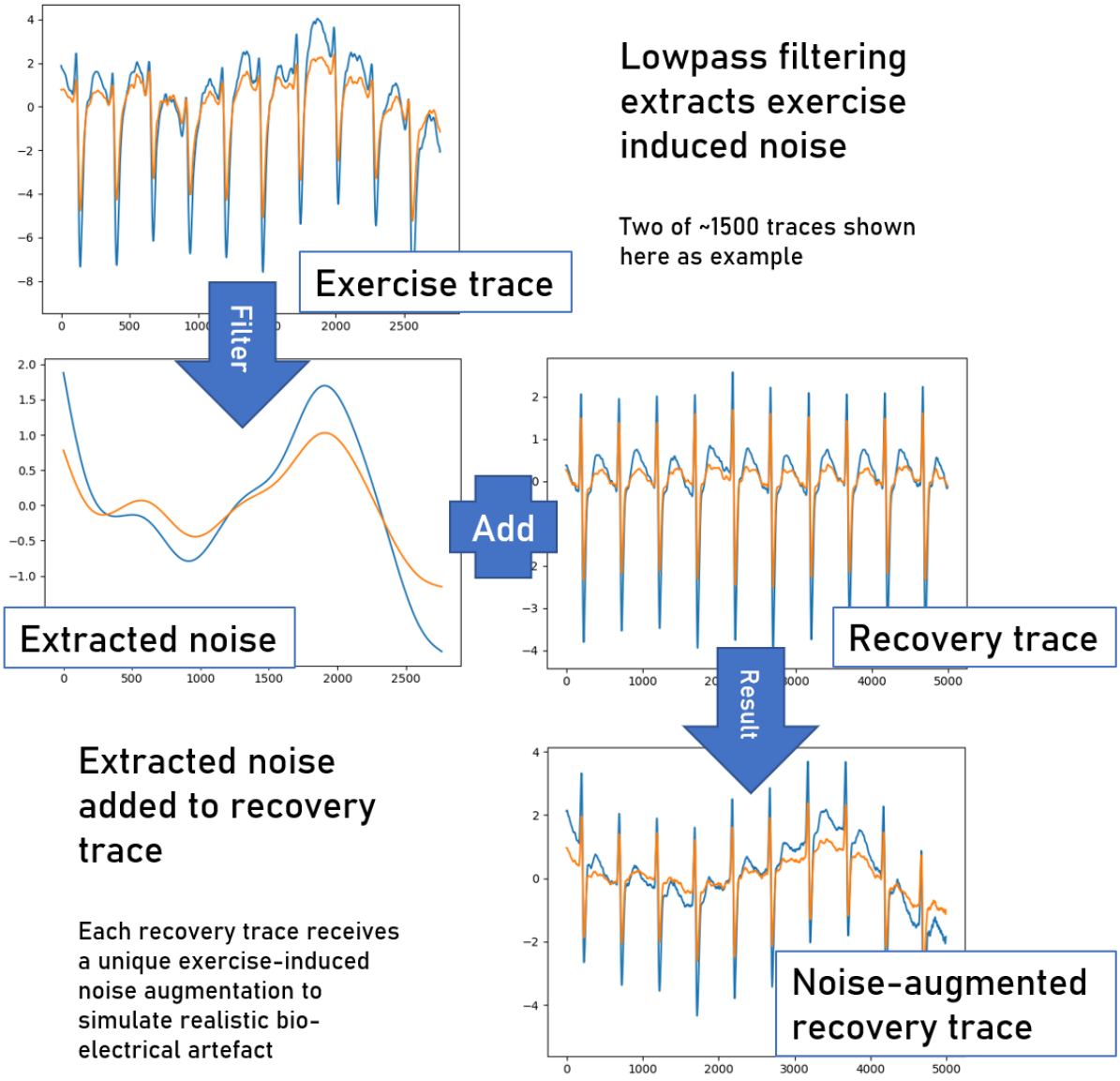

Figure 5.5: Summary of the noise simulation method. For a given patient, the exercise trace is lowpass filtered to produce extracted noise. Following interpolation, this is added to the recovery traces producing a synthetic electrogram with the QRS complex of recovery but the baseline noise characteristics of exercise. This augmented recovery trace is then used for comparison in the V-CoS software.

Statistical analysis

In summary, for each patient, three V-CoS matrices were constructed for statistical analysis:

1. True exercise (versus recovery) matrix
2. Noise-augmented synthetic (versus recovery) matrix
3. Recovery (versus recovery) matrix as a control.

True exercise, true recovery and noise-augmented recovery V-CoS matrix values were compared using t-test.

5.2.3 Results

True exercise induced V-CoS scores were lower than both noise-augmented and true recovery V-CoS scores ($p < 2.2 \times 10^{-16}$ for both comparisons). Noise-augmented V-CoS scores were not significantly different from true recovery V-CoS scores ($p = 0.47$). Mean ±SD V-CoS scores were 97.4 ±3.0% V-CoS for true exercise, 99.9 ±0.19% V-CoS for noise-augmented synthetic and 99.9 ±0.18% V-CoS for true recovery.

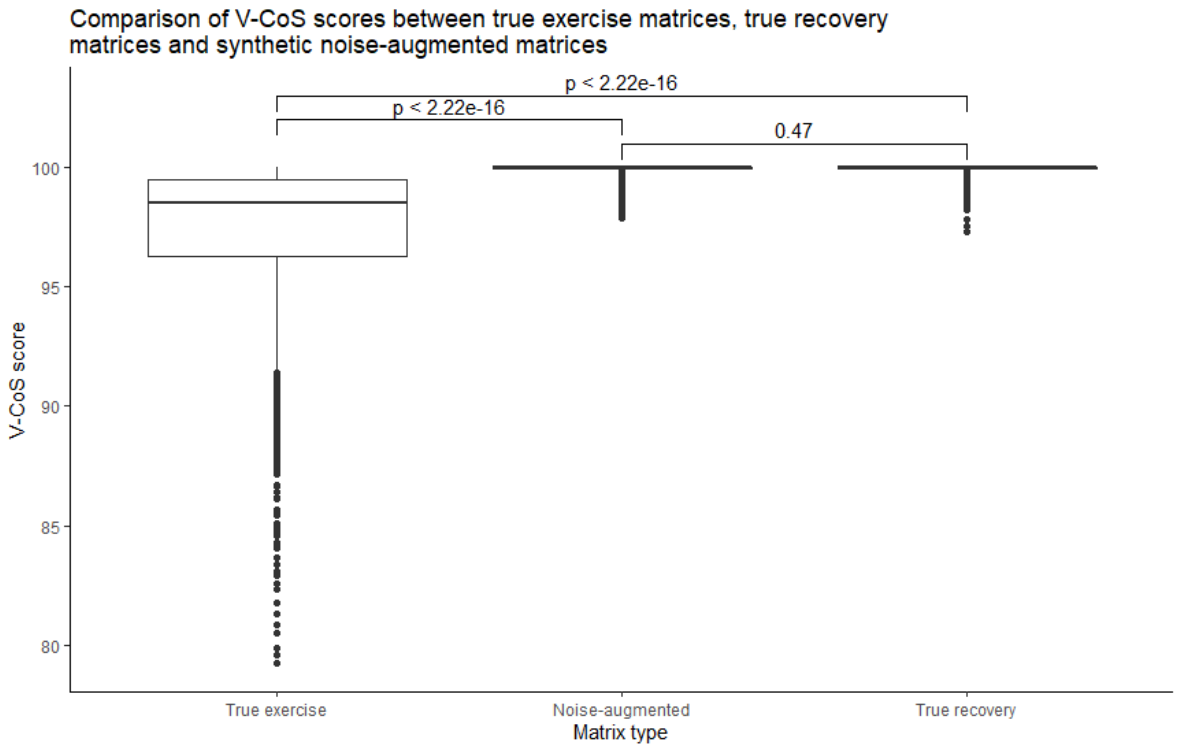

Figure 5.6: Comparison of the individual ventricular conduction stability values between true exercise scores – i.e. those used in patient differentiation in Chapter 5.1 – and those with the bio-electrical noise of exercise added onto the recovery QRS characteristics to form synthetic signals. V-CoS values from the recovery scores are provided for comparison. Ventricular conduction stability, V-CoS.

V-CoS matrices were graphically expressed with consecutive peak exercise beats in the horizontal axis and consecutive recovery beats in the vertical axis. Colour scaling was standardized across all patients; V-CoS scores were shaded yellow if 100%, with increasing red intensity to a lower bound of 85%. All scores below 85% were shaded a constant red colour.

For each patient, the appearance of three V-CoS matrices could be compared. One patient from each experimental group is displayed in Figure 5.7.

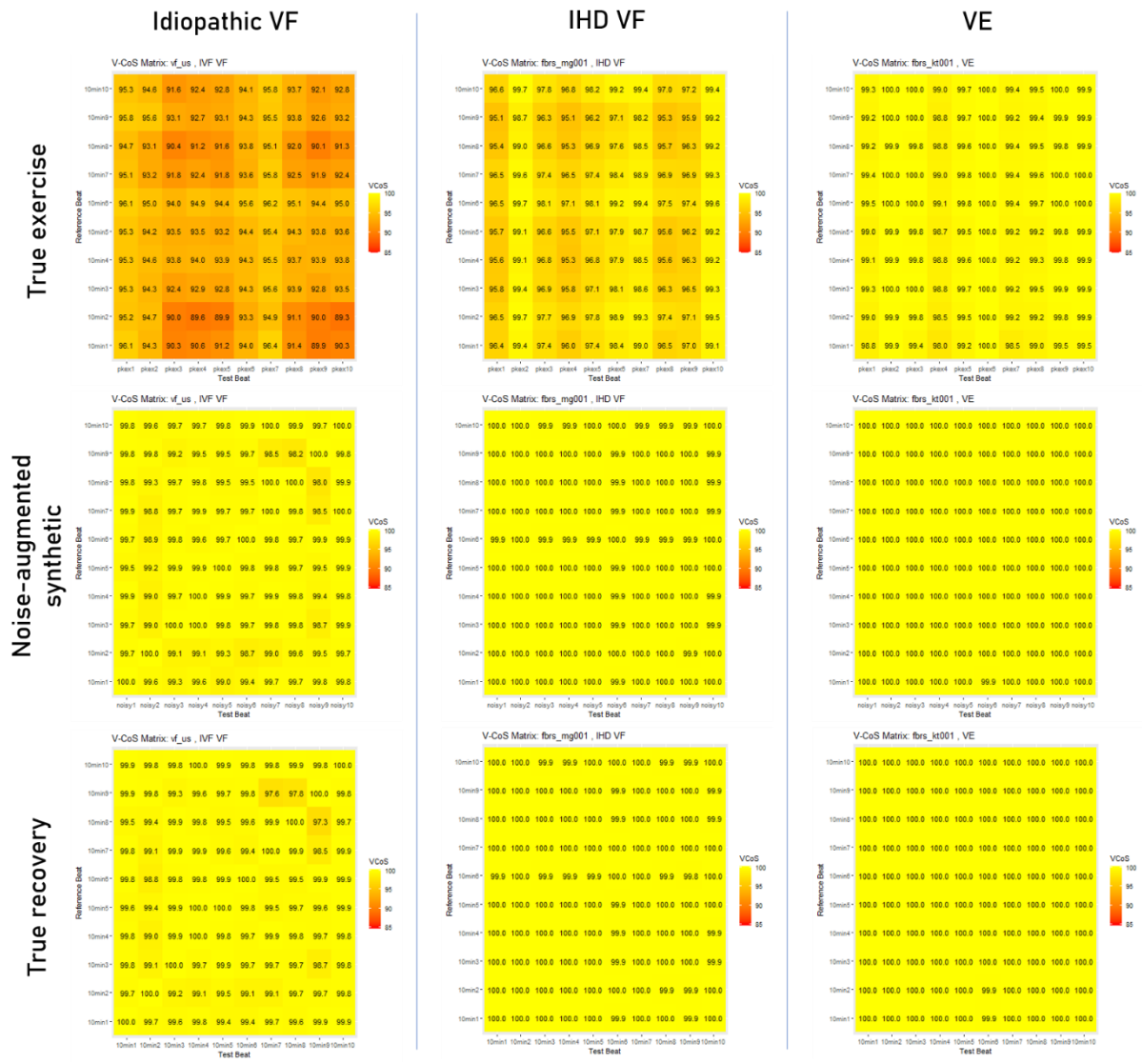

Figure 5.7: Three V-CoS matrices for each of 3 patients: one survivor of idiopathic ventricular fibrillation, one ischaemic ventricular fibrillation survivor and one patient with benign ventricular ectopy. Each patient occupies a column; the first row demonstrates V-CoS scores when exercise and recovery beats are compared, the second when a synthetic combination of recovery beats and extracted bio-electrical noise are compared to non-augmented recovery beats and the third row comparing non-augmented recovery beats to each other. The exercise V-CoS matrices demonstrate lower scores with periodic loss of uniform conduction, absent in recovery matrices. The synthetic matrices cannot replicate the exercise scores, suggesting that periodic noise is unlikely to be the cause of periodic low V-CoS scores.

In the idiopathic VF patient, the differences between the matrices are the starkest. The true exercise matrix (top left) demonstrates periodic drops in V-CoS score as shown in the results for section 5.1.3. The noise-augmented matrix (middle left) and the recovery matrix (bottom left) are near identical in

appearance, with some variation in V-CoS score but not to the same magnitude as the true exercise matrix. The difference between the noise-augmented matrix and the true exercise matrix is greatest in the idiopathic VF patient, followed by the IHD VF patient and then the benign VE patient.

5.2.4 Discussion

Idiopathic VF, Brugada syndrome, ischaemic heart disease and healthy controls all demonstrate periodic loss of uniform activation in the 0-1Hz range, although the magnitude is higher in ventricular fibrillation survivors. In this simulation experiment, we extracted bio-electric noise in the 0-1Hz range and added it to V-CoS comparisons with little to no periodic loss of activation. These noise-augmented comparison matrices failed to replicate the V-CoS changes induced by exercise.

Many biological phenomena are periodic, or oscillatory; the periods can vary significantly from milliseconds to days (Li and Yang 2018). Pathological processes have also been noted to have periodic patterns. Low frequency ventricular repolarization instability known as periodic repolarization dynamics (PRD) are seen following acute myocardial infarction and long-QT syndrome, and at lower magnitudes in healthy patients (Rizas, Hamm et al. 2016). Much like exercise induced V-CoS, sympathetic stimulation during exercise or tilt testing enhances the magnitude of PRD, and the frequency range matches that of oscillatory patterns in muscle sympathetic nerves (Ang and Marina 2020). Our study describes similarly oscillating activation pattern change as a potential risk marker for ventricular arrhythmia.

Limitations

This result would at first appear to confirm that bio-electric noise is not responsible for the exercise-induced changes seen in the V-CoS matrices, but there are some experimental limitations which must be considered. Firstly, the extraction of noise was performed by a low-pass filter of frequency 1Hz. Any higher frequency components that might influence V-CoS would not be included in the extracted noise. This was performed because the periodicity of uniform conduction loss suggested aberrations in this frequency range would be responsible, but we cannot rule out that intermittent higher frequency signals might produce the patterns seen in exercise induced V-CoS matrices. Secondly, the exercise-induced noise extraction was interpolated to match the length of the recovery electrogram traces. This would have led to an interpolation factor of approximately 1.4 to 1.6. The resultant dominant frequencies of the extracted noise would have therefore also fallen by this amount.

However, we can say from this experiment that low-amplitude bio-electrical noise does not produce the low-amplitude loss of activation uniformity detected by V-CoS. The difference between the patterns seen in exercise-induced V-CoS matrices and their noise-augmented counterparts must be due to signal differences in the QRS complex range of frequencies and above. It is unlikely that supra-QRS frequency noise causes periodicity, because the 3-5 beat regular patterns seen in the results would not be expected.

5.2.5 Conclusion

Exercise-induced periodic loss of uniform activation occurs in patients with life-threatening cardiac conditions and healthy controls. This occurs in the 0-1Hz frequency range; exercise induced changes cannot be replicated by adding electrical noise in this frequency range to electrograms sampled during full recovery. The implication is that subtle QRS changes occur in exercise which are quantifiable by V-CoS and not a result of extra-cardiac noise sources. This supports the observation that patients surviving past ventricular fibrillation have the greater periodic losses of uniform activation than healthy controls, and that this might be a true physiological indication of arrhythmogenic substrate.

Chapter 6: Strategies for improving ECGi reproducibility

6.1 A method for automating repolarization methods in electrocardiographic imaging

6.1.1 Introduction

Although ventricular conduction stability can differentiate cardiac arrest survivors from controls, more basic electrophysiological measurements like local activation and repolarization times may be useful in understanding the arrhythmogenic substrate. In the future this may lead to the development of viable risk stratifiers based on electrophysiological measurements.

The ability of electrographic imaging to reconstruct epicardial signals during physiological activity leads to vulnerability to extrinsic noise sources such as movement artefacts and baseline wander. This may be more exaggerated than direct invasive recording from immobilized patients or ex-vivo preparations.

Extensive use of pre-filtering has been shown to alter the results of the inverse solution, and as such may lead to inaccurate interpretations of epicardial electrophysiology (Bear, Dogrusoz et al. 2018). As body surface mapping uses large numbers of physical electrodes, common practice is to exclude poorly recorded traces after visual inspection by the operator (Issa, Miller et al. 2009). Areas with missing data can be interpolated from surrounding electrodes (Serinagaoglu Dogrusoz, Bear et al. 2019). Reconstructed electrograms can also be excluded based on visual assessment of unwanted noise but reporting of this step varies in studies utilizing electrocardiographic imaging. Number of rejected electrograms is stated as 1% in a single paper (Cuculich, Zhang et al. 2011); this metric is not specified in other studies (Ghosh, Rhee et al. 2008; Zhang, Sacher et al. 2015; Andrews, Srinivasan et al. 2017; Zhang, Hocini et al. 2017; Haïssaguerre, Hocini et al. 2018).

From the prior work performed in other groups, there can be three broad strategies to limit the effect of extrinsic noise on measurement accuracy. First, the patient could be totally immobilized. This would reduce the need for electrode deselection or pre-filtering but negates the advantage of being able to record patients performing physiological tasks like exercising and resting. Second, pre-filtering could be used so all electrodes remain intact. This has the advantage of being reproducible as each signal undergoes the same mathematical transform but has already been shown to alter the

results away from ground truth in simulations. Third, in the subject of this chapter we will examine electrogram deselection. To date, no objective criteria or algorithm has been described to achieve this. User-determined deselection could allow for bias and poor reproducibility.

We hypothesized that repolarization measurements following manual electrogram cleaning would be especially inconsistent due to their low amplitude and peak gradients, and that automated processing of multiple beats could improve reproducibility.

6.1.2 Methods

Patient population and source data

15 patients underwent body surface mapping and non-invasive electrogram (EGM) reconstruction by the CardioINSIGHT™ inverse solution using a combination of 252-electrode sensor vest and low dose computerized tomography of the chest. 20 consecutive sinus beats were mapped with the patients in supine recovery.

An ECG or EGM trace can be considered a graph of voltage (V) against time (t). CardioINSIGHT returns both the source body surface ECG and reconstructed epicardial EGMs in a 2-dimensional array of size $m \times n$ where m is the number of recorded ECG/EGM traces and n is the number of time samples. Value $a_{i,j}$ is equivalent to the recorded voltage of reconstructed EGM i at time j. Sampling for CardioINSIGHT is at 1kHz; number of recorded body surface ECG traces is between 0-252 and number of reconstructed epicardial EGMs is generally between 1000-2000.

Signal pre-processing

For a reconstructed EGM array containing multiple cardiac cycles, signal quality can be improved by both filtering and signal averaging. This solution utilizes Python packages NumPy and SciPy (Oliphant 2007; Walt, Colbert et al. 2011).

A high pass finite impulse response (FIR) filter can be utilized to remove baseline wander from the tracing, demonstrated in Figure 6.1. Because measurements were made immediately after exercise whilst volunteers were still breathing heavily, we utilized a higher filter frequency than filters considering resting ECG only (Kher 2019).

Code snippet 1: Baseline filtering

The use of `**kwargs` in the function allows the filter to be vectorized over all EGM traces by the `axis` argument of `ss.filtfilt`.

For an ECGi array `ECGi_array` of size $m \times n$:

```
import numpy as np
import scipy.signal as ss

def FIR_filter(array, order = 600, sampling_rate = 1000,
               frequency = 1, **kwargs):
    b, a = [], []

    # Normalise the frequency
    nfrequency = 2.*float(frequency)/float(sampling_rate)

    # FIR filter construction
    if order % 2 == 0:
        order += 1
    a = np.array([1])
    b = ss.firwin(numtaps=order,
                  cutoff=nfrequency,
                  pass_zero=False)

    # Calculate the padding length
    padlen = 3 * max(len(a), len(b))

    if padlen > array.shape[array.ndim-1]:
        padlen = array.shape[array.ndim-1]-1

    # Apply the filter
    filtered = ss.filtfilt(b, a, array, **kwargs, padlen=padlen)

    return filtered

filtered_ECGi_array = FIR_filter(ECGi_array, axis = 1)
```

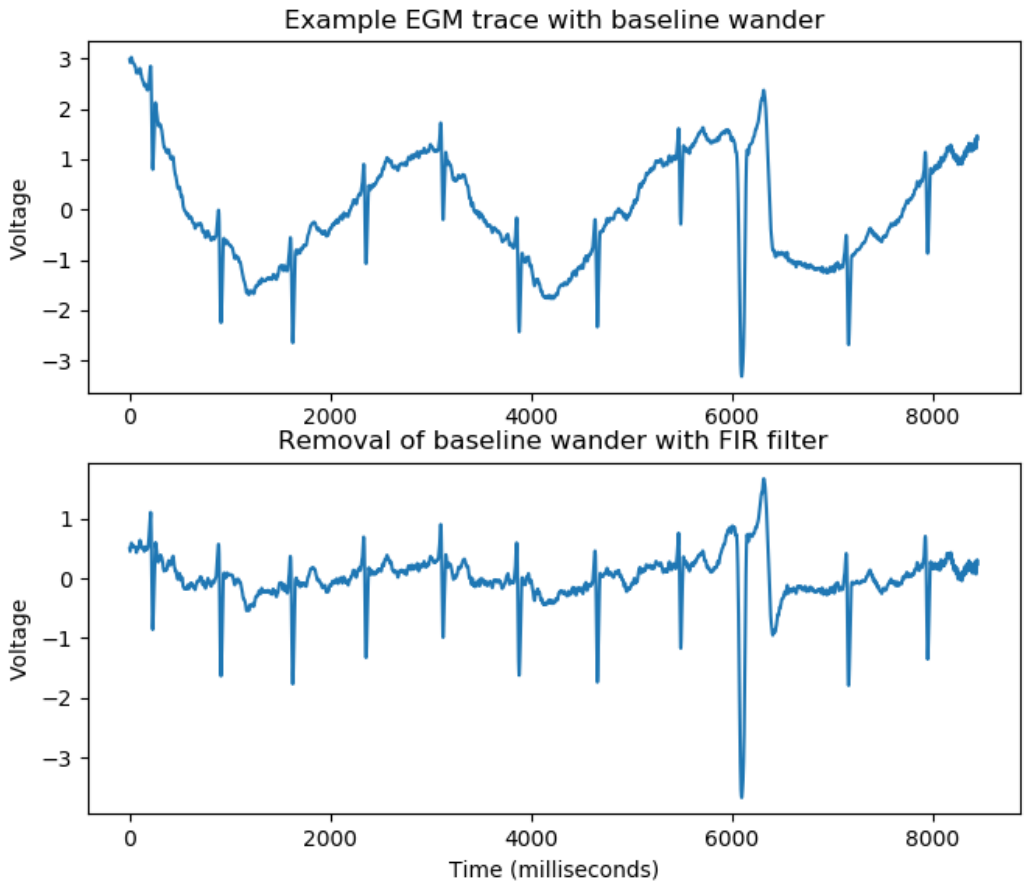

Figure 6.1: Use of a finite impulse response filter to remove the majority of baseline wander from a trace of electrograms. FIR = finite impulse response, EGM = electrogram.

Higher frequency noise components have some crossover with the frequency domains of QRS complexes and T waves, meaning that application of aggressive filtering here could alter end results. An alternative strategy is to perform signal averaging.

To perform signal averaging, several cardiac cycles must be identified. As ECGi recordings may have a variety of beat types (e.g. sinus rhythm, ventricular ectopic, ventricular tachycardia), it is important to find beat types representative of the target cardiac cycle for signal averaging. This can be performed by providing a template bounded by 2 time points `template_start` and `template_end`.

Once the template has been defined, this can be used to create an autocorrelation value for points along the time axis of each EGM, shown in Figure 6.2. Peaks in this trace correspond to regions of

similarity between the trace and the template. These peaks can be identified, and in this case, the ten best matches are selected – the number selected can be customized to the number of beats the end user wishes to average from those available. These are stacked to form an array of shape $m \times n \times s$ where m is the number of EGMs, n is the number of samples in time and s is the number of segment matches that will eventually be signal averaged.

The signal averaged EGM array can be found by taking the mean in the s axis, leaving an array of shape $m \times n$.

Code snippet 2: Template autocorrelation

```
# Create the template
signal = filtered_ECGi_array
template = filtered_ECGi_array[:, template_start:template_end]
template_length = np.abs(template_start-template_end)

# Determine autocorrelation
autocorr_mtx = np.zeros((signal.shape[0],signal.shape[1]), 'float')

for egm in range(template.shape[0]):
      autocorr = np.correlate(signal[egm], template[egm], 'same')
      normalised_autocorr = autocorr/np.max(autocorr)
      autocorr_mtx[egm, :] = normalised_autocorr

mean_autocorr = np.mean(autocorr_mtx, axis = 0)

# Detect peaks
peaks, props = ss.find_peaks(mean_autocorr, height=(None, None))
heightarray = props['peak_heights']
tenth = np.sort(heightarray)[-11]
topten = np.squeeze(np.argwhere(heightarray > tenth))

# Define start and end of each detected cardiac cycle
starts = []
ends = []

for n in range(len(topten)):
      starts.append(peaks[topten][n] - template_length/2)
      ends.append(peaks[topten][n] + template_length/2)

roicount = len(starts)
egmcount = signal.shape[0]
segmentstack = np.zeros((egmcount, template_length+1, roicount), 'float')

# Stack segments with some padding
for n, roi in enumerate(self.starts):
      roi_start = starts[n]
      roi_end = ends[n]
```

```
        segment = signal[:, roi_start:roi_end]
        padding_length = segmentstack.shape[1]-segment.shape[1]
        segmentstack[:, :, n] = np.pad(segment, ((0,0), (0,
        padding_length)), 'edge')

# Signal average
signal_averaged_EGMs = np.mean(segmentstack, axis = 2)
```

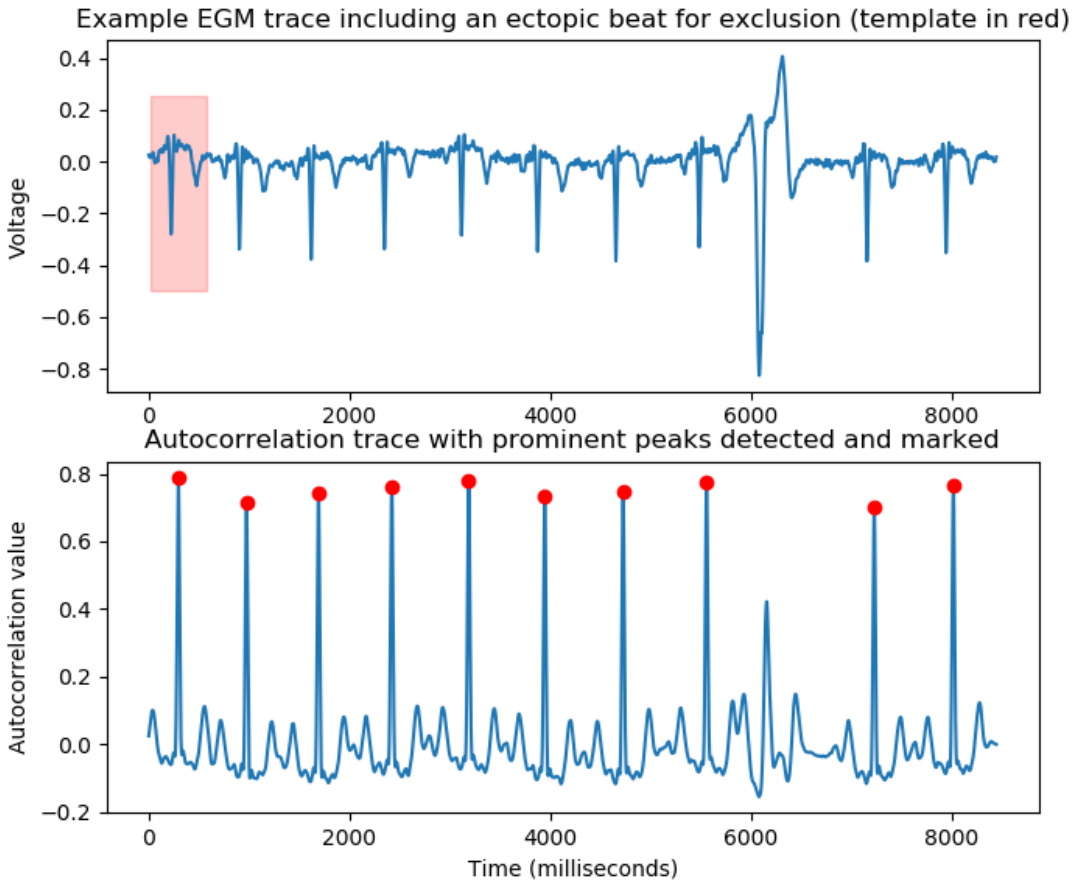

Figure 6.2: Use of template-derived autocorrelation to select similar beats for signal averaging. The lower panel is not an EGM – it is an autocorrelation trace. The appearance of pseudo P, QRS and T waves is because it is an autocorrelation trace of an EGM. EGM = electrogram.

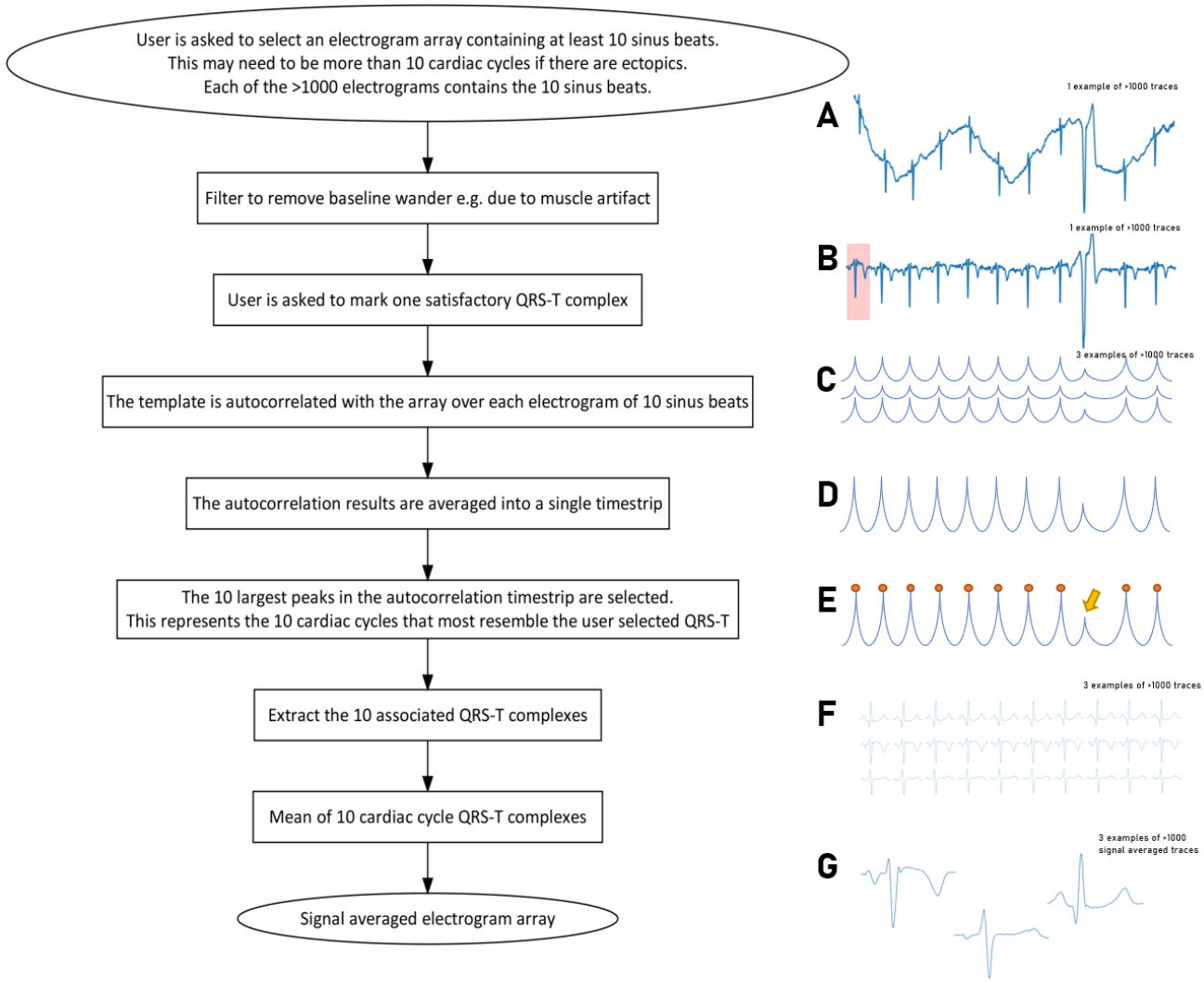

Figure 6.3: Flowchart summarizing pre-processing of data prior to determination of activation and repolarization characteristics. (A) 1 of >1000 raw electrogram traces containing at least 10 sinus cardiac cycles. (B) Baseline wander filter applied and a satisfactory QRS-T complex [pink box] defined by the user as a template of >1000 QRS-Ts – one per electrogram trace. (C) The template is autocorrelated with EGM traces, resulting in >1000 autocorrelation traces. Higher values [y-axis] mean more similarity to the template. These are stylized traces; a real example can be seen in Figure 6.2. (D) >1000 autocorrelation traces are averaged to a mean timestrip to guide complex selection. (E) Top 10 peaks are marked in the mean autocorrelation timestrip [red circles] to represent the QRS-T complexes best matching the user template. The yellow arrow demonstrates that the ventricular ectopic has been rejected by the algorithm. (F) 10 QRS-T complexes per the >1000 original raw traces are extracted based on the peaks in the autocorrelation timestrip. (G) One signal averaged QRS-T complex is calculated for each of >1000 original raw traces for use in further analysis.

Marking activation and repolarization

As beat morphology can vary significantly between different pathology types that may be evaluated by ECGi, user-defined bounds are recommended to segment the QRS complex and T wave. These values can be stored for future use to improve reproducibility and save time in re-analysis. Figure 6.3 demonstrates activation and repolarization point marking within user-defined bounds.

For the unipolar epicardial EGM, the steepest downward slope of the QRS complex is considered to be the best marker of local activation (Shenasa, Hindricks et al. 2019). Mathematically this can be defined as a maximum negative first differential of the voltage-time graph, or $max\left(-\frac{dV}{dt}\right)$. A 1D array of activation times of size m will be returned.

Code snippet 3: Marking activation times

For a QRS complex bounded by `qrs_start` and `qrs_end`:

```
pot = signal_averaged_EGMs
pot_diff = np.diff(-pot, axis=1)
# Filters may be added at this point if required

pot_diff[:,:qrs_start] = 0
pot_diff[:, qrs_end:] = 0

local_activation_times = np.argmax(pot_diff[:], axis=1)
```

Repolarization time has a more varied definition. There are two main strategies, the Wyatt (Wyatt, Burgess et al. 1981) method and the Yue method (Yue, Betts et al. 2005). The Wyatt is more commonly used in ECGi papers to date (Andrews, Srinivasan et al. 2017; Zhang, Hocini et al. 2017; Leong, Ng et al. 2018). The Wyatt method can be defined as the steepest upward slope of the T wave, or $max\left(\frac{dV}{dt}\right)$.

T waves are often lower amplitude than QRS complexes and therefore have an inherently lower signal to noise ratio. Fortunately, there are only 3 accepted morphologies of T wave (Yue, Betts et al. 2005), unlike the multitude for QRS. Thus, the danger of removing small but significant deflections by aggressive filtering is reduced. To accurately find the repolarization time, we used a Savitzsky-

Golay (Savitzky and Golay 1964) filter of order 3 and window length 51ms to remove high-frequency noise components. 1D array of repolarization times of size m can be returned and following this, a 1D array of activation recovery intervals (ARI) of size m can be found by subtracting the activation time array from the repolarization time array.

Code snippet 4: Marking repolarization times and defining activation-recovery interval

For a T wave bounded by `t_start` and `t_end`, a 1D array of repolarization times of size m can be returned:

```
pot_diff = np.diff(ss.savgol_filter(pot, 51, 3, axis=1))

pot_diff[:,:t_start] = 0
pot_diff[:,t_end:] = 0

pot_repol = np.argmax(pot_diff[:,t_start:t_end], axis=1)+ t_start
local_repolarization_times = pot_repol
```

A 1D array of activation-recovery intervals of size m can therefore be returned by subtracting the local repolarization time from the local activation time:

```
local_ARIs = local_activation_times - local_repolarization_times
```

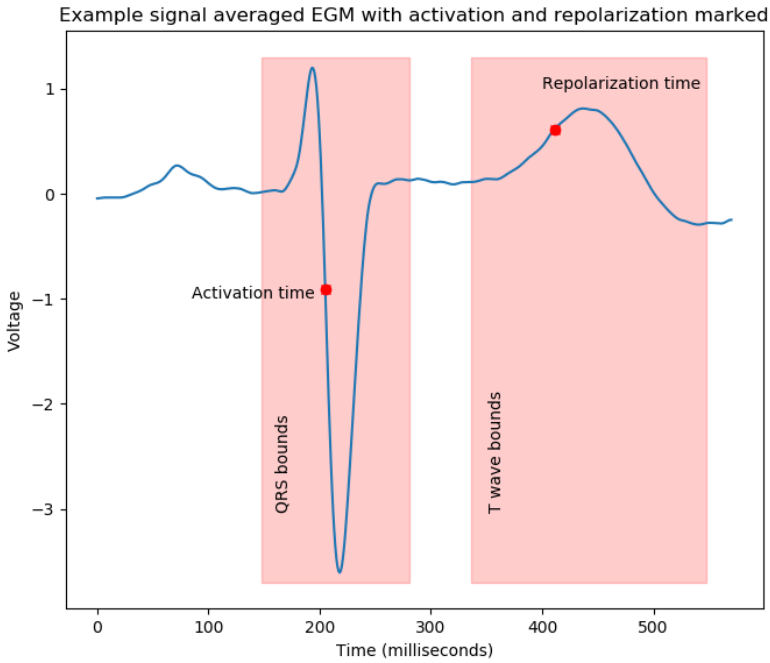

Figure 6.4: Marking of local activation and repolarization using the first differential of the electrogram. Local activation is defined as the greatest negative slope of the electrogram-QRS and local repolarization the greatest positive slope of the electrogram-T. EGM = electrogram.

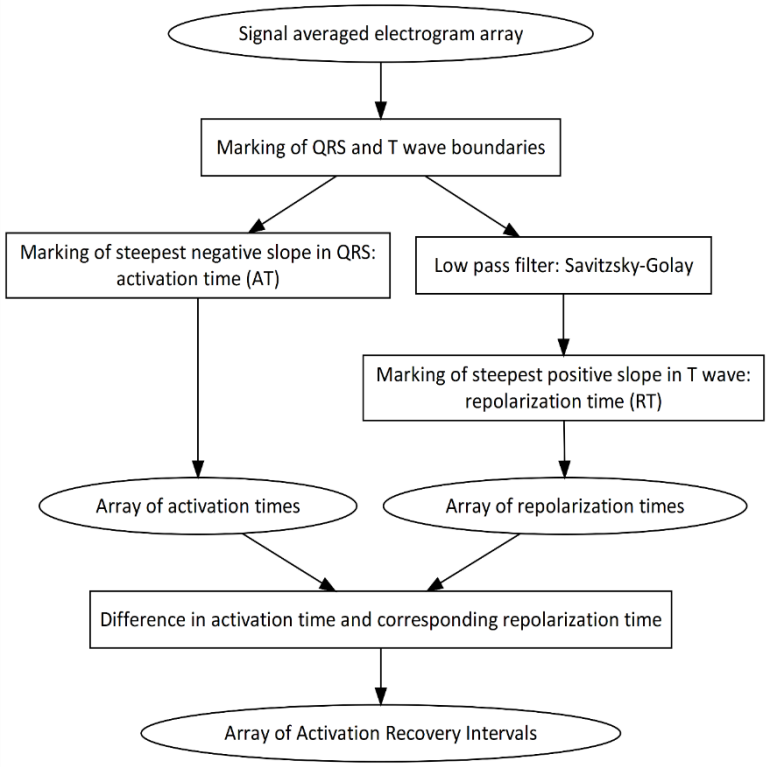

Figure 6.5: Flowchart summarizing the process of marking activation and repolarization characteristics in the electrogram array

Deselection of unsuitable electrograms

A varying number of electrograms may be unsuitable for analysis due to noise or ambiguous morphology, or a combination of both. Due to the zero-order regularization used in CardioINSIGHT, amplitude is constrained, negatively affecting reconstruction of the T wave, which as previously mentioned has an inherently lower signal to noise ratio. For this reason, this section focuses on T waves which cannot be interpreted.

Given the previously mentioned constraints on accepted T wave morphology (Yue, Betts et al. 2005), two main rules were set for T-wave rejection:

1. T waves amplitude had to be a certain percentage of the QRS amplitude – we chose 3% as a very low amplitude wave may not be accurately assessed for gradient in the context of background noise.
2. T waves could have no more than 2 deflections (biphasic accepted, triphasic and above rejected).

These characteristics of T waves may be stored in two further 1D arrays of size m.

Initially, a further baseline wander correction is applied to enable the T wave amplitude to be more accurately calculated. To ensure position of the maximum gradient was unchanged we used a linear correction (Figure 6.6).

Code snippet 5: Applying constraints using the T wave identification and selection technique (TWIST)

For a T wave bounded by `t_start` and `t_end` linear correction is achieved by:

```
t_pots = pot[:,self.t_start:self.t_end]
array_gradients = np.mean(np.diff(t_pots, axis=1), axis=1)
array_gradients = array_gradients.reshape(array_gradients.shape[0],1)
correction_mtx = np.zeros_like(t_pots)
correction_mtx[:] = np.arange(t_pots.shape[1])
correction_mtx = correction_mtx*array_gradients
corrected_t_pots = pot_array-correction_mtx
```

With a QRS complex bounded by `qrs_start` and `qrs_end`, the ratio of T wave amplitude to QRS amplitude can be calculated:

```
qrspot = pot[:,qrsstart:qrsend]
qrsheights = np.ptp(qrspot, axis=1)
theights = np.ptp(corrected_t_pots, axis=1)
t_qrs_ratios = theights/qrsheights
```

The number of deflections on a T wave can be determined by how many discrete peaks there are greater than a certain threshold prominence. In this example the threshold ratio is 10%:

```
def countpeaks(tpot):
      theight = np.ptp(tpot)
      threshold = 0.1*theight
      peaks, _ = ss.find_peaks(tpot, prominence=threshold)
      negpeaks, _ = ss.find_peaks(-tpot, prominence=threshold)
      allpeaks = peaks.shape[0]+negpeaks.shape[0]
      return allpeaks

t_peaks = np.apply_along_axis(countpeaks, 1, corrected_t_pots)
```

Finally, a further 1D array can be used to store the indices of EGMs that fulfil suitability for analysis criteria:

```
is_bad = np.bitwise_or(t_peaks>2, t_qrs_ratios<0.03)
is_good = np.logical_not(is_bad)
good = np.argwhere(is_good).ravel()
```

Slicing the arrays of activation of repolarisation times by this array allows the calculation of metrics from only suitable EGMs. In this example, the mean activation time is calculated:

```
mean_AT = np.mean(local_activation_times[good])
```

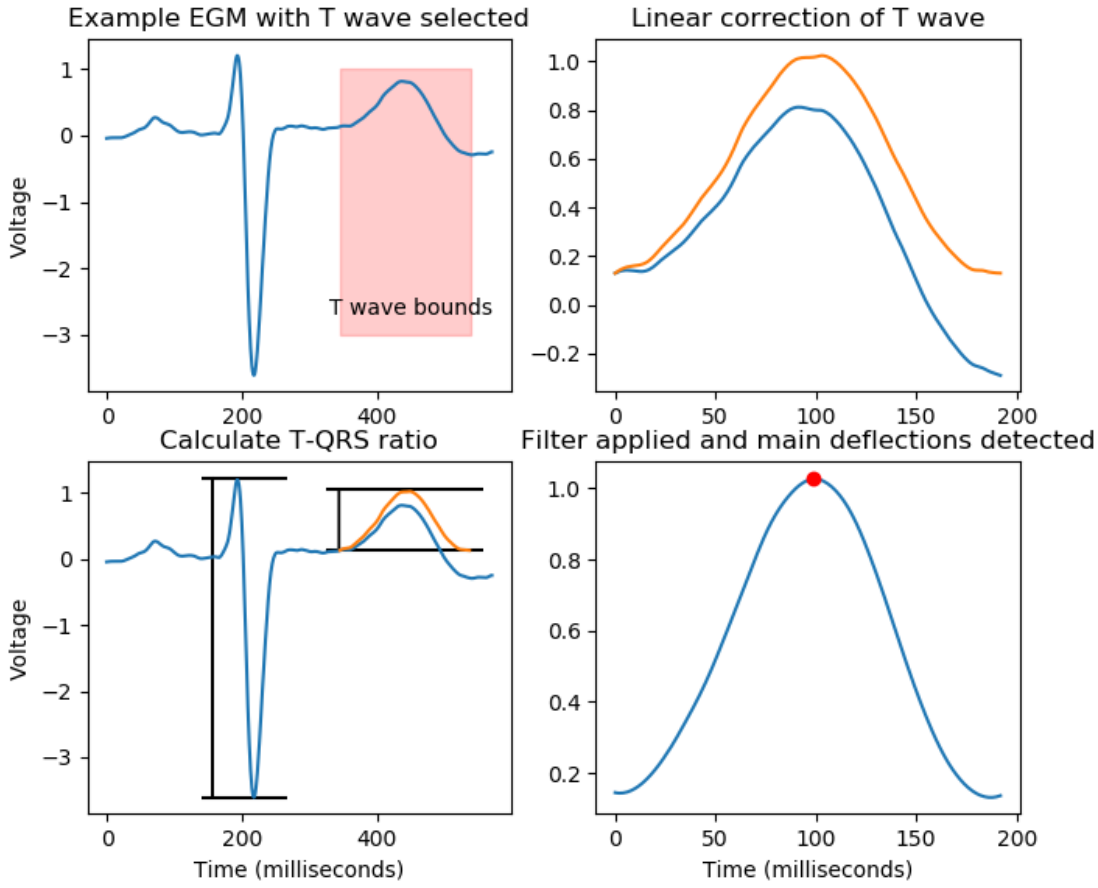

Figure 6.6: Stages of T wave feature analysis. The T wave is user-defined and linearly corrected. The amplitude is compared to the QRS amplitude. The number of deflections is determined following application of Savitzsky-Golay filter. EGM = electrogram.

With a QRS complex bounded by `qrs_start` and `qrs_end`, the ratio of T wave amplitude to QRS amplitude can be calculated. The number of deflections on a T wave can be determined by how many discrete peaks there are greater than a certain threshold prominence (Figure 6.7). In our algorithm the threshold ratio is 10%. A 1D array of suitable electrograms of size m will be returned

and can be used to dictate which EGMs are used in summary statistic calculation. We have termed this the T wave identification and selection technique (TWIST).

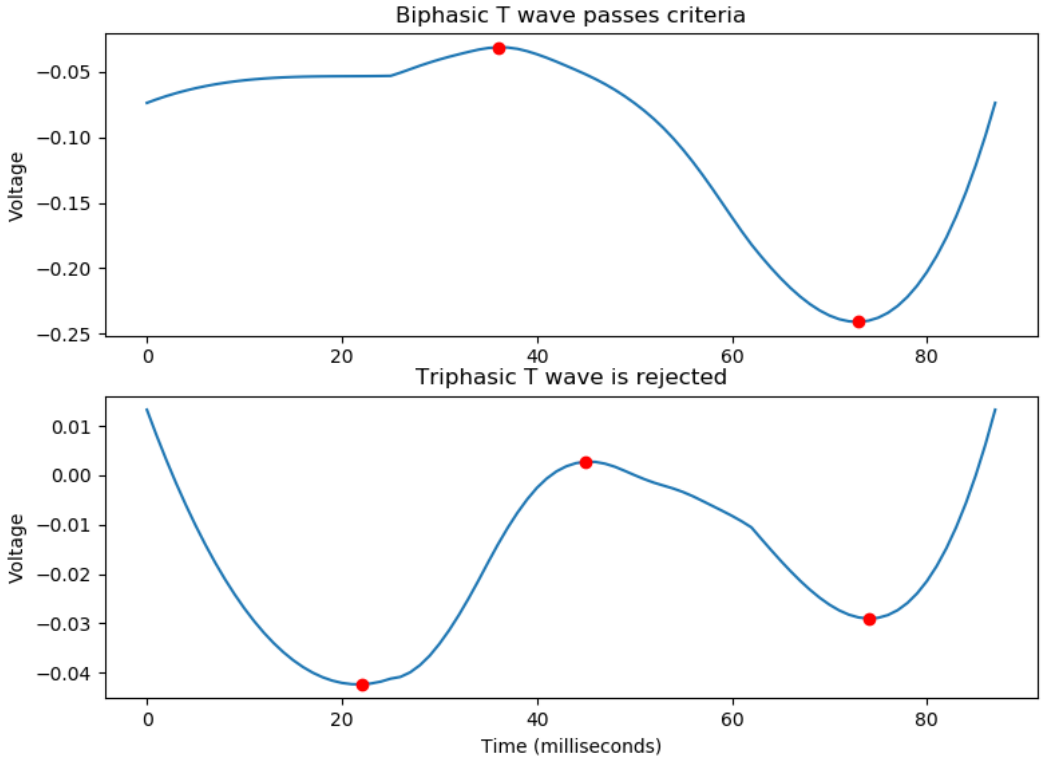

Figure 6.7: Biphasic and triphasic T wave detection, enabling exclusion of the triphasic T wave. The user can set an a priori exclusion threshold to ensure consistency in electrogram exclusion.

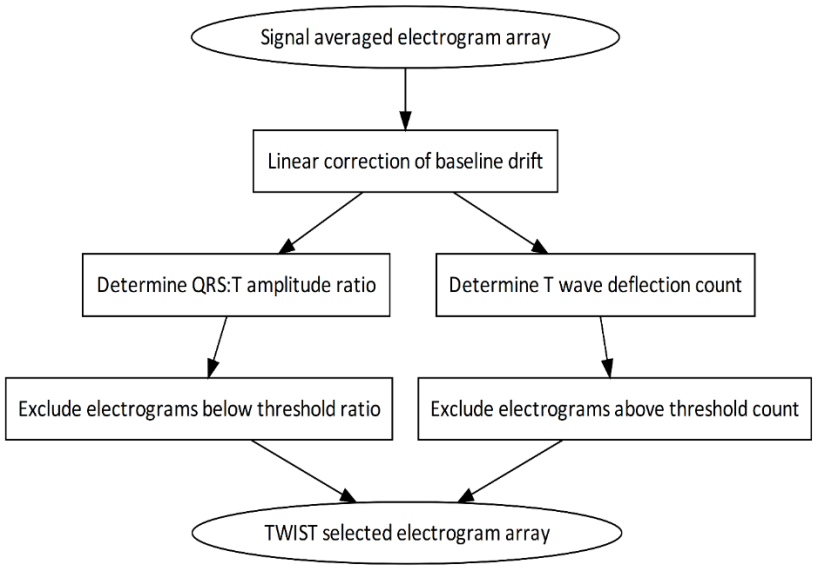

Figure 6.8: Flowchart summarizing the process of the T wave identification and selection technique (TWIST)

Automatic segmentation of QRS and T waves

In previous examples we have shown segmentation of the EGM complex to provide bounds for QRS and T wave used in later processing. An alternative method is to use machine learning to determine the wave boundaries. Inspired by a previously published convolutional neural network combined with conditional random fields (Jia, Zhao et al. 2019) we developed a purely 1D convolutional strategy to segment EGM like waves. The convolutional neural network (CNN) is composed of a degradation and reconstruction stage, linked by skip connections. It outputs a label for each sample (millisecond) of data, determining whether than sample is part of a P wave, QRS complex, T wave or isoelectric baseline. The architecture is shown in Figure 6.9.

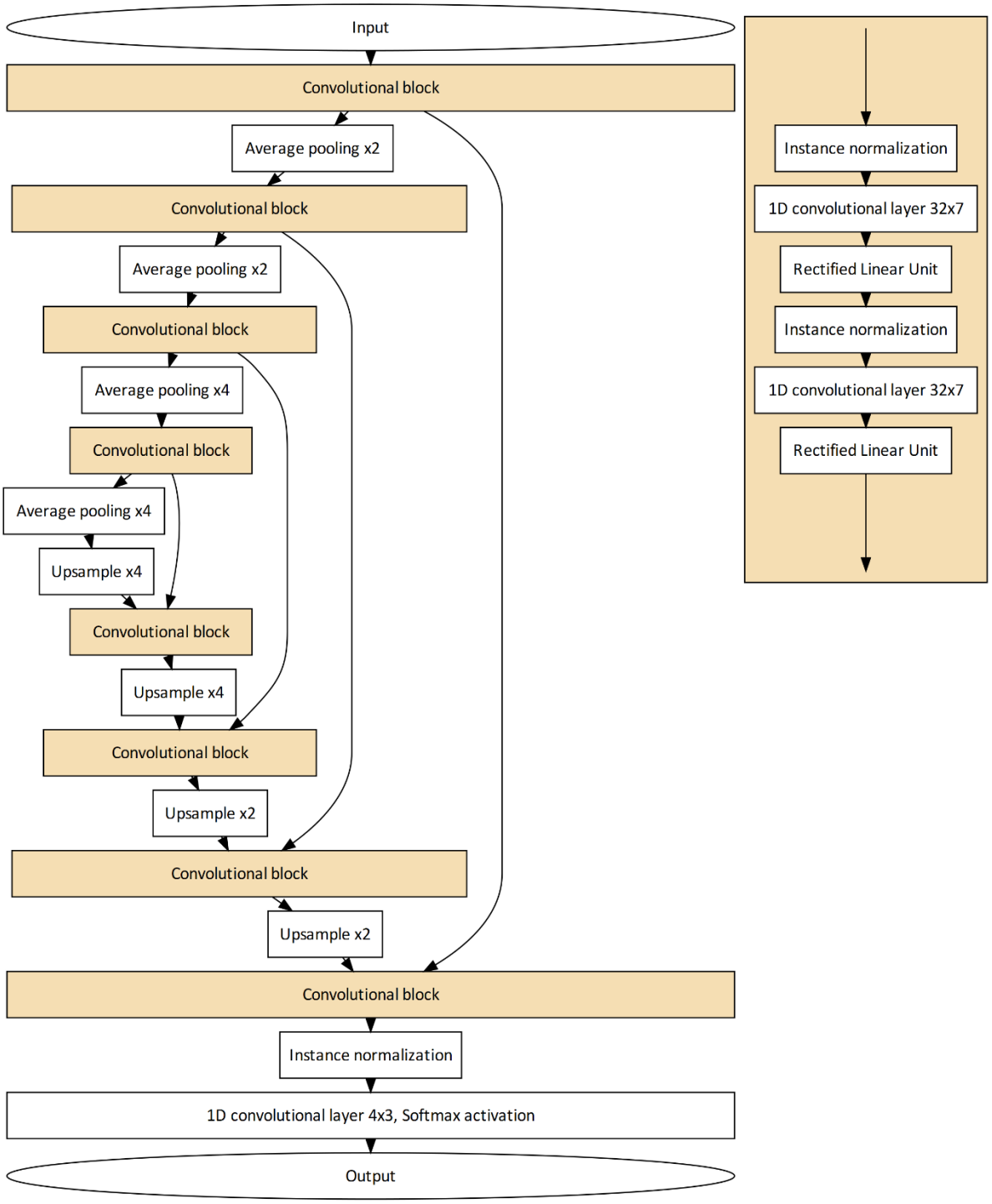

Figure 6.9: Architecture of convolutional neural network with skip connections for electrogram or electrocardiogram segmentation. The convolutional block (highlighted in orange) repeats within the larger network and is explored further in the right side of the diagram, containing normalization, convolutional and rectified linear unit (ReLU) layers.

Code snippet 6: Training a convolutional neural network to recognize labelled surface ECG data segmentation

For an ECG array `data` and labels `labels` of size $m \times n$:

```
from keras import layers
from keras.models import Model
from keras_contrib.layers import InstanceNormalization
import pickle

def conv_block(tensorinput):
    t1 = InstanceNormalization()(tensorinput)
    t2 = layers.Conv1D(32, 7, strides=1, padding='same')(t1)
    t3 = layers.ReLU()(t2)
    t4 = InstanceNormalization()(t3)
    t5 = layers.Conv1D(32, 7, strides=1, padding='same')(t4)
    t6 = layers.ReLU()(t5)
    return t6

# Input
inputs = layers.Input((input_len, 1))

# DEGRADE
de1 = conv_block(inputs)
de2 = layers.AveragePooling1D(pool_size=2)(de1)
de3 = conv_block(de2)
de4 = layers.AveragePooling1D(pool_size=2)(de3)
de5 = conv_block(de4)
de6 = layers.AveragePooling1D(pool_size=4)(de5)
de7 = conv_block(de6)
de8 = layers.AveragePooling1D(pool_size=4)(de7)

# RECONSTRUCT
re1 = layers.UpSampling1D(size=4)(de8)
re2 = conv_block(layers.concatenate([re1, de7]))
re3 = layers.UpSampling1D(size=4)(re2)
re4 = conv_block(layers.concatenate([re3, de5]))
re5 = layers.UpSampling1D(size=2)(re4)
re6 = conv_block(layers.concatenate([re5, de3]))
re7 = layers.UpSampling1D(size=2)(re6)
```

```
re8 = conv_block(layers.concatenate([re7, de1]))
re9 = InstanceNormalization()(re8)
outputs = re10 = layers.Conv1D(4, 3, strides=1, padding='same',
activation='softmax')(re9)

epochs = 10
input_len = 2048
# Pre-process data

def normalise(data):
    data -= data.mean(axis=0)
    data /= data.std(axis=0)
    return data

def trace_padder(traceblock, target_len=input_len, pad_mode='constant',
constant=None):
    (_,startlen) = traceblock.shape
    padlen = target_len-startlen
    if pad_mode=='constant':
        padblock = np.pad(traceblock, ((0,0), (0,padlen)), pad_mode,
constant_values=constant)
    else:
        padblock = np.pad(traceblock, ((0, 0), (0, padlen)), 'edge')
    return padblock[:,:,np.newaxis]



data = np.nan_to_num(normalise(data))
datastack = trace_padder(data, pad_mode='edge')
labelints = trace_padder(labels, pad_mode='constant', constant=0)

data_train, data_test, labels_train, labels_test =
train_test_split(datastack, labelints, test_size=0.2)

model = Model(inputs=inputs, outputs=outputs)
model.summary()
model.compile(optimizer='adam',
              loss='sparse_categorical_crossentropy',
              metrics=['sparse_categorical_accuracy'])
```

```
history = model.fit(data_train, labels_train, epochs=epochs,
batch_size=40, validation_data=(data_test,labels_test))

def save_model(model):
    model_json = model.to_json()
    with open(filename + '.json', 'w') as json_file:
        json_file.write(model_json)
    with open(filename + '.history', 'wb') as historyfile:
        pickle.dump(history.history, historyfile)
    model.save_weights(filename + '.h5')
    print('Model saved to disk')
```

Due to the lack of large volume labelled datasets of EGM data, we used ~22,000 labelled surface ECG beats from the Lobachevsky University ECG database (Kalyakulina, Yusipov et al. 2018), separate from the data used in this analysis. Following training, the un-altered CNN was used to make predictions about wave location and bounds for each EGM in the array.

To deal with gaps in segmented waves (e.g. sections in the middle of a T wave inappropriately labelled as isoelectric baseline), a custom searching algorithm was developed to process the raw CNN predictions. The longest segment pertaining to a particular waveform (for example T wave) is sought and designated the primary location of the wave. Shorter segments are then sought; if they fall within an a priori defined threshold (200 milliseconds in this example), these are incorporated into the primary wave location. All other wave segments are rejected. This process is summarized by the flowchart Figure 6.10.

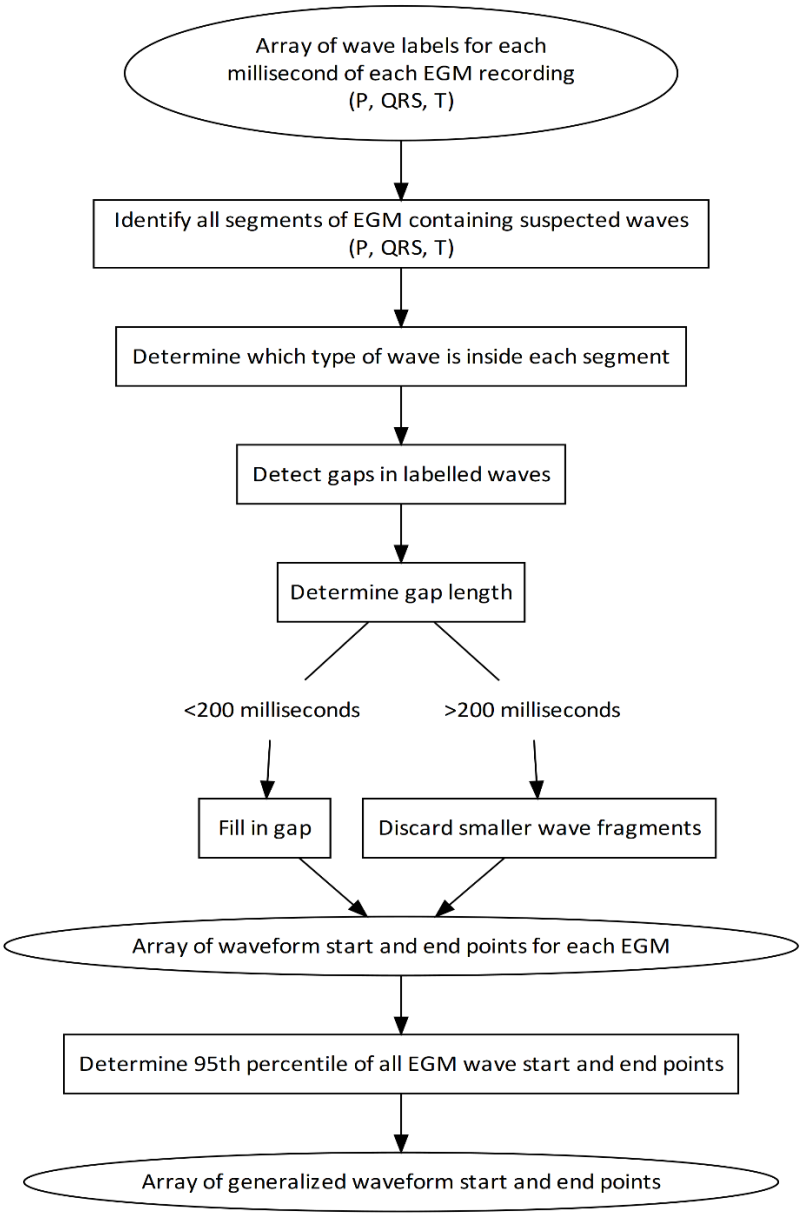

Figure 6.10: Flowchart summarizing the process of segmenting the entire EGM array using the neural network predictions. To deal with unintended gaps in waveform bounds, a search algorithm groups all segments of the same class within a defined window (200 milliseconds in this example). To deal with anomalous detections in a noisy electrogram, the whole-array bounds are set at the 95th percentile of start and end points – encompassing all but the most extreme measurements.

Code snippet 7: Automated delineation of QRS complex and T wave using a pre-trained neural network

For a saved `Keras` neural network composed of `.history`, `.json` and `.h5` files and an ECGi array `ecgi_dataset` of size $m \times n$:

```
MODEL = '<history filename>.history'
class ECGi_segmenter:
    def __init__(self, modelfile = None, ecgi_dataset = None):
        self.model = None
        self.history = None
        self.results = None
        self.allbounds = None
        self.bounds95 = None
        self.ecgi_dataset = ecgi_dataset
        self.ecgidata = None
        self.modelfile = modelfile
        self.getfiles()

    def run_segmentation(self):
        self.ecgidata = self.trace_padder(self.ecgi_dataset)
        self.results = self.predict_ecgi(self.ecgidata, self.model)
        self.allbounds = self.find_all_boundaries(self.results)
        self.bounds95 =
self.define_egmstack_bounds(self.allbounds,percentile=90)

    def getfiles(self):
        custom_objects = {'InstanceNormalization':InstanceNormalization}

        if not self.modelfile:
            firstfp = askopenfilename(initialdir=os.getcwd())
        else:
            firstfp = self.modelfile

        if '.json' in firstfp:
            jsonfp = firstfp
            histfp = firstfp.replace('json', 'history')
```

```
            h5fp = firstfp.replace('json', 'h5')
        elif '.history' in firstfp:
            histfp = firstfp
            jsonfp = firstfp.replace('history', 'json')
            h5fp = firstfp.replace('history', 'h5')
        else:
            h5fp = firstfp
            histfp = firstfp.replace('h5', 'history')
            jsonfp = firstfp.replace('h5', 'json')


        with open(jsonfp, 'r') as jsonfile:
            modeljson = jsonfile.read()
            self.model = model_from_json(modeljson, custom_objects)
            jsonfile.close()

        with open(histfp, 'rb') as histfile:
            self.history = pickle.load(histfile)
            histfile.close()

        self.model.load_weights(h5fp)

    def trace_padder(self, traceblock, target_len=2048):
        '''
        CI arrays come as EGMs x length
        We need them to be EGMs x length expected by model x features
        Generally features are 1 (voltage) so we just add an axis
        '''
        (_, startlen) = traceblock.shape
        padlen = target_len - startlen
        padblock = np.pad(traceblock, ((0, 0), (0, padlen)), 'edge')
        return padblock[:, :, np.newaxis]

    def plot_history(self):
        fig,ax = plt.subplots(1)
        for key,val in self.history.items():
            ax.plot(val, label=key)
        ax.legend()
```

```
        ax.set_title('Training history for current model')
        fig.show()

    def predict_ecgi(self, ecgidata, model):
        return model.predict(ecgidata, batch_size=40, verbose=1)

    def find_1d_boundaries(self, prediction, wavethresh=200):
        '''
        Will take either a samples*4 set of probabilities and convert it,
or the samples*1 set of predicted labels
        Wavethresh is the longest allowed wave for joining up non-
contiguous pieces of detected T wave etc
        If two areas are further apart than the wavethresh then the
largest found segment will be returned as the predicted boundaries
        '''

        if prediction.shape[-1] == 4:
            prediction = np.argmax(prediction, axis=-1)

        valid_p = False
        valid_qrs = False
        valid_t = False

        # Create an array of zeros where index 0 is P start through to
index 5 is T end
        boundsary = np.zeros(6)
        plist = []
        qlist = []
        tlist = []
        segslist = [plist, qlist, tlist]

        enumerated_segments, _ = sn.label(prediction)
        segments = sn.find_objects(enumerated_segments)
        segment_contents = np.zeros(len(segments))
        try:
            segment_contents =
np.array([int(stats.mode(prediction[x])[0]) for x in segments])
        except:
```

```
            for n, segment in enumerate(segments):
                try:
                    segment_contents[n] =
int(stats.mode(prediction[segment])[0])
                except:
                    segment_contents[n] = None

        for n,content in enumerate(segment_contents):
            if content == 1:
                try:
                    plist.append(segments[n][0])
                    valid_p = True
                except:
                    print('No P waves for this EGM')
            elif content == 2:
                try:
                    qlist.append(segments[n][0])
                    valid_qrs = True
                except:
                    print('No QRS for this EGM')
            elif content == 3:
                try:
                    tlist.append(segments[n][0])
                    valid_t = True
                except:
                    print('No T wave for this EGM')
            else:
                continue

        for n, sublist in enumerate(segslist):
            if len(sublist) == 1:
                boundsary[2 * n] = sublist[0].start
                boundsary[2 * n + 1] = sublist[0].stop
            elif len(sublist) == 0:
                boundsary[2 * n] = np.nan
                boundsary[2 * n + 1] = np.nan
                # print('No {} for this EGM'.format(sublist))
            else:
```

```
                print('Assessing multiple candidate segments')
                starts = [x.start for x in sublist]
                ends = [x.stop for x in sublist]
                starts.sort()
                ends.sort(reverse=True)
                gaps = np.array(ends) - np.array(starts)
                gaps[gaps < 0] = 0
                gaps[gaps > wavethresh] = 0
                if np.sum(gaps) != 0:
                    joinedindex = np.argmax(gaps)
                    boundsary[2 * n] = starts[joinedindex]
                    boundsary[2 * n + 1] = ends[joinedindex]
                else:
                    ends.sort()
                    intervals = np.array(ends) - np.array(starts)
                    chosenindex = np.argmax(intervals)
                    boundsary[2 * n] = starts[chosenindex]
                    boundsary[2 * n + 1] = ends[chosenindex]

        return boundsary, valid_p, valid_qrs, valid_t

    def find_all_boundaries(self, prediction, wavethresh=200):
        '''
        Will take a block of predictions and return an EGMs*6 array
where:
        index 0 is P start through to index 5 is T end
        '''
        vpfalse = []
        vqfalse = []
        vtfalse = []
        boundsary = np.zeros((prediction.shape[0], 6))
        for n in range(prediction.shape[0]):
            # print('Assessing EGM {}'.format(n))
            boundsary[n], vp, vq, vt =
self.find_1d_boundaries(prediction[n], wavethresh=wavethresh)
            if not vp:
                vpfalse.append(n)
            if not vq:
```

```
                vqfalse.append(n)
            if not vt:
                vtfalse.append(n)
        print('Summary: Missing P = {}; Missing QRS = {}; Missing T =
{}'.format(len(vpfalse), len(vqfalse),

len(vtfalse)))
        print(vpfalse)
        print(vqfalse)
        print(vtfalse)
        return boundsary

    def define_egmstack_bounds(self, bounds_array, percentile=95):
        '''
        Takes the full results of an EGM*6 bounds array and returns the
required percentile of results (default 95)
        Indices 0,2,4 are the starts, indices 1,3,5 are the ends
        '''
        bounds95 = np.zeros(6)
        offstart = (100 - percentile) / 2
        offend = percentile + offstart
        starts = [0, 2, 4]
        ends = [1, 3, 5]
        for s in starts:
            bounds95[s] = int(np.nanpercentile(bounds_array[:, s],
(offstart)))
        for e in ends:
            bounds95[e] = int(np.nanpercentile(bounds_array[:, e],
(offend)))
        return bounds95
```

Validation

To determine the performance of our automated system against current practice, reproducibility of the central 95% range of total repolarization time (TRT95) was examined.

Beat-to-beat reproducibility for successive cardiac cycles is also important to producing a meaningful result for a patient. To determine the improvement made by considering multiple beats, we quantified the reduction in mean absolute difference when 1, 2, 3 and up to 10 beats were considered. Two strategies were considered – signal averaging: the creation of a synthetic cardiac cycle from multiple beats in pre-processing; and result averaging: the post-calculation mean of results from several single beats. Figure 6.11 summarizes the manual and automatic workflows in full.

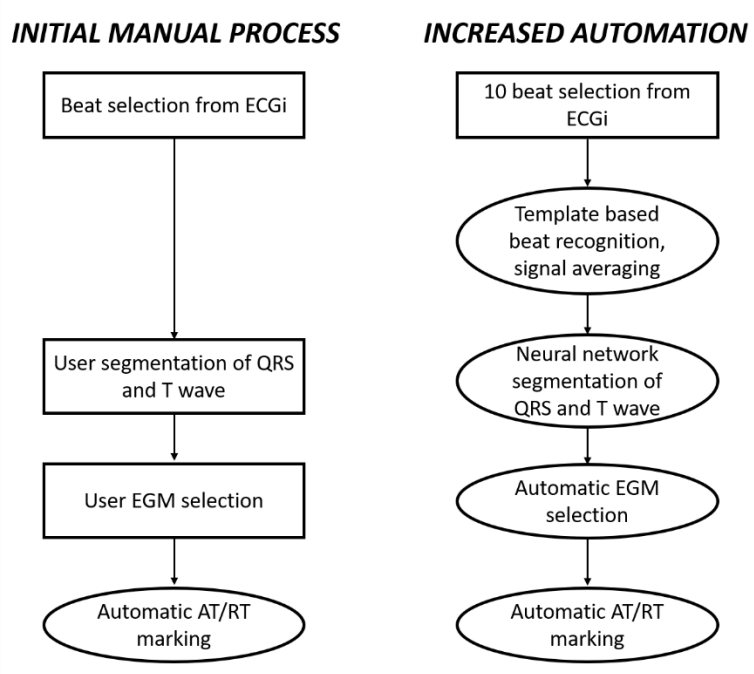

Figure 6.11: Comparison of the initial manual analysis and the increasingly automated analysis using the algorithms described in the paper. Rectangular boxes are user driven; oval boxes are automated. ECGi = electrocardiographic imaging, EGM = electrocardiogram, TRT95 = total repolarization time (central 95 percent range).

The mean absolute difference (MAD) was used to quantify reproducibility. Paired T-tests were used to test whether the automatic methods produced a smaller reproducibility error than manual methods.

6.1.3 Results

Neural network performance

After training over 10 epochs with a 80:20 train:validate split using the ADAM optimizer, validation set accuracy exceeded 97%. Overfitting was not seen, with the validation set accuracy continuing to rise with the training set accuracy (Figure 6.12).

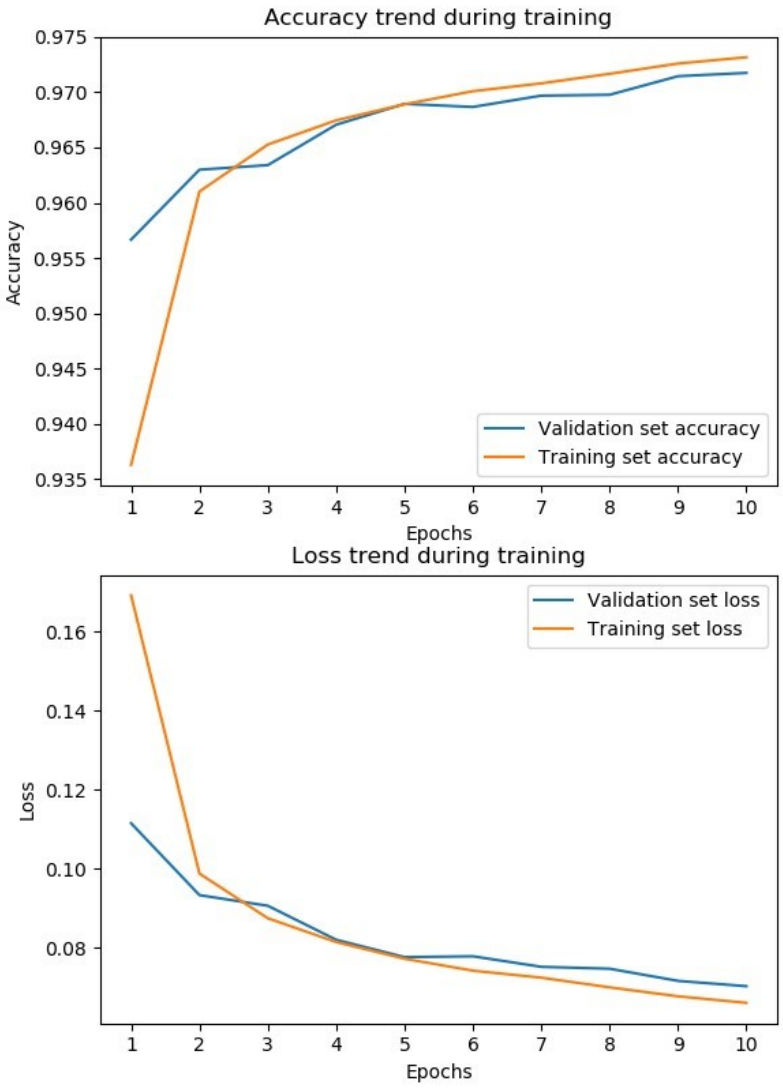

Figure 6.12: Accuracy and loss changes during training of the neural network. A high level (>96%) accuracy is reached for defining each millisecond of signal as baseline, P wave, QRS complex or T wave. Validation set results closely match the test group result, indicating that overfitting is unlikely.

Figure 6.13 demonstrates four real EGM examples of the CNN output and aids in understanding the classification mechanism. For each millisecond of signal, the CNN calculates how likely it is to be a P wave, QRS complex, T wave or baseline millisecond. The highest probability waveform is labelled to this millisecond.

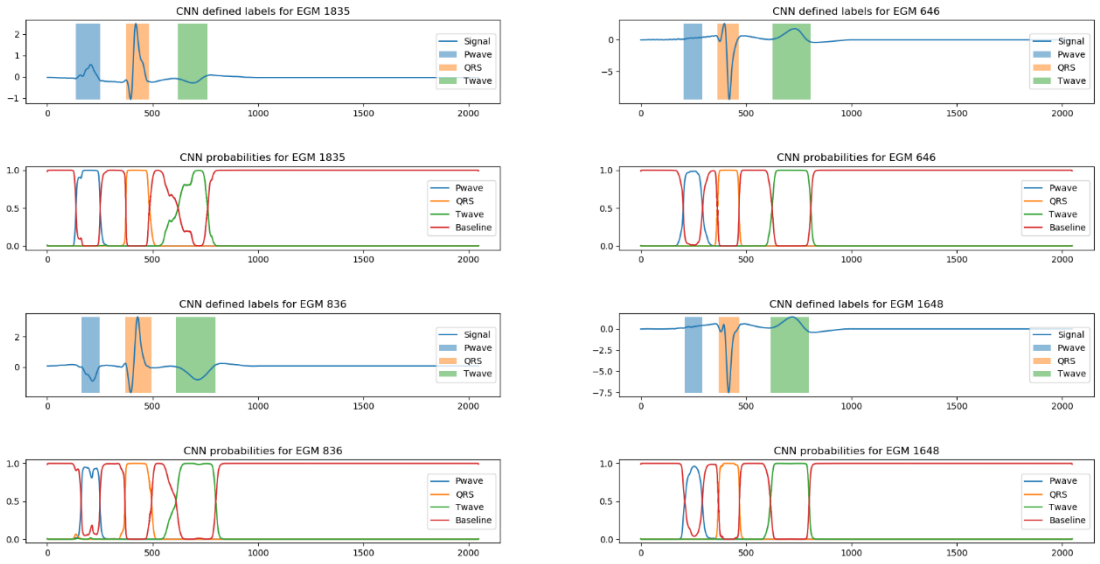

Figure 6.13: Raw results of the convolutional neural network (CNN) on four example electrograms (EGMs 1835, 646, 836 and 1648). Each pair of graphs (CNN defined labels and CNN probabilities) pertain to the same EGM. In the top graph of every pair, the shading denotes the waveform boundaries. In the bottom graph of every pair, the line chart denotes the probability of each millisecond belonging to either P, QRS, T or baseline signal. The CNN assigns the highest probability waveform to each millisecond of the trace, producing the defined labels.

Some examples of CNN misprediction are highlighted in Figure 6.14. In Panel A the P wave has been misclassified altogether as baseline. Between Panel A and Panel B, there is some discrepancy in the labelling of the ST segment as baseline or part of the T wave. In Panel B, part of the P wave is misclassified as baseline, but this segment is surrounded by appropriately classified P wave. In Panel C, the initial part of the P wave has been misclassified as QRS complex.

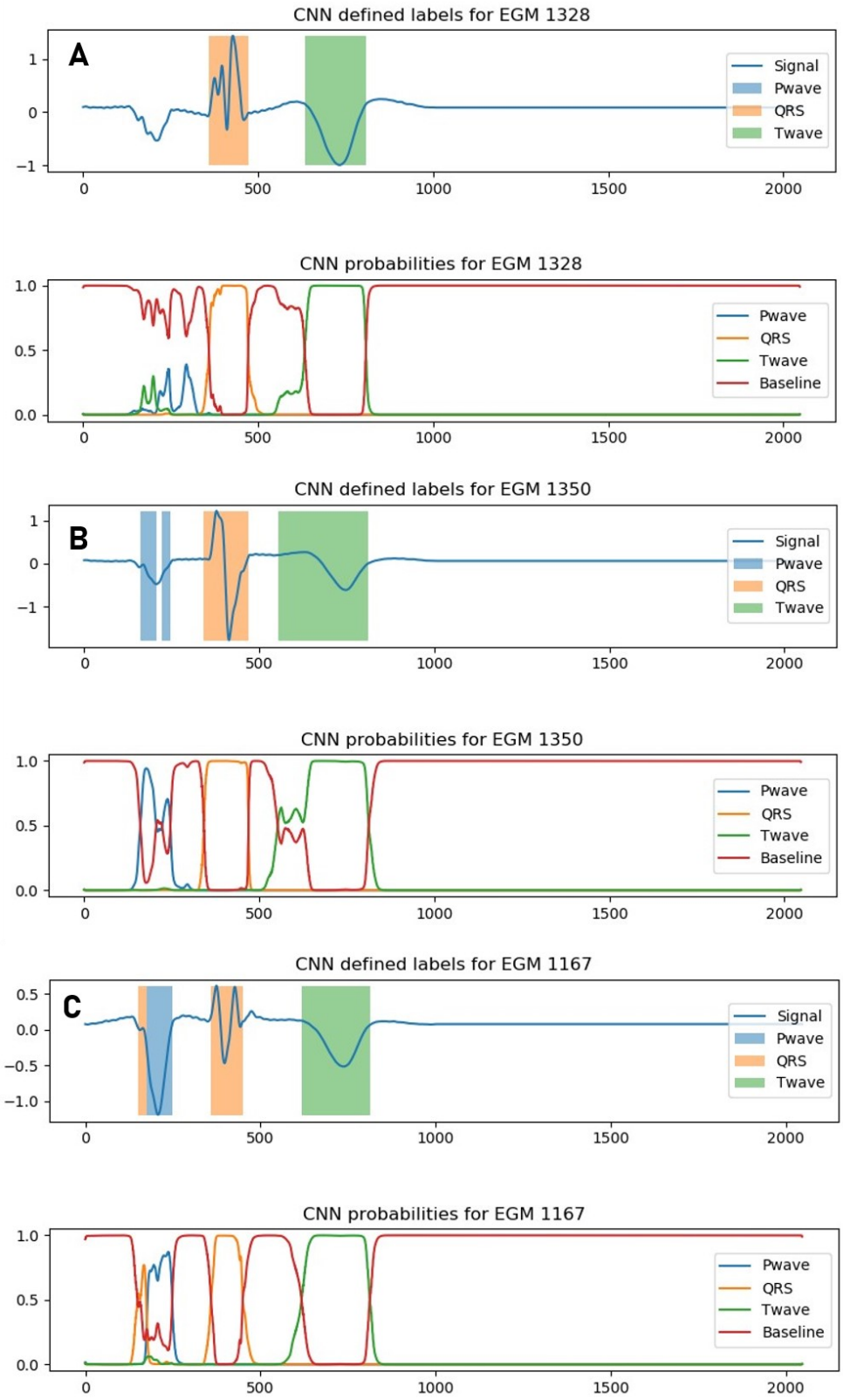
CNN defined labels for EGM 1328
A
Signal
Pwave
QRS
Twave
CNN probabilities for EGM 1328
Pwave
QRS
Twave
Baseline
CNN defined labels for EGM 1350
B
Signal
Pwave
QRS
Twave
CNN probabilities for EGM 1350
Pwave
QRS
Twave
Baseline
CNN defined labels for EGM 1167
C
Signal
Pwave
QRS
Twave
CNN probabilities for EGM 1167
Pwave
QRS
Twave
Baseline

Figure 6.14: Examples of convolutional neural network (CNN) misprediction for electrograms (EGM). Panel A demonstrates misclassification of the whole P wave as baseline. Panel B demonstrates misclassification of only a segment of P wave as baseline, surrounded by correctly labelled signal. Panel C demonstrates misclassification of P wave start as QRS complex.

Using the bounding strategy demonstrated by Figure 6.10 and Code Snippet 7, segmentation results were supplied to the user for human verification. Figure 6.15 demonstrates screenshots from this process.

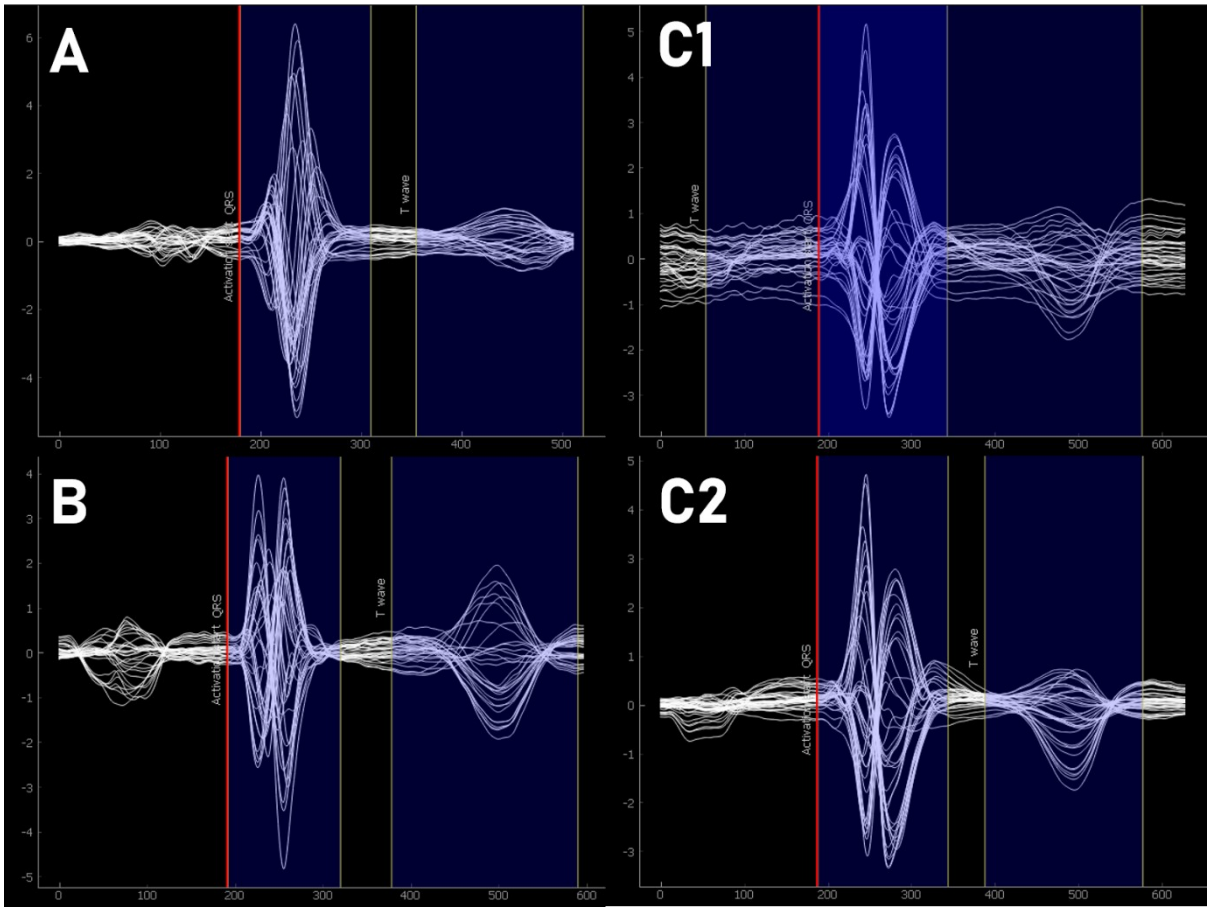

Figure 6.15: Screenshots from the Graphic User Interface (GUI) used for window selection verification following neural network segmentation. Each graph is an overlay of several hundred electrograms and the overall bounds calculated by the segmentation algorithm. Panels A and B demonstrate good segmentation – the waveform is fully contained within the boundaries without excessive baseline signal selection. C1 and C2 are from the same patient, C1 without signal averaging and C2 with signal averaging of 10 beats. Panel C1 demonstrates overclassification of the T wave whilst C2 demonstrates the correct waveform segmentation.

Panels A and B demonstrate good segmentation – the waveform is fully contained within the boundaries without excessive baseline signal selection. C1 and C2 are from the same patient, C1 without signal averaging and C2 with signal averaging of 10 beats. Panel C1 demonstrates a system

error, in this case incorrectly identifying part of the P wave as T wave. The user at this point can correct the selection. However, the signal averaged trace in C2 is much better segmented – strengthening the case for signal averaging prior to machine segmentation.

To perform the various calculations in this experiment, each patient underwent 50 separate segmentations with varying amounts of signal averaging. In 3 out of 750 segmentations (0.4%), the wave boundaries were clearly mislabelled in a similar fashion to Figure 6.15, Panel C1.

Result reproducibility for single beats

The central 95% of total repolarization times for single identical beats were calculated twice over by both manual and automated methods. Figure 6.16 demonstrates the results.

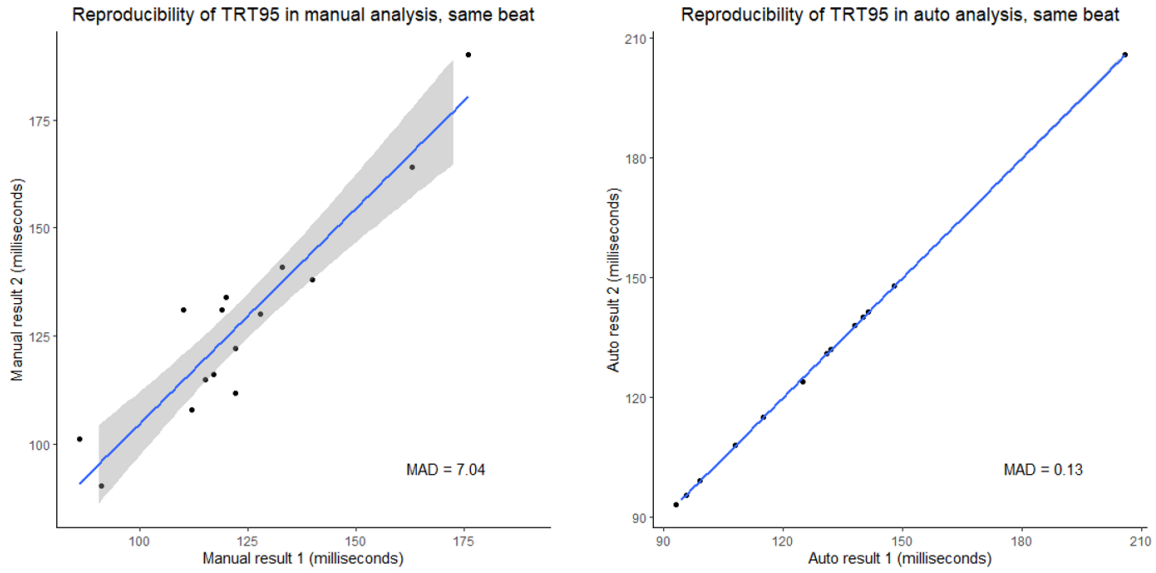

Figure 6.16: Reproducibility of same-beat repeated analysis by both manual and automatic analysis. The central 95% of total repolarization time (TRT95) is the assessed measure. Automatic analysis has better reproducibility than manual analysis.

Manual identical beat analysis for a single cardiac cycle had a significantly worse MAD than automated analysis of the same beats (manual 7.0 vs automatic 0.1 milliseconds, p = 0.002).

Successive single beat reproducibility was worse than for identical beats, despite automated selection of the time windows and EGMs suitable for analysis (successive 19.4 vs identical 0.1 milliseconds, p = 0.0007).

Result reproducibility for multiple beats

Signal averaging improved reproducibility significantly when combined with the automatic analysis, improving MAD from 19.4 milliseconds with a single beat to 12.8 milliseconds once 10 beats had been ensembled ($p = 0.0002$ for the trend). For an ensemble of 2 beats, the MAD worsened to 22.9 milliseconds, and for an ensemble of 9 beats the MAD was better than the final result at 11.9 milliseconds.

Result averaging combined with automatic analysis performed even better, improving MAD from 19.4 milliseconds with a single beat to 7.2 milliseconds once results from 10 beats had been averaged ($p = 0.009$ for the trend). Like signal averaging, result averaging showed some fluctuation in improvement, with the lowest MAD occurring with the 7^{th} beat (5.9 milliseconds).

Whilst result averaging produced lower absolute MAD for a given number of beats used (result averaging mean 9.99 vs signal averaging mean 15.9 milliseconds, $p = 0.0002$), the trend for improvement was stronger for signal averaging ($R = -0.77$ vs -0.92, p-values = 0.009 vs 0.0002). Figure 6.17 summarizes the result.

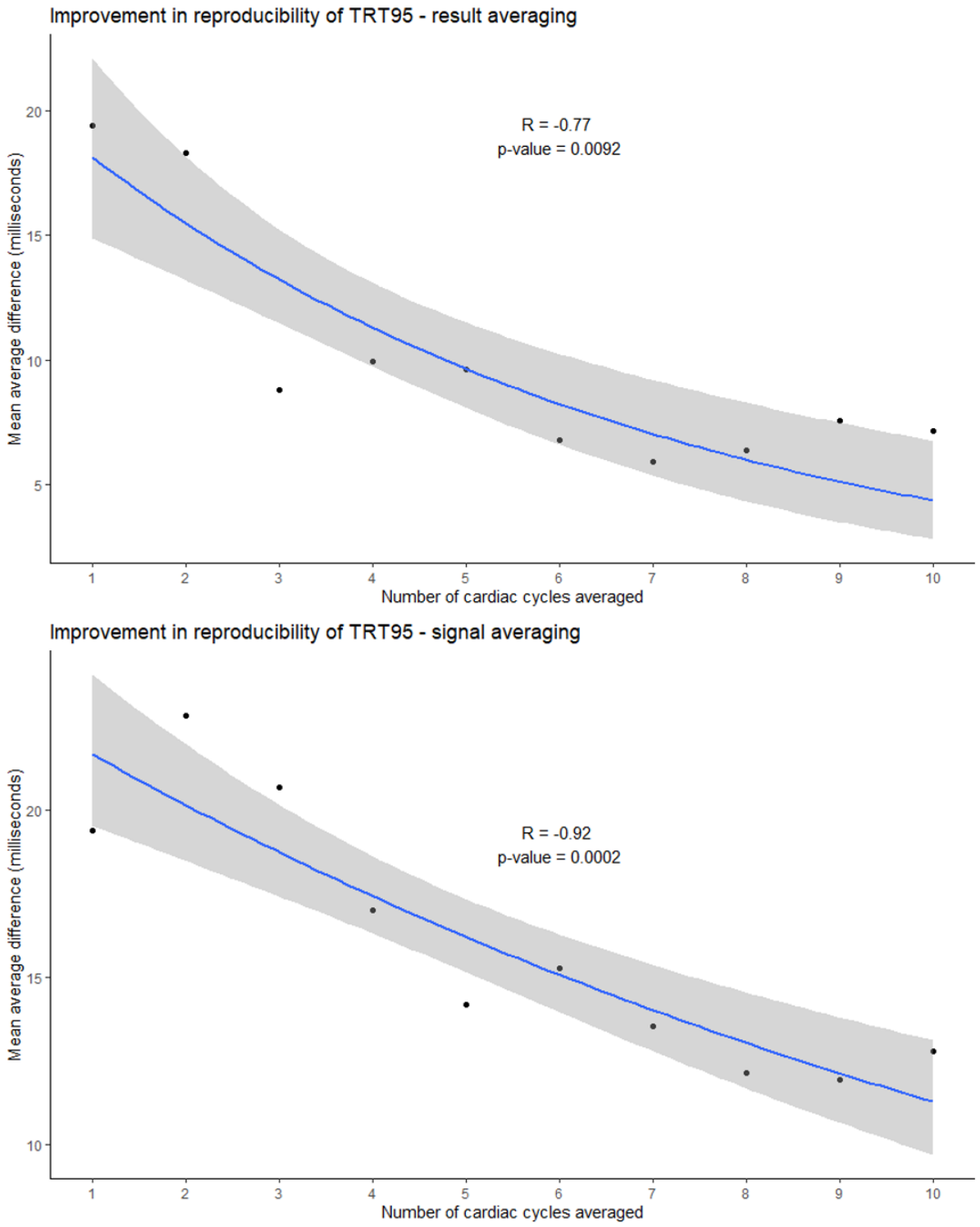

Figure 6.17: Reproducibility improves as more cardiac cycles are considered in analysis. Signal averaging produces a synthetic average electrogram from 10 consecutive beats prior to analysis. Result averaging performs analysis on 10 consecutive beats, and then averages the result.

6.1.4 Discussion

Operator selection of time-windows and clean electrograms for analysis can be critical in making clinical judgements when presented with a single dataset. This study explores how manual strategies can lead to poor reproducibility between successive and even identical cardiac cycles, as well as potential techniques for improving reproducibility in the research context.

Human versus automated reproducibility

Our initial reproducibility experiment demonstrated how evaluation of even an identical cardiac cycle can demonstrate significant intra-rater variability. Small amounts of variability were also seen in the automatic analysis, a likely consequence of the initial template QRS-T complex selection by the operator. There is an opportunity to automate this step, but with a mean absolute difference of 0.13 milliseconds the benefit would be marginal. The system would then also be disadvantaged by not being able to select a particular type of beat for analysis – whilst arrhythmia classification can be achieved to 99.7% accuracy by deep learning (Ebrahimi, Loni et al. 2020), the operator would have to specific the class of cardiac cycle desired for analysis, at which point it is likely simpler to simply select manually.

Performance of neural networks for electrogram segmentation

In this chapter we present a simplified neural network segmenting electrograms similar to that used in recent ECG segmentation (Jia, Zhao et al. 2019). Compared to Jia's neural network, we have removed the sequential conditional random fields element which adds extra processing time during both learning and prediction. Without this layer our network still achieved a high degree (>97%) of accuracy classifying each millisecond of the surface ECG dataset.

Currently no labelled reconstructed cardiac electrogram datasets are available. We used our neural network trained on surface ECG to directly predict the waveform boundaries for epicardial signals. Due to the lack of available labels in a large dataset, the millisecond-accuracy for cardiac electrograms cannot be stated but visually segmentation was successful in most beats (>99%). Further improvements could be made using transfer learning – taking a pre-trained neural network on a similar dataset (surface ECG) and fine-tuning the response in a smaller but more specific labelled dataset. A future goal should be to expertly label epicardial electrograms for this purpose. Transfer learning is extensively used in machine vision, but currently only a single paper exists

describing pre-training a neural network on human ECG and transferring this learning to equine ECG (Van Steenkiste, van Loon et al. 2020).

It remains unclear whether we can claim 'good accuracy' of segmenting epicardial electrograms using this method as only sinus beats have been considered from a small number of patients. To be confident that our system segments successfully in a wider range of situations further testing would be needed.

For this reason, user-editable waveform boundaries remain available in our software. Whilst the user-edit may harm reproducibility, it may be essential for the true segmentation of the epicardial electrogram.

Summary statistics for improving reproducibility

In this experiment, both signal averaging and result averaging were effective methods of improving reproducibility in non-identical beat analyses. In both strategies, the greater the number of beats used, the smaller the difference between two consecutive runs of 10 cardiac cycles. Result averaging seemed to produce a slightly lower mean average difference in this experiment, but it is not clear that this is more than a chance finding as the magnitude of the difference is very small.

There is a balance to be struck between dynamic changes in cardiac electrophysiology and reproducibility. A key advantage of ECG imaging is the ability to panoramically map a single cardiac cycle. In traditional roving-catheter mapping, several hundred cardiac cycles may be averaged into a single activation map. If cardiac electrophysiology has altered over this time, this would not be appreciated; worse, if the alteration were not periodic, or the period were greater than the mapping time, the sequence in which cardiac segments were mapped would change the interpretation. Whilst choosing to analyse longer runs of beats could improve reproducibility, it could also reduce precision for detecting the effects of short-term stressors.

Although we can say how similar the results are for two consecutive runs of beats, we cannot tell what the relationship is to ground truth. To achieve the intact, innervated and physiologically active heart we purposefully did not perform invasive measurements. An epicardial electrode sock would be the ideal measurement of panoramic ground truth, but this would require a sternotomy and preclude the application of realistic physiological stressors.

6.1.5 Conclusion

Human reproducibility for ECG imaging datasets can be markedly improved by the introduction of automation. However, the differences between neighbouring cardiac cycles can also significantly hamper reproducibility. Summary methods such as signal averaging or result averaging improve reproducibility, but the full extent and superiority of one strategy over the other has yet to be determined. Further study either by experimentation or simulation would be needed to form a definitive opinion.

6.2 Comparison of signal and result averaging against a simulated noise dataset

6.2.1 Introduction

In the previous section, a small number of real patients underwent two rounds of repeat analysis after which it was difficult to conclude whether a signal averaging or result averaging strategy was more appropriate for further work.

Although real data has the advantage of demonstrating actual reproducibility between two different beats, the actual ground truth remains unknown. To understand the relationship between ground truth and measured values in the presence of noise, simulation studies can be useful.

In our previous noise simulation experiment we utilized noise from a narrow band of frequencies and magnitudes. In this experiment we aimed to test the accuracy of signal averaging against result averaging when a wide variety of noise frequencies and amplitudes to determine which strategy would be more robust in different situations. Importantly, we aimed to be able to finely control the noise spectra in this experiment – which is not possible in real world experimentation.

6.2.2 Methods

To produce synthetic clean data, a set of m electrograms containing 10 cardiac cycles ($10n$ samples) was obtained from a patient at rest. This was signal averaged to a single synthetic cardiac cycle array of size $m \times n$ and then filtered using a Savitzky-Golay filter, window length 51 milliseconds and order 3. The ground truth local repolarization time for the trace was calculated as QRS start subtracted by the steepest upward slope location of the T wave, or $max\left(\frac{dV}{dt}\right)$.

To produce synthetic noise for addition to this clean data, a visually noisy single electrogram containing 10 cardiac cycles was filtered using a Savitzky-Golay filter, window length 51 milliseconds and order 7. The resultant filtered trace was then subtracted from the original, leaving only the noise. This noise was then multiplied by 1 to 20 times in length (using 1-dimensional interpolation) and magnitude to produce 400 unique noise patterns with a range of frequencies and amplitudes.

To ensure the noise patterns were not simply duplicated every time, a random segment of noise equivalent sample length to the clean data was chosen at random and added onto this clean data. The effect of small errors in autocorrelation were simulated by the random addition or subtraction of up to 10 milliseconds to the start of the trace.

Local repolarization time was calculated for the synthetic noisy electrograms using the methods in section 6.1.2. Briefly, for each clean electrogram studied, ten synthetic noisy electrograms with

varying amounts of simulated autocorrelation error were created. In the result averaging strategy, local repolarization time was calculated for each of the ten and averaged to find the final value. In the signal averaging strategy, the mean of the ten synthetic noisy traces was calculated and the local repolarization time calculated for this. Figure 6.18 visually describes the method.

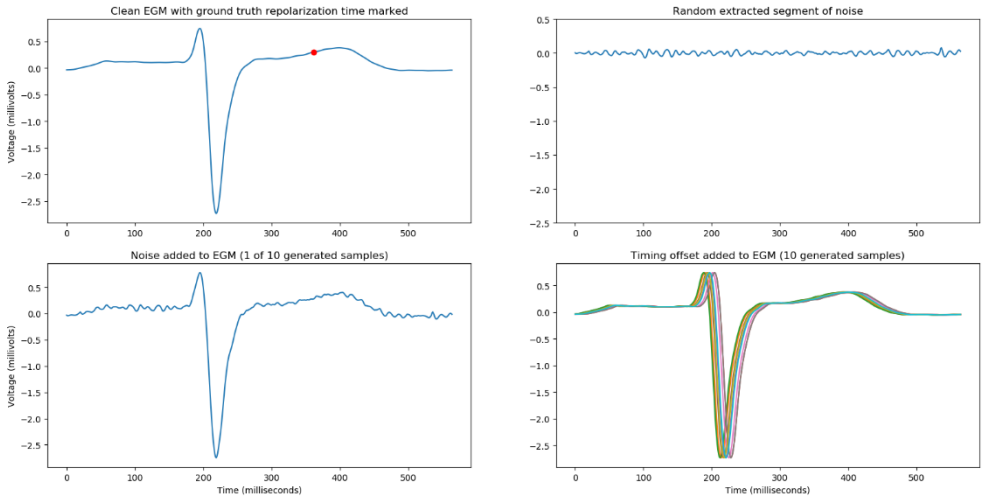

Figure 6.18: Visual summary of methods in this simulation study. Top left: a clean electrogram (EGM) has repolarization time marked using the Wyatt method. Top right: a random segment of extracted noise is chosen by filtering from a real noisy electrogram trace. Bottom left: the extracted noise is added to the electrogram to form a synthetic EGM with controllable noise characteristics. Bottom right: a random timing offset is introduced to the electrogram to simulate errors in autocorrelation

For each combination of noise amplitude and frequency spectrum this allowed comparison of the two methods by their deviation from ground truth. To determine the effects noise on the two methods in a larger group, each electrogram measurement was repeated 100 times. T-tests were performed to determine the significance of the difference between the methods.

6.2.3 Results

Simulation statistics

Approximately 50 hours of computing was performed on a laptop computer (Intel™ Core i7-10510U central processing unit @ 2.3GHz with 16 gigabytes of random-access memory). 1158 electrograms were assessed for typical amplitudes and frequencies. 232 clean electrograms – 1 in 5 – underwent ground truth calculation, noise and autocorrelation error addition before result and signal averages were performed. In total, from 100 repeats using 400 different synthetic noise additions, ~9.2 million electrogram simulations were performed for this analysis.

Raw spectral characteristics

For the mean clean electrogram, QRS frequency content extended up to 50Hz, peaking at approximately 20 Hz. T wave frequency content extended up to 20Hz, peaking at approximately 5Hz. Understanding this distribution is key because when the noise spectrum is identical to the waveform spectrum, filtering is impossible. Graphical expressions of the spectra are shown in Figure 6.18.

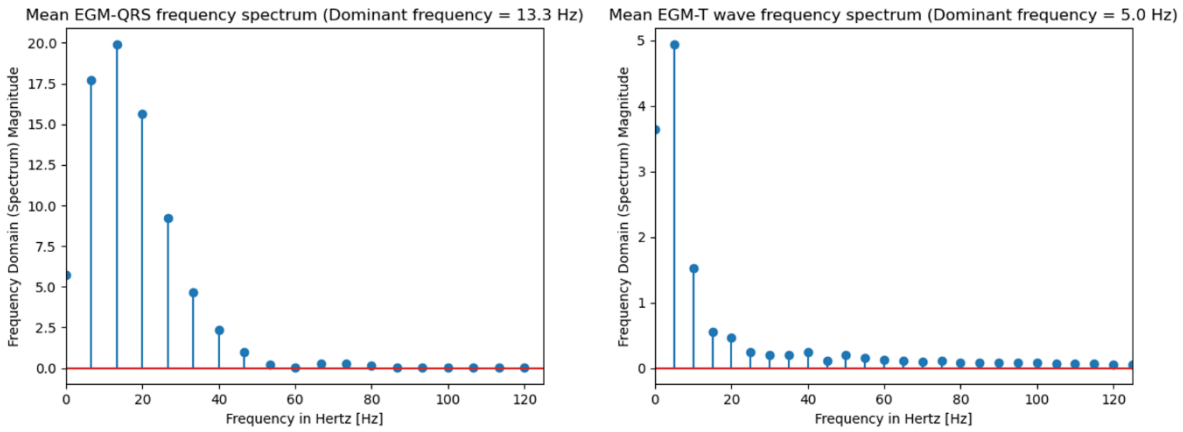

Figure 6.19: Frequency spectra of QRS complex and T wave for the mean electrogram (EGM) in the clean dataset.

QRS amplitudes peaked at 10mV with the bulk of values around 2-4mV. T wave amplitudes peaked at 3.8mV with the bulk of values under 1mV. Distribution of the amplitudes from the clean electrogram dataset are shown in Figure 6.19.

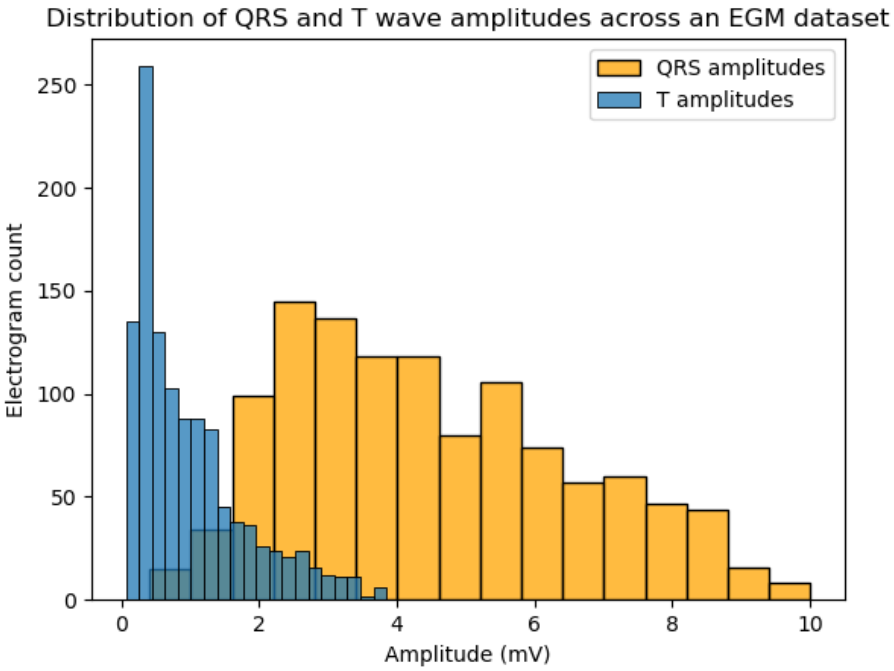

Figure 6.20: Distribution of amplitudes for QRS complex and T waves across the whole clean electrogram (EGM) array (n = 1158).

Extracted noise occupied a broad band of frequencies upwards of 25Hz, peaking at approximately 70Hz. Peak amplitude of noise was 0.21mV. Therefore, to reach similar spectral characteristics to the T wave, the period would have to be extended by a factor of approximately 16 and the amplitude increased by approximately factor 20. The noise spectrum is displayed in Figure 6.20.

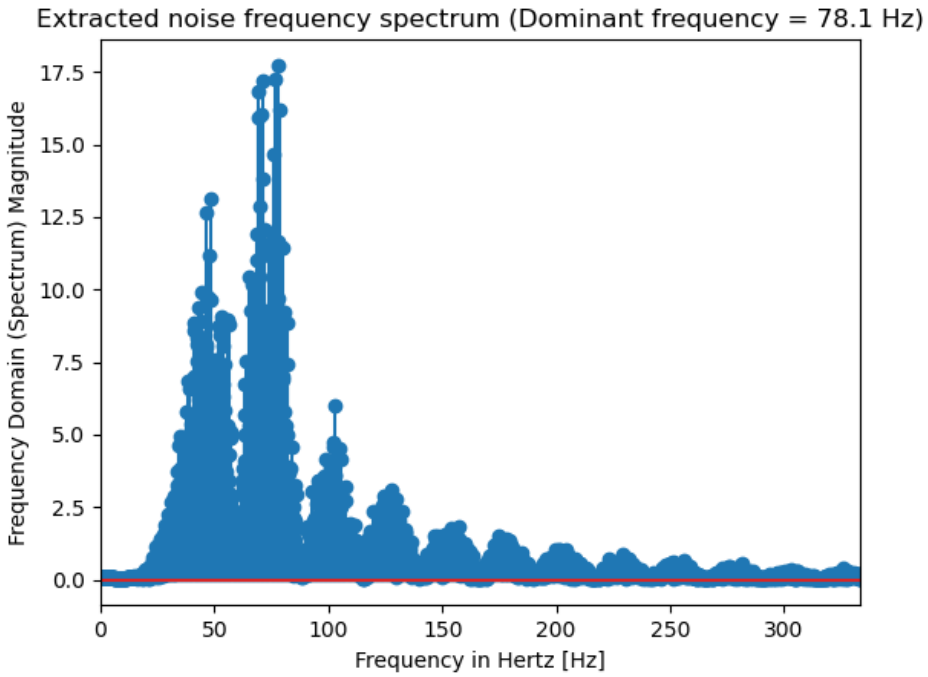

Figure 6.21: Frequency spectrum of extracted noise used in this simulation

Synthetic noise characteristics

Following interpolation and multiplication, 400 noise samples were created with different frequency spectra and amplitudes. These are shown in Figure 6.22.

Figure 6.22: Four hundred noise signals with varying amplitudes and frequency. The asterisk (*) marks the original noise signal used to generate the other 399 synthetic signals.

These were then added to the electrograms, an example of which is demonstrated with the variant noise signals in Figure 6.23. Noise is easily visually detected when high frequency and high amplitude (Figure 6.23, bottom left). When noise is added that is closer to the spectra of a typical QRS complex or T wave, it is less obvious which components are part of the original clean electrogram.

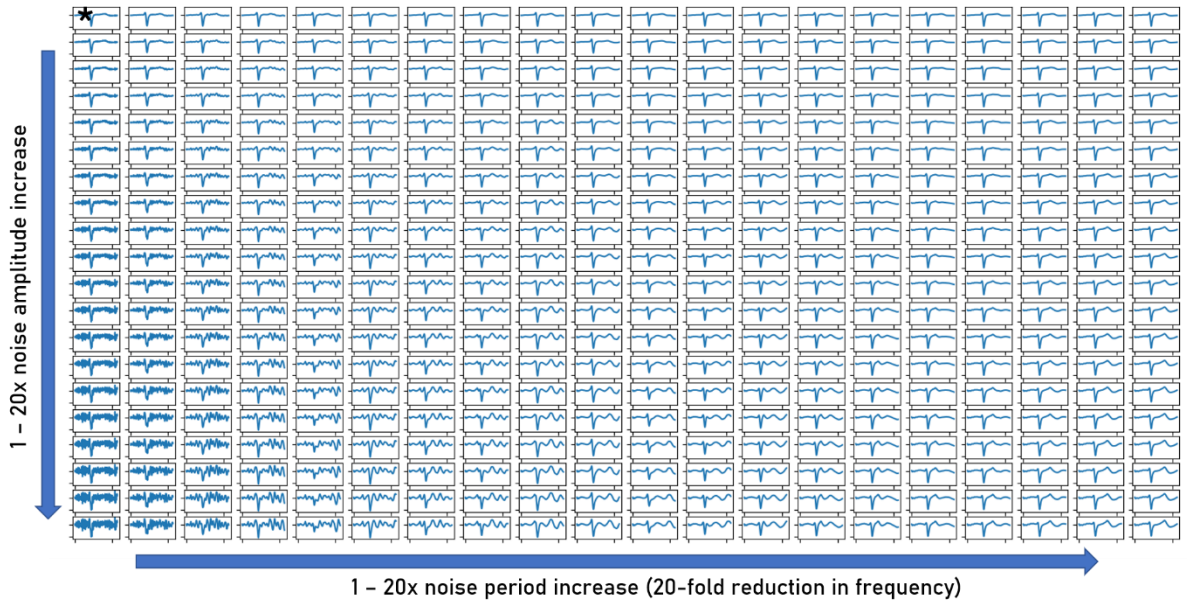

Figure 6.23: Four hundred noise signals with varying amplitudes and frequency added to an example clean electrogram. Top left – the original noise signal added to the clean electrogram (*). Bottom left: high frequency, high amplitude noise is easily identified as being abnormal – the electrogram is hardly identifiable. Bottom right: as the frequency aligns with the spectral peak of QRS complexes and T waves, it is progressively more difficult to determine whether signal components are noise or real parts of the clean electrogram.

Simulation of signal and result averaging outcomes

Mean difference from the ground truth over all 400 noise sets was 4.87 milliseconds for signal averaging and 5.22 milliseconds for result averaging (T-test $p < 0.00001$). The distribution of method superiority is demonstrated in Figure 6.24. Signal averaging is superior in most amplitudes and frequencies, but result averaging has an advantage with noise around 1.5mV amplitude and lower dominant frequencies (>20Hz).

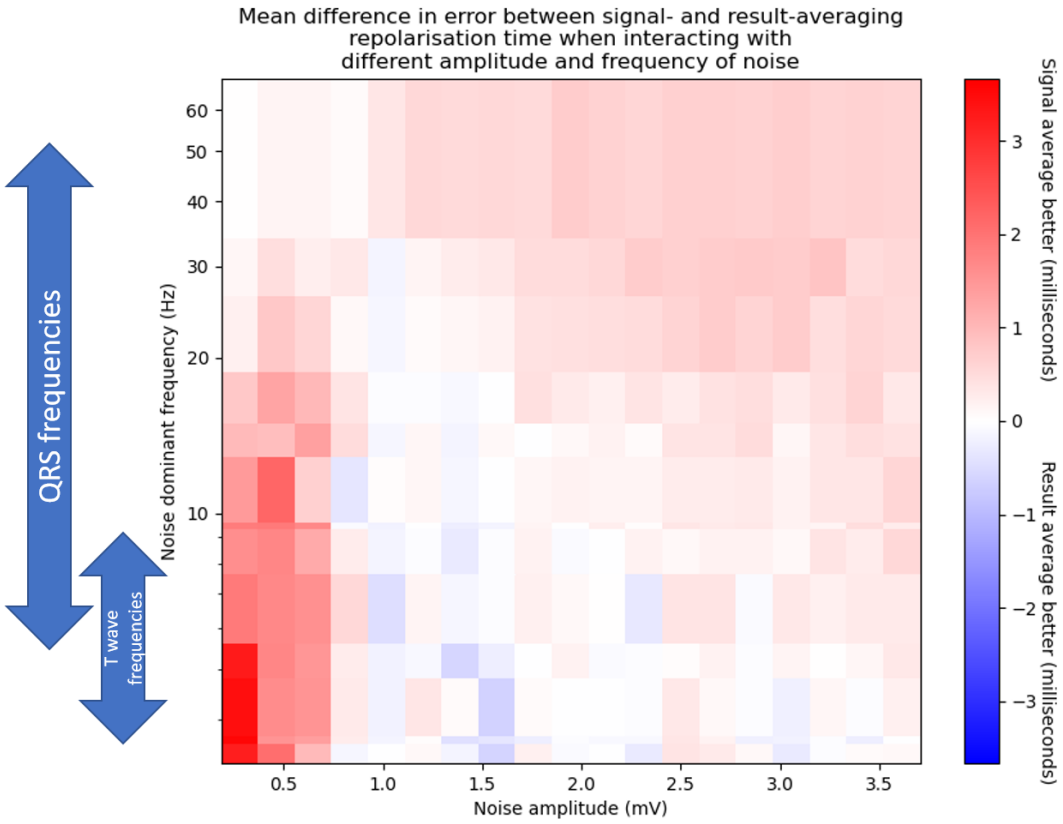

Figure 6.24: Distribution of signal vs result averaging superiority by noise frequency and amplitude characteristics. Millivolts, mV; Hertz, Hz.

To understand the relationship between T wave morphology and error, the peak T wave gradient for each of the 232 electrograms studied was plotted against the mean error of all simulations for that electrogram. The results are shown in Figure 6.25. The range of errors with very low T wave gradients <0.01 millivolts/milliseconds can be ±100 milliseconds from ground truth. Excluding T wave gradients <0.01 or <0.02 millivolts/milliseconds would exclude 98 or 148 out of 232 electrograms (48 or 63%) from analysis and reduce mean absolute error to 6.2 and 3.7 milliseconds respectively.

The same analysis for only the original extracted noise source is shown in Figure 6.26. Error at lower gradients is reduced compared to the mean of all 400 noise sets. Excluding the 61 electrograms (26%) with peak T gradient <0.005 millivolts/millisecond would result in a mean absolute error of 1.97 milliseconds. Increasing this threshold to 0.01 and 0.02 millivolts/milliseconds would give mean absolute errors of 1.95 and 1.59 milliseconds respectively. Below the 0.02 millivolts/milliseconds cut-off, 50 of 148 (34%) of electrograms had mean absolute error ≤ 1.59 milliseconds.

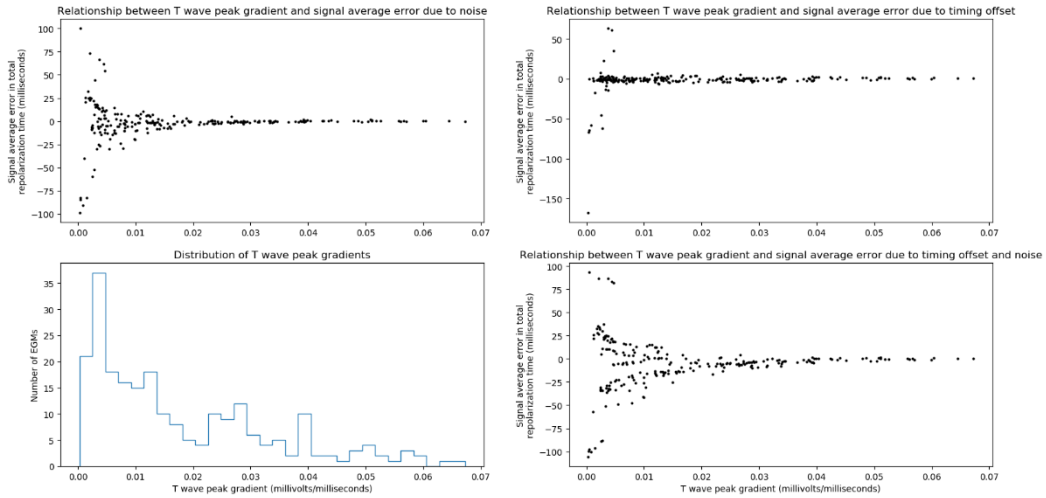

Figure 6.25: The relationship between T wave peak gradient in 232 electrograms and error over all synthetic noise spectra and amplitudes. Top left – relationship between T wave gradient and error induced by noise alone. Top right – relationship between T wave gradient and error induced by autocorrelation inconsistency alone. Bottom left – distribution of T wave peak gradients. Bottom right – relationship between T wave gradient and error induced by a combination of noise and autocorrelation inconsistency. Electrogram, EGM.

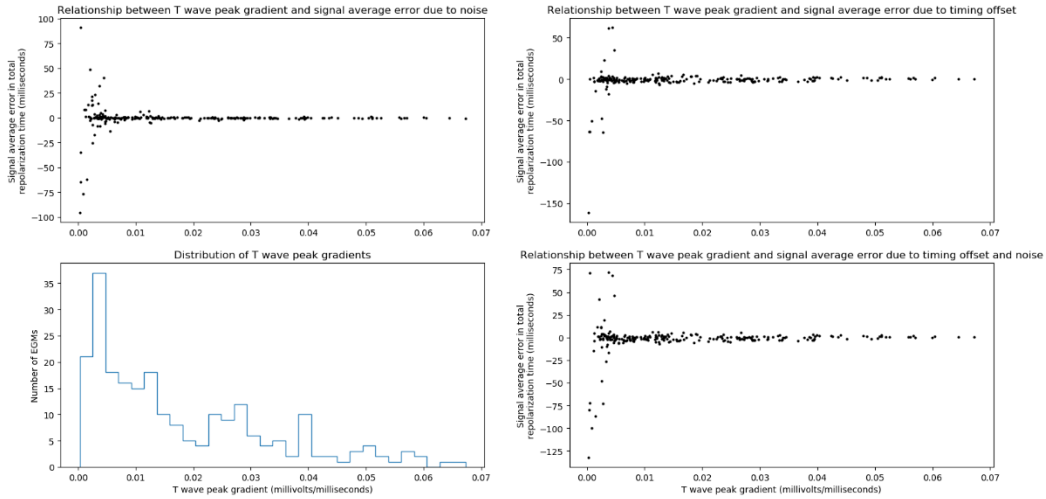

Figure 6.26: The relationship between T wave peak gradient in 232 electrograms and error over the original, extracted noise spectrum and amplitude. Top left – relationship between T wave gradient and error induced by noise alone. Top right – relationship between T wave gradient and error induced by autocorrelation inconsistency alone. Bottom left – distribution of T wave peak gradients. Bottom right – relationship between T wave gradient and error induced by a combination of noise and autocorrelation inconsistency. Electrogram, EGM.

6.2.4 Discussion

In this experiment we examined the effect of synthetic noise on error in repolarization measurement. Compared with the real patient experimentation in the previous section, we have been able to both set a 'ground truth' and finely control the frequency and amplitude characteristics of the synthetic noise.

Noise characteristics

There are several ways we can measure the frequency and amplitude of noise affecting a given electrogram. Each method has assumptions and weaknesses. First, a filter could be applied until a 'clean-looking' electrogram is formed. The value of the data removed by the filter could then be said to be noise. This is highly subjective as the ground truth of the clean electrogram is unknown. The result of this analysis is simply the operator's idea of what noise looks like. Second, signal averaging could be used to form a synthetic clean electrogram. This assumes that the signal (i.e. the true waveform shape) is always identical, that timing is matched exactly and that all noise is random: none of which are guaranteed. Third, an artificial patient model or cadaver could be used, but this assumes that all noise originates from the measurement equipment – not true as respiratory and muscle activity are known to be significant components of ECG artefact. Last, a live patient with temporarily ceased ventricular activation could be measured, for example after adenosine induced atrioventricular block. Whilst likely the most robust measurement, it is also riskiest for the patient and does not guarantee that non-cardiac signals are preserved.

For this reason, assessment of methods should occur using a wide range of sample noise frequencies and amplitude. Figure 6.23 demonstrates that for frequencies and amplitudes approaching QRS and T wave values, it is difficult to say if an electrogram is noisy or there are genuine abnormalities in activation or repolarization that should be preserved for measurement.

Performance of signal and result averaging

Signal averaging outperformed result averaging both overall and for most noise frequencies and amplitudes tested. These frequencies and amplitudes included values in the range of representative T waves, so the amount of noise added can be judged to be as extensive as any readings analysed by cardiologists. Any higher amplitudes would obscure the T waves.

For the purposes of further experimentation, this result would appear to recommend signal averaging as the default method for approximating ground truth.

Cut-offs for exclusion

Exploratory analysis was performed on the simulation dataset to determine if an exclusion threshold could be set for T wave characteristics. As T wave peak gradient rises, mean absolute error falls. This is not a surprising result as larger, steeper signals should be less vulnerable to most noise and less altered by filtering.

In our example dataset, large numbers of electrograms (26-63%) would have been discarded to remove the greatest outliers. Summary statistics such as whole-heart conduction could be drastically affected by discarding this many electrograms, and low amplitude 'diseased' electrograms could be preferentially deselected. This fact strengthens the case for simply excluding outlier values assuming they must be erroneous, for example by using the central 95% of total repolarization time.

Limitations

One caveat is that we do not know which extrinsic noise frequencies and amplitudes are truly most common (see section Noise Characteristics). In a minority of noise frequencies and amplitudes result averaging may be superior.

This simulation also only considered a set of 232 T wave morphologies, which should be extended to ensure that any proposed cut-offs are applicable to wider groups. However, this experimental method could be used as a framework for future determination of the optimal cut-offs for T wave rejection.

6.2.5 Conclusion

Signal averaging appears superior to result averaging for the analysis of noisy electrograms – we would recommend that it be used in any electrogram analysis process which is prone to poor reproducibility. In a wider experiment it may be possible to determine optimal cut-offs for electrogram rejection based on the measured characteristics. The true extent of noise in our signal is difficult to know, as at certain frequencies and amplitudes, noise can be indistinguishable from pathological signs. This forces us to make the key assumption underlying signal averaging: that the ground truth is static. In the highly dynamic interplay of trigger and substrate for arrhythmia, this remains an inherent challenge to the measuring electrophysiological characteristics in diseased hearts.

Chapter 7: The arrhythmic substrate of Brugada syndrome

7.1 Introduction

Ventricular conduction stability was shown to successfully differentiate Brugada syndrome patients from controls in chapter 4, but electrophysiological differentiators of ventricular fibrillation survivors are still lacking.

Invasive descriptions of the arrhythmic substrate in Brugada syndrome are becoming established, and even forming the basis of ablative treatment that has been shown to reduce short term arrhythmia inducibility (Brugada, Pappone et al. 2015). Electrocardiographic imaging (ECGi) has also been used to non-invasively describe the difference between patients with a spontaneous Type 1 ECG, demonstrating ST segment elevation, delayed right ventricular outflow tract activation, prolonged recovery and steep repolarization gradients.

Patients with spontaneous Type 1 ECG are a minority of modern Brugada syndrome cohorts – including many patients suffering cardiac arrest (Raju, Papadakis et al. 2011; Leong, Ng et al. 2019). The effect of previous ventricular fibrillation on epicardial electrophysiology is unknown.

Using the automated and reproducible methods from chapter 6, we hypothesise that ECGi can demonstrate electrophysiological differences between Brugada patients and their unaffected relatives, and potentially be used to identify Brugada patients with a personal history of cardiac arrest.

7.2 Methods

7.2.1 Patient selection

The patient cohort from Chapter 4 was re-analysed. To recapitulate:

Fifty-two patients were selected from our cohort.

4. 21 survivors of ventricular fibrillation or sustained ventricular tachycardia and haemodynamic compromise with Brugada syndrome (‘BrS VF’).

5. 20 patients with Brugada syndrome without previous ventricular fibrillation or sustained ventricular tachycardia ('BrS')
6. 11 asymptomatic relatives of patients with Brugada syndrome, proven not to have the same condition by a negative Ajmaline challenge reaching dose endpoint of 1mg/kg (up to 120mg total dose).

Exclusion criteria were identical to those described in Chapter 4.

7.2.2 Exercise ECGi testing and epicardial reconstruction

Each volunteer underwent the following procedures as detailed in Chapter 2: Methods:

- Drug cessation if necessary
- Torso preparation and vest application
- Maximal Bruce protocol exercise testing
- Supine recovery for a minimum 10 minutes or to return of resting pulse rate
- Low dose-CT scan of chest
- Epicardial reconstruction of electrograms.

7.2.3 Measures of epicardial electrophysiology

Measurements were made in anatomical subdivisions of the epicardial shell as well as the whole heart. Magnitude, spread and gradient measures were calculated for each of activation and repolarization in these subdivisions for both exercise and recovery.

Finite impulse response filtering, signal averaging and electrogram segmentation by convolutional neural network were performed as described in Chapter 6.

To better understand the electrophysiology of the three groups, three domains were defined for analysis:

1. The mean of activation or repolarization times was used to describe overall *conduction or repolarization delay*.
2. The central 95% range of activation or repolarization times was used to describe *conduction or repolarization dispersion*.
3. The mean gradient of activation or repolarization times in space was used to detect the presence of *steep gradients in conduction or repolarization*.

7.2.3.1 Activation measures

QRS complex start for each reconstructed epicardial electrogram was predicted by the convolutional neural network. The 2.5th percentile of all electrogram QRS starts was taken to represent whole-heart activation start in order to exclude prediction outliers.

Local activation time was defined as the steepest negative deflection, or $max\left(-\frac{dV}{dt}\right)$ of the electrogram QRS complex. Whole-heart activation start was used as the reference timing, and the mean was calculated. Spread was measured by the central 95% range of activation times to exclude likely outliers.

For two neighbouring vertices i and j on the epicardial shell, the activation gradient in milliseconds/millimeter can be expressed as $g = \frac{AT_i - AT_j}{d(i,j)}$, where AT is the local activation time for a given vertex, and $d(i,j)$ is the Euclidean distance between the vertices in 3-dimensional space. Euclidean distances were calculated using the Pythagorean formula $d(i,j) = \sqrt{(i_1 - j_1)^2 + (i_2 - j_2)^2 + (i_3 - j_3)^2}$ where the coordinates of vertices i and j are (i_1, i_2, i_3) and (j_1, j_2, j_3) respectively. To determine the local mean gradient for a given vertex, this calculation was performed for all neighbouring vertices within a given distance and averaged. The mean of these local gradients could then be expressed over the whole heart or within an anatomical segment.

Exploratory testing in 6 patients using multiple search distances revealed that 5 millimeters allowed the whole-heart gradient to stabilize for each patient with no advantage to searching further (Figure 7.1). Using a 5 mm search distance, Figure 7.2 demonstrates how the mean gradient measure can numerically express irregularities in conduction seen in traditional activation maps.

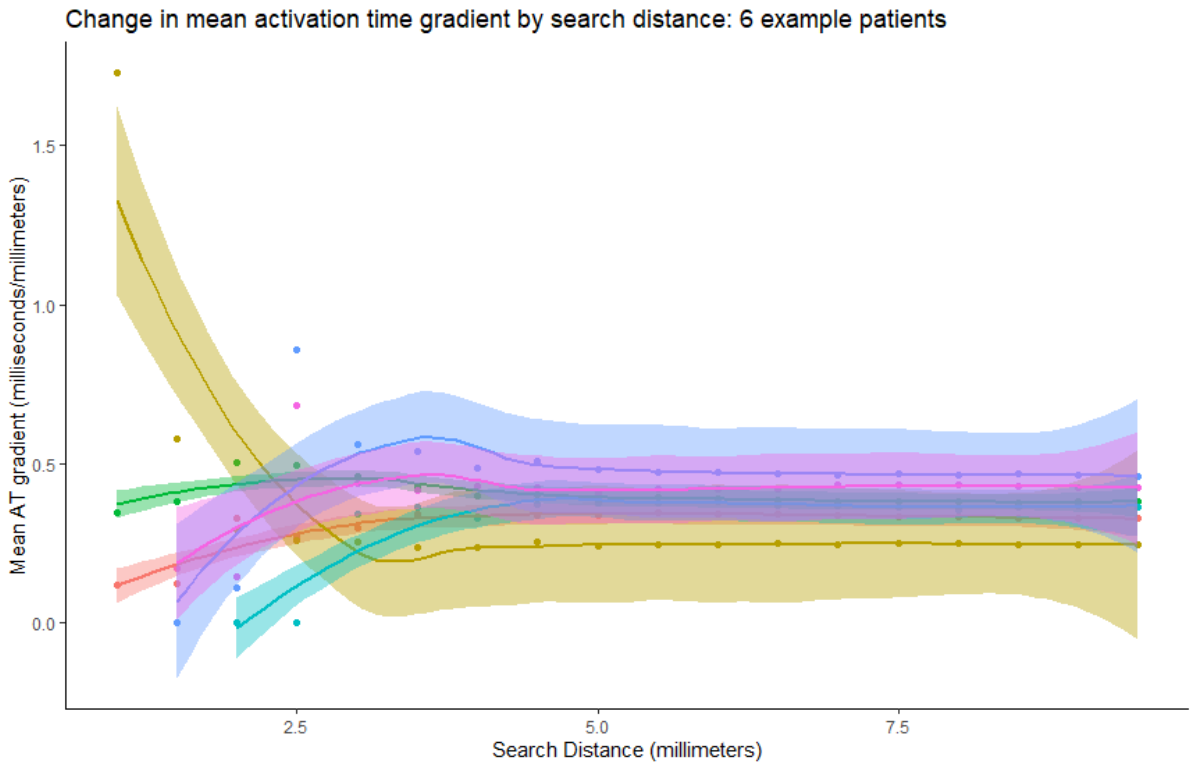

Figure 7.1: To determine optimal search distance to express activation gradients over, search distances were increased from 0 to 10 millimetres. Under 5 millimetres, changes in search distance were accompanied by poor reproducibility for repeat measurement. At 5 millimetres and above, gradients were consistently replicated. Activation time, AT.

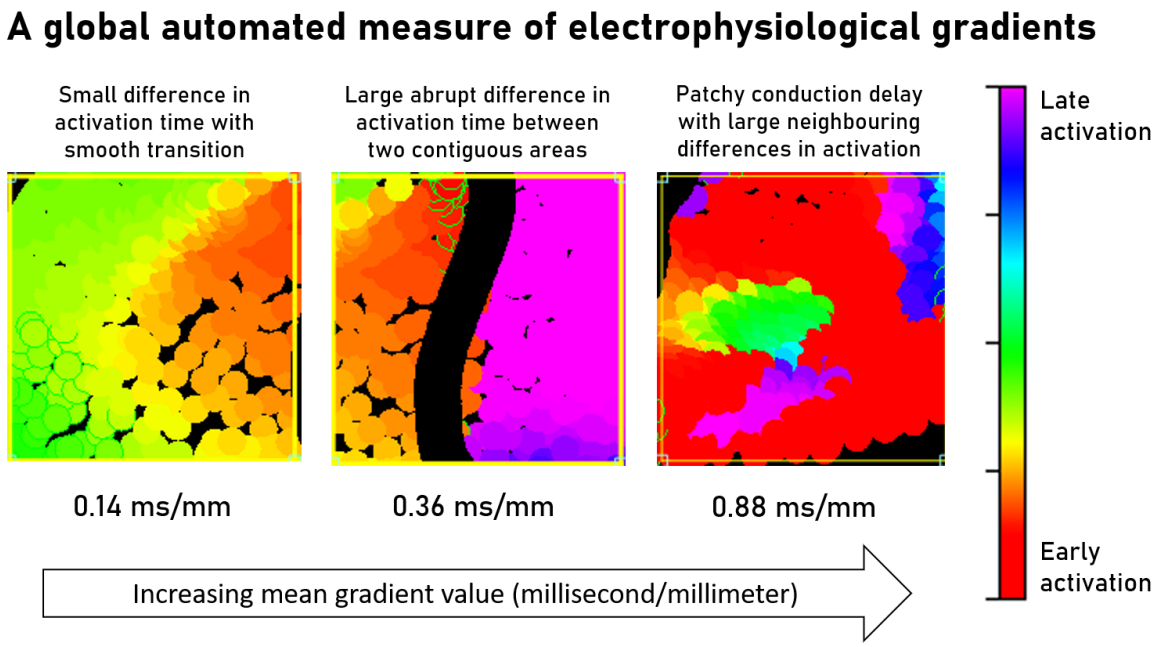

Figure 7.2: To illustrate the visual implications of mean activation gradient, three example segments of activation maps are shown. On the left, smooth transition between two closely activating areas produces the lowest gradient of 0.14ms/mm. In the middle two contiguous areas separated by a line of block under the left anterior descending artery (black line, surrogate for septum) produces an intermediate gradient of 0.36ms/mm. On the right, patchy areas of late conduction embedded within early activation produce the highest gradient of 0.88ms/mm.

7.2.3.2 Repolarization measures

Local repolarization time was defined as the steepest negative deflection, or $max\left(\frac{dV}{dt}\right)$ of the electrogram T wave. Whole-heart activation start was used as the reference timing, and the mean was calculated. Spread was measured by the central 95% range of repolarization times to exclude likely outliers. Activation recovery intervals (ARI) were also calculated for each vertex as $ARI = AT - RT$ where AT is the local activation time and RT is the local repolarization time. Mean and central 95% range were calculated.

Repolarization time was used in the measures of delay and dispersion to closer reflect the spatial variation in refractoriness at any given point in time. As spatial information is included in the gradient, activation recovery interval was used for gradient calculations to accentuate any deviation from normal action potential duration gradients seen in normal tissue (Myles, Bernus et al. 2010).

Corrections for heart rate were made using the Fridericia formula. Gradients were also calculated in a similar method to the activation times for rate-corrected activation recovery intervals only. Search distance was preserved at 5mm for consistency.

7.2.3.3 Surface measures

To ensure direct concordance with the epicardial measurements, raw surface ECG data was extracted from the CardioINSIGHT™ vest alongside reconstructed potentials. The visually cleanest body surface signal from vest electrodes 71-79 was selected as a surrogate for V2 on a 12 lead ECG. As the central terminal for the CardioINSIGHT™ vest is only an approximation of Wilson's, no comments were made on morphology and the measurements were made of timings only.

Heart rate, QRS duration, QT interval and correction by Fridericia formula were obtained for comparison to the epicardial measurements using a PyQt5 based graphical user interface.

7.2.3.4 Anatomical subdivisions

Left and right ventricle divisions were made using the left anterior descending artery as a surrogate for the septum as this cannot be segmented from the non-contrast scans used by CardioINSIGHT™. The right ventricular outflow tract was defined as the area of the right ventricle immediately proximal to the pulmonary trunk.

To ensure concordance between exercise and recovery epicardial reconstructions, epicardial shell coordinates were saved to a custom file per-patient denoting the vertices assigned to each segment. These could then be loaded for each new beat, ensuring identical subdivisions of anatomy.

7.2.4 Statistical analysis

Three-way comparisons were made using the Kruskal-Wallis test, and pairwise comparisons made using the Wilcoxon rank-sum test. Significance was defined as $p < 0.05$. Any significant three-way comparisons were further examined for pairwise significance.

Repeat analysis was performed excluding patients exhibiting a Type 1 ECG at any time to assess electrophysiological differences in patients with a concealed pattern.

7.3 Results

7.3.1 Patient characteristics and surface measures

Study groups were not significantly different in gender balance, age, heart rates and peak exercise or recovery. QRS durations were also not significantly different during exercise or recovery. Corrected

QT intervals at peak exercise were however different for both BrS VF versus BrS and BrS VF versus BrS relatives (means 372.4, 340.7 and 332.1 milliseconds, pairwise comparisons p = 0.04, p = 0.011 respectively). QTc for peak exercise was not significantly different between BrS and BrS relatives (p = 0.33). Corrected QT intervals at end recovery were different between BrS VF and BrS relatives (means 415.8 and 376.1 milliseconds, p = 0.012). Comparisons of BrS VF versus BrS and BrS versus BrS relatives did not yield a significant difference (pairwise comparisons p = 0.093 and 0.33 respectively).

There was a significant difference between the proportion of electrograms selected by the automated method as suitable for analysis. BrS VF underwent the greatest deselection, followed by BrS then BrS relative (p = 0.04).

*Table 7.1: Characteristics of volunteers undergoing electrocardiographic imaging exercise testing. Peak and recovery phase heart rates were those when signal was clean enough for measurement using the electrocardiographic imaging system. *Spontaneous type 1 ECG was defined as positive if the ECG pattern were seen during the exercise test or any ECG recording from clinic. Brugada syndrome, BrS; Brugada ventricular fibrillation or haemodynamically unstable sustained ventricular tachycardia survivor, BrS VF; Electrocardiogram, ECG.*

Parameter	**BrS VF**	**BrS**	**BrS relative**	**p-value**
Males (proportion)	85.7%	75%	72.7%	0.60
Age (years, mean)	46.9	46.1	45.5	0.93
Spontaneous type 1 ECG (proportion)*	23.8%	15.0%	-	0.21
Syncope (proportion)	14.3%	15.0%	-	0.41
Peak phase heart rate (bpm, mean)	145.4	144.1	135.3	0.39
Peak phase QRS duration (ms, mean)	103.3	100.8	88.4	0.26
Peak phase corrected QT interval (ms, mean)	372.4	340.7	332.1	**0.02**
Recovery phase heart rate (bpm, mean)	91.5	91.8	96.1	0.16
Recovery phase QRS duration (ms, mean)	113.0	118.6	101.1	0.09
Recovery phase corrected QT interval (ms, mean)	415.8	390.4	376.1	**0.03**
Electrograms automatically selected for analysis (proportion)	92.4%	92.6%	95.5%	**0.04**

7.3.2 Activation

Full results are summarized in Table 7.2.

7.3.2.1 Peak exercise

During peak exercise, the three groups differed significantly in mean whole heart activation time (mean times BrS VF = 56.8ms, BrS = 52.5ms, BrS relatives = 49.8ms, p = 0.01). In the pairwise comparisons of Figure 7.3, BrS relatives were significantly different from BrS VF (p = 0.004) but not the BrS group (p = 0.21). The BrS VF group were also not significantly different from the BrS group (p = 0.08). The greatest difference in activation times was seen in the right ventricular segment (mean times BrS VF = 52.1ms, BrS = 46.8ms, BrS relative = 44.1ms, p = 0.009).

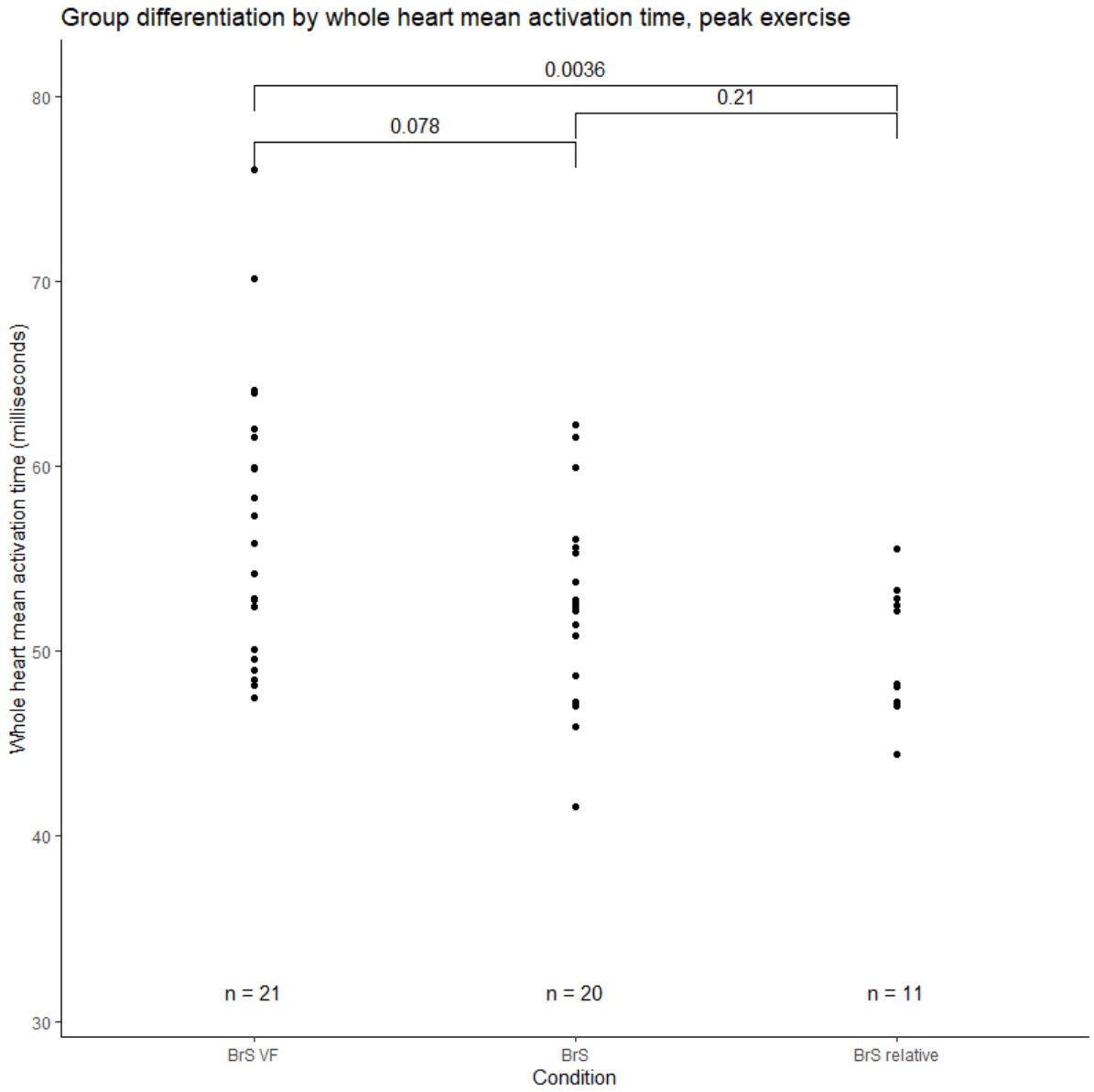

Figure 7.3: Comparison of whole heart mean activation time immediately following peak exercise between Brugada VF survivors (BrS VF), Brugada syndrome patients without a history of potentially lethal arrhythmia (BrS) and unaffected, asymptomatic relatives (BrS relatives). Local activation time was defined as the onset of the first epicardial QRS complex to the steepest negative slope of the electrogram-QRS. The mean of all times across the heart is reported per patient.

7.3.2.2 End recovery

During end recovery, activation times differences widened (mean times BrS VF = 60.6ms, BrS = 55.7ms, BrS relatives 52.4ms, p = 0.0008). In the pairwise comparisons of Figure 7.4, all three groups were significantly differentiated (BrS VF vs BrS, p = 0.017; BrS vs BrS relative, p = 0.016; BrS VF vs BrS relative, p = 0.0006). The greatest difference between groups was again seen in the right ventricle (p

= 0.0006); focusing on the right ventricular outflow tract and left ventricle also yielded significant results (p = 0.008 and p = 0.01 respectively).

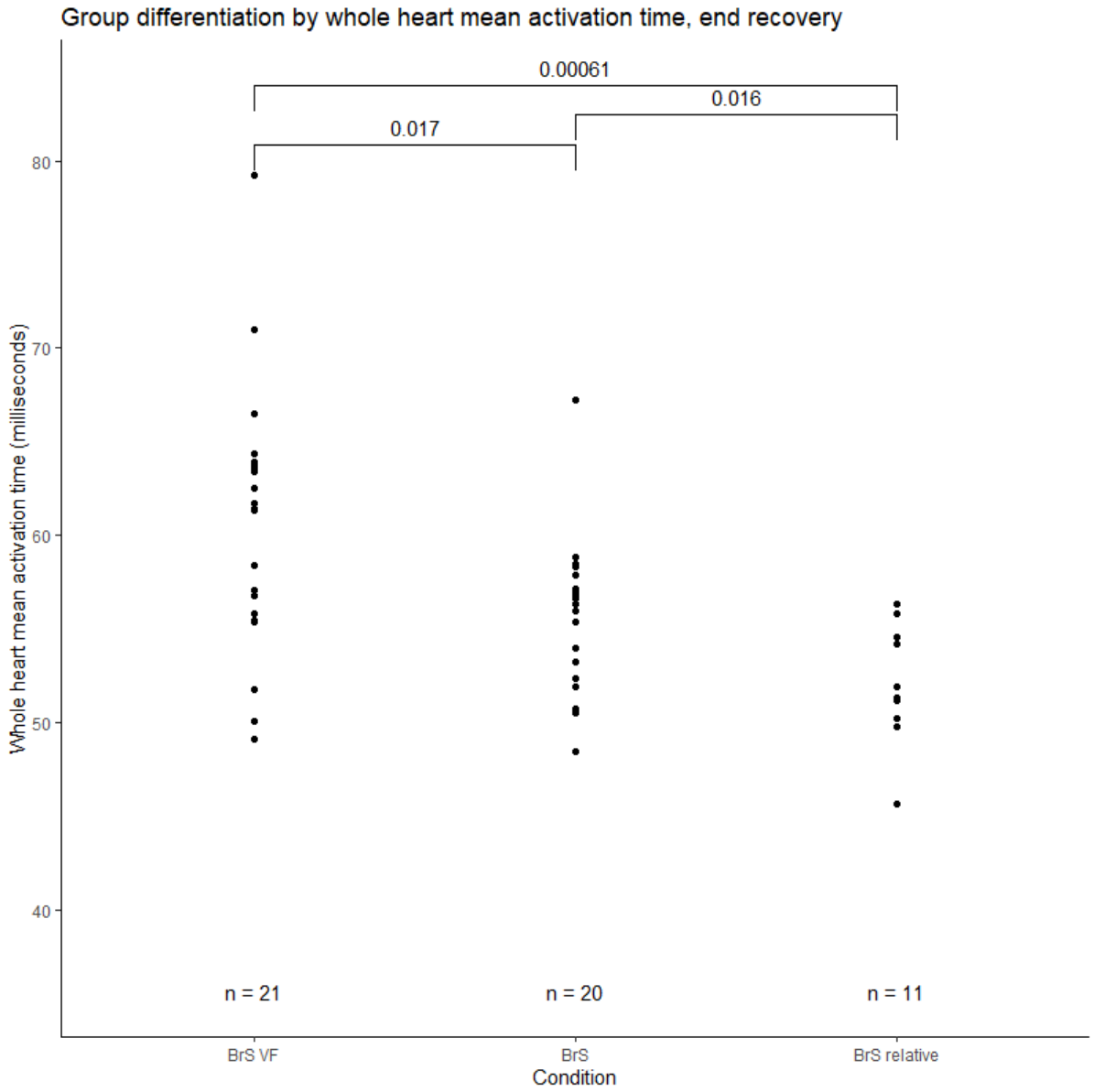

Figure 7.4: Comparison of whole heart mean activation time in end recovery between Brugada VF survivors (BrS VF), Brugada syndrome patients without a history of potentially lethal arrhythmia (BrS) and unaffected, asymptomatic relatives (BrS relatives). Local activation time was defined as the onset of the first epicardial QRS complex to the steepest negative slope of the electrogram-QRS. The mean of all times across the heart is reported per patient.

In the right ventricle, all three groups were differentiated (BrS VF vs BrS, p = 0.02; BrS vs BrS relative, p = 0.02; BrS VF vs BrS relative, p = 0.0002). In the right ventricular outflow tract BrS VF and BrS

groups could not be significantly differentiated (p = 0.13) and in the left ventricle the BrS and BrS relatives could not be significantly differentiated (p = 0.21).

Table 7.2: Comparison of automated epicardial activation measurements between Brugada VF survivors (BrS VF), Brugada syndrome patients without a history of potentially lethal arrhythmia (BrS) and unaffected, asymptomatic relatives (BrS relatives).

Measure	**BrS VF**	**BrS**	**BrS relative**	**p-value**
Peak exercise				
Whole heart				
Mean whole heart activation time (AT_{mean}, milliseconds)	56.8	52.5	49.8	**0.01**
Whole heart total activation time (TAT95, milliseconds)	56.6	46.3	47.1	0.55
Whole heart mean activation gradient (AT-$Gradient_{mean}$, millisecond/millimeters)	0.46	0.41	0.39	0.81
Right ventricular outflow tract (RVOT)				
Mean RVOT activation time (RVOT-AT_{mean}, milliseconds)	50.5	48.5	45.8	0.43
RVOT total activation time (RVOTAT95, milliseconds)	34.4	30.0	29.9	0.97
RVOT mean activation gradient (RVOT-AT-$Gradient_{mean}$, millisecond/millimeters)	0.53	0.55	0.62	0.98
Right ventricle (RV)				
Mean RV activation time (RV-AT_{mean}, milliseconds)	52.1	46.8	44.1	**0.009**
RV total activation time (RVAT95, milliseconds)	46.9	38.1	44.4	0.47
RV mean activation gradient (RV-AT-$Gradient_{mean}$, millisecond/millimeters)	0.46	0.38	0.39	0.81
Left ventricle (LV)				

Mean LV activation time (LV-AT_{mean}, milliseconds)	62.0	58.5	55.9	0.07
LV total activation time (LVAT95, milliseconds)	53.9	46.6	42.2	0.20
LV mean activation gradient (LV-AT-$Gradient_{mean}$, millisecond/millimeters)	0.45	0.42	0.39	0.42
End recovery				
Whole heart				
Mean whole heart activation time (AT_{mean}, milliseconds)	60.6	55.7	52.4	**0.0008**
Whole heart total activation time (TAT95, milliseconds)	57.2	46.9	43.9	0.07
Whole heart mean activation gradient (AT-$Gradient_{mean}$, millisecond/millimeters)	0.47	0.42	0.43	0.91
Right ventricular outflow tract (RVOT)				
Mean RVOT activation time (RVOT-AT_{mean}, milliseconds)	55.3	50.7	46.1	**0.008**
RVOT total activation time (RVOTAT95, milliseconds)	37.2	28.3	23.7	0.54
RVOT mean activation gradient (RVOT-AT-$Gradient_{mean}$, millisecond/millimeters)	0.76	0.54	0.43	0.27
Right ventricle (RV)				
Mean RV activation time (RV-AT_{mean}, milliseconds)	55.6	50.1	46.1	**0.0006**
RV total activation time (RVAT95, milliseconds)	43.0	36.2	34.2	0.87
RV mean activation gradient (RV-AT-$Gradient_{mean}$, millisecond/millimeters)	0.44	0.41	0.38	0.53
Left ventricle (LV)				

Mean LV activation time (LV-AT_{mean}, milliseconds)	65.9	62.0	59.2	**0.01**
LV total activation time (LVAT95, milliseconds)	55.8	47.3	46.3	0.13
LV mean activation gradient (LV-AT-$Gradient_{mean}$, millisecond/millimeters)	0.49	0.42	0.46	0.21

7.3.3 Repolarization

Full results are summarized in Table 7.3.

7.3.3.1 Peak exercise

During peak exercise the three groups were differentiated significantly by whole heart total corrected repolarization time (mean ranges BrS VF = 153.8ms, BrS = 133.7ms, BrS relatives = 111.5ms, p = 0.001). In the pairwise comparisons of Figure 7.5, the BrS VF and BrS groups could not be significantly differentiated (p = 0.24), but the BrS relatives were significantly differentiated from them both (p = 0.0048, 0.049 against BrS VF and BrS respectively). This was most exaggerated in the right ventricle, where all three groups were differentiated significantly (BrS VF vs BrS, p = 0.04; BrS vs BrS relative, p = 0.04; BrS VF vs BrS relative, p = 0.0027), and less so in the left ventricle, where BrS VF and BrS groups could not be significantly differentiated (p = 0.23).

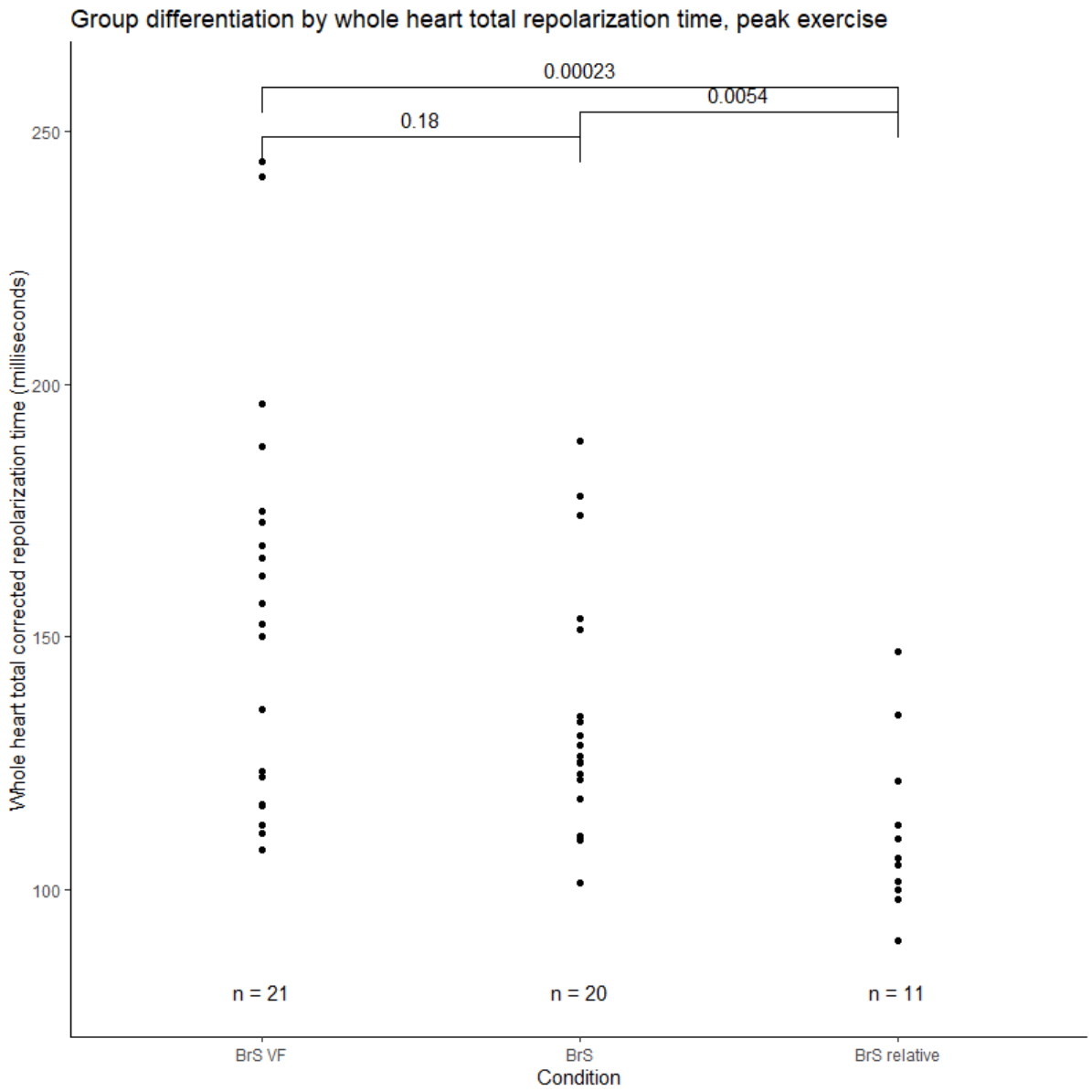

Figure 7.5: Comparison of whole heart total repolarization time immediately following peak exercise between Brugada VF survivors (BrS VF), Brugada syndrome patients without a history of potentially lethal arrhythmia (BrS) and unaffected, asymptomatic relatives (BrS relatives). Local repolarization time was defined as the onset of the first epicardial QRS complex to the steepest positive slope of the electrogram-T wave. The central 95% range across the heart is reported per patient. Correction for heart rate was made using the Fridericia method.

Mean repolarization time of the left ventricle weakly differentiated the BrS relatives from BrS VF and BrS groups (mean times BrS VF = 283.8ms, BrS = 269.9ms, BrS relatives = 226.9ms, p = 0.02). This was not in the context of a detectable whole heart difference (p = 0.07).

Whole heart repolarization gradients were significantly steeper in Brugada patients than BrS relatives (mean gradients BrS VF = 1.86ms/mm, BrS = 1.68ms/mm, BrS relatives = 1.39ms/mm, p =

0.016). In the pairwise comparisons of Figure 7.6 the BrS relatives were significantly differentiated from BrS VF and BrS groups (p = 0.0048, 0.049 respectively) but BrS VF patients could not be differentiated from BrS patients (p = 0.24). This effect was significant only in the right ventricle (p = 0.01). Pairwise significant differences again only existed between BrS relatives and both Brugada groups (p = 0.0073 against BrS VF and p = 0.032 against BrS).

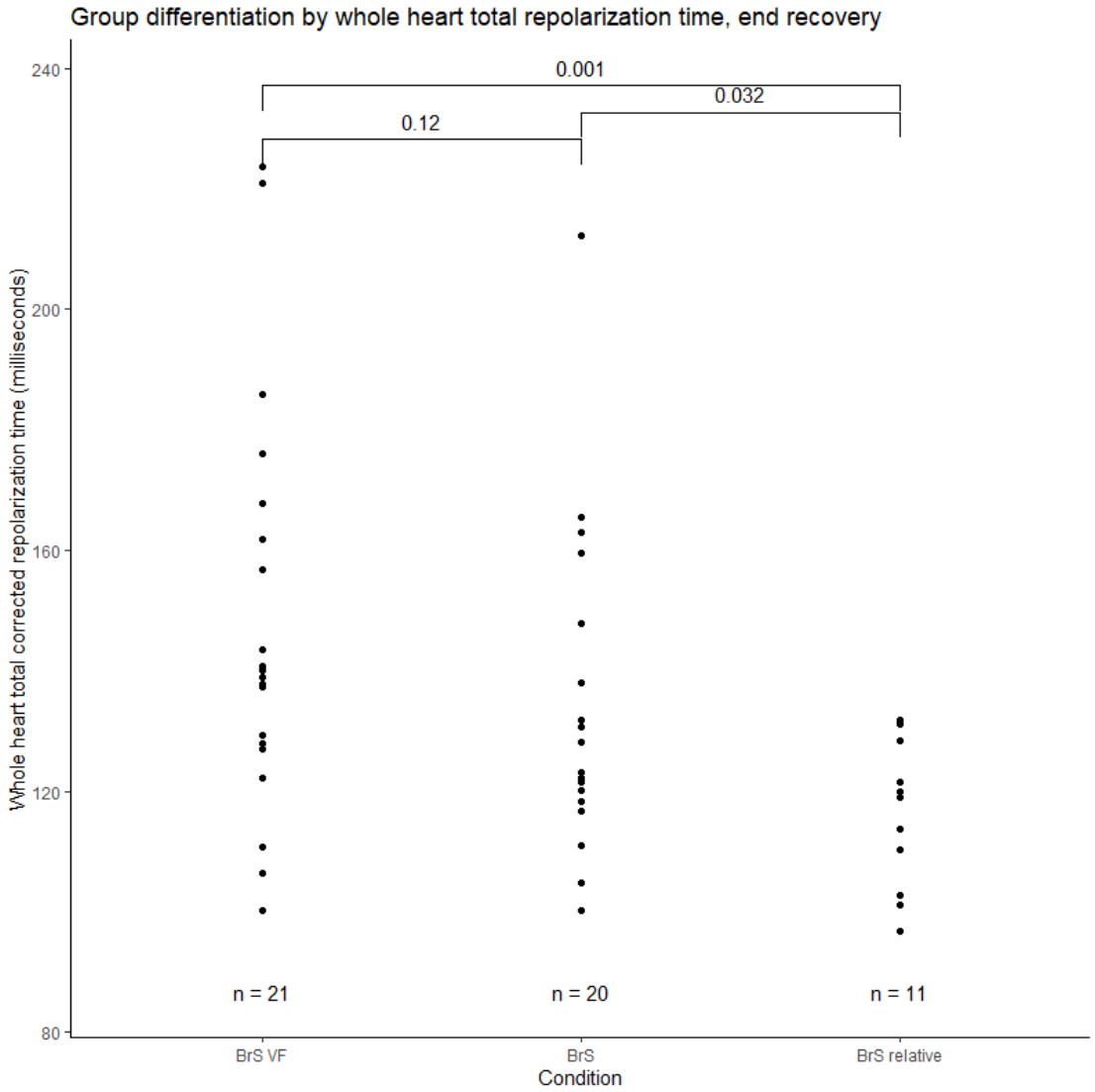

Figure 7.6: Comparison of whole heart total repolarization time in end recovery between Brugada VF survivors (BrS VF), Brugada syndrome patients without a history of potentially lethal arrhythmia (BrS) and unaffected, asymptomatic relatives (BrS relatives). Local repolarization time was defined as the onset of the first epicardial QRS complex to the steepest positive slope of the electrogram-T wave. The central 95% range across the heart is reported per patient. Correction for heart rate was made using the Fridericia method.

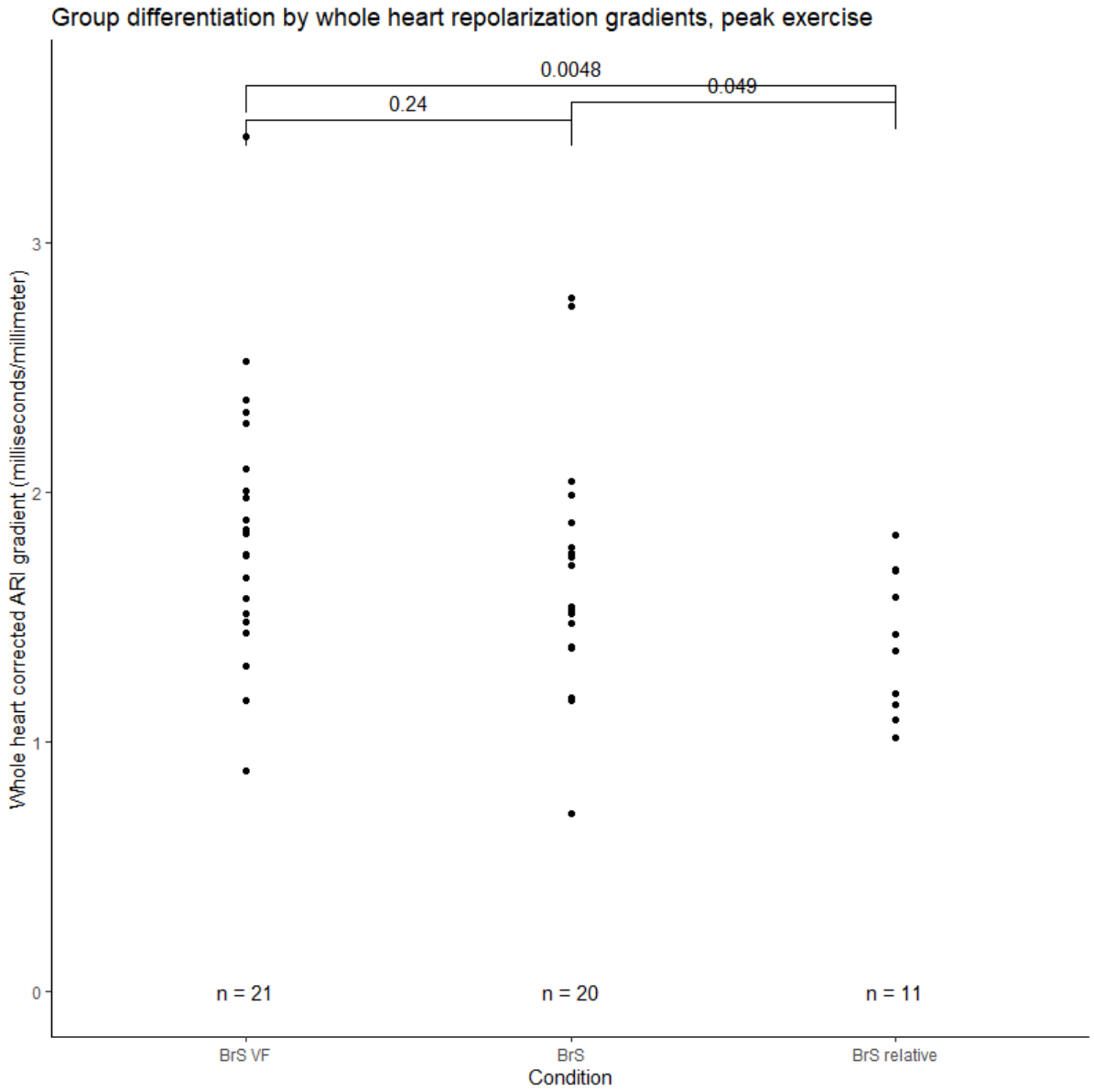

Figure 7.7: Comparison of whole heart corrected activation recovery interval (ARI) gradients immediately following peak exercise between Brugada VF survivors (BrS VF), Brugada syndrome patients without a history of potentially lethal arrhythmia (BrS) and unaffected, asymptomatic relatives (BrS relatives). ARI was defined as the steepest negative slope in the electrogram-QRS to the steepest positive slope in the electrogram-T wave. Gradients between individual nodes are calculated by the difference in ARI divided by the Euclidean distance between them. Each individual node is assigned the mean gradient against all neighbours within a search distance of 5mm and the mean value is reported across the heart for each patient. Correction for heart rate was made using the Fridericia method.

7.3.3.2 End recovery

During end recovery, whole heart repolarization times were significantly different across the groups (mean times BrS VF = 334.4ms, BrS = 319.2ms, BrS relatives = 317.7ms, p = 0.048). Pairwise

differences only existed between the two Brugada groups (p = 0.028) whilst BrS relatives could not be differentiated for either group (p = 0.061 against BrS VF, p = 0.82 against BrS). Significant differences were seen in the right ventricular outflow tract (p = 0.0003) and right ventricle (p = 0.03). In the right ventricular outflow tract, mean repolarization time significantly differentiated both BrS VF from BrS (means 358 vs 325ms, p = 0.012) and BrS relatives (means 358 vs 306ms, p = 0.00002). BrS and BrS relatives were not significantly different in the RVOT or right ventricle (p = 0.1, 9,56 respectively). In the right ventricle, BrS VF were significantly differentiated from BrS (means 346 vs 328ms, p = 0.026) and BrS relatives (means 346 vs 325ms, p = 0.031).

Whole heart total repolarization time was also different in end recovery (mean ranges BrS VF = 147.4ms, BrS = 134.2ms, BrS relatives = 116.0ms, p = 0.004). The pairwise comparisons of Figure 7.7 demonstrated that BrS relatives were differentiated from both Brugada groups (p = 0.001 against BrS VF, p = 0.032 against BrS). The two Brugada groups could not be differentiated (p = 0.12). The right ventricle also demonstrated this significant difference in total repolarization time (p = 0.01) whereas the right ventricular outflow tract and left ventricle did not (p = 0.52 and 0.08 respectively).

Table 7.3: Comparison of automated epicardial repolarization measurements between Brugada VF survivors (BrS VF), Brugada syndrome patients without a history of potentially lethal arrhythmia (BrS) and unaffected, asymptomatic relatives (BrS relatives).

Measure	**BrS VF**	**BrS**	**BrS relative**	**p-value**
Peak exercise				
Whole heart				
Mean whole heart corrected repolarization time (RTc_{mean}, milliseconds)	295.3	282.4	275.4	0.07
Whole heart total corrected repolarization time (TRT95, milliseconds)	153.8	133.7	111.5	**0.001**
Whole heart mean corrected ARI gradient (ARIc-$Gradient_{mean}$, millisecond/millimeters)	1.86	1.68	1.39	**0.016**
Right ventricular outflow tract (RVOT)				

Mean RVOT corrected repolarization time (RVOT-RTc_{mean}, milliseconds)	315.6	295.0	279.9	0.05
RVOT total corrected repolarization time (RVOTRT95, milliseconds)	115.9	113.2	104.6	0.20
RVOT mean corrected ARI gradient (RVOT-ARIc-$Gradient_{mean}$, millisecond/millimeters)	2.71	2.49	2.54	0.81
Right ventricle (RV)				
Mean RV corrected repolarization time (RV-RTc_{mean}, milliseconds)	306.1	294.6	283.5	0.17
RV total corrected repolarization time (RVRT95, milliseconds)	154.2	132.9	117.3	**0.004**
RV mean corrected ARI gradient (RV-ARIc-$Gradient_{mean}$, millisecond/millimeters)	2.09	1.77	1.43	**0.01**
Left ventricle (LV)				
Mean LV corrected repolarization time (LV -RTc_{mean}, milliseconds)	283.8	269.9	226.9	**0.02**
LV total corrected repolarization time (LVRT95, milliseconds)	141.7	127.9	105.8	**0.009**
LV mean corrected ARI gradient (LV-ARIc-$Gradient_{mean}$, millisecond/millimeters)	1.57	1.59	1.35	0.42
End recovery				
Whole heart				
Mean whole heart corrected repolarization time (RTc_{mean}, milliseconds)	334.4	319.2	317.7	**0.048**
Whole heart total corrected repolarization time (TRT95, milliseconds)	147.4	134.2	116.0	**0.004**

Whole heart mean corrected ARI gradient (ARIc-Gradient$_{mean}$, millisecond/millimeters)	1.89	1.77	1.57	0.13
Right ventricular outflow tract (RVOT)				
Mean RVOT corrected repolarization time (RVOT-RTc$_{mean}$, milliseconds)	358.8	324.7	306.4	**0.0003**
RVOT total corrected repolarization time (RVOTRT95, milliseconds)	110.2	121.5	106.2	0.40
RVOT mean corrected ARI gradient (RVOT-ARIc-Gradient$_{mean}$, millisecond/millimeters)	2.81	2.89	2.32	0.52
Right ventricle (RV)				
Mean RV corrected repolarization time (RV-RTc$_{mean}$, milliseconds)	345.7	327.5	324.8	**0.03**
RV total corrected repolarization time (RVRT95, milliseconds)	145.9	136.1	112.4	**0.01**
RV mean corrected ARI gradient (RV-ARIc-Gradient$_{mean}$, millisecond/millimeters)	1.97	1.82	1.53	0.12
Left ventricle (LV)				
Mean LV corrected repolarization time (LV -RTc$_{mean}$, milliseconds)	322.1	310.1	310.6	0.09
LV total corrected repolarization time (LVRT95, milliseconds)	132.8	123.4	113.5	0.08
LV mean corrected ARI gradient (LV-ARIc-Gradient$_{mean}$, millisecond/millimeters)	1.87	1.71	1.58	0.34

7.3.4 Visual representations of automated measurements

Activation and repolarization maps from two patients in both peak exercise and end recovery are displayed in Figure 7.8: one with Brugada syndrome and a Brugada relative – normal heart. These patients have been selected to help visualize the group differences measured by the automated

measures. The Brugada syndrome heart has delayed conduction and slower repolarization than the normal heart. Although activation and repolarization gradients were often not significantly different between the groups, lines of steep activation or repolarization change can be visualized in the Brugada epicardium, contrasting with the smooth graduation of colours in the normal heart. Upon inspection of electrograms from the right ventricular outflow tract, the Brugada electrograms clearly demonstrate abnormal ST segment elevation followed by T wave inversion, not seen in the electrograms from the normal heart subject.

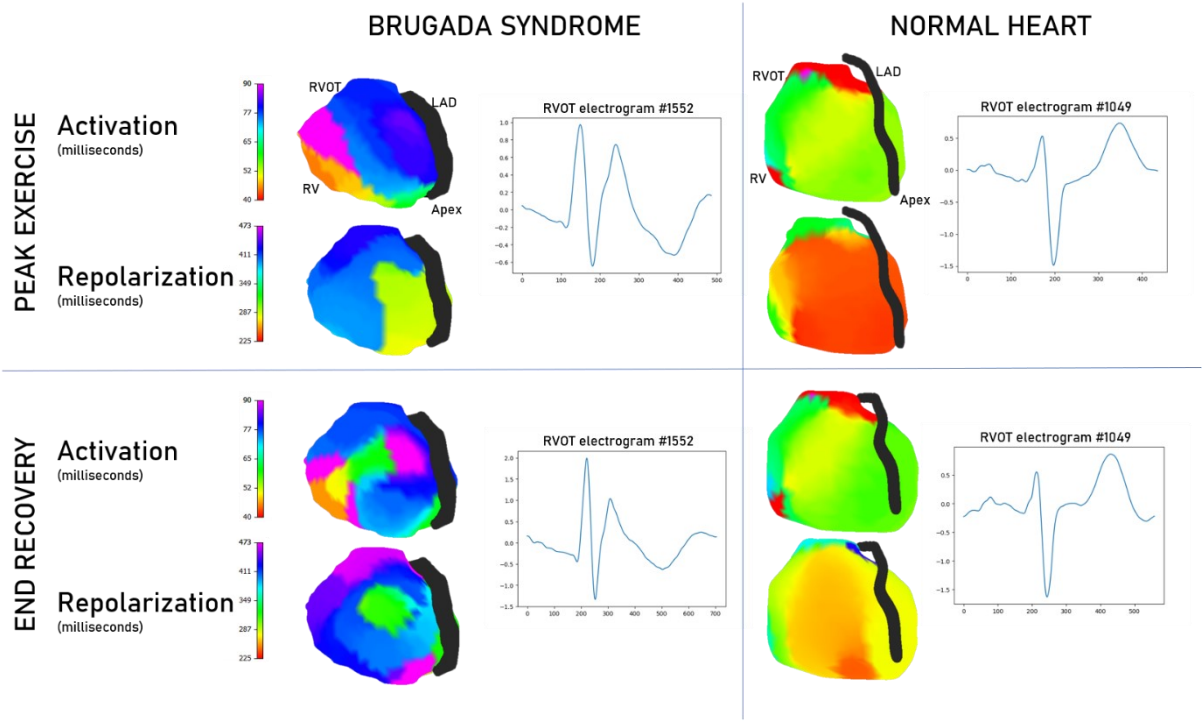

Figure 7.8: Comparison of non-invasive epicardial maps between a patient with Brugada syndrome and an asymptomatic, unaffected relative. Scales are matched for activation and repolarization separately to aid comparison. Examples are selected to illustrate the differences seen in the overall cohort. In activation, the Brugada syndrome heart (left panel) has delayed conduction and repolarization compared to the normal heart (right panel). The normal heart appears to have a smoother colour progression, not indicative of steep activation or repolarization gradients that may be seen in the Brugada heart. Right ventricular outflow tract (RVOT) electrograms are displayed for both hearts, with the Brugada heart exhibiting abnormal ST segment elevation. Right ventricle, RV; Left ventricle, LV; Left anterior descending artery, LAD.

7.3.5 Differentiation of concealed Brugada syndrome patients from unaffected relatives

33 Brugada patients from our cohort had never been seen to exhibit a spontaneous Type 1 ECG. They were compared to the 11 unaffected Brugada relatives. Concealed Brugada values are reported first.

7.3.5.1 Peak exercise

Whole heart mean activation time only trended towards significance between concealed Brugada patients and unaffected relatives (means ±SD: 54.1 ±6.9ms vs 49.9 ±3.5ms, p = 0.057). Total activation time was not significantly different (means ±SD: 48.9 ±18.9ms vs 47.1 ±8.3ms, p = 0.53). Whole heart activation gradients were also similar (means ±SD: 0.40 ±0.2ms/mm vs 0.39 ±0.1ms/mm, p = 0.87).

Whole heart mean repolarization time was not significantly different between groups (means ±SD: 287 ±23.0ms vs 275 ±18.9ms, p = 0.15). However, total repolarization time was significantly higher in the concealed Brugada group (means ±SD: 139 ±30.0ms vs 112 ±16.9ms, p = 0.0007). Repolarization gradients were also significantly higher in the concealed Brugada group (means ±SD 1.7 ±0.4ms/mm vs 1.4 ±0.3ms/mm, p = 0.029).

7.3.5.2 End recovery

Whole heart mean activation time was longer in concealed Brugada patients than unaffected relatives (means ±SD: 57.6 ±5.9ms vs 52.5 ±3.3ms, p = 0.0022). Total activation time was not significantly different (means ±SD: 49.1 ±15.1ms vs 44.0 ±5.6ms, p = 0.55). Likewise, whole heart activation gradients were similar (means SD: 0.4 ±0.2ms/mm vs 0.4 ±0.2ms/mm, p = 0.83).

Whole heart mean repolarization time was not significantly different between groups (means ±SD: 326 ±20.5ms vs 318 ±14.8ms, p = 0.3). However, total repolarization time was significantly higher in the concealed Brugada group (means ±SD: 136 ±25.2ms vs 116 ±12.2ms, p = 0.0094). Repolarization gradients were not higher in the concealed Brugada group (means ±SD 1.8 ±0.5ms/mm vs 1.6 ±0.3ms/mm, p = 0.083).

7.3.5.3 Differences in VF survivors, BrS without potentially lethal arrhythmia and relatives when spontaneous Type 1 ECGs are excluded

Mean activation times were higher in BrS VF survivors than Brugada relatives in peak exercise (effect size 6.1ms, p = 0.02) and end recovery (effect size 6.7ms, p = 0.006). BrS and BrS relatives were differentiated by mean activation time in end recovery only (effect size = 3.6ms, p = 0.0093).

Repolarization dispersion was greater in BrS VF survivors than Brugada relatives in peak exercise (effect size 30ms, p = 0.0022) and end recovery (effect size = 20ms, p = 0.009). Repolarization gradients were greater in BrS VF survivors than Brugada relatives in peak exercise only (effect size 0.32ms/mm, p = 0.026). BrS and BrS relatives were differentiated by repolarization dispersion in peak exercise (effect size = 23ms, p = 0.004) and end recovery (effect size = 20ms, p = 0.047)

Once spontaneous Type 1 ECGs were excluded, there were no significant differences between Brugada VF survivors and other Brugada syndrome patients.

7.3.6 Differentiation of spontaneous Type 1 ECG Brugada patients from unaffected relatives

8 Brugada patients from our cohort had been seen to exhibit a spontaneous Type 1 ECG either during routine follow up or during ECGi exercise testing. They were compared to the 11 unaffected Brugada relatives. Spontaneous Brugada values are reported first.

7.3.6.1 Peak exercise

Whole heart mean activation time was significantly longer in spontaneous Brugada patients compared to unaffected relatives (means ±SD: 57.3 ±6.1ms vs 49.9 ±3.5ms, p = 0.007). Total activation time was not significantly different (means ±SD: 62.9 ±16.4ms vs 47.1 ±8.3ms, p = 0.09). Whole heart activation gradients were higher in the Brugada patients (means ±SD: 0.56 ±0.2ms/mm vs 0.39 ±0.1ms/mm, p = 0.03).

Whole heart mean repolarization time was significantly longer in spontaneous Brugada syndrome (means ±SD: 295 ±22.2ms vs 275 ±18.9ms, p = 0.034). Total repolarization time was also significantly longer in the spontaneous Brugada group (means ±SD: 167 ±43.6ms vs 112 ±16.9ms, p = 0.0036). Repolarization gradients were also significantly higher in the concealed Brugada group (means ±SD 2.1 ±0.7ms/mm vs 1.4 ±0.3ms/mm, p = 0.0012).

7.3.6.2 End recovery

Whole heart mean activation time was longer in spontaneous Brugada patients than unaffected relatives (means ±SD: 60.9 ±7.0ms vs 52.5 ±3.3ms, p = 0.009). Total activation time was significantly longer (means ±SD: 64.8 ±17.7ms vs 44.0 ±5.6ms, p = 0.012). Whole heart activation gradients were longer in spontaneous Brugada patients (means ±SD: 0.6 ±0.2ms/mm vs 0.4 ±0.2ms/mm, p = 0.04).

Whole heart mean repolarization time was not significantly different between groups (means ±SD: 329 ±22.5ms vs 318 ±14.8ms, p = 0.27). However, total repolarization time was significantly higher in the spontaneous Brugada group (means ±SD: 162 ±40.9ms vs 116 ±12.2ms, p = 0.001). Repolarization gradients were not higher in the Brugada group (means ±SD 2.0 ±0.5ms/mm vs 1.6 ±0.3ms/mm, p = 0.11).

7.3.7 Correlation of activation and repolarization measures within-patient

To determine the independence of activation and repolarization measures within patients, correlation plots and resultant Pearson correlation coefficients were examined in Figure 7.9. The

range of correlation coefficients between any activation and any repolarization measure was 0.13 to 0.51.

As expected, activation measures correlated best with other activation measures (coefficients 0.68 to 0.82). Repolarization measures showed more independence (coefficients 0.23 to 0.61).

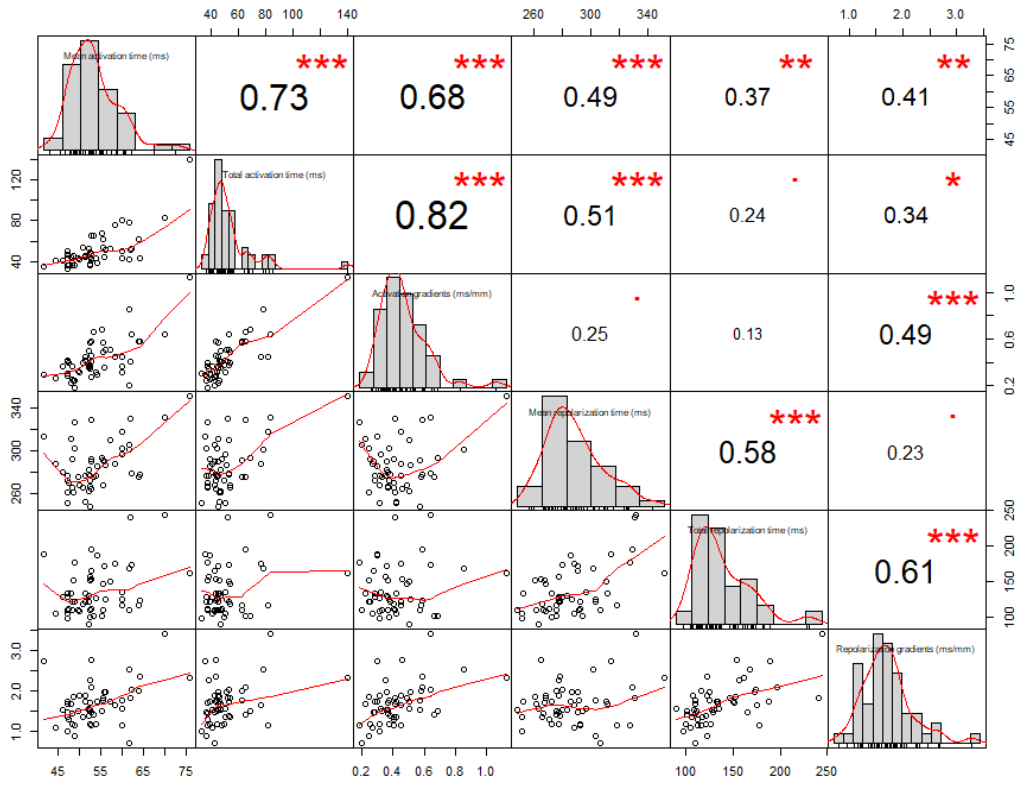

*Figure 7.9: Correlation matrix plot between activation and repolarization measures in Brugada syndrome patients and their unaffected relatives. The diagonal squares going from top left to bottom right contain histograms of activation metrics (top three) and repolarization metrics (bottom three). Squares to the bottom left of this diagonal contain scatter plots depicting the interaction between two metrics. Squares to the top right of this diagonal contain the Pearson correlation coefficient and the significance (***: p <0.001, **: p<0.01, *: p<0.05, · [dot] : p <0.1, [empty]: p >0.1).*

*Table 7.4: Summary for pairwise significance of automated epicardial measurements differentiating Brugada syndrome patients with and without potentially lethal arrhythmia (BrS VF, BrS), and unaffected asymptomatic Brugada relatives (BrS relative). Significance levels in brackets indicate the values once spontaneous Type 1 ECGs are excluded. Significance: * = p>0.05, ** = p>0.005, *** = p>0.0005.*

Measure	**BrS VF vs BrS relative**	**BrS vs BrS relative**	**BrS VF vs BrS**
Peak exercise			
Activation delay	** (*)		

Activation dispersion			
Activation gradients			
Repolarization delay	* (-)		
Repolarization dispersion	*** (**)	* (**)	
Repolarization gradients	** (*)	* (-)	
End recovery			
Activation delay	** (*)	* (*)	* (-)
Activation dispersion	* (-)		
Activation gradients			
Repolarization delay			* (-)
Repolarization dispersion	** (*)	* (*)	
Repolarization gradients			

*Table 7.5: Summary for pairwise significance of automated epicardial measurements differentiating concealed Brugada syndrome patients and unaffected asymptomatic Brugada relatives (BrS relative). Significance: * = p>0.05, ** = p>0.005.*

Measure	**Concealed BrS vs BrS relative**	**Spontaneous BrS vs BrS relative**
Peak exercise		
Activation delay		**
Activation dispersion		
Activation gradients		*
Repolarization delay		*
Repolarization dispersion	**	*
Repolarization gradients	*	*
End recovery		
Activation delay	**	**
Activation dispersion		*
Activation gradients	*	
Repolarization delay		
Repolarization dispersion	*	**
Repolarization gradients		

7.4 Discussion

In this subchapter we have compared basic electrophysiological measurements in patients with Brugada syndrome and their unaffected relatives. Unlike previous studies into epicardial Brugada electrophysiology, we have not stipulated that patients require a Type 1 ECG to take part and have also focused on the group surviving ventricular fibrillation.

Table 7.4 summarizes the pairwise differences between the group epicardial measurements. Table 7.5 summarizes the pairwise differences between concealed Brugada syndrome patients and unaffected relatives.

7.4.1 Mechanisms in Brugada syndrome: the depolarization and repolarization hypotheses

Two competing hypotheses exist for the mechanisms underlying Brugada syndrome – the depolarization and repolarization hypotheses.

The depolarization hypothesis holds that conduction delay in the right ventricle leads to the Brugada syndrome phenotype, drawing on the use of sodium channel blockade to unmask the ECG pattern, the association with right bundle branch block (RBBB) and prolonged His-Ventricular intervals, the association with SCN5A and the detection of late potentials during contact epicardial mapping as evidence. The repolarization hypothesis counters that simultaneous monophasic action potential measurements of endo- and epicardium demonstrate deep notching of the epicardial action potential without conduction delay, and transmembrane potential measurements of canine wedge preparations demonstrate repolarization heterogeneity causing ST elevation and phase 2 re-entry leading to arrhythmia upon exposure to either flecainide and acetylcholine or pinacidil.

These theories may not be mutually exclusive. The broad methodologies differ – contact electrograms for the depolarization hypothesis and action potentials for the repolarization hypothesis. Although conversion strategies are commonly used and accepted (such as activation-recovery interval for 90% of action potential duration), significant variability is also noted (Haws and Lux 1990). It is also possible that Brugada syndrome may contain two sub-conditions, one repolarization dominant and the other depolarization dominant.

ECGi has previously been used to differentiate the pathognomonic Type 1 Brugada ECG from right bundle branch block and normal ECG (Zhang, Sacher et al. 2015). Delayed right ventricular outflow tract activation, prolonged recovery time and steep repolarization gradients were found. Six patients

were measured with increased heart rate: outflow tract activation delay worsened but repolarization gradients lessened when compared to other areas of the heart.

Surface ECG data for Brugada syndrome subjects undergoing exercise testing has previously revealed that QRS duration increases more in Brugada patients with an SCN5A mutation than either SCN5A negative or control subjects (Amin Ahmad, de Groot Elisabeth et al. 2009). Corrected QT was found to lengthen in Brugada patients during exercise and not return to baseline at end recovery, unlike matched controls who had corrected QT interval shortening on exercise and recovered fully.

Our data for 11 patients with spontaneous Type 1 ECG demonstrated that whole heart activation times were longer both with and without exercise. Effect size was comparable at 8ms in recovery and 7.5ms in exercise. Activation dispersion was increased during recovery but not in exercise. Repolarization changes were evident during peak exercise – delay, increased dispersion and steep gradients were all noted – furthermore these changes were not as evident during recovery. Although the p-value of repolarization dispersion differences were lower in recovery ($p = 0.001$ vs 0.0052), the effect size was still larger in exercise (41 vs 37ms).

Our data suggests that compared to unaffected relatives, exercise suppresses differences in activation dispersion in spontaneous Type 1 patients but increases the extent of repolarization changes. In concealed Brugada syndrome, activation delays are suppressed by exercise, but once again, repolarization changes are accentuated. This does not necessarily contrast with the other published ECGi data as their comparisons were made within-subject whereas we have made comparisons between BrS and control. Our data would suggest that the finding of poor recovery in corrected QT interval found in the ECG data is a combination of activation delay and greater repolarization dispersion.

Both activation and repolarization changes have been demonstrated in this study, supporting neither hypothesis outright. By examining the correlation between markers of depolarization and repolarization we can determine whether patients with significant abnormalities in one domain also have greater abnormalities in the other, or whether the Brugada cohort might be a mixture of depolarization dominant and repolarization dominant patients.

No correlation coefficient between a depolarization measure or a repolarization measure was above 0.51, indicating that there should be a significant number of patients with greater repolarization abnormality than depolarization, and vice versa. This would support a conclusion that Brugada

syndrome may be a heterogenous diagnosis. This conclusion is also supported by the range of genetic mutations associated with the condition (Hedley, Jørgensen et al. 2009).

7.4.2 Brugada syndrome beyond the Type 1 ECG

Expected differences were demonstrated between patients with a spontaneous Type 1 ECG pattern at any time and unaffected relatives. Activation delay was present in both exercise and recovery, whilst steep gradients existed in exercise and greater dispersion in recovery. Greater repolarization dispersion was present in both test phases, whereas repolarization delay and steep gradients were primarily exercise related.

Although the 12 lead ECGs for a concealed Brugada patient and an unaffected relative may be visually similar, the high-density body surface mapping used in ECGi may be sufficiently sensitive to differentiate the groups. Furthermore, previous exercise ECG work has shown that Brugada groups with predominantly concealed ECG (~80%) can demonstrate surface measurement differences with healthy controls (Amin Ahmad, de Groot Elisabeth et al. 2009). Sub-analysis for concealed Brugada syndrome only was not performed.

Our exclusion of spontaneous Type 1 ECG for this sub-analysis was stringent. If a patient had exhibited spontaneous Type 1 pattern at any time (that is, even if their surface ECG during ECGi measurement was normal), they were excluded. From the remaining patients, several differences with unaffected relatives remained. Activation delay in end recovery was evident despite the lack of a significant difference between QRS duration on the surface ECG. Increased repolarization dispersion was present in both exercise and recovery, which tallies with the longer corrected QT intervals in Brugada patients, especially those with a personal history of life-threatening arrhythmia.

Similar to our conclusions for the whole group, this indicates that depolarization and repolarization abnormalities exist in patients with concealed Brugada syndrome, and whilst recovery relatively accentuates the activation differences, repolarization differences are more evident in peak exercise. In a similar way to V-CoS in Chapter 4, these simple automated exercise ECGi measurements could inform diagnosis of Brugada syndrome without having to resort to the potentially dangerous sodium channel blocker challenge.

7.4.3 ECGi electrophysiological measurements for risk stratification of life-threatening arrhythmia

Contrasting with the multiple differences with normal subjects, only two comparisons within Brugada syndrome proved to be statistically significant – activation delay and repolarization delay in recovery. However, when viewed with the exclusion of spontaneous type 1 subjects, these differences are no longer significant. It may be that the presence of a Type 1 ECG during analysis is a confounder in the difference between VF survivors and those without life threatening arrhythmia – a spontaneous Type 1 ECG was more common in the BrS VF group than the BrS group, but this did not reach significance (27.3% vs 14.3%, $p = 0.27$).

It is plausible that no electrophysiological difference exists between these groups that can be elicited by ECGi exercise testing. This notion is backed up by difficult risk stratification by traditional measures mentioned Chapters 1 and 3 of this thesis, and that exercise is only one anecdotal trigger for arrhythmia – sleep, fever, drugs and large meals are also cited (Olde Nordkamp, Vink et al. 2015). More comprehensive ECGi testing including hyperthermia, sodium channel blockade and so on may well have a higher chance of eliciting a significant difference, but this must be balanced with the ethically acceptable risk to a research participant or a future patient.

Alternatively, our sub-analysis may be simply underpowered. Evidence supporting this view comes from Table 7.4: we can see that concealed VF survivors have more differences from control than Brugada patients without life threatening arrhythmia. During exercise the difference between relatives and VF survivors is stronger for activation delay and repolarization gradients. If there are greater differences between the VF survivors and relatives than for the other Brugada patients, our small study may have failed to detect the difference between BrS VF and BrS groups.

7.4.4 Limitations

Due to the small number of patients tested in this analysis, it is not possible to draw definitive conclusions on the utility of ECGi measures for clinical applications such as diagnosis or risk stratification. Continuous 12-lead analysis was not undertaken to compare with ECGi measurements and this means that correlating the commonly used 12-lead ECG to ECGi findings is not easy. Further study would be possible to review the body surface traces from areas on the vest analogous to the traditional ECG lead positions. We were stringent with our exclusion of Type 1 ECG patients – rejecting any showing a spontaneous pattern at any point in their clinical follow up from concealed analyses regardless of what their ECG showed on the day of the test. Further review of the body

surface ECG from the vest could allow us to power the analysis better by including patients with previous spontaneous Type 1 pattern but concealed on the day.

7.5 Conclusion

Exercise ECG imaging can pick up multiple differences between Brugada patients and their unaffected relatives, even when surface ECG markers are not significantly different and when analysis is restricted to only concealed Brugada patients. This may form the basis for improved diagnosis of concealed Brugada syndrome with a lower risk to life than gold standard sodium channel blocker challenges. Furthermore, both activation and repolarization abnormalities can be detected, with some degree of independence from each other, suggesting that the diagnosis of Brugada syndrome may be more heterogenous than first thought.

Differentiation of ventricular fibrillation survivors from Brugada patients without a personal history of life-threatening arrhythmia is more difficult and may be almost totally confounded by the higher prevalence of spontaneous Type 1 Brugada patterns in the VF survivors or inclusion of Brugada patients without current evidence of arrhythmias in our ‘control' BS group who then go on to develop fatal arrhythmias (noting event rates are low). For ECGi to become useful in risk stratification for sudden death, different stimuli should be considered to elicit measurable electrophysiological responses non-invasively.

Chapter 8: The arrhythmic substrate of hypertrophic cardiomyopathy

8.1 Introduction

Hypertrophic cardiomyopathy (HCM) is the commonest genetic cardiovascular disease. The most devastating sequela is sudden cardiac death – but accurate risk stratification remains a challenge.

HCM has been mainly studied as a structural abnormality of the ventricles. The presence or absence of non-sustained ventricular tachycardia (NSVT) on 24-hour continuous ECG monitoring is the only electrophysiological marker backed by current guidelines (American College of Cardiology Foundation/American Heart Association Task Force on, American Association for Thoracic et al. 2011; O'Mahony, Jichi et al. 2014). Yet NSVT has the highest hazard ratio of any of the risk factors – indicating the importance of electrophysiology in this condition (O'Mahony, Jichi et al. 2014).

Electrophysiological markers of sudden death risk in HCM are affected by increased myocyte size, disarray and fibrosis causing slow and discontinuous conduction (Roberts and Sigwart 2005). Invasive paced fractionation, a marker of this disordered conduction, has already been shown an effective risk stratifier (Saumarez, Pytkowski et al. 2008).

Non-invasively: longer QRS duration, corrected QTc and more complex T waves were found in HCM subjects than controls (Barletta, Lazzeri et al. 2004). ECG abnormalities correlate with structural changes detected on MRI (Fronza, Raineri et al. 2016). At the cellular level, repolarization abnormalities are detectable in human HCM models which are partially reversible with anti-arrhythmic drugs (Passini, Minchole et al. 2016).

ECG imaging (ECGi) has been used to non-invasively describe the epicardial arrhythmogenic substrate of HCM, finding greater activation dispersion in HCM than ischemic cardiomyopathy and healthy controls (Perez-Alday, Haq et al. 2020). Repolarization characteristics were not studied, nor were cardiac arrest survivors examined separately. The ability of ECGi to risk stratify sudden death in patients with HCM has not been prospectively established; a pilot study to determine useful biomarkers would be essential to that end.

To serve these gaps in our knowledge, we tested two hypotheses. First, that HCM is differentiable from controls using epicardial electrophysiological measures. Second, that VF/VT survivors are differentiable within the HCM cohort from those without a personal history of life-threatening arrhythmia.

8.2 Methods

Ethics were granted by the UK Health Research Authority and the Fulham Research Ethics Committee (London, UK) under references 14/LO/1318 and 17/LO/1660.

8.2.1 Patient selection

Sixty-nine patients were screened, approached, and recruited from cardiology clinics at Imperial College NHS Trust, Barts Health NHS Trust and Oxford University Hospitals NHS Trust in the United Kingdom:

1. 17 survivors of ventricular fibrillation or sustained ventricular tachycardia and haemodynamic compromise with HCM ('HCM VF/VT').
2. 20 patients with HCM without previous ventricular fibrillation or sustained ventricular tachycardia ('HCM controls')
3. 10 survivors of ventricular fibrillation in the context of single vessel total occlusion and ST-elevation, or critical three vessel disease. All patients had full revascularization, recovery of left ventricular function by echocardiographic criteria and return to full exercise capacity and asymptomatic status for >1 year ('IHD VF controls').
4. 11 patients attending for clinically indicated ablation of benign ventricular ectopy ('VE controls') with ECGi guidance. These patients had normal echocardiography and/or MRI, no family history of cardiac electrical disease and no symptoms of cardiac ischemia. Recruitment and testing took place prior to ablation.
5. 11 asymptomatic relatives of patients with Brugada syndrome ('BrS relative controls'), proven not to have the same condition by a negative Ajmaline challenge reaching dose endpoint of 1mg/kg (up to 120mg total dose).

8.2.2 Exercise ECGi testing and epicardial mapping

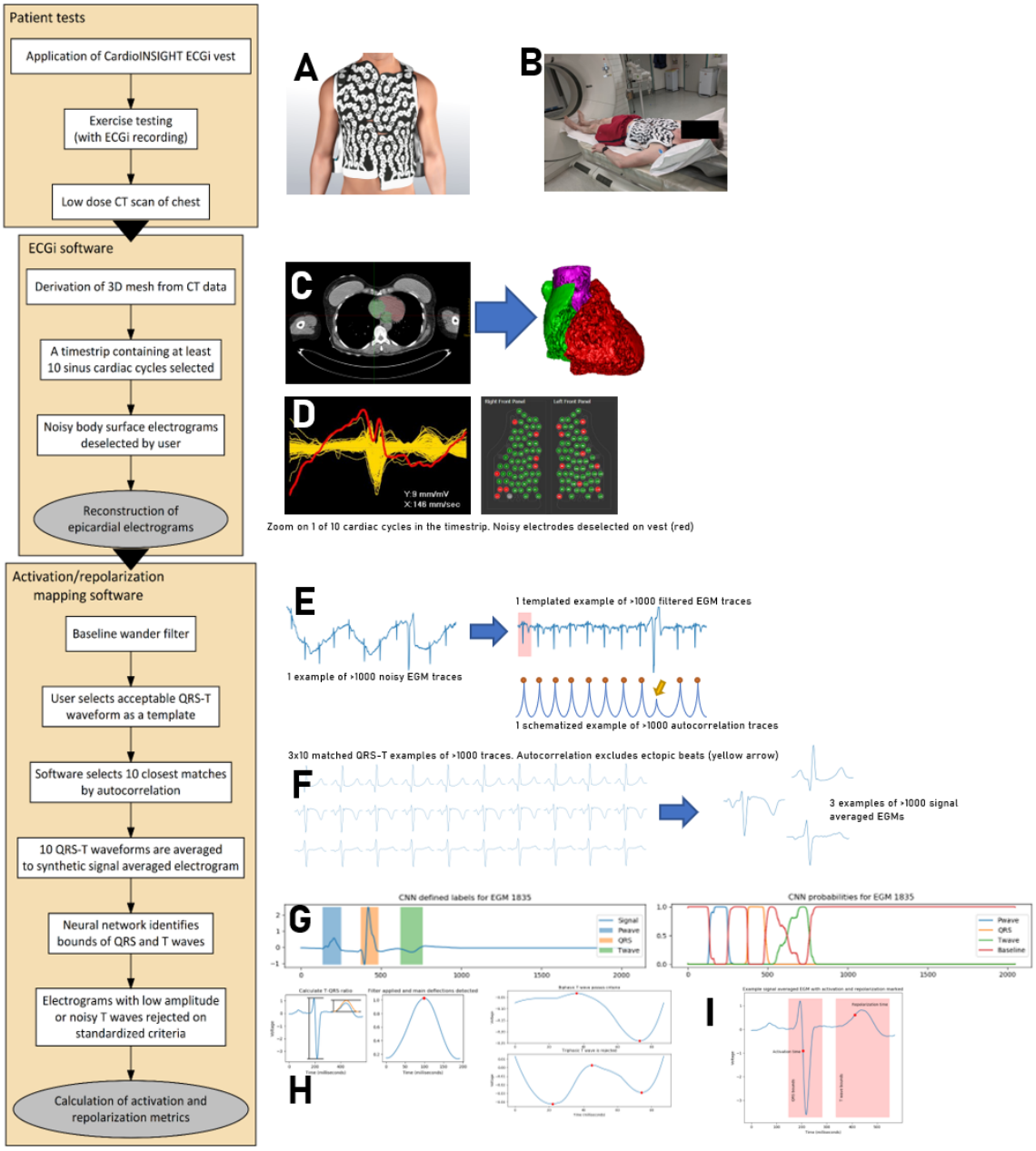

Figure 8.1: The activation-repolarization mapping process. (A) The 252-electrode sensor vest is applied to the patient undergoing maximal Bruce protocol exercise. Recordings are made during 10 minutes of supine recovery which is followed by non-contrast CT scan of chest (B). The CT scan is segmented (C, left) into a 3D mesh (C, right). A timestrip containing 10 cardiac cycles from the recording are selected for analysis and body surface signals from the vest too noisy for analysis are identified (D, left), and removed from the vest recording (D, right). Epicardial electrograms are reconstructed and extracted to our custom software. In this mapping software, reconstructed electrograms (cf. the body surface signals from step D) are filtered for baseline wander (E, left). The user selects a template QRS-T complex and the software uses autocorrelation to search for the most similar 10 regions of interest (E, right). These 10 matched regions of interest containing the QRS complexes are signal averaged to a synthetic EGM per epicardial location (F). A pre-trained neural network identifies the

bounds of the QRS complex and the T wave for further processing (G, left). It does this by working out the probability that a given timepoint is within a P wave, QRS complex, T wave or the baseline based on its value and the values of its neighbours (G, right). EGMs with low amplitude relative to QRS or T waves with 3 or more deflections are rejected (indicative of poor interpretability, H). Following this, local activation and repolarization times can be calculated (I). Electrocardiographic imaging, ECGi; Computerized tomography, CT; three-dimensional, 3D; Electrogram, EGM; Convolutional neural network, CNN.

The ECGi mapping process is graphically represented in Figure 8.1. Each volunteer was fitted with the appropriately sized 252 electrode CardioInsight™ vest based on their height and body shape, and a heart rate monitor. Volunteers exercised to peak effort (defined as exhaustion and exceeding 85% of predicted maximum heart rate) using the treadmill Bruce Protocol, then underwent 10 minutes of recording in a supine position. A non-contrast CT scan of the chest was performed.

Epicardial EGM reconstruction has been previously described (Rudy and Lindsay 2015). A 3D mesh of the heart is derived from the CT scan alongside the position of each electrode in the vest. CardioInsight™ software then calculates epicardial EGMs by combining information from the body surface electrodes and the 3D coordinates from the CT derived mesh. Approximately 1,200 epicardial electrograms could be extracted per 3D mesh.

Peak exercise and 10 minutes of recovery were bookmarked at the time of testing. The earliest 10 cardiac cycles considered sufficiently artefact-free for analysis were selected following each of these bookmarks. Heart rates were recorded for each of the sampled segments to detect inter-group differences.

To reduce the effect of random noise, finite impulse response filtering and signal averaging were performed, summarizing each timestrip of 10 cardiac cycles to a single, signal averaged beat. To minimize user bias, electrogram segmentation and curation were fully automated. We developed a convolutional neural network (CNN) based on an existing model to bound QRS complexes and T waves (Jia, Zhao et al. 2019). Our CNN was trained on over 20,000 labelled beats from a separate public database (Kalyakulina, Yusipov et al. 2018). Once the neural network had estimated the start and end bounds of QRS and T waves for each electrogram, the overall bounds were taken from the 2.5^{th} to 97.5^{th} percentiles of times to diminish outlier effects. Elimination of electrograms unsuitable for analysis was automated to two pre-specified criteria: T-waves less than 3% the size of the QRS complex or having more than 3 deflections (Wyatt, Burgess et al. 1981).

8.2.3 Analysis of surface ECG markers

To examine for body surface recording signs of conduction pathology, QRS durations were measured for the peak exercise and recovery datasets. The vest output rather than conventional 12-lead was used to avoid timing issues with the exercise machine output. The positional equivalent of 12-lead ECG V2 was used (electrodes 71-76 on the CardioINSIGHT™ vest), with the first beat from the sample as the representative measurement.

8.2.4 Measures of epicardial electrophysiology

For a given epicardial electrogram, local activation time was defined as the period from QRS start to steepest negative point of the QRS complex, and local repolarization time as QRS start to steepest positive point of the T wave (Wyatt method (Wyatt, Burgess et al. 1981)). The Wyatt method is favored by ECGi mapping papers to date (Zhang, Sacher et al. 2015; Andrews, Srinivasan et al. 2017; Zhang, Hocini et al. 2017; Leong, Ng et al. 2018). Local activation recovery interval (ARI) was defined as the difference between activation and repolarization times.

To search for steep electrical gradients, each electrogram location on the epicardial shell was linked to neighboring locations within a 5mm Euclidean search distance. For each node-neighbor pair, the difference in local activation or repolarization times was divided by the distance between the locations, giving a gradient in milliseconds/millimeter. For each node on the epicardial surface, the mean gradient within a 5mm radius was calculated, and these values were averaged across the epicardial shell to give a whole-heart estimation of steep electrical gradients.

To fully understand the electrophysiology of the three groups, three domains were defined for analysis:

1. The mean of activation, ARI or repolarization times was used to describe overall *conduction, ARI or repolarization delay*.
2. The central 95% range of times was used to describe *dispersion*.
3. The mean gradient of activation and ARI times in space was used to detect the presence of *steep gradients*.

8.2.5 Logistic regression for the description of the arrhythmogenic substrate in HCM

To understand the contribution of different parameters from our panel to the arrhythmogenic substrate in HCM, we built multiple variable logistic models from the significant variables. Activation and ARI measures were considered; repolarization times were not as both activation and ARI

contributed to these figures. To qualify for inclusion, a measure would have to significantly differentiate HCM VF and HCM volunteers ($p < 0.05$).

Qualifying measures were scaled to the mean and variance of the whole dataset. To improve the ability of the model to predict on unseen data, collinearity was reduced by rejecting one measure of any pair with a Pearson correlation of >0.8 (Mason and Perreault 1991). A multiple logistic model was then fitted using Newton's method. Backward stepwise selection was used to reject variables with $p>0.15$ (Hosmer Jr, Lemeshow et al. 2013; Chowdhury and Turin 2020). Odds ratios were calculated by exponent of the model coefficients. The predicted probability of an observation falling into the HCM VF group was compared for the true HCM VF group, and the HCM group without previous arrhythmia.

8.2.6 Ability of a multiple logistic model to predict in unseen data

A single logistic model only tested on training data cannot guarantee that it will generalize to a larger population. Validation in unseen data must be performed to determine wider applicability.

To determine the ability of logistic models to predict whether a patient was in the HCM or HCM VF group based on our ECGi measures, k-folds validation was performed. K-folds validation is used in small datasets because it tests on the entire population (n), thereby avoiding the potentially large effect of single outliers in small validation sets (Kohavi 1995; Kim 2009). Briefly, a subset of patients is reserved for testing (size $\frac{n}{k}$, a 'fold'), and the remaining patient data is used to train a logistic regression model. The accuracy of this model is then assessed on the reserved testing group. This is repeated by reserving a new testing group and training another model on the remaining data. Once all k folds are tested, the accuracy results are aggregated to estimate sensitivity and specificity.

8.2.7 Comparison of logistic regression with other machine learning techniques for discriminating arrhythmogenic substrates

Logistic regression models are popular due to their interpretability. Although these techniques are well understood and established, there is growing interest in machine learning (ML) as an alternative in the classification problem, in this case discerning risk groups.

To understand possible contributions of machine learning (ML) to risk models, three readily implementable ML strategies were compared to logistic regression using k-folds validation. All non-collinear variables were used. A full methodology is outside the scope of this paper, but each strategy is briefly described. Each model was initialised with Scikit-Learn's default hyperparameters

and are available at www.scikit-learn.org, but method references and selected initialization values are provided below.

8.2.7.1 Support vector machine

Support vector machines (SVM) plot data points in space in such a way that different classes can be separated by a hyperplane. The number of dimensions is the number of features (e.g. activation time, repolarization time). New validation data points which land on a particular side of the hyperplane are predicted to have the same class as the training data points on this same side. SVMs are able to generate more complex decision boundaries than logistic regression, allowing the prediction of non-linear relationships between variables; furthermore, SVMs may be less sensitive to outlier data (Pochet and Suykens 2006).

Scikit-Learn's Support Vector Classification function (`sklearn.svm.SVC`) was initialized with a regularization parameter of 1 and radial basis function kernel with a scaled coefficient.

8.7.2.2 Random forests

Random forests (RF) are built from decision trees, which are simple binary questions (e.g. is activation time greater than 50ms?). A random forest is a large collection of trees which vote for a particular class – the class with the greatest number of votes is the prediction for a given data point. They can also separate non-linear problems, but increased forest complexity leads to a greater chance that the model will overfit – that is, it will not generalize well to previously unseen data.

Scikit-Learn's Random Forest Classifier function (`sklearn.ensemble.RandomForestClassifier`) was initialized with 100 trees; quality of the split was measured by Gini impurity, trees had no maximum depth and the bootstrap method was used.

8.2.7.3 Artificial neural network

Artificial neural networks (ANN) are collections of computer neurons which take a numerical input and output a number transformed by a function particular to that neuron. Neurons can take multiple inputs which can be weighted. The weights are altered until the ANN has learned the best way to separate the groups. Neural networks have gained recent attention for their ability to surpass human performance in certain problems not well solved by other programming techniques, such as suboptimal image recognition (Cireşan, Meier et al. 2012) or even complex board games (Silver, Schrittwieser et al. 2017).

Scikit-Learn's Multi-layer Perceptron was used (`sklearn.neural_network.MLPClassifier`) with a single hidden layer of 100 neurons and the rectifier linear unit activation function with L2 regularization parameter 0.0001. The Limited memory Broyden-Fletcher-Goldfarb-Shanno algorithm was used for optimization.

8.2.8 General statistical analysis

Comparisons across more than two groups was carried out using the Kruskal-Wallis test. Pairwise comparisons were made using the Wilcoxon rank-sum test. Significance was defined as $p < 0.05$. Data were analysed in R v4.0.3 and Python v3.7.

8.3 Results

8.3.1 Patient characteristics and surface measures

Table 8.1: Characteristics of volunteers undergoing electrocardiographic imaging exercise testing. Peak and recovery phase heart rates were those when signal was clean enough for measurement using the electrocardiographic imaging system. Hypertrophic cardiomyopathy, HCM; HCM ventricular fibrillation or haemodynamically unstable sustained ventricular tachycardia survivor, HCM VF; Ischaemic heart disease, IHD; Ventricular ectopy, VE; Brugada syndrome, BrS; European society of Cardiology, ESC; ventricular tachycardia, VT.

Parameter	**HCM VF**	**HCM**	**IHD VF**	**VE**	**BrS relative**	**p-value**
Males (proportion)	0.76	0.76	0.9	0.54	0.72	0.18
Age (years, mean)	45.5	52.0	58.3	44.5	45.4	**0.047**
Mean ESC score (5-year risk, %)	5.90	2.85	-	-	-	**0.023**
Syncope (proportion)	0.17	0.05	-	-	-	0.20
Max left ventricular hypertrophy (mm)	19.4	18.6	-	-	-	0.40
Left atrial size (mm)	40.3	39.5	-	-	-	0.82
Left ventricle outflow gradient (mmHg)	26.8	23	-	-	-	0.54
Non sustained VT history (proportion)	0.53	0.29	-	-	-	0.13
Early familial sudden death	0.35	0.14	-	-	-	0.14

Peak phase heart rate (bpm, mean)	125.3	138.4	119.0	132.4	136.2	0.26
Recovery phase heart rate (bpm, mean)	70.3	86.5	81.5	91.6	97.4	**0.0001**
Peak phase QRS duration (ms, mean)	94.2	88.2	92.6	91.2	90.9	0.61
Recovery phase QRS duration (ms, mean)	104.7	101.7	100.3	106.7	102.8	0.87
Peak phase corrected QT interval (ms, mean)	361.3	351.2	350.1	340.9	331.6	0.11
Recovery phase corrected QT interval (ms, mean)	427.4	400.1	391.4	418.1	375.4	**0.001**

Table 8.1 summarizes patient characteristics and surface ECG markers.

All patients reached 85% of age-predicted maximal heart rate during peak exertion. One patient from the HCM VF group was excluded as their implantable device began back-up pacing during recovery.

The groups had similar gender balance. Across-group comparison of age showed a significant difference (p = 0.047). Pairwise analysis indicated that the IHD VF group were older than the HCM VF, VE and BrS relatives (p = 0.037, 0.025, 0.01 respectively) but not the HCM group (p = 0.33). The HCM VF group had higher European Society of Cardiology (ESC) scores than the HCM group, although 8 of 17 HCM VF patients had a score <4%/5-year risk and 11 had a score <6%/5-year risk (p=0.023). None of the subcomponents of the ESC score reached significance, although approximately double the proportion of patients in the HCM VF group had a history of non-sustained ventricular tachycardia or a history of early familial sudden death.

Following peak exercise, heart rates and QRS durations and QTc intervals between groups were similar. During end recovery, heart rates were significantly different (p = 0.0001). Pairwise analysis showed no difference between HCM, VE and IHD VF but HCM VF patients had lower heart rates (vs HCM, p = 0.0014; vs BrS relative, p = 0.0001; HCM VF vs VE, p = 0.0028). BrS relatives tended towards higher recovery heart rates (vs HCM, p = 0.017; vs IHD VF, p = 0.0048). End recovery QRS

durations were similar. Recovery corrected QT was significantly different between groups (p = 0.001). Pairwise comparisons showed that HCM VF patients had significantly longer recovery QTc than any group except VE (vs BrS relatives, p = 0.00014; vs IHD VF, p = 0.002; vs HCM, p = 0.01).

8.3.2 Electrophysiological phenotype of hypertrophic cardiomyopathy

To determine the electrophysiological features of hypertrophic cardiomyopathy, we compared a pooled HCM group with our control groups. Figure 8.2 summarizes the significant variables. All variables (including nonsignificant) are graphed in the Supplement.

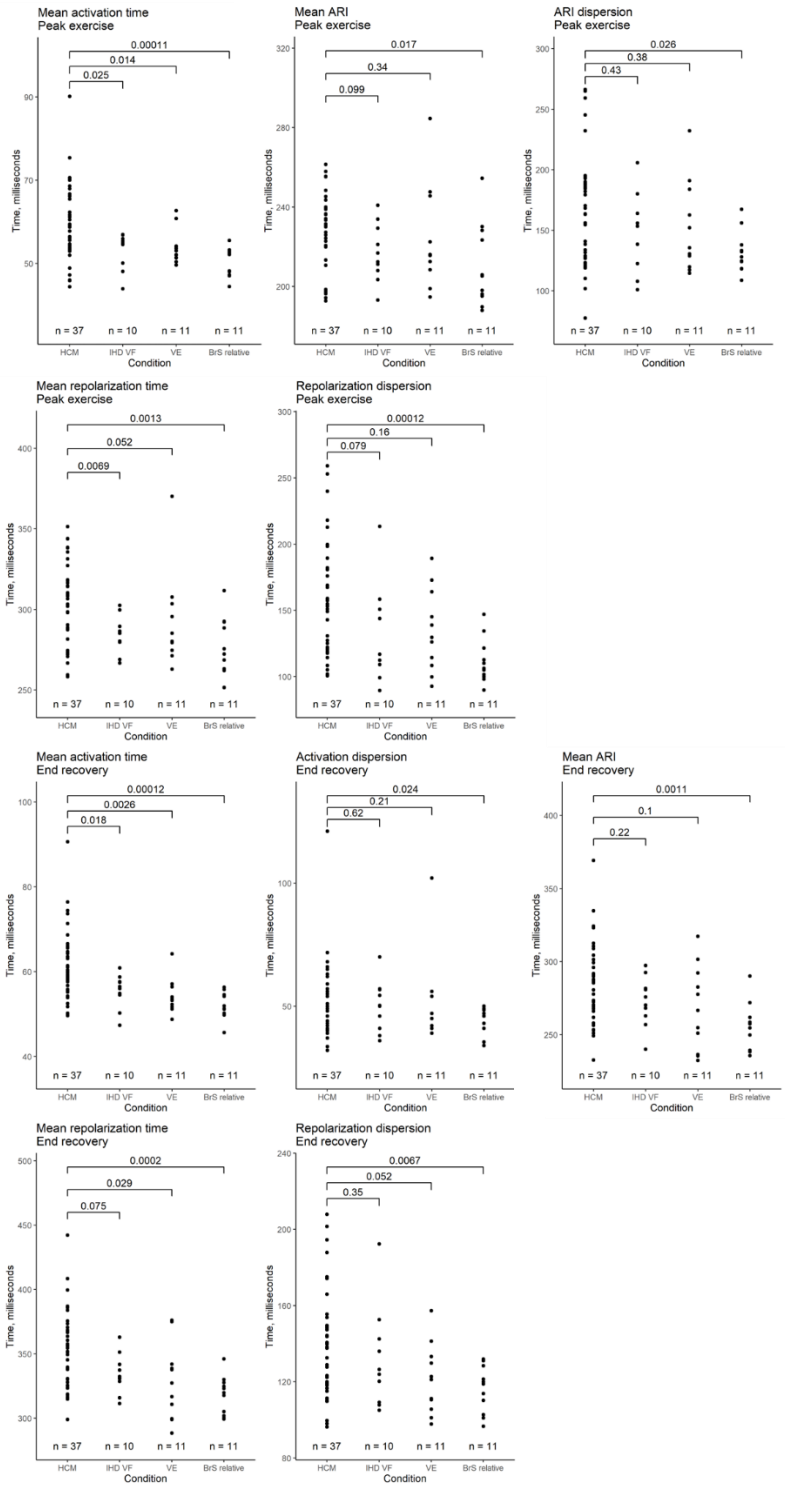

Figure 8.2: Comparison of whole heart activation and repolarization metrics immediately after peak exercise and in end recovery between hypertrophic cardiomyopathy (HCM) and a selection of structurally normal heart control groups: (I) fully recovered and revascularized ischaemic VF survivors, IHD VF; (II) patients with benign but symptomatic idiopathic ventricular ectopy, VE; (III) the unaffected relatives of patients with Brugada syndrome, BrS relative. Local activation time (LAT) was defined as the onset of the first epicardial QRS complex to the steepest negative slope of the electrogram-QRS

complex. Local repolarization time (LRT) was defined as the onset of the first epicardial QRS complex to the steepest positive slope of the electrogram-T wave. Activation recovery interval (ARI) is the difference between LAT and LRT. Mean time is the average of all LAT/LRT/ARI across the heart. Dispersion is the central 95% range of LAT/LRT/ARI across the heart. Gradient is the whole-heart mean rate of range in LAT/ARI over a 5mm search distance around each epicardial location.

8.3.2.1 Peak exercise

Following exercise, whole heart mean activation times were longer in the HCM group than any of the control groups (mean 60.1ms, across groups p = 0.0003). All pairwise comparisons were significant (vs IHD VF, mean 53.2ms, p = 0.025; vs VE, mean 53.7ms, p = 0.014; vs BrS relative, mean 49.7, p = 0.0001). Whole heart activation dispersion was similar between HCM and the controls (across groups p = 0.17), as were activation gradients (across groups p = 0.92).

The HCM group had longer mean ARI than the BrS relatives (means 227.2ms vs 210.4ms, p = 0.017), but was not significantly different from the other groups (across groups p = 0.06). ARI dispersion was also higher in the HCM group than BrS relatives (means 164.1ms vs 131.7ms, p = 0.026) but similar to the other groups (across groups p = 0.15). ARI gradients were not significantly different across groups (p = 0.25).

Combining activation and ARI, mean repolarization times were longer in HCM than the control groups (mean 304.7ms, across groups p = 0.001). All but the VE pairwise comparisons were significant (vs IHD VF, mean 283.9ms, p = 0.0069; vs VE, mean 291.8ms, p = 0.05; vs BrS relative, mean 275.4ms p = 0.0013). Repolarization dispersion was higher in HCM patients than the BrS relatives (means 156.1ms vs 111.5ms, p = 0.00012). Although the trend for HCM patients to have more repolarization dispersion than the IHD VF and VE patients did not reach significance (p = 0.079 and 0.16 respectively), the across groups comparison did (p = 0.002).

8.3.2.2 End recovery

After 10 minutes of recovery, whole heart mean activation times were longer in the HCM group (mean 61.3ms, across groups p = 0.0001). All pairwise comparisons were significant – (vs IHD VF, mean 55.4ms, p = 0.018; vs VE, mean 54.5ms, p = 0.0026; vs BrS relatives, mean 52.5ms, p = 0.00012). HCM activation dispersion was significantly higher than in BrS relatives (means 53.2ms vs 42.9ms, p = 0.024) but other comparisons were not significant (across groups p = 0.1). Activation gradients were similar (across groups p = 0.32).

The HCM group had longer mean ARI than controls (mean 285.9ms, across groups p = 0.009). Pairwise comparisons demonstrated that this was due to differences with the BrS relatives (mean

256.1ms, p = 0.001); there was no significant difference against IHD VF or VE (p = 0.22, 0.1 respectively). ARI gradients were similar (across groups p = 0.38).

Mean repolarization times were longest in HCM (mean 352.5ms, across groups p = 0.001). Pairwise comparisons revealed significant differences against VE and BrS relatives (means 328.2ms and 317.7ms, p = 0.029 and 0.0002 respectively). Repolarization dispersion was highest in HCM patients (mean 139.8ms, across groups p = 0.025). The only pairwise significance was against BrS relatives (mean 116.0ms, p = 0.0067). No significant difference was demonstrated against IHD VF or VE (p = 0.35, 0.05 respectively).

8.3.3 Visual representations of automated measurements

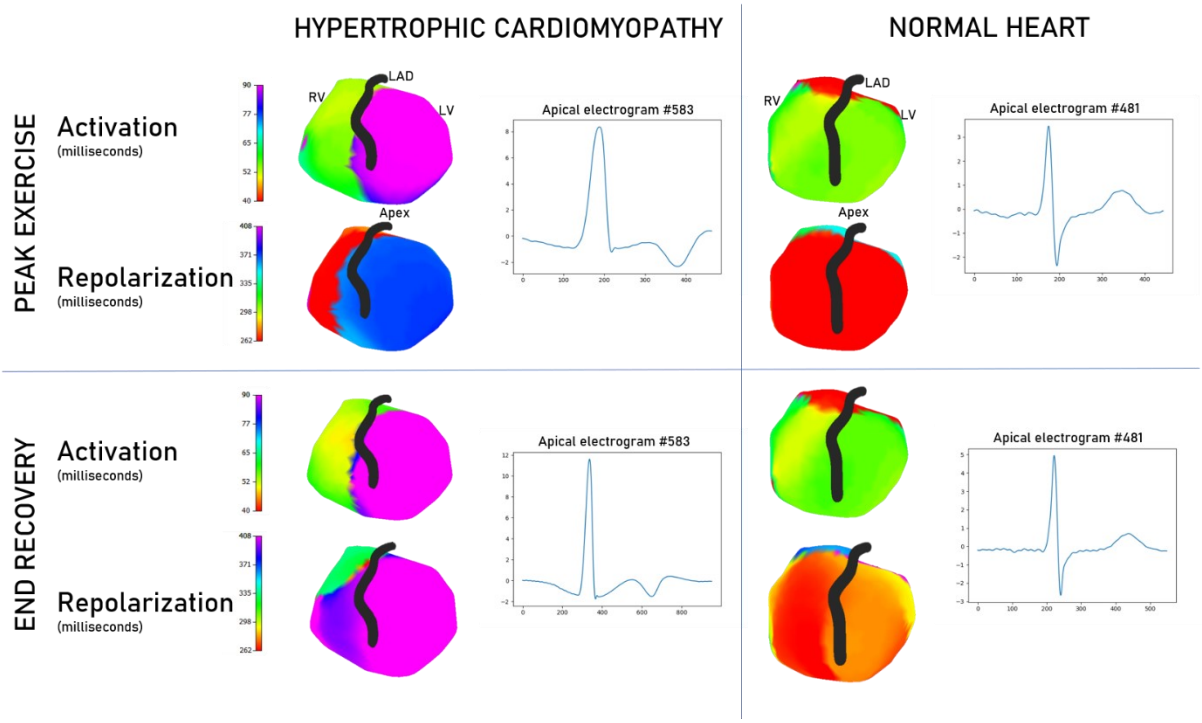

Figure 8.3: Comparison of non-invasive epicardial maps between a patient with hypertrophic cardiomyopathy and an asymptomatic, unaffected Brugada relative. Scales are matched for activation and repolarization separately to aid comparison. Examples are selected to illustrate the differences seen in the overall cohort. In activation, the hypertrophic cardiomyopathy heart (left panel) has delayed conduction and repolarization compared to the normal heart (right panel). Apical electrograms are displayed for both hearts, with the HCM heart exhibiting T wave inversion. Right ventricle, RV; Left ventricle, LV; Left anterior descending artery, LAD.

Activation and repolarization maps from two patients in both peak exercise and end recovery are displayed in Figure 8.3: one with hypertrophic cardiomyopathy and a Brugada relative (normal heart). The hypertrophic cardiomyopathy patient's heart has delayed conduction and slower

repolarization than the normal heart. Lines of steep activation or repolarization change can be seen on the hypertrophic cardiomyopathy epicardium, contrasting with the smooth graduation of colors in the normal heart. Upon inspection of electrograms from the apex, the hypertrophic cardiomyopathy electrograms show abnormal T wave inversion, not seen in the electrograms from the normal heart subject.

8.3.4 Electrophysiological phenotype of ventricular fibrillation survivors with HCM

To determine the electrophysiological features of HCM VF survivors, we compared them to HCM patients without a personal history of arrhythmia. Figure 8.4 summarizes the significant variables. All variables (including nonsignificant) are graphed in the Supplement.

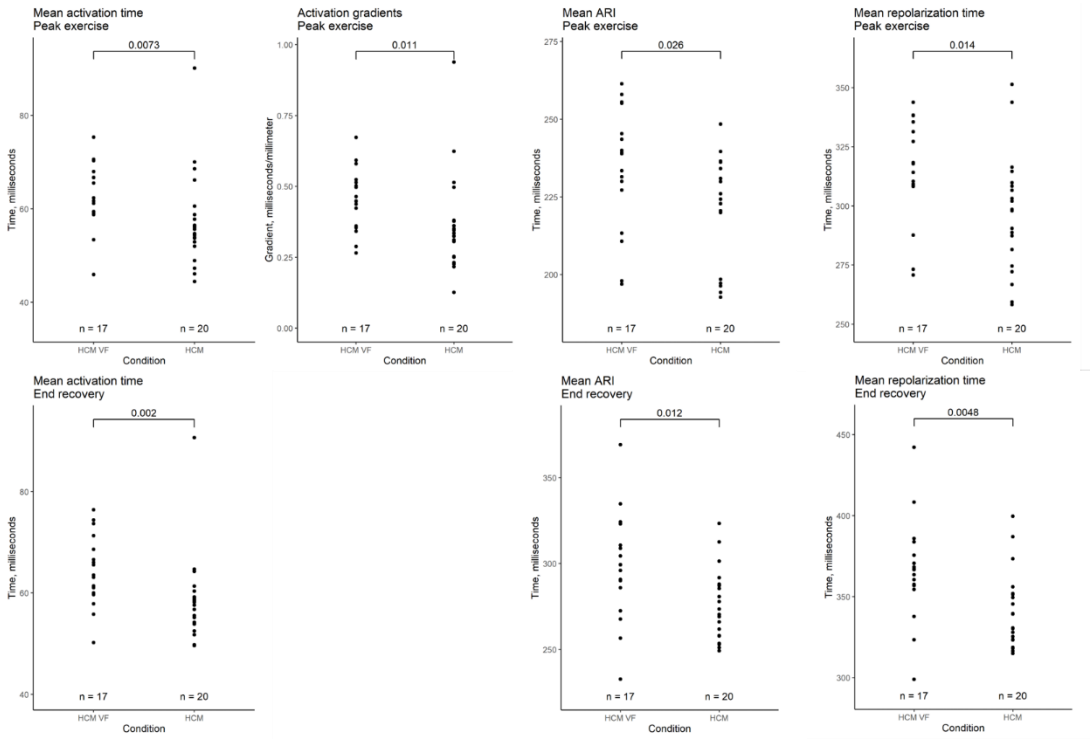

Figure 8.4: Comparison of whole heart activation and repolarization metrics immediately after peak exercise and in end recovery between hypertrophic cardiomyopathy (HCM) patients without a personal arrhythmic history and VF or haemodynamically unstable VT survivors (HCM VF). Local activation time (LAT) was defined as the onset of the first epicardial QRS complex to the steepest negative slope of the electrogram-QRS complex. Local repolarization time (LRT) was defined as the onset of the first epicardial QRS complex to the steepest positive slope of the electrogram-T wave. Activation recovery interval (ARI) is the difference between LAT and LRT. Mean time is the average of all LAT/LRT/ARI across the heart. Dispersion is the central 95% range of LAT/LRT/ARI across the heart. Gradient is the whole-heart mean rate of range in LAT/ARI over a 5mm search distance around each epicardial location.

8.3.4.1 Peak exercise

Following peak exercise, mean activation times in VF survivors were longer than HCM patients without personal history of arrhythmia (means 63.2ms vs 57.4ms, p = 0.0073). Activation dispersion trended towards being longer in HCM VF than HCM patients (mean ranges 56.9ms vs 53.6ms, p =

0.067). Activation gradients were steeper in HCM VF patients (means 0.45ms/mm vs 0.36ms/mm, p = 0.011).

Activation recovery intervals were longer in HCM VF patients than their HCM counterparts (means 234.0ms vs 221.4ms, p = 0.026). ARI dispersion was similar between the groups (p = 0.18) but ARI gradients trended to being steeper in HCM VF patients (means 1.89ms/mm vs 1.58ms/mm, p = 0.06).

Mean repolarization times were significantly longer in HCM VF survivors (means 314.3ms vs 296.6ms, p = 0.014). Corrected repolarization time dispersion was longer in HCM VF survivors, trending towards significance (mean 169.1ms vs 145.2ms p = 0.06).

8.3.4.2 End recovery

After 10 minutes of recovery, whole heart mean activation times were longer in HCM VF survivors (means 64.4ms vs 58.6ms, p = 0.002). Activation dispersion and gradients were not significantly different between groups (p = 0.27, 0.14 respectively).

Activation recovery intervals were longer in HCM VF patients than their unaffected HCM counterparts (means 298.0ms vs 275.5ms, p = 0.012). ARI dispersion and gradients were similar (p = 0.23, 0.17 respectively). Mean repolarization times were significantly longer in HCM VF patients (means 365.9ms vs 341.1ms, p = 0.0048). The dispersion in repolarization times was not significantly different between groups (p = 0.24).

8.3.5 Ventricular conduction stability

Our group has previously described Ventricular Conduction Stability (V-CoS) as a tool to quantify activation heterogeneity in response to exercise (Shun-Shin, Leong et al. 2019). We tested V-CoS on the current population. The pooled HCM cohort had significantly less preserved activation patterns in response to exercise than the controls (means 96.5 +/- 3.9% vs 98.5% +/- 1.0% V-CoS respectively, p = 0.0083). This difference was most evident in the BrS relatives (98.9% +/- 0.8% V-CoS, p = 0.015 against HCM); neither IHD VF nor VE patients could be differentiated in the pairwise analysis (p = 0.26, 0.065 respectively). HCM VF patients were not significantly different from HCM patients without arrhythmic history (p = 0.89).

8.3.6 Logistic regression for the description of the arrhythmogenic substrate in HCM

To understand the contribution of different parameters from our panel to the arrhythmogenic substrate in HCM, we built multiple variable logistic models from the significant variables. Five ECGi

measures of epicardial electrophysiology significantly differentiated the HCM VF group from their HCM counterparts without ventricular arrhythmia:

1. Mean activation time (exercise)
2. Mean activation time (recovery)
3. Mean activation gradients (exercise)
4. Mean ARI (exercise)
5. Mean ARI (recovery).

The only collinear pair of measures were mean activation time in exercise and recovery (Pearson R = 0.93, p >0.001). The mean activation time in exercise was excluded from analysis to reduce collinearity. The remaining 4 variables had Pearson correlations from 0.21 to 0.72 (Table 8.2).

Table 8.2: Correlation matrix to detect intervariable dependence. High Pearson correlation between two variables suggests a 1:1 relationship and predisposes models to collinearity. In our study we chose to eliminate one of any pair of variables more with a Pearson correlation >0.8 (high inter-dependence). In this case, mean activation time in exercise was eliminated (high correlation with mean activation time in recovery). Activation recovery interval, ARI.

	Recovery mean activation time	**Exercise mean activation time**	**Recovery mean ARI**	**Exercise mean ARI**	**Exercise activation gradients**
Recovery mean activation time	1.00	0.93	0.23	0.32	0.72
Exercise mean activation time	0.93	1.00	0.21	0.34	0.72
Recovery mean ARI	0.23	0.21	1.00	0.57	0.21
Exercise mean ARI	0.32	0.34	0.57	1.00	0.31
Exercise activation gradients	0.72	0.72	0.21	0.31	1.00

The 4 variable model achieved a log likelihood ratio (LLR) p-value of 0.04 (lower is better) and divided the training group with a sensitivity of 0.82 and a specificity of 0.8. Individual coefficients however were non-significant (p = 0.14-0.82, see Supplement). Stepwise exclusion of the least significant coefficient was performed until all coefficients reached the pre-specified stop criterion (p>0.15). A nested 2-variable model was reached a LLR p-value of 0.008. The remaining variables were mean activation time and mean ARI in full recovery. This 2-variable model differentiated the HCM VF and HCM groups better than any single variable from our panel (Figure 8.5), and similarly to the 4-variable model.

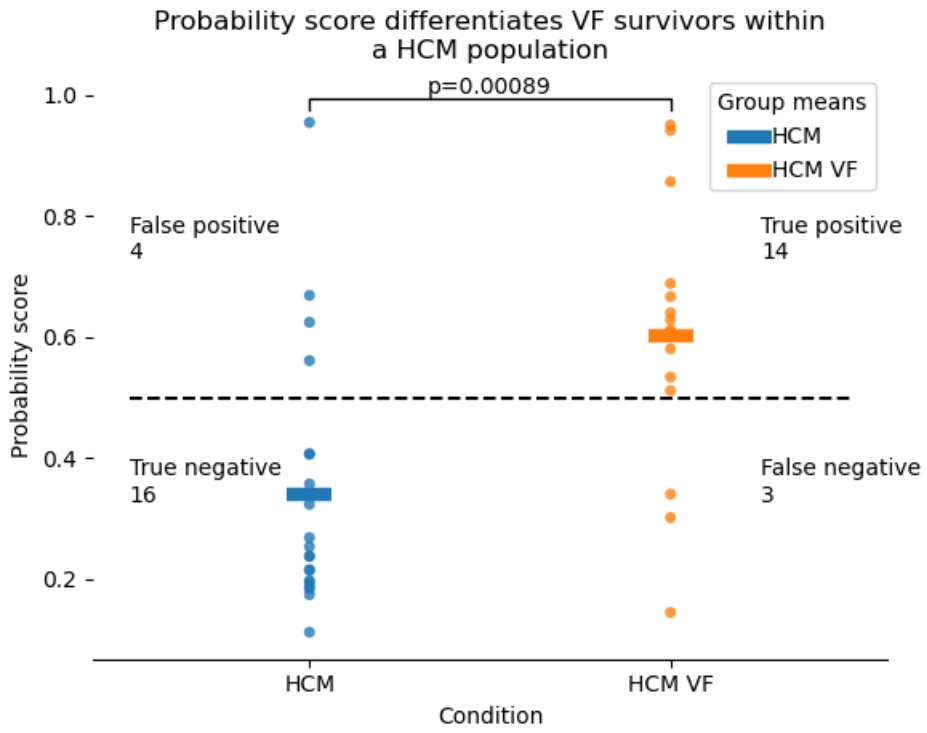

Figure 8.5: Probability distributions for HCM VF or unstable VT survivors as well as HCM patients without a personal history of life-threatening arrhythmia, produced by a 2-variable logistic model of mean activation time and mean activation recovery interval at rest. Higher probability scores refer to the chance that the patient in question falls in the HCM VF group. The dotted line represents a probability of 0.5. Correct classification was defined as p>0.5 for HCM VF and p<0.5 for HCM, although this threshold can be defined differently by the clinician. Hypertrophic cardiomyopathy, HCM; Ventricular fibrillation, VF; Ventricular tachycardia, VT.

To understand the relationship between the mean activation time, mean ARI and the likelihood of being in the VF group, odds ratios were calculated. Mean activation time had an odds ratio of 1.1 (95% confidence intervals 0.98-1.23) per millisecond increase, and mean ARI had an odds ratio of 1.03 (95% confidence intervals 1.00-1.06) per millisecond increase.

8.3.7 Ability of a multiple logistic model to predict in unseen data

A single logistic regression model tested on training data cannot guarantee generalization to a larger population. Validation in unseen data must be performed to determine wider applicability.

To understand the ability of a logistic model containing mean activation time and mean ARI to predict whether a volunteer was in the HCM VF or HCM group on unseen data, we performed a 5-fold validation.

The balanced accuracy of the 2-variable models was 0.75 (95% confidence intervals 0.70-0.80, Figure 8.6A). Individual accuracy for conditions was 0.80 for HCM (95% confidence interval 0.8-0.8) and 0.72 for HCM VF (95% confidence interval 0.63-0.8). In comparison, use of 4-variable models would have only produced accuracies of 0.8 and 0.62 for HCM and HCM VF respectively. The receiver operating characteristic demonstrated an area under the curve of 0.76 (95% confidence intervals 0.72-0.81, Figure 8.6B). Using Youden's method to evaluate the best threshold, the aggregated models could achieve a sensitivity of 78.6% with a specificity of 79.8% for identifying a patient from the HCM VF group.

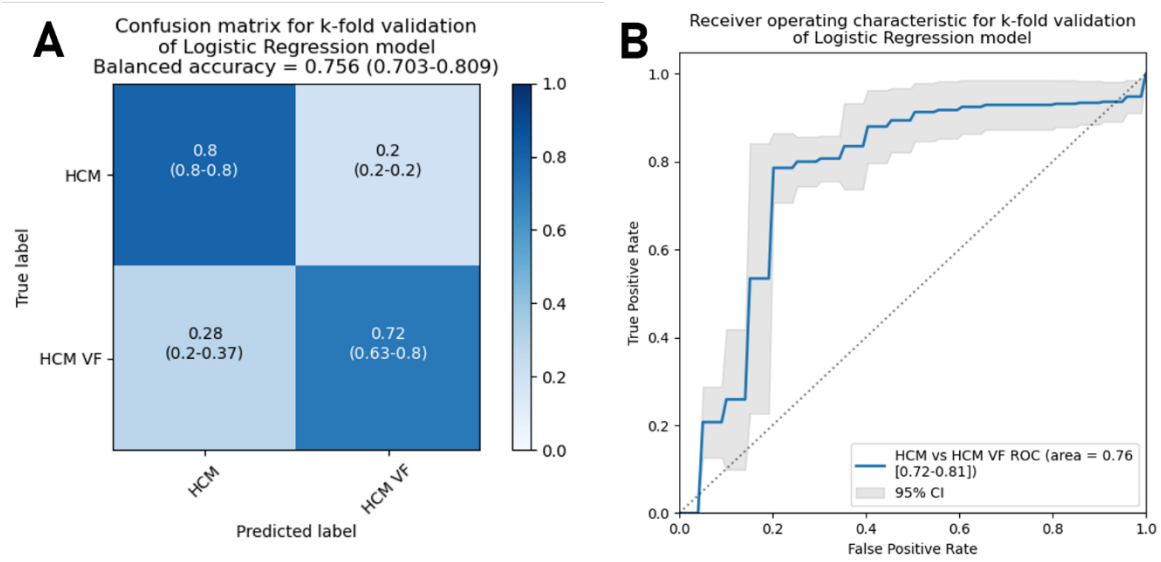

Figure 8.6: Results for a k-fold validation of 2-variable logistic models including mean activation times and ARI at rest in patients with HCM without a personal history of life-threatening arrhythmia and HCM VF or haemodynamically unstable VT survivors. This analysis simulates unseen data to provide a more reliable estimate of how a model with the same input variables will generalize. The classification threshold was set to p=0.5 and the dataset was split into 5 folds. Hypertrophic cardiomyopathy, HCM; Ventricular fibrillation, VF; Ventricular tachycardia, VT.

8.3.8 Comparison of logistic regression with other machine learning techniques for discriminating arrhythmogenic substrates

The discriminative power of support vector machines, random forests and neural networks were tested against logistic regression in the HCM vs HCM VF problem to assess the potential future contribution to risk stratification problems. 5-fold validation was again used to simulate unseen data.

In terms of accuracy, all predictive models performed comparably with overlapping confidence intervals. Support vector machines performed best (accuracy 76.7%, CI: 71.3-82.1%), followed by logistic regression (75.6%, CI: 70.3-80.9%), random forests (70.8%, CI: 63.8-77.8%) and finally the neural network (65.9%, CI: 57.8-73.9%).

Models were also evaluated by area under the receiving operator curve (AUC). Again, models were comparable with overlapping confidence intervals. Support vector machines again performed best (AUC 0.82, CI: 0.79-0.86), followed by random forests (0.79, CI: 0.75-0.83), logistic regression (0.76, CI: 0.72-0.81) and finally the neural network (0.64, CI: 0.56-0.72). Using Youden's method to evaluate thresholds on these receiver operating characteristic curves, the highest sensitivity and specificity would have been achieved by the SVM model at 80.0% and 79.8% respectively.

8.4 Discussion

We sought to understand the electrophysiological differences between patients with hypertrophic cardiomyopathy and various control groups. This pilot study uses non-invasive ECGi to describe significant differences in activation and repolarization between patients with HCM and a range of control groups. Logistic regression and machine learning analysis of these markers can improve the identification rate of VF survivors from the HCM cohort.

8.4.1 Traditional risk markers and surface ECG characteristics

Aside from a personal history of life-threatening arrhythmia, no traditional risk marker significantly differentiated the HCM VF group from the HCM group. In contrast, the ESC scores were significantly higher in the HCM VF than the HCM scores. This demonstrates the utility of multiparametric analysis to differentiate groups when individual risk factors may (in small samples) fail.

Even for the significantly different ESC scores, around half of the patients would not have had an implantable cardioverter-defibrillator (ICD) mandated by either the 4% "consider" cut-off or the 6% "definite" cut-off for 5-year risk. This corroborates earlier observations that many HCM patients

surviving sudden cardiac arrest would not be offered an ICD if assessed by their presenting characteristics on the ESC risk calculator (Maron, Casey et al. 2015; Leong, Chow et al. 2018).

Corrected QT intervals were significantly higher in the HCM VF population than HCM, IHD VF and BrS relatives in the recovery phase. The observation of prolonged QT intervals in patients at higher risk of potentially lethal arrhythmia has been noted before, but has never been included in risk stratification guidelines (Gray, Ingles et al. 2013).

8.4.2 The HCM epicardial electrotype

Activation and repolarization differences are seen between the HCM patients and the control groups. Especially with the HCM VF group, activation happens later with respect to the QRS start (delay), takes longer to complete (dispersion) and is subject to higher gradients between neighbouring areas of the heart. These differences appear to be present immediately after exercise and in the later stages of recovery.

Our activation findings are consistent with previous publications. During endocardial mapping of the left ventricle in 9 patients, long stimulus-to-V times were found in hypertrophic areas of the HCM heart during multisite stimulation (Schumacher, Gietzen et al. 2005). ECGi mapping of 10 HCM patients demonstrated a greater degree of activation dispersion in HCM patients, especially in the basal areas (Perez-Alday, Haq et al. 2020). The authors did not measure recovery times but theorized that activation dispersion would contribute to repolarization dispersion and therefore promote arrhythmogenesis. Our study confirms that abnormal repolarization exists, but in fact repolarization metrics show independence from activation metrics (Table 8.2).

Surface markers of repolarization have been compared between HCM patients and controls in the past – showing that HCM patients with above average maximal wall thickness had longer corrected QT intervals and T peak-T end measurements than healthy controls without genetic mutations associated with HCM or evidence of ventricular hypertrophy (Jalanko, Väänänen et al. 2018). These measurements are correlates of mean and dispersion of epicardial repolarization times. Our healthy control group clearly showed differences in mean and dispersion of repolarization in both exercise and recovery (HCM vs BrS relatives, $p = 0.0001$-0.006). Interestingly, our control groups with a known non-HCM pathology were only sometimes differentiable by epicardial repolarization times. Exercise seemed to accentuate the differences, and mean repolarization time (the correlate of surface QTc) was a stronger differentiator. This suggests that exercise is important in revealing the epicardial substrate of HCM.

The independence of activation and repolarization measures support the idea of HCM as a heterogenous condition; further study would be required to subtype HCM patients with activation predominant or repolarization predominant disease. This would open the possibility for tailored risk stratification or therapy based on reconstructed ECGi measurements.

8.4.3 Understanding contributors to ventricular fibrillation in HCM using logistic regression

As well as the differences between HCM and control groups, our study demonstrated that HCM VF survivors could be differentiated from HCM patients without a personal history of ventricular arrhythmia by longer mean activation times and steeper activation gradients, as well as longer mean ARIs. Unlike with repolarization time against the controls, the only marker affected by exercise in this analysis was the presence of steep activation gradients in peak exercise.

Epicardial activation and repolarization times have not previously been directly examined in high risk HCM patients; surrogates have been described. Accepted electrophysiological differences between HCM VF and HCM patients include non-sustained VT (Elliott, Poloniecki et al. 2000; Monserrat, Elliott et al. 2003; O'Mahony, Jichi et al. 2014), paced fractionated electrograms (Saumarez, Camm et al. 1992), and longer QTc (Gray, Ingles et al. 2013). It is also possible to compare electrophysiological markers in HCM patients with higher risk features, such as a higher HCM-SCD risk score (O'Mahony, Jichi et al. 2014) or any of its constituents. An unsupervised machine learning study on surface ECG in HCM patients found an association with isolated repolarization abnormalities and higher HCM-SCD scores (Lyon, Bueno-Orovio et al. 2018). HCM patients with greater maximum wall thickness were found to have longer surface QTc and T peak-T end measurements than controls or HCM patients with milder hypertrophy (Jalanko, Väänänen et al. 2018).

The paced fractionated electrogram technique was designed to detect the effects of myocardial disarray on intraventricular conduction (Saumarez, Camm et al. 1992). Our results show this conduction slowing non-invasively and as a continuous variable in patients who cannot be differentiated by QRS duration. Whilst QTc combines both activation and repolarization, our epicardial study has allowed ARI to be measured, an accepted correlate of APD (Haws and Lux 1990), showing that ventricular repolarization is elongated in HCM VF survivors independent of activation pattern.

Our logistic regression model could be simplified down to two variables: mean activation time in recovery and mean ARI in recovery. Odds ratios suggest that longer activation time and ARI independently increase the risk of falling in the VF category, although the 95% confidence interval

crosses zero for activation time. This could be because our study was small. Further work would be needed to confidently determine the additional risk per millisecond increase in activation time or ARI.

As with the findings between the pooled HCM group and controls, the independence and poor correlation of activation and repolarization measures in our model suggest that there is more than one mechanism for VF in HCM. Future therapies may be tailored by the findings of mapping studies.

8.4.4 Comparison of logistic regression to (other) machine learning methods

Logistic regression allowed us to understand the relationships between variables and the arrhythmic substrate, but it was not clear whether this would be the optimal strategy for future risk prediction. In this analysis, logistic regression was one of the strongest models in terms of overall classification accuracy but was matched or perhaps bettered by other ML methods in receiver operating characteristic (ROC) analysis.

The range of ROC AUC values for all models except for ANN was comparable to the initially reported performance of modern risk stratification scores. Our models scored between 0.76-0.82. CHADSVASC had a ROC AUC of 0.606 in the original paper (Lip, Nieuwlaat et al. 2010), compared to 0.81 for the Sieira Brugada score (Sieira, Conte et al. 2017) and 0.7 for the HCM-SCD risk score (O'Mahony, Jichi et al. 2014).

The underperformance of neural networks for tabular data is well known in the machine learning community and expresses itself in user preference for decision tree-based models in the biggest ML competitions (Kaggle 2019). Recent developments have been made in Google's TabNet (Arik and Pfister 2019), but this architecture has yet to make it into popular off-the-shelf learning libraries. Although neural networks have traditionally been viewed as 'black boxes', newer architectures like TabNet are specifically designed with interpretability in mind, and the data science community's understanding of how to interpret the workings of other architectures is also rapidly advancing (Fan, Xiong et al. 2020). The relative strength of logistic regression as an interpretable statistical tool may further diminish in the future.

The biggest limitation in our analysis is the lack of optimization of any of the machine learning algorithms, which potentially disadvantages SVM, RF and ANN against logistic regression which has been optimized by stepwise backward elimination. The decision to use unoptimized models was deliberate. Only a small dataset was available, with every datapoint well known to the investigators; although cross validation was used to estimate performance on unseen data, it might be possible for

the investigators to 'over-tune' hyperparameters to the dataset (Eggensperger, Lindauer et al. 2019). Using the Scikit-Learn defaults provided an unbiased but pessimistic view of the ability of machine learning to compete with logistic regression. In some ways, the fairest comparison in our analysis may be between the full, unselected logistic regression model and SVM, RF or ANNs.

In the future and with a larger dataset, optimization should occur with the data analysis team blinded to the full dataset. A training and validation set can be reserved from the end data for the purpose of model selection and development, with final evaluation in a test set never seen by the analysis team.

In the literature there is no clear winner between logistic regression and other machine learning techniques, with articles supporting opposing viewpoints (Verplancke, Van Looy et al. 2008; Maroco, Silva et al. 2011; Huang, Xu et al. 2014; Mustafa, Rienow et al. 2018; Panesar, D'Souza et al. 2018). Like for variable selection, model selection should be guided by the purpose of the research: whether we are searching for predictive or descriptive models. Despite being disadvantaged by lack of optimization, the competitive sensitivity and specificity of SVM suggests that machine learning methods should be strongly considered for predictive model building in future populations.

8.4.5 Feasibility of a prospective study into ECGi derived predictors for sudden death

A prospective study would be the ideal for assessing the ability of ECGi to discriminate HCM patients who will go on to have life threatening arrhythmia, but the parameters which should be examined are unknown. Even with a limited sample size we were able to show a significant difference in several electrophysiological parameters between HCM VF survivors and HCM patients without a history of life-threatening arrhythmia.

Single parameters were limited in their ability to differentiate the groups by a significant overlap in values. Whilst combining many variables separated the training data well, two of the parameters (mean activation gradients and mean ARI in recovery) did not meet our pre-specified significance criteria and were dropped to reduce overfitting. This proved to be the optimal strategy as the 2-variable models outperformed the 4-variable models in K-fold validation (which simulates unseen data). We would therefore recommend risk models with fewer variables for both simplicity and the avoidance of overfitting.

Our study took place in a balanced population of VF survivors and those without arrhythmic history. In reality, the incidence of VF in an unselected HCM population is only about 1-2% per year (O'Mahony, Jichi et al. 2014), and the prevalence of VF in the HCM cohort is far less than 50%. One

approach for future studies might be to recruit only primary prevention patients considered to be high risk by an existing score, to maximize the event rate. Assuming a five-year study of HCM patients considered high to intermediate risk (4% HCM-SCD 5-year risk and above (O'Mahony, Jichi et al. 2014)) reached a mean risk of 5% per 5 years, the positive predictive value of our model would be 0.16, but the negative predictive value would be 0.98. This early data would suggest that an ECGi based risk model is superior predictor of safety than of actual events. Given that sudden cardiac arrest is far less survivable than the complications of ICD implantation, clinicians and patients may accept this limitation.

8.4.6 Limitations

The small size of this pilot predisposes it to type II error, so as well as mean activation time and mean ARI other ECGi derived measures for risk prediction could reasonably be considered as hypotheses. The univariate significance of measures such as activation gradients in exercise but not in recovery could be important in larger studies and explain the possible link between exercise and HCM death in the young (Margey, Roy et al. 2011).

Our study used the only commercially and clinically available ECGi platform (CardioInsight™), which allows applicability for healthcare teams already using ECGi in the catheter laboratory. The methods with which ECGi reconstructions can be calculated vary (Cluitmans, Brooks et al. 2018) and it was important for our study goal to use a system with the widest clinical access. CardioInsight™ uses zero-order Tikhonov regularization, optimized for activation, but second-order Tikhonov regularization optimizes T wave amplitude (Ramanathan, Jia et al. 2003). It is unknown whether this would cause error in our measurements, but to lessen the possibility we did not compare absolute T wave amplitudes or gradients between patients. Relative calculations were used to either reject uninterpretable electrograms or define local repolarization time; no error should result if regularization order affects T wave amplitude uniformly in time.

The agreement of ECGi compared with invasive mapping has been examined previously, and the debate surrounding the validity of these measurements goes on. Correlation coefficients between epicardial maps and ECGi reconstructions have been quoted between 0.03 and 0.86 (Cluitmans, Bonizzi et al. 2017; Graham, Orini et al. 2018; Duchateau, Sacher et al. 2019). However, all in-vivo invasive mapping comparisons to date have suffered from difficulty co-localizing and timing against ECGi reconstructed points. Invasive maps are collected over multiple cardiac cycles whilst ECGi maps are collected in a single beat – so beat-to-beat variations cannot be captured by invasive methods.

Spatial mismatch in these studies could reach 20mm, which in our normal controls could lead to activation time mismatch of up to 10 milliseconds. Graham and colleagues recognized this effect directly in their validation paper (Graham Adam, Orini et al. 2019). To reduce the effect of spatiotemporal disagreement with invasive ground truth, we took the approach of signal averaging over 10 beats and taking whole heart means rather than quoting per-epicardial segment values. Concordance with the (unknown) ground truth will be a problem for any ECGi based project of this type.

8.5 Conclusion

ECGi can differentiate HCM from mixed control groups. The HCM epicardial electrotype is characterized by slow, dispersed conduction and delayed, dispersed repolarization, often accentuated by exercise. These factors occur with some independence between patients, corroborating the view from imaging that hypertrophic cardiomyopathy is a heterogenous disease. These parameters may be useful for risk stratification of sudden cardiac arrest, but larger prospective trials would be recommended to test the findings generated by this pilot.

8.6 Supplemental material

8.6.1 Supplementary figure 1

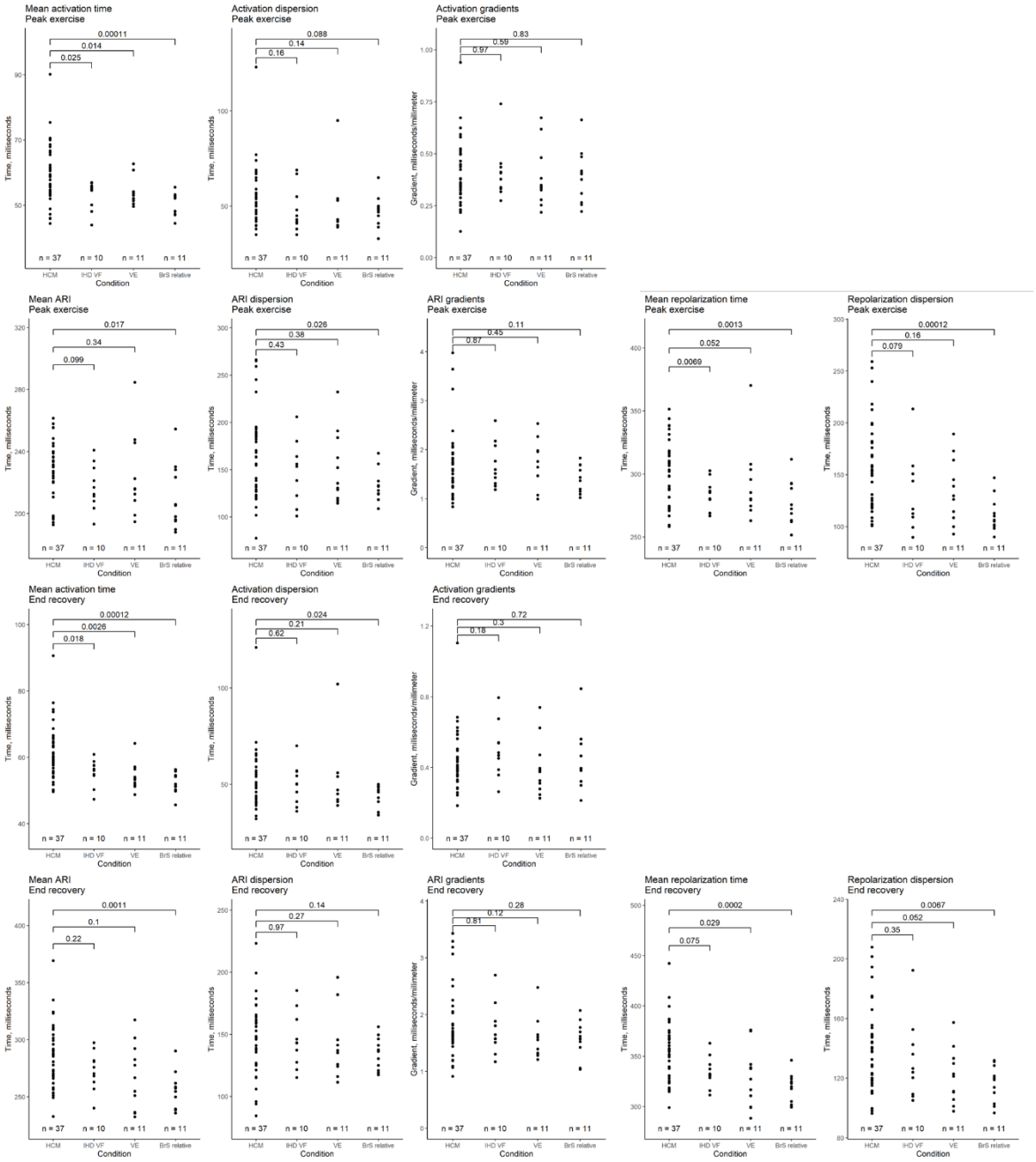

Supplementary figure 8.1: Comparison of whole heart activation and repolarization metrics immediately after peak exercise and in end recovery between hypertrophic cardiomyopathy (HCM) and a selection of structurally normal heart control groups: (I) fully recovered and revascularized ischaemic VF survivors, IHD VF; (II) patients with benign but symptomatic idiopathic ventricular ectopy, VE; (III) the unaffected relatives of patients with Brugada syndrome, BrS relative. Local activation time (LAT) was defined as the onset of the first epicardial QRS complex to the steepest negative slope of the electrogram-QRS complex. Local repolarization time (LRT) was defined as the onset of the first epicardial QRS complex to

the steepest positive slope of the electrogram-T wave. Activation recovery interval (ARI) is the difference between LAT and LRT. Mean time is the average of all LAT/LRT/ARI across the heart. Dispersion is the central 95% range of LAT/LRT/ARI across the heart. Gradient is the whole-heart mean rate of range in LAT/ARI over a 5mm search distance around each epicardial location.

8.6.2 Supplementary figure 2

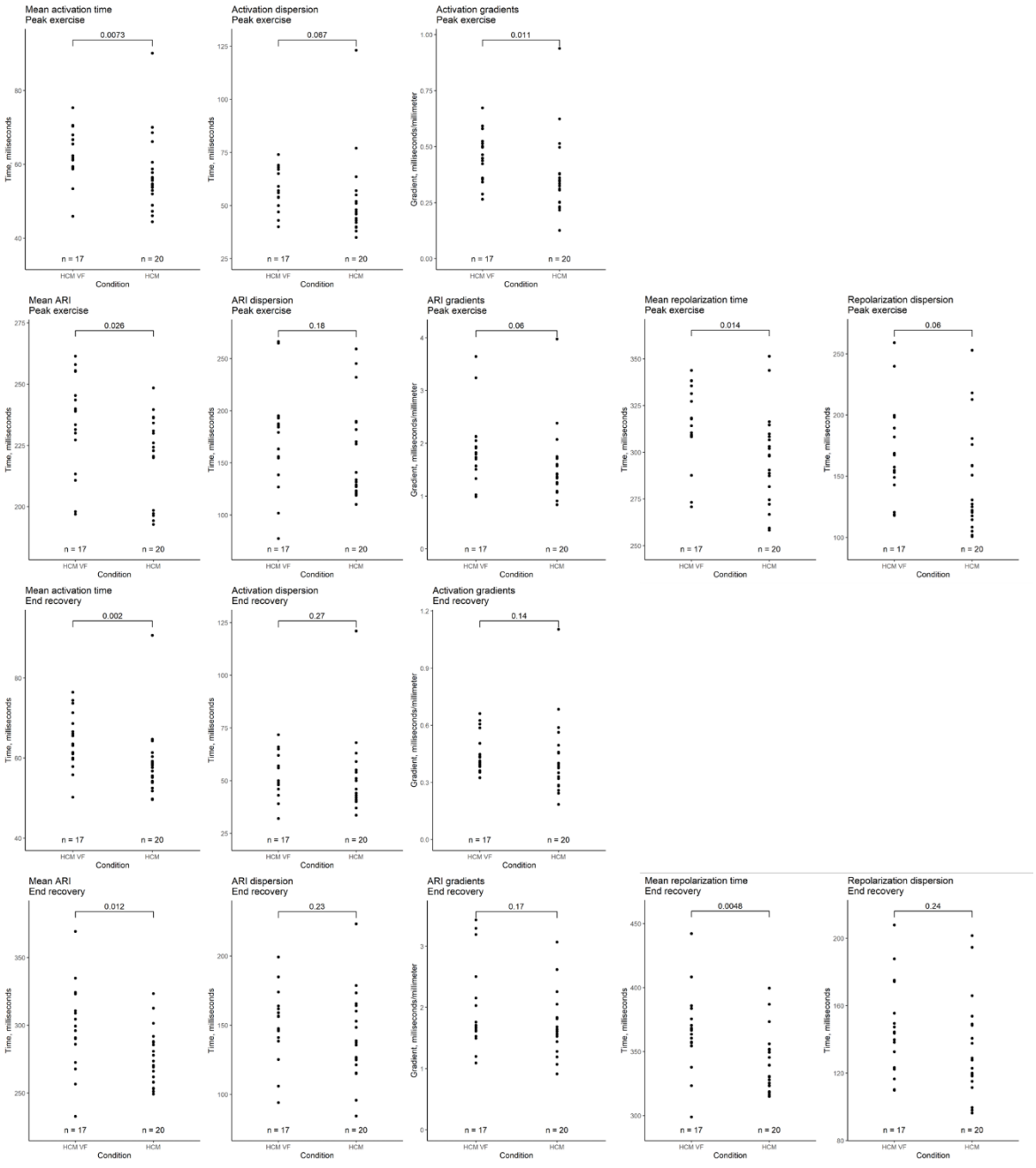

Supplementary figure 8.2: Comparison of whole heart activation and repolarization metrics immediately after peak exercise and in end recovery between hypertrophic cardiomyopathy (HCM) patients without a personal arrhythmic history and VF or haemodynamically unstable VT survivors (HCM VF). Local activation time (LAT) was defined as the onset of the first

epicardial QRS complex to the steepest negative slope of the electrogram-QRS complex. Local repolarization time (LRT) was defined as the onset of the first epicardial QRS complex to the steepest positive slope of the electrogram-T wave. Activation recovery interval (ARI) is the difference between LAT and LRT. Mean time is the average of all LAT/LRT/ARI across the heart. Dispersion is the central 95% range of LAT/LRT/ARI across the heart. Gradient is the whole-heart mean rate of range in LAT/ARI over a 5mm search distance around each epicardial location.

8.6.3 Supplementary table 1

4-variable model regression results	
No. Observations:	37
Df Residuals:	32
Df Model:	4
Pseudo R-squared:	0.1930
Log-Likelihood:	-20.600
LL-Null:	-25.525
LLR p-value:	0.04302

	coefficient	**SE**	**z-value**	**P>|z|**	**[0.025**	**0.975]**
constant	-14.7861	6.239	-2.370	0.018	-27.015	-2.557
Recovery mean activation time	0.0784	0.071	1.102	0.270	-0.061	0.218
Recovery mean ARI	0.0283	0.019	1.476	0.140	-0.009	0.066
Exercise mean ARI	0.0062	0.027	0.232	0.816	-0.046	0.059
Exercise mean activation gradients	0.8177	3.674	0.223	0.824	-6.383	8.019

Supplementary table 8.1: Regression parameters for 4-variable model differentiating hypertrophic cardiomyopathy patients with and without a personal history of life-threatening arrhythmia. Standard error of the coefficient, SE; coefficient divided by standard error, z-value; significance of the coefficient, P>|z|; lower and upper 95% confidence bound, [0.025 0.975].

8.6.4 Supplementary table 2

2-variable model regression results	
No. Observations:	37
Df Residuals:	34
Df Model:	2
Pseudo R-squared:	0.1904
Log-Likelihood:	-20.665
LL-Null:	-25.525

LLR p-value:	0.007754

	coefficient	std err	z-value	P>|z|	[0.025	0.975]
constant	-14.6505	5.667	-2.585	0.010	-25.758	-3.543
Recovery mean activation time	0.0918	0.057	1.614	0.107	-0.020	0.203
Recovery mean ARI	0.0311	0.016	1.963	0.050	4.95e-05	0.062

Supplementary table 8.2: Regression parameters for 2-variable model differentiating hypertrophic cardiomyopathy patients with and without a personal history of life-threatening arrhythmia. Standard error of the coefficient, SE; coefficient divided by standard error, z-value; significance of the coefficient, P>|z|; lower and upper 95% confidence bound, [0.025 0.975].

8.6.5 Detailed characteristics of the control groups

8.6.5.1 Ischaemic VF

Count	10
Age (years)	58.3 ±8.0
Gender M:F	9:1
VF during presentation	10/10
Anginal symptoms in year prior to testing	0/10
ECG at testing	3 normal sinus rhythm 3 residual ST elevation (<1mm) 1 anterior early repolarization 3 residual T wave inversion
MRI	Performed in 1, late Gad enhancement of papillary muscle but no regional motion abnormality
Normal LV function, no regional wall motion abnormalities on echocardiogram	10/10
Infarct location/revascularization	2 LAD 2 Circumflex/OM 2 RCA/PDA 4 triple vessel disease
Mean peak troponin I (ng/L)	15387 ±20919

8.6.5.2 Brugada relatives

Count	11
Age (years)	45.5 ±11.0
Gender M:F	8:3
ECG at testing	8 normal sinus rhythm 1 RSR' in V1-2 1 early repolarization in V1-2 1 W pattern in V1
Echocardiogram	10 normal 1 bicuspid aortic valve, otherwise normal
MRI	Performed in 1, normal
Coronary assessment	10 normal ETT 1 normal ETT and DSE
Negative Ajmaline challenge	11/11
Family history	4 (aborted) sudden death 4 spontaneous Type 1 ECG 3 concealed Type 1 ECG

8.6.5.3 Ventricular ectopy ablation

Count	11
Age (years)	44.5 ±14.3
Gender M:F	6:5
ECG (excluding ectopy)	10 normal sinus rhythm 1 anterior T wave abnormality
Echocardiogram	10 normal 1 mitral valve prolapse, otherwise normal
MRI	3 normal 2 mild LV dysfunction in the context of ectopy without evidence of fibrosis 6 not performed

Ectopy location	8 RVOT 1 LVOT 1 Basal septal LV 1 inferior LV
Ectopy burden	17.2 ±10.2%

Chapter 9: Conclusions

Risk stratification of sudden death in the inherited cardiac conditions is still dominated by clinical history taking and imaging, despite the unifying problem – ventricular tachyarrhythmia – being an electrophysiological phenomenon. This is in part due to the difficulties in understanding the electrodynamics of the diseased heart within a patient – the most detailed work takes place in-vitro, in animal models or immobilized patients despite knowing the importance of the heart's interaction with the body's homeostatic systems and environmental stressors. Non-invasive technologies previously lacked the resolution to compete with other study modalities.

Electrocardiographic imaging has allowed us to study epicardial electrophysiology in higher resolution and a more physiological setting than ever before. The scientific community has used this to study the mechanisms of multiple cardiac conditions, giving us a unique look at in-vivo electrical conditions for Brugada syndrome (Zhang, Sacher et al. 2015), Hypertrophic cardiomyopathy (Perez-Alday, Haq et al. 2020), long-QT syndrome (Vijayakumar, Silva et al. 2014) and early repolarization (Zhang, Hocini et al. 2017). None of these achievements have yet translated into clinical practice.

Although the scientific discoveries enabled by ECGi are impressive, it is unclear if this could be used for improving risk stratification. To be useful, a tool would have to surpass the performance of currently available strategies; it would need to be usable for clinicians handling large, busy clinics; it would need to be reproducible.

This thesis is an exploration of these criteria. In our final chapter, I will draw conclusions on the findings, implications and limitations of the work carried out.

9.1 Key findings and clinical implications

Despite a multitude of risk factors determined from careful patient registry and the development of multivariate scores, we found modern risk stratification methods still lacking, with a poor sensitivity and specificity for cardiac arrest in our multicenter cohort.

Registry of patients to determine risk factors of sudden cardiac death has inherent issues that are unlikely to be resolved by exclusive study using this strategy. First, by the time a registry is published

the data may be outdated – by the time of publication the Sieira score cohort was at least 4 years old. With rapid changes in the diagnosis and classification of Brugada syndrome, we showed that there are fewer patients with high-risk features in modern registries (Brugada, Brugada et al. 2003; Probst, Veltmann et al. 2010; Priori, Gasparini et al. 2012; Sieira, Conte et al. 2017), so model coefficients from old studies may not be representative of today's clinic attendance. Second, clinical features attracting high risk scores tend to be exhibited by fewer patients, meaning that small chance changes in the register (such as recruiting a single extra patient) could significantly alter recommendations. Third, the score model was sensitive to whether patients had undergone invasive electrophysiological study, which occurs with a high rate in some areas, but was found in our survey to be largely unacceptable to a UK based cohort of cardiologists.

Similar findings in a multivariable score for hypertrophic cardiomyopathy encouraged our group to explore non-invasive electrophysiological differences between cardiac arrest survivors and those unaffected by potentially lethal arrhythmia. Following our investigation into the Sieira score, we also elected to take this route using electrographic imaging (ECGi).

Our first step was to test the latest ECGi electrophysiological score, Ventricular Conduction Stability (V-CoS) (Leong, Ng et al. 2020). We found that reproducibility of this score was poor when different cardiac cycles from the same patients were considered.

The V-CoS scoring process is complex and there are multiple stages where variance may occur – the exercise test, CT scan, 3D mesh reconstruction, cardiac cycle selection and exclusion of electrical signals deemed too noisy for accurate analysis. Many of these steps rely on human judgement, which is subject to significant variation. We described the V-CoS matrix, a fully automated summary of 100 V-CoS scores. This method significantly improved reproducibility between exercise tests.

Furthermore, the previous strategy of identifying the lowest V-CoS score to represent a patient's arrhythmic substrate enabled bias, as more values could be measured if a result seemed inappropriately 'normal'. The use of a fully automated system allows every patient an equal opportunity to manifest an abnormal score but might result in poorer sensitivity when shielded from the sharp eyes of the specialist. Cardiology is guided by qualitative human decisions – judgements on electrogram noise, coronary stenosis severity and visual ejection fraction being just a few examples.

To determine whether this more reproducible but possibly insensitive tool could still differentiate those at risk of cardiac arrest from controls, we explored the performance of the V-CoS matrix in a range of volunteer groups.

In previous study, all control patients had either a benign arrhythmia or an inherited cardiac condition but were judged to be low risk (Leong, Ng et al. 2020). In this study we tested asymptomatic relatives of Brugada syndrome patients. These individuals had normal electrocardiogram, no structural abnormality on imaging, nor evidence of channelopathy on drug challenge testing. Activation patterns were remarkably conserved despite exercise stress. Conservation of activation patterns in response to stress is a logical outcome in patients with normal hearts and no history of arrhythmia – we were able to show this conclusively. Patients with benign ventricular ectopy and structurally normal hearts (VE) were also tested to determine if non-lethal ventricular arrhythmia was associated with reduced V-CoS score, but again activation patterns were well conserved – in line with previous research.

Asymptomatic survivors of ischaemic ventricular fibrillation with full ventricular recovery and revascularization (IHD VF) were also tested to determine whether reduced V-CoS was associated with previous cardiac arrest, or extant arrhythmic substrates. These patients had slightly more activation heterogeneity in response to stress but were indistinguishable from the normal patients. This finding supports the hypothesis that once the ventricle is adequately supplied with blood and there is no large permanent damage, the electrophysiology returns to near normal. In clinical practice these patients would not be routinely offered defibrillators because prognosis is good in those with normal ejection fraction. Our evidence corroborates the epidemiological findings.

We followed this by studying patients with cardiac arrest syndromes.

Unlike in previous works, V-CoS poorly identified cardiac arrest survivors, but did show promise when combined with traditional risk factors spontaneous Type 1 ECG and syncope as seen in Chapter 4 of this thesis. Despite the poor differentiation of cardiac arrest survivors, V-CoS could separate unaffected relatives from patients with Brugada syndrome. This difference persisted when spontaneous Type 1 ECG patients were excluded, allowing good diagnostic specificity and sensitivity. The current gold standard Ajmaline challenge test poses a small but lethal risk to patients – our data suggest V-CoS could be a safer alternative especially in lower risk individuals.

Previous ECGi mapping focused on Brugada patients with Type 1 ECG patterns at the time of recording (Zhang, Sacher et al. 2015). Our work in patients with concealed ECG patients shows that ECGi can resolve a difference with unaffected relatives even when the 12 lead ECG is similar. Although we cannot draw a direct conclusion, it is interesting that a drug induced Brugada patient is closer to a Brugada cardiac arrest survivor than the normal controls. There is some debate over

whether asymptomatic, drug-induced Brugada patients are truly outside the spectrum of normal (Viskin, Rosso et al. 2015). Our findings, along with the observation of cardiac arrest in many asymptomatic concealed Brugada patients (Raju, Papadakis et al. 2011; Leong, Ng et al. 2019) seem to suggest these patients have definite electrophysiological abnormalities even when the Type 1 ECG is not readily seen.

Patients with hypertrophic cardiomyopathy (HCM) were found to have lower V-CoS scores than our control patients. Like Brugada syndrome, the survivors of VF or sustained VT had similar V-CoS scores to the HCM patients without a personal history of potentially lethal arrhythmia. V-CoS's diagnostic ability here is likely to be less useful than in Brugada syndrome – imaging is a well-established and low risk method of identifying HCM. A niche application might be in cases where imaging is indeterminate – although these patients are unlikely to have an ESC score mandating ICD consideration. Interval imaging would be a better evidenced and preferable strategy.

Patients with idiopathic ventricular fibrillation or tachycardia (VF/VT) were found to have significantly lower V-CoS scores than both IHD VF survivors and VE patients. This suggests the V-CoS describes extant arrhythmic substrate present in idiopathic VF/VT patients rather than remnant disease from previous cardiac arrest as might be found in the IHD VF group. A high degree of variation was noted in the idiopathic VF/VT cohort, underlining the heterogenous nature of this group. Patients with multiple VF/VT events trended towards lower scores, suggesting that in a larger study V-CoS might correlate with arrhythmia recurrence.

The low V-CoS idiopathic VF subgroup warrants further investigation – the syndrome of exercise induced activation heterogeneity could well become defined as a distinct condition. If patients with multiple events could be differentiated by V-CoS in a larger study this would strengthen the case. Conversely, cardiac arrest survivors with normal ECGi could be considered close to normal – although this finding is unlikely to persuade clinicians that a secondary prevention ICD could be avoided. Family screening might be possible for relatives of those with low V-CoS scores – there is currently low yield in screening relatives of idiopathic VF survivors with conventional tests (Mellor, Blom et al. 2021).

In all groups tested we saw evidence of periodic patterns in V-CoS. Most patients have cardiac cycles with V-CoS scores close to 100%, but patients in the cardiac arrest syndrome cohorts showed periodic drops in concordance. Whilst fluctuations in beat-to-beat activation concordance could be seen in controls, the magnitude was greater in idiopathic VF/VT, Brugada syndrome and

hypertrophic cardiomyopathy. Alternans patterns are well documented in both patients and cardiac models, and have been linked to arrhythmia (Kulkarni, Merchant et al. 2019). The reason underlying periodic drops in V-CoS is not clear and warrants further investigation – but we have shown that exercise induced ECG artefact is not responsible, despite similar frequency.

Our data suggest a shared final arrhythmic pathway across multiple pathologies that relies on discordance between consecutive cardiac cycles in response to stress. This phenomenon appeared to be broadly successful at identifying patients with cardiac arrest syndromes, but not necessarily risk stratifying them. To further examine the possibility of improving risk stratification in these conditions we opted to return to more basic electrophysiological measurements from our dataset.

Invasive and ex-vivo experimentation has demonstrated disorders of conduction and repolarization in all three cardiac arrest syndromes examined in this thesis (Yan and Antzelevitch 1999; Janse and De Bakker 2001; Saumarez, Pytkowski et al. 2008; Wilde, Postema et al. 2010; Haïssaguerre, Hocini et al. 2018). The inability to study intact individuals undergoing physiological stress is a significant disadvantage. Non-invasive studies of activation and repolarization have been performed in those with type 1 Brugada ECG, long-QT and early repolarization syndromes (Vijayakumar, Silva et al. 2014; Zhang, Sacher et al. 2015; Zhang, Hocini et al. 2017).

After our experience with V-CoS, we investigated and sought to improve the reproducibility of basic ECG imaging measurements before interrogating our cohort. Due to lower signal to noise ratio, variable user segmentation and noise exclusion for electrogram T waves, repolarization measurements were found to be the most vulnerable to poor reproducibility.

Through a combination of signal averaging, neural network guided ECG segmentation and rule-based T wave rejection we were able to greatly improve reproducibility against manual measurement. The process was almost fully automated, reducing opportunity for user bias. As with the V-CoS matrix, this has the disadvantage of removing the expertise of the experienced cardiologist.

For our strategy to be match ground truth, noise must be assumed random and with zero mean due to the signal averaging. In practice this is difficult to know as direct contact measurement to non-invasive recording co-registration can be challenging. We minimized use of neural networks in our strategy to only the simplest task – segmenting the ECG trace – to avoid the training dataset biasing future decisions. The use of rule-based T wave rejection allows easy modification of the software when a consensus on acceptable morphology is reached for ECGi electrograms. In direct contact electrograms we have the Wyatt and Yue standards (Wyatt, Burgess et al. 1981; Yue, Betts et al.

2005) based on correlation to action potential duration, but ECGi T waves have yet to be validated in this way.

Importantly, standardizing the measurement would mean consistency across sites and research teams if this saw widespread adoption. Our software had a graphical user interface and was designed with usability in mind: this might open up ECGi post-processing to a wider audience and accelerate discovery of electrophysiological phenomena in a wide range of conditions. We cannot confidently say how best to use ECGi parameters for risk stratification from our small cohort, but reproducible techniques would be the cornerstone of a larger effort toward defining cut-offs for ICD implantation.

Using these reproducible methods, we examined epicardial electrograms from our Brugada and HCM cohorts.

Despite similar resting 12-lead ECG, patients with concealed Brugada syndrome could be differentiated from their asymptomatic, unaffected relatives by greater repolarization dispersion and steeper gradients in exercise. Activation delay and steep activation gradients were also evident at full recovery. The longstanding debate between proponents of the activation and repolarization hypotheses in Brugada syndrome is not settled by our data. Poor correlation between activation and repolarization times suggests that for some patients, repolarization is the dominant abnormality whilst for others, activation is disordered. Brugada syndrome may be more heterogenous than first thought – an idea supported by morphological, histopathological, electrophysiological and genetic evidence (Gray, Semsarian et al. 2014).

Differences between normal controls and concealed Brugada patients again raises the possibility of using ECGi to help diagnose the syndrome. The same cannot be said of risk stratification – although longer activation and repolarization times were seen in the VF survivor group, but there were more spontaneous Type 1 ECG patients in the VF group. Once these patients had been excluded, no significant differences remained, corroborating earlier data showing electrophysiologic abnormalities manifest more in those with Type 1 patterns at the time of testing (Brugada, Pappone et al. 2015; Zhang, Sacher et al. 2015).

Compared to a range of controls, we described longer, more dispersed and steeper gradients of both activation and repolarization in patients with HCM. This appeared to be a continuum, with the VF/VT survivors having the highest values of all. Once again, poor correlation was seen between activation and repolarization measures, suggesting a degree of heterogeneity within the cohort.

The longer activation and repolarization times in HCM VF/VT survivors indicate that ECGi might have a role in risk stratifying patients for sudden death with HCM. Despite significant group differences, there is much overlap between the VF/VT survivors and those without previous significant arrhythmia. Drawing a cut-off value for any one of these parameters would entail poor sensitivity or specificity, limiting usefulness for guiding ICD implantation.

Multivariate analysis showed that longer mean activation times and mean activation recovery intervals (ARI) at rest identified the HCM VF/VT survivors with the greatest independence. Using a logistic regression model, we achieved an area under the ROC curve similar to the currently recommended HCM risk score (O'Mahony, Jichi et al. 2014). Our cohort was significantly smaller, so the result should be interpreted with extreme caution. We used a highly polarized cohort of cardiac arrest survivors and low ESC risk score patients in roughly equal proportions – very different to the intake of an inherited cardiac conditions clinic. A project looking at patients in the intermediate risk band is needed to generate a more realistic view of these biomarkers.

In recent years, machine learning has gained great traction in classification problems – we tested 3 common strategies: support vector machines, random forests and neural networks. Support vector machines and random forests scored higher areas under the ROC curve than logistic regression – but confidence intervals showed overlap. Furthermore, interpretability of regression models is far more accessible to clinicians. Without a clear advantage in performance, machine learning strategies should be considered alongside, rather than instead of logistic regression for clinical classification problems.

However they are processed, our data suggests that ECGi measurements can indeed quantify electrophysiological substrates for life threatening arrhythmia. These measurements could be used as adjunct to currently available tools to improve the risk stratification of sudden death in the inherited cardiac conditions.

9.2 Limitations

Despite the detailed electrophysiological measurements made in this thesis, patient selection suffers from similar limitations to many of the registry studies we previously examined.

All data here is analyzed retrospectively. To demonstrate true utility, risk stratifiers must show prospective performance. In considering cardiac arrest survivors, we exclude patients who did not survive ventricular arrhythmia, and assume that the only difference between life and death was the efficacy and promptness of resuscitation. In considering patients with appropriate therapy from an

ICD equivalent to those with aborted cardiac arrest we assume that ventricular tachyarrhythmia never self terminates after the programmed therapy delay, which is known to be false (Gasparini, Proclemer et al. 2013). The rarity of ventricular tachyarrhythmia necessitates this assumption, but it must be recognized that whilst we might be able to draw conclusions about a combined groups of cardiac arrest survivors and appropriate therapy recipients, the results may not be totally applicable to a pure primary prevention cohort.

Our study was also small, meaning that outlier patients might have significant effect on final conclusions, but also that true electrophysiological differences may be masked by Type II error.

Electrocardiographic imaging provides the only current method to reconstruct epicardial electrophysiology non-invasively for intact patients undergoing physiological stress, but there is extensive debate over how accurate it is (Rudy and Lindsay 2015; Duchateau, Sacher et al. 2019; Graham Adam, Orini et al. 2019). Ground truth is ambiguously defined – although contact mapping allows direct recording of electrograms, operators must assume that activation and repolarization patterns are conserved beat to beat as a map is made up of perhaps thousands of catheter positions taken across as many cardiac cycles. Our experimentation suggests that beat to beat electrophysiology is not well conserved in the intact, innervated heart, but this claim may be unfalsifiable.

For this reason, we must be cautious when drawing mechanistic conclusions from our data. Despite the failure of simulated artefact to nullify our results, it would be prudent to consider detectable change within subject, or as a reference against normal subjects rather than absolute values derived from ECGi. The similarity of our findings to invasively gained data can give us some confidence, but we can never be sure of the relationship between our findings and the true epicardial picture.

Modern cardiac MRI techniques have demonstrated great utility in diagnostics and as of the latest HCM guidelines have also been given a role in risk stratification. Lack of MRI data, especially contemporaneous is a limitation of this study. Although MRI-ECGi systems do exist, they are not widely used and have not achieved clinical deployment to date. They were also not CE Marked at the start of this study, which is the reason they were not selected. ECGi-MRI is inherently more difficult to perform in those with implanted cardiac devices; our population had a high prevalence of ICDs. Many of the cardiac arrest survivors were first seen and treated years prior to the common availability of cardiac MRI, and the study did not have funding to repeat scans in these patients. This would be an excellent opportunity for further study.

Use of exercise alone may also limit the quantification of arrhythmic substrates. Vagal stimulation, ectopic beats, emotional stress and sleep have all been anecdotally linked to cardiac arrest. Exercise was chosen for our study as it had the most evidence behind it, was easy to perform and standardize. However, the heterogeneity displayed by all 3 cardiac arrest survivor groups suggests that perhaps exercise is not the optimal stressor for everyone.

9.3 Future directions

At the time of writing, our group has initiated a multi-centre prospective study of intermediate- and high- ESC risk HCM patients without a history of cardiac arrest either being offered or with a primary prevention ICD. Each patient undergoes exercise ECGi which will allow us to measure the parameters examined in this thesis. Alongside this, clinical history, blood tests, 12 lead electrocardiography, echocardiographic and in a subset of patients, magnetic resonance imaging will be performed. Twice yearly follow up will be used to determine whether patients went onto have life threatening ventricular tachyarrhythmia. This comprehensive dataset provides the opportunity to fill remaining gaps in our knowledge.

This prospective data will allow us to know whether V-CoS, or one of the other non-invasive ECGi measurements is effective at guiding ICD implantation. Aside from this clinical conclusion, many basic science goals could also be pursued.

The relationship between structural and electrical measurements is still unknown. MRI data was lacking in this thesis. Longer, more dispersed conduction and repolarization times with steeper gradients would be hypothesized to occur in patients with more myocardial fibrosis, or thicker ventricular walls. We had not considered the distribution of electrophysiologic abnormalities in this thesis, but it is plausible that localized scar or thick ventricular walls would be associated with localized electrophysiological abnormality. The effect of septal fibrosis on epicardial ECGi measurements is also unknown and could be assessed in a larger group of MRI evaluated patients.

A significant issue with interpretation of multiple modalities is anatomic co-registration. This is used extensively by clinical radiotherapists. Although co-localized substrates and electrical measurements are described in the literature, automation is rare and resolution is in the >1cm range, when myocardial abnormalities may be smaller. Further work into electroanatomic co-registration would allow better understanding of how structural abnormalities affect conduction and repolarization. This work would also benefit the nascent field of non-invasive cardiac radiotherapy for ventricular tachycardia, which currently has a coarse targeting system(Cuculich, Schill et al. 2017).

The ECGi system is expensive and requires exposure to ionizing radiation. Although we were able to detect ECGi differences in patients with broadly similar 12-lead ECGs, machine vision may detect abnormalities in this cheap tool that we are unable to with standard clinical measurements like QRS duration. An extension of the convolutional neural network (CNN) used for ECG segmentation in our work could be turned to classification, using either ECGi derived or clinical measurements as the labels.

As body surface signals are used in the reconstruction of epicardial electrograms, it is plausible that this vest data contains sufficient information to differentiate our clinical groups without CT scan. Our data could be retrospectively analyzed using automatic QRS and QTc measurements – these being gained from tools based on our ECG segmenting CNN.

9.4 Closing thoughts

This thesis began with an appraisal of risk models using currently known biomarkers implicated in sudden cardiac death. We found these to be lacking.

Trying to close gaps in our knowledge, we found that electrocardiographic imaging could detect differences between patients with and without a history of life-threatening arrhythmia. We found that activation patterns in normal patients were unchanged by stress, and periodically deranged in those with known arrhythmogenic syndromes. We found computing solutions to improve reproducibility and risk stratification. From the new biomarkers we identified, we constructed a multivariable model to describe the arrhythmic substrate.

A globally-collaborative continually updated registry with follow-up should be a future direction; risk model coefficients can be expected to change with time and our clinical scores should reflect that. The medical problem of static databases is mirrored in the wider machine learning community (Parisi, Kemker et al. 2019). Patients and clinicians should be well counselled that risk stratification remains a steep challenge and will likely be so for time to come.

References

Abdalla, I. S., R. J. Prineas, J. D. Neaton, D. R. Jacobs, Jr. and R. S. Crow (1987). "Relation between ventricular premature complexes and sudden cardiac death in apparently healthy men." Am J Cardiol **60**(13): 1036-1042.

Abiodun, O. O., M. O. Balogun, A. O. Akintomide, R. A. Adebayo, O. E. Ajayi, S. A. Ogunyemi, V. N. Amadi and V. O. Adeyeye (2015). "Comparison between treadmill and bicycle ergometer exercise tests in mild-to-moderate hypertensive Nigerians." Integrated blood pressure control **8**: 51-55.

Al-Khatib Sana, M., G. Stevenson William, J. Ackerman Michael, J. Bryant William, J. Callans David, B. Curtis Anne, J. Deal Barbara, T. Dickfeld, E. Field Michael, C. Fonarow Gregg, M. Gillis Anne, B. Granger Christopher, C. Hammill Stephen, A. Hlatky Mark, A. Joglar José, G. N. Kay, D. Matlock Daniel, J. Myerburg Robert and L. Page Richard (2018). "2017 AHA/ACC/HRS Guideline for Management of Patients With Ventricular Arrhythmias and the Prevention of Sudden Cardiac Death." Circulation **138**(13): e272-e391.

American College of Cardiology Foundation/American Heart Association Task Force on, P., S. American Association for Thoracic, E. American Society of, C. American Society of Nuclear, A. Heart Failure Society of, S. Heart Rhythm, A. Society for Cardiovascular, Interventions, S. Society of Thoracic, B. J. Gersh, B. J. Maron, R. O. Bonow, J. A. Dearani, M. A. Fifer, M. S. Link, S. S. Naidu, R. A. Nishimura, S. R. Ommen, H. Rakowski, C. E. Seidman, J. A. Towbin, J. E. Udelson and C. W. Yancy (2011). "2011 ACCF/AHA guideline for the diagnosis and treatment of hypertrophic cardiomyopathy: a report of the American College of Cardiology Foundation/American Heart Association Task Force on Practice Guidelines." J Thorac Cardiovasc Surg **142**(6): e153-203.

Amin Ahmad, S., A. A. de Groot Elisabeth, M. Ruijter Jan, A. M. Wilde Arthur and L. Tan Hanno (2009). "Exercise-Induced ECG Changes in Brugada Syndrome." Circulation: Arrhythmia and Electrophysiology **2**(5): 531-539.

Andrews, C. M., N. T. Srinivasan, S. Rosmini, H. Bulluck, M. Orini, S. Jenkins, A. Pantazis, W. J. McKenna, J. C. Moon, P. D. Lambiase and Y. Rudy (2017). "Electrical and Structural Substrate of Arrhythmogenic Right Ventricular Cardiomyopathy Determined Using Noninvasive Electrocardiographic Imaging and Late Gadolinium Magnetic Resonance Imaging." Circ Arrhythm Electrophysiol **10**(7).

Ang, R. and N. Marina (2020). "Low-Frequency Oscillations in Cardiac Sympathetic Neuronal Activity." Front Physiol **11**: 236.

Antzelevitch, C. and A. Burashnikov (2011). "Overview of Basic Mechanisms of Cardiac Arrhythmia." Cardiac electrophysiology clinics **3**(1): 23-45.

Antzelevitch, C., G.-X. Yan, M. J. Ackerman, M. Borggrefe, D. Corrado, J. Guo, I. Gussak, C. Hasdemir, M. Horie, H. Huikuri, C. Ma, H. Morita, G.-B. Nam, F. Sacher, W. Shimizu, S. Viskin and A. A. M. Wilde (2016). "J-Wave syndromes expert consensus conference report: Emerging concepts and gaps in knowledge." Journal of Arrhythmia **32**(5): 315-339.

Arik, S. O. and T. Pfister (2019). "Tabnet: Attentive interpretable tabular learning." arXiv preprint arXiv:1908.07442.

Arutunyan, A., L. M. Swift and N. Sarvazyan (2002). "Initiation and propagation of ectopic waves: insights from an in vitro model of ischemia-reperfusion injury." American Journal of Physiology-Heart and Circulatory Physiology **283**(2): H741-H749.

Asada, S., H. Morita, A. Watanabe, K. Nakagawa, S. Nagase, M. Miyamoto, Y. Morimoto, S. Kawada, N. Nishii and H. Ito (2020). "Indication and prognostic significance of programmed ventricular stimulation in asymptomatic patients with Brugada syndrome." EP Europace.

Authors/Task Force, P. M. Elliott, A. Anastasakis, M. A. Borger, M. Borggrefe, F. Cecchi, P. Charron, A. A. Hagege, A. Lafont, G. Limongelli, H. Mahrholdt, W. J. McKenna, J. Mogensen, P. Nihoyannopoulos, S. Nistri, P. G. Pieper, B. Pieske, C. Rapezzi, F. H. Rutten, C. Tillmanns and H. Watkins (2014). "2014 ESC Guidelines on diagnosis and management of hypertrophic cardiomyopathy: the Task Force for the Diagnosis and Management of Hypertrophic Cardiomyopathy of the European Society of Cardiology (ESC)." Eur Heart J **35**(39): 2733-2779.

Avitall, B., J. McKinnie, M. Jazayeri, M. Akhtar, A. J. Anderson and P. Tchou (1992). "Induction of ventricular fibrillation versus monomorphic ventricular tachycardia during programmed stimulation. Role of premature beat conduction delay." Circulation **85**(4): 1271-1278.

Babai Bigi, M. A., A. Aslani and S. Shahrzad (2007). "aVR sign as a risk factor for life-threatening arrhythmic events in patients with Brugada syndrome." Heart Rhythm **4**(8): 1009-1012.

Barletta, G., C. Lazzeri, F. Franchi, R. Del Bene and A. Michelucci (2004). "Hypertrophic cardiomyopathy: electrical abnormalities detected by the extended-length ECG and their relation to syncope." International Journal of Cardiology **97**(1): 43-48.

Baruscotti, M., A. Bucchi and D. DiFrancesco (2005). "Physiology and pharmacology of the cardiac pacemaker (“funny”) current." Pharmacology & Therapeutics **107**(1): 59-79.

Bear, L. R., Y. S. Dogrusoz, J. Svehlikova, J. Coll-Font, W. Good, E. van Dam, R. Macleod, E. Abell, R. Walton, R. Coronel, M. Haissaguerre and R. Dubois (2018). "Effects of ECG Signal Processing on the Inverse Problem of Electrocardiography." Computing in cardiology **45**: 10.22489/CinC.22018.22070.

Bear, L. R., P. R. Huntjens, R. D. Walton, O. Bernus, R. Coronel and R. Dubois (2018). "Cardiac electrical dyssynchrony is accurately detected by noninvasive electrocardiographic imaging." Heart Rhythm **15**(7): 1058-1069.

Behr, E. R., C. Dalageorgou, M. Christiansen, P. Syrris, S. Hughes, M. T. Tome Esteban, E. Rowland, S. Jeffery and W. J. McKenna (2008). "Sudden arrhythmic death syndrome: familial evaluation identifies inheritable heart disease in the majority of families." European Heart Journal **29**(13): 1670-1680.

Beltz, N. M., A. L. Gibson, J. M. Janot, L. Kravitz, C. M. Mermier and L. C. Dalleck (2016). "Graded Exercise Testing Protocols for the Determination of VO(2)max: Historical Perspectives, Progress, and Future Considerations." Journal of sports medicine (Hindawi Publishing Corporation) **2016**: 3968393-3968393.

Bezzina, C. R., R. Pazoki, A. Bardai, R. F. Marsman, J. de Jong, M. T. Blom, B. P. Scicluna, J. W. Jukema, N. R. Bindraban, P. Lichtner, A. Pfeufer, N. H. Bishopric, D. M. Roden, T. Meitinger, S. S. Chugh, R. J. Myerburg, X. Jouven, S. Kääb, L. R. C. Dekker, H. L. Tan, M. W. T. Tanck and A. A. M. Wilde (2010). "Genome-wide association study identifies a susceptibility locus at 21q21 for ventricular fibrillation in acute myocardial infarction." Nat Genet **42**(8): 688-691.

Bikkina, M., M. G. Larson and D. Levy (1992). "Prognostic implications of asymptomatic ventricular arrhythmias: the Framingham Heart Study." Ann Intern Med **117**(12): 990-996.

Bisbal, F., J. Fernández-Armenta, A. Berruezo, L. Mont and J. Brugada (2014). "Use of MRI to guide electrophysiology procedures." Heart **100**(24): 1975.

Blom, L. J., S. A. Groeneveld, B. M. Wulterkens, B. van Rees, U. C. Nguyen, R. W. Roudijk, M. Cluitmans, P. G. A. Volders and R. J. Hassink (2020). "Novel use of repolarization parameters in electrocardiographic imaging to uncover arrhythmogenic substrate." Journal of Electrocardiology **59**: 116-121.

Boehringer, T., P. Bugert, M. Borggrefe and E. Elmas (2014). "SCN5A mutations and polymorphisms in patients with ventricular fibrillation during acute myocardial infarction." Mol Med Rep **10**(4): 2039-2044.

Boineau, J. P. and J. Cox (1973). "Slow Ventricular Activation in Acute Myocardial Infarction." Circulation **48**(4): 702-713.

Brown, H. F., D. Difrancesco and S. J. Noble (1979). "How does adrenaline accelerate the heart?" Nature **280**(5719): 235-236.

Bruce, R. A., J. R. Blackmon, J. W. Jones and G. Strait (1963). "EXERCISING TESTING IN ADULT NORMAL SUBJECTS AND CARDIAC PATIENTS." Pediatrics **32**: Suppl 742-756.

Brugada, J., R. Brugada and P. Brugada (2003). "Determinants of sudden cardiac death in individuals with the electrocardiographic pattern of Brugada syndrome and no previous cardiac arrest." Circulation **108**(25): 3092-3096.

Brugada, J., C. Pappone, A. Berruezo, G. Vicedomini, F. Manguso, G. Ciconte, L. Giannelli and V. Santinelli (2015). "Brugada Syndrome Phenotype Elimination by Epicardial Substrate Ablation." Circulation: Arrhythmia and Electrophysiology **8**(6): 1373-1381.

Brugada, P. and J. Brugada (1992). "Right bundle branch block, persistent ST segment elevation and sudden cardiac death: A distinct clinical and electrocardiographic syndrome: A multicenter report." Journal of the American College of Cardiology **20**(6): 1391-1396.

Buendía-Fuentes, F., M. A. Arnau-Vives, A. Arnau-Vives, Y. Jiménez-Jiménez, J. Rueda-Soriano, E. Zorio-Grima, A. Osa-Sáez, L. V. Martínez-Dolz, L. Almenar-Bonet and M. A. Palencia-Pérez (2012). "High-Bandpass Filters in Electrocardiography: Source of Error in the Interpretation of the ST Segment." ISRN Cardiol **2012**: 706217.

Cadrin-Tourigny, J., L. P. Bosman, A. Nozza, W. Wang, R. Tadros, A. Bhonsale, M. Bourfiss, A. Fortier, O. H. Lie, A. M. Saguner, A. Svensson, A. Andorin, C. Tichnell, B. Murray, K. Zeppenfeld, M. P. van den Berg, F. W. Asselbergs, A. A. M. Wilde, A. D. Krahn, M. Talajic, L. Rivard, S. Chelko, S. L. Zimmerman,

I. R. Kamel, J. E. Crosson, D. P. Judge, S. C. Yap, J. F. van der Heijden, H. Tandri, J. D. H. Jongbloed, M. C. Guertin, J. P. van Tintelen, P. G. Platonov, F. Duru, K. H. Haugaa, P. Khairy, R. N. W. Hauer, H. Calkins, A. Te Riele and C. A. James (2019). "A new prediction model for ventricular arrhythmias in arrhythmogenic right ventricular cardiomyopathy." Eur Heart J **40**(23): 1850-1858.

Calo, L., C. Giustetto, A. Martino, L. Sciarra, N. Cerrato, M. Marziali, J. Rauzino, G. Carlino, E. de Ruvo, F. Guerra, M. Rebecchi, C. Lanzillo, M. Anselmino, A. Castro, F. Turreni, M. Penco, M. Volpe, A. Capucci and F. Gaita (2016). "A New Electrocardiographic Marker of Sudden Death in Brugada Syndrome: The S-Wave in Lead I." J Am Coll Cardiol **67**(12): 1427-1440.

Calvo, N., M. Jongbloed and K. Zeppenfeld (2013). "Radiofrequency catheter ablation of idiopathic right ventricular outflow tract arrhythmias." Indian pacing and electrophysiology journal **13**(1): 14-33.

Carmeliet, E. (1984). Existence of pacemaker current if in human atrial appendage fibers. JOURNAL OF PHYSIOLOGY-LONDON, CAMBRIDGE UNIV PRESS 40 WEST 20TH STREET, NEW YORK, NY 10011-4211.

Casella, M., A. Gasperetti, F. Gaetano, M. Busana, E. Sommariva, V. Catto, R. Sicuso, S. Rizzo, E. Conte, S. Mushtaq, D. Andreini, L. Di Biase, C. Carbucicchio, A. Natale, C. Basso, C. Tondo and A. Dello Russo (2020). "Long-term follow-up analysis of a highly characterized arrhythmogenic cardiomyopathy cohort with classical and non-classical phenotypes–a real-world assessment of a novel prediction model: does the subtype really matter." EP Europace.

Cassidy, D. M., J. A. Vassallo, J. M. Miller, D. S. Poll, A. E. Buxton, F. E. Marchlinski and M. E. Josephson (1986). "Endocardial catheter mapping in patients in sinus rhythm: relationship to underlying heart disease and ventricular arrhythmias." Circulation **73**(4): 645-652.

Chen, S. A., C. E. Chiang, C. J. Yang, C. C. Cheng, T. J. Wu, S. P. Wang, B. N. Chiang and M. S. Chang (1994). "Sustained atrial tachycardia in adult patients. Electrophysiological characteristics, pharmacological response, possible mechanisms, and effects of radiofrequency ablation." Circulation **90**(3): 1262-1278.

Chen, Z., M. Sohal, T. Voigt, E. Sammut, C. Tobon-Gomez, N. Child, T. Jackson, A. Shetty, J. Bostock, M. Cooklin, M. O'Neill, M. Wright, F. Murgatroyd, J. Gill, G. Carr-White, A. Chiribiri, T. Schaeffter, R. Razavi and C. A. Rinaldi (2015). "Myocardial tissue characterization by cardiac magnetic resonance imaging using T1 mapping predicts ventricular arrhythmia in ischemic and non–ischemic cardiomyopathy patients with implantable cardioverter-defibrillators." Heart Rhythm **12**(4): 792-801.

Cheung, C. C., G. Mellor, M. W. Deyell, B. Ensam, V. Batchvarov, M. Papadakis, J. D. Roberts, R. Leather, S. Sanatani, J. S. Healey, V. S. Chauhan, D. H. Birnie, J. Champagne, P. Angaran, G. J. Klein, R. Yee, C. S. Simpson, M. Talajic, M. Gardner, J. A. Yeung-Lai-Wah, S. Chakrabarti, Z. W. Laksman, S. Sharma, E. R. Behr and A. D. Krahn (2019). "Comparison of Ajmaline and Procainamide Provocation Tests in the Diagnosis of Brugada Syndrome." JACC: Clinical Electrophysiology **5**(4): 504-512.

Chowdhury, M. Z. I. and T. C. Turin (2020). "Variable selection strategies and its importance in clinical prediction modelling." Family Medicine and Community Health **8**(1): e000262.

Cireşan, D., U. Meier, J. Masci and J. Schmidhuber (2012). "Multi-column deep neural network for traffic sign classification." Neural Netw **32**: 333-338.

Cluitmans, M., D. H. Brooks, R. MacLeod, O. Dössel, M. S. Guillem, P. M. van Dam, J. Svehlikova, B. He, J. Sapp, L. Wang and L. Bear (2018). "Validation and Opportunities of Electrocardiographic Imaging: From Technical Achievements to Clinical Applications." Frontiers in Physiology **9**(1305).

Cluitmans, M. J. M., P. Bonizzi, J. M. H. Karel, M. Das, B. L. J. H. Kietselaer, M. M. J. de Jong, F. W. Prinzen, R. L. M. Peeters, R. L. Westra and P. G. A. Volders (2017). "In Vivo Validation of Electrocardiographic Imaging." JACC: Clinical Electrophysiology **3**(3): 232-242.

Cole, C. R., E. H. Blackstone, F. J. Pashkow, C. E. Snader and M. S. Lauer (1999). "Heart-Rate Recovery Immediately after Exercise as a Predictor of Mortality." New England Journal of Medicine **341**(18): 1351-1357.

Conte, G., J. Sieira, G. Ciconte, C. de Asmundis, G. B. Chierchia, G. Baltogiannis, G. Di Giovanni, M. La Meir, F. Wellens, J. Czapla, K. Wauters, M. Levinstein, Y. Saitoh, G. Irfan, J. Julia, G. Pappaert and P. Brugada (2015). "Implantable cardioverter-defibrillator therapy in Brugada syndrome: a 20-year single-center experience." J Am Coll Cardiol **65**(9): 879-888.

Conte, G., J. Sieira, A. Sarkozy, C. de Asmundis, G. Di Giovanni, G. B. Chierchia, G. Ciconte, M. Levinstein, R. Casado-Arroyo, G. Baltogiannis, J. Saenen, Y. Saitoh, G. Pappaert and P. Brugada (2013). "Life-threatening ventricular arrhythmias during ajmaline challenge in patients with Brugada syndrome: incidence, clinical features, and prognosis." Heart Rhythm **10**(12): 1869-1874.

Coronel, R., A. Baartscheer, J. M. E. Rademaker, J. T. Vermeulen and J. M. T. de Bakker (2001). The Arrhythmogenic Substrate in Ischemic and Non-ischemic Cardiomyopathies. Progress in Catheter Ablation: Clinical Application of New Mapping and Ablation Technology. L. B. Liem and E. Downar. Dordrecht, Springer Netherlands**:** 3-11.

Coumel, P. (1987). "The management of clinical arrhythmias. An overview on invasive versus non-invasive electrophysiology." Eur Heart J **8**(2): 92-99.

Cuculich, P. S., M. R. Schill, R. Kashani, S. Mutic, A. Lang, D. Cooper, M. Faddis, M. Gleva, A. Noheria, T. W. Smith, D. Hallahan, Y. Rudy and C. G. Robinson (2017). "Noninvasive Cardiac Radiation for Ablation of Ventricular Tachycardia." New England Journal of Medicine **377**(24): 2325-2336.

Cuculich, P. S., J. Zhang, Y. Wang, K. A. Desouza, R. Vijayakumar, P. K. Woodard and Y. Rudy (2011). "The electrophysiological cardiac ventricular substrate in patients after myocardial infarction: noninvasive characterization with electrocardiographic imaging." J Am Coll Cardiol **58**(18): 1893-1902.

de Bakker, J. M., F. J. van Capelle, M. J. Janse, S. Tasseron, J. T. Vermeulen, N. de Jonge and J. R. Lahpor (1993). "Slow conduction in the infarcted human heart. 'Zigzag' course of activation." Circulation **88**(3): 915-926.

Dekker, L. R., C. R. Bezzina, J. P. Henriques, M. W. Tanck, K. T. Koch, M. W. Alings, A. E. Arnold, M. J. de Boer, A. P. Gorgels, H. R. Michels, A. Verkerk, F. W. Verheugt, F. Zijlstra and A. A. Wilde (2006). "Familial sudden death is an important risk factor for primary ventricular fibrillation: a case-control study in acute myocardial infarction patients." Circulation **114**(11): 1140-1145.

Delise, P., G. Allocca, E. Marras, C. Giustetto, F. Gaita, L. Sciarra, L. Calo, A. Proclemer, M. Marziali, L. Rebellato, G. Berton, L. Coro and N. Sitta (2011). "Risk stratification in individuals with the Brugada type 1 ECG pattern without previous cardiac arrest: usefulness of a combined clinical and electrophysiologic approach." European heart journal **32**(2): 169-176.

Dereci, A., S. C. Yap and A. F. L. Schinkel (2019). "Meta-Analysis of Clinical Outcome After Implantable Cardioverter-Defibrillator Implantation in Patients With Brugada Syndrome." JACC Clin Electrophysiol **5**(2): 141-148.

Doi, Y. L., W. J. McKenna, S. Chetty, C. M. Oakley and J. F. Goodwin (1980). "Prediction of mortality and serious ventricular arrhythmia in hypertrophic cardiomyopathy. An echocardiographic study." Br Heart J **44**(2): 150-157.

Duchateau, J., F. Sacher, T. Pambrun, N. Derval, J. Chamorro-Servent, A. Denis, S. Ploux, M. Hocini, P. Jaïs, O. Bernus, M. Haïssaguerre and R. Dubois (2019). "Performance and limitations of noninvasive cardiac activation mapping." Heart Rhythm **16**(3): 435-442.

Ebrahimi, Z., M. Loni, M. Daneshtalab and A. Gharehbaghi (2020). "A review on deep learning methods for ECG arrhythmia classification." Expert Systems with Applications: X **7**: 100033.

Eggensperger, K., M. Lindauer and F. Hutter (2019). "Pitfalls and best practices in algorithm configuration." Journal of Artificial Intelligence Research **64**: 861-893.

Eisner, D. A., J. L. Caldwell, K. Kistamás and A. W. Trafford (2017). "Calcium and Excitation-Contraction Coupling in the Heart." Circulation Research **121**(2): 181-195.

Elliott, P. M., J. Poloniecki, S. Dickie, S. Sharma, L. Monserrat, A. Varnava, N. G. Mahon and W. J. McKenna (2000). "Sudden death in hypertrophic cardiomyopathy: identification of high risk patients." J Am Coll Cardiol **36**(7): 2212-2218.

Fan, F., J. Xiong and G. Wang (2020). "On interpretability of artificial neural networks." arXiv preprint arXiv:2001.02522.

Fenoglio, J. J., Jr., T. D. Pham, A. H. Harken, L. N. Horowitz, M. E. Josephson and A. L. Wit (1983). "Recurrent sustained ventricular tachycardia: structure and ultrastructure of subendocardial regions in which tachycardia originates." Circulation **68**(3): 518-533.

Ferrick, K. J., J. Luce, S. Miller, A. D. Mercando, S. G. Kim, J. A. Roth and J. D. Fisher (1992). "Reproducibility of electrophysiologic testing during antiarrhythmic therapy for ventricular arrhythmias secondary to coronary artery disease." Am J Cardiol **69**(16): 1296-1299.

Ferrick, K. J., M. Maher, J. A. Roth, S. G. Kim and J. D. Fisher (1995). "Reproducibility of electrophysiological testing during antiarrhythmic therapy for ventricular arrhythmias unrelated to coronary artery disease." Pacing Clin Electrophysiol **18**(7): 1395-1400.

Fink, M., P. J. Noble and D. Noble (2011). "Ca^{2+}-induced delayed afterdepolarizations are triggered by dyadic subspace $Ca2^{2+}$ affirming that increasing SERCA reduces aftercontractions." American journal of physiology. Heart and circulatory physiology **301**(3): H921-H935.

Fisher F, D. and A. Tyroler Herman (1973). "Relationship between Ventricular Premature Contractions on Routine Electrocardiography and Subsequent Sudden Death from Coronary Heart Disease." Circulation **47**(4): 712-719.

Fleg, J. L. and H. L. Kennedy (1992). "Long-term prognostic significance of ambulatory electrocardiographic findings in apparently healthy subjects greater than or equal to 60 years of age." Am J Cardiol **70**(7): 748-751.

Franz, M. R., J. Schaefer, M. Schöttler, W. A. Seed and M. I. Noble (1983). "Electrical and mechanical restitution of the human heart at different rates of stimulation." Circ Res **53**(6): 815-822.

From, A. M., J. J. Maleszewski and C. S. Rihal (2011). Current status of endomyocardial biopsy. Mayo Clinic Proceedings, Elsevier.

Fronza, M., C. Raineri, A. Valentini, E. M. Bassi, L. Scelsi, M. L. Buscemi, A. Turco, G. Castelli, S. Ghio and L. O. Visconti (2016). "Relationship between electrocardiographic findings and Cardiac Magnetic Resonance phenotypes in patients with Hypertrophic Cardiomyopathy." Int J Cardiol Heart Vasc **11**: 7-11.

Fye, W. B. (1999). "Rudolf albert von koelliker." Clinical cardiology **22**(5): 376.

Gao, Z., T. P. Rasmussen, Y. Li, W. Kutschke, O. M. Koval, Y. Wu, Y. Wu, D. D. Hall, M.-l. A. Joiner, X.-Q. Wu, P. D. Swaminathan, A. Purohit, K. Zimmerman, R. M. Weiss, K. D. Philipson, L.-s. Song, T. J. Hund and M. E. Anderson (2013). "Genetic inhibition of Na+-Ca2+ exchanger current disables fight or flight sinoatrial node activity without affecting resting heart rate." Circulation research **112**(2): 309-317.

Garcia-Dorado, D., M. Ruiz-Meana, J. Inserte, A. Rodriguez-Sinovas and H. M. Piper (2012). "Calcium-mediated cell death during myocardial reperfusion." Cardiovascular Research **94**(2): 168-180.

Gasparini, M., A. Proclemer, C. Klersy, A. Kloppe, M. Lunati, J. B. M. Ferrer, A. Hersi, M. Gulaj, M. C. E. F. Wijfels, E. Santi, L. Manotta and A. Arenal (2013). "Effect of Long-Detection Interval vs Standard-Detection Interval for Implantable Cardioverter-Defibrillators on Antitachycardia Pacing and Shock Delivery: The ADVANCE III Randomized Clinical Trial." JAMA **309**(18): 1903-1911.

Ghasemzadeh, N. and A. M. Zafari (2011). "A Brief Journey into the History of the Arterial Pulse." Cardiology Research and Practice **2011**: 164832.

Ghosh, S., E. K. Rhee, J. N. Avari, P. K. Woodard and Y. Rudy (2008). "Cardiac memory in patients with Wolff-Parkinson-White syndrome: noninvasive imaging of activation and repolarization before and after catheter ablation." Circulation **118**(9): 907-915.

Giavarina, D. (2015). "Understanding Bland Altman analysis." Biochemia medica **25**(2): 141-151.

Gibbons Raymond, J., J. Balady Gary, W. Beasley John, F. null, J. T. Bricker, F. C. Duvernoy Wolf, F. Froelicher Victor, B. Mark Daniel, H. Marwick Thomas, D. McCallister Ben, D. Thompson Paul, F. null, L. Winters William and G. Yanowitz Frank (1997). "ACC/AHA Guidelines for Exercise Testing: Executive Summary." Circulation **96**(1): 345-354.

Gradel, C., D. Jain, W. P. Batsford, F. J. Wackers and B. L. Zaret (1997). "Relationship of scar and ischemia to the results of programmed electrophysiological stimulation in patients with coronary artery disease." J Nucl Cardiol **4**(5): 379-386.

Graham Adam, J., M. Orini, E. Zacur, G. Dhillon, H. Daw, T. Srinivasan Niel, D. Lane Jem, A. Cambridge, J. Garcia, J. O'Reilly Nanci, S. Whittaker-Axon, P. Taggart, M. Lowe, M. Finlay, J. Earley Mark, A. Chow, S. Sporton, M. Dhinoja, J. Schilling Richard, J. Hunter Ross and D. Lambiase Pier (2019). "Simultaneous Comparison of Electrocardiographic Imaging and Epicardial Contact Mapping in Structural Heart Disease." Circulation: Arrhythmia and Electrophysiology **12**(4): e007120.

Graham, A. J., M. Orini, E. Zacur, G. Dhillon, S. Van Duijvenboden, H. Daw, A. Cambridge, J. Garcia, R. Hunter, M. Dhinoja and P. D. Lambiase (2018). "42First simultaneous invasive validation of electrocardiographic imaging (ECGi) in intact human heart with epicardial mapping." EP Europace **20**(suppl_4): iv20-iv20.

Gray, B., J. Ingles, C. Medi and C. Semsarian (2013). "Prolongation of the QTc Interval Predicts Appropriate Implantable Cardioverter-Defibrillator Therapies in Hypertrophic Cardiomyopathy." JACC: Heart Failure **1**(2): 149-155.

Gray, B., C. Semsarian and R. W. Sy (2014). "Brugada Syndrome: A Heterogeneous Disease with a Common ECG Phenotype?" Journal of Cardiovascular Electrophysiology **25**(4): 450-456.

Haïssaguerre, M., F. Extramiana, M. Hocini, B. Cauchemez, P. Jaïs, J. A. Cabrera, G. Farre, A. Leenhardt, P. Sanders, C. Scavée, L.-F. Hsu, R. Weerasooriya, D. C. Shah, R. Frank, P. Maury, M. Delay, S. Garrigue and J. Clémenty (2003). "Mapping and Ablation of Ventricular Fibrillation Associated With Long-QT and Brugada Syndromes." Circulation **108**(8): 925-928.

Haïssaguerre, M., M. Hocini, G. Cheniti, J. Duchateau, F. Sacher, S. Puyo, H. Cochet, M. Takigawa, A. Denis, R. Martin, N. Derval, P. Bordachar, P. Ritter, S. Ploux, T. Pambrun, N. Klotz, G. Massoullié, X. Pillois, C. Dallet, J.-J. Schott, S. Scouarnec, J. Ackerman Michael, D. Tester, O. Piot, J.-L. Pasquié, C. Leclerc, J.-S. Hermida, E. Gandjbakhch, P. Maury, L. Labrousse, R. Coronel, P. Jais, D. Benoist, E. Vigmond, M. Potse, R. Walton, K. Nademanee, O. Bernus and R. Dubois (2018). "Localized Structural Alterations Underlying a Subset of Unexplained Sudden Cardiac Death." Circulation: Arrhythmia and Electrophysiology **11**(7): e006120.

Haissaguerre, M., D. C. Shah, P. Jais, M. Shoda, J. Kautzner, T. Arentz, D. Kalushe, A. Kadish, M. Griffith, F. Gaita, T. Yamane, S. Garrigue, M. Hocini and J. Clementy (2002). "Role of Purkinje conducting system in triggering of idiopathic ventricular fibrillation." Lancet **359**(9307): 677-678.

Haïssaguerre, M., M. Shoda, P. Jaïs, A. Nogami, C. Shah Dipen, J. Kautzner, T. Arentz, D. Kalushe, D. Lamaison, M. Griffith, F. Cruz, A. de Paola, F. Gaïta, M. Hocini, S. Garrigue, L. Macle, R. Weerasooriya and J. Clémenty (2002). "Mapping and Ablation of Idiopathic Ventricular Fibrillation." Circulation **106**(8): 962-967.

Hardarson, T., R. Curiel, C. S. De La Calzada and J. F. Goodwin (1973). "PROGNOSIS AND MORTALITY OF HYPERTROPHIC OBSTRUCTIVE CARDIOMYOPATHY." The Lancet **302**(7844): 1462-1467.

Hasdemir, C., S. Payzin, U. Kocabas, H. Sahin, N. Yildirim, A. Alp, M. Aydin, R. Pfeiffer, E. Burashnikov, Y. Wu and C. Antzelevitch (2015). "High prevalence of concealed Brugada syndrome in patients with atrioventricular nodal reentrant tachycardia." Heart Rhythm **12**(7): 1584-1594.

Haws, C. W. and R. L. Lux (1990). "Correlation between in vivo transmembrane action potential durations and activation-recovery intervals from electrograms. Effects of interventions that alter repolarization time." Circulation **81**(1): 281-288.

Hayashi, M., W. Shimizu and C. M. Albert (2015). "The spectrum of epidemiology underlying sudden cardiac death." Circulation research **116**(12): 1887-1906.

Hedley, P. L., P. Jørgensen, S. Schlamowitz, J. Moolman-Smook, J. K. Kanters, V. A. Corfield and M. Christiansen (2009). "The genetic basis of Brugada syndrome: A mutation update." Human Mutation **30**(9): 1256-1266.

Hernandez-Ojeda, J., E. Arbelo, R. Borras, P. Berne, J. M. Tolosana, A. Gomez-Juanatey, A. Berruezo, O. Campuzano, G. Sarquella-Brugada, L. Mont, R. Brugada and J. Brugada (2017). "Patients With Brugada Syndrome and Implanted Cardioverter-Defibrillators: Long-Term Follow-Up." J Am Coll Cardiol **70**(16): 1991-2002.

Hocini, M., A. J. Shah, T. Neumann, M. Kuniss, D. Erkapic, A. Chaumeil, S. J. Copley, P. B. Lim, P. Kanagaratnam, A. Denis, N. Derval, R. Dubois, H. Cochet, P. Jais and M. Haissaguerre (2015). "Focal Arrhythmia Ablation Determined by High-Resolution Noninvasive Maps: Multicenter Feasibility Study." J Cardiovasc Electrophysiol **26**(7): 754-760.

Hodges, D. C. and L. M. Schell (1988). "Power analysis in biological anthropology." American Journal of Physical Anthropology **77**(2): 175-181.

Hoenig, J. M. and D. M. Heisey (2001). "The Abuse of Power." The American Statistician **55**(1): 19-24.

Hoffman, B. F. and P. F. Cranefield (1964). "The physiological basis of cardiac arrhythmias." The American Journal of Medicine **37**(5): 670-684.

Honarbakhsh, S., R. Providencia and P. D. Lambiase (2018). "Risk Stratification in Brugada Syndrome: Current Status and Emerging Approaches." Arrhythmia & electrophysiology review **7**(2): 79-83.

Hosmer Jr, D. W., S. Lemeshow and R. X. Sturdivant (2013). Applied logistic regression, John Wiley & Sons.

Huang, H.-H., T. Xu and J. Yang (2014). "Comparing logistic regression, support vector machines, and permanental classification methods in predicting hypertension." BMC proceedings **8**(Suppl 1): S96-S96.

Huiskamp, G. and A. Van Oosterom (1988). "The depolarization sequence of the human heart surface computed from measured body surface potentials." IEEE Trans Biomed Eng **35**(12): 1047-1058.

Ideker, R. E., J. M. Rogers, V. Fast, L. Li, G. N. Kay and S. M. Pogwizd (2009). "Can mapping differentiate microreentry from a focus in the ventricle?" Heart rhythm **6**(11): 1666-1669.

Igarashi, M., A. Nogami, K. Kurosaki, Y. Hanaki, Y. Komatsu, S. Fukamizu, I. Morishima, K. Kaitani, S. Nishiuchi, A. K. Talib, T. Machino, K. Kuroki, H. Yamasaki, N. Murakoshi, Y. Sekiguchi, K. Kuga and K. Aonuma (2018). "Radiofrequency Catheter Ablation of Ventricular Tachycardia in Patients With Hypertrophic Cardiomyopathy and Apical Aneurysm." JACC: Clinical Electrophysiology **4**(3): 339-350.

Ikeda, T., H. Sakurada, K. Sakabe, T. Sakata, M. Takami, N. Tezuka, T. Nakae, M. Noro, Y. Enjoji, T. Tejima, K. Sugi and T. Yamaguchi (2001). "Assessment of noninvasive markers in identifying patients at risk in the Brugada syndrome: insight into risk stratification." J Am Coll Cardiol **37**(6): 1628-1634.

Issa, Z. F., J. M. Miller and D. P. Zipes (2009). CHAPTER 3 - Mapping and Navigation Modalities. Clinical Arrhythmology and Electrophysiology. Z. F. Issa, J. M. Miller and D. P. Zipes. Philadelphia, W.B. Saunders**:** 57-99.

Jabbari, R., T. Engstrøm, C. Glinge, B. Risgaard, J. Jabbari, B. G. Winkel, C. J. Terkelsen, H. H. Tilsted, L. O. Jensen, M. Hougaard, S. E. Chiuve, F. Pedersen, J. H. Svendsen, S. Haunsø, C. M. Albert and J. Tfelt-Hansen (2015). "Incidence and risk factors of ventricular fibrillation before primary angioplasty in patients with first ST-elevation myocardial infarction: a nationwide study in Denmark." J Am Heart Assoc **4**(1): e001399.

Jakobsen, J. C., C. Gluud, J. Wetterslev and P. Winkel (2017). "When and how should multiple imputation be used for handling missing data in randomised clinical trials – a practical guide with flowcharts." BMC Medical Research Methodology **17**(1): 162.

Jalanko, M., H. Väänänen, M. Tarkiainen, P. Sipola, P. Jääskeläinen, K. Lauerma, T. Laitinen, T. Laitinen, M. Laine, T. Heliö, J. Kuusisto and M. Viitasalo (2018). "Fibrosis and wall thickness affect ventricular repolarization dynamics in hypertrophic cardiomyopathy." Annals of Noninvasive Electrocardiology **23**(6): e12582.

James, G. a. (2013). An Introduction to Statistical Learning with Applications in R. D. a. Witten, T. a. Hastie and R. a. Tibshirani.

Jamil-Copley, S., R. Bokan, P. Kojodjojo, N. Qureshi, M. Koa-Wing, S. Hayat, A. Kyriacou, B. Sandler, A. Sohaib, I. Wright, D. W. Davies, Z. Whinnett, S. P. N, P. Kanagaratnam and P. B. Lim (2014). "Noninvasive electrocardiographic mapping to guide ablation of outflow tract ventricular arrhythmias." Heart Rhythm **11**(4): 587-594.

Janette Busby, M., E. A. Shefrin and J. L. Fleg (1989). "Prevalence and long-term significance of exercise-induced frequent or repetitive ventricular ectopic beats in apparently healthy volunteers." Journal of the American College of Cardiology **14**(7): 1659-1665.

Janse, M. J. and C. N. D'Alnoncourt (1987). "Reflections on reentry and focal activity." The American Journal of Cardiology **60**(11): 21-26.

Janse, M. J. and J. M. T. De Bakker (2001). "Arrhythmia substrate and management in hypertrophic cardiomyopathy: from molecules to implantable card ioverter-defibrillators." European Heart Journal Supplements **3**(suppl_L): L15-L20.

Jia, D., W. Zhao, Z. Li, J. Hu, C. Yan, H. Wang and T. You (2019). An Electrocardiogram Delineator via Deep Segmentation Network. 2019 41st Annual International Conference of the IEEE Engineering in Medicine and Biology Society (EMBC), IEEE.

Josephson, M. E. and E. Anter (2015). "Substrate Mapping for Ventricular Tachycardia: Assumptions and Misconceptions." JACC Clin Electrophysiol **1**(5): 341-352.

Kaggle (2019). "Kaggle's State of Data Science and Machine Learning 2019: Enterprise Executive Summary."

Kalyakulina, A. I., I. I. Yusipov, V. A. Moskalenko, A. V. Nikolskiy, A. A. Kozlov, K. A. Kosonogov, N. Y. Zolotykh and M. V. Ivanchenko (2018). "LU electrocardiography database: a new open-access validation tool for delineation algorithms." arXiv preprint arXiv:1809.03393.

Kaplinsky, E., J. H. Yahini and H. N. Neufeld (1972). "On the mechanism of sustained ventricular arrhythmias associated with acute myocardial infarction1." Cardiovascular Research **6**(2): 135-142.

Karagueuzian, H. S. (2004). "Ventricular fibrillation: an organized delirium or uncoordinated reason?" Heart rhythm **1**(1): 24-26.

Katzung, B. G. (1975). "Effects of extracellular calcium and sodium on depolarization-induced automaticity in guinea pig papillary muscle." Circulation Research **37**(1): 118-127.

Kher, R. (2019). "Signal Processing Techniques for Removing Noise from ECG signals." Journal of Biomedical Engineering and Research **1**: 1-9.

Kienzle, M. G., J. Miller, R. A. Falcone, A. Harken and M. E. Josephson (1984). "Intraoperative endocardial mapping during sinus rhythm: relationship to site of origin of ventricular tachycardia." Circulation **70**(6): 957-965.

Kim, J.-H. (2009). "Estimating classification error rate: Repeated cross-validation, repeated hold-out and bootstrap." Computational statistics & data analysis **53**(11): 3735-3745.

Knecht, S., F. Sacher, M. Wright, M. Hocini, A. Nogami, T. Arentz, B. Petit, R. Franck, C. De Chillou, D. Lamaison, J. Farré, T. Lavergne, T. Verbeet, I. Nault, S. Matsuo, L. Leroux, R. Weerasooriya, B. Cauchemez, N. Lellouche, N. Derval, S. M. Narayan, P. Jaïs, J. Clementy and M. Haïssaguerre (2009). "Long-Term Follow-Up of Idiopathic Ventricular Fibrillation Ablation: A Multicenter Study." Journal of the American College of Cardiology **54**(6): 522-528.

Kohavi, R. (1995). A study of cross-validation and bootstrap for accuracy estimation and model selection. Ijcai, Montreal, Canada.

Kostis, J. B., K. McCrone, A. E. Moreyra, S. Gotzoyannis, N. M. Aglitz, N. Natarajan and P. T. Kuo (1981). "Premature ventricular complexes in the absence of identifiable heart disease." Circulation **63**(6): 1351-1356.

Kulkarni, K., F. M. Merchant, M. B. Kassab, F. Sana, K. Moazzami, O. Sayadi, J. P. Singh, E. K. Heist and A. A. Armoundas (2019). "Cardiac Alternans: Mechanisms and Clinical Utility in Arrhythmia Prevention." Journal of the American Heart Association **8**(21): e013750.

Kurita, T., W. Shimizu, M. Inagaki, K. Suyama, A. Taguchi, K. Satomi, N. Aihara, S. Kamakura, J. Kobayashi and Y. Kosakai (2002). "The electrophysiologic mechanism of ST-segment elevation in Brugada syndrome." J Am Coll Cardiol **40**(2): 330-334.

Lakatta, E. G. and D. DiFrancesco (2009). "What keeps us ticking: a funny current, a calcium clock, or both?" Journal of molecular and cellular cardiology **47**(2): 157-170.

Leong, K. M. W., J.-J. Chow, F. S. Ng, E. Falaschetti, N. Qureshi, M. Koa-Wing, N. W. F. Linton, Z. I. Whinnett, D. C. Lefroy, D. W. Davies, P. B. Lim, N. S. Peters, P. Kanagaratnam and A. M. Varnava (2018). "Comparison of the Prognostic Usefulness of the European Society of Cardiology and American Heart Association/American College of Cardiology Foundation Risk Stratification Systems for Patients With Hypertrophic Cardiomyopathy." The American journal of cardiology **121**(3): 349-355.

Leong, K. M. W., F. S. Ng, S. Jones, J.-J. Chow, N. Qureshi, M. Koa-Wing, N. W. F. Linton, Z. I. Whinnett, D. C. Lefroy, D. W. Davies, P. B. Lim, N. S. Peters, P. Kanagaratnam and A. M. Varnava (2019). "Prevalence of spontaneous type I ECG pattern, syncope, and other risk markers in sudden cardiac arrest survivors with Brugada syndrome." Pacing and Clinical Electrophysiology **42**(2): 257-264.

Leong, K. M. W., F. S. Ng, S. Jones, J. J. Chow, N. Qureshi, M. Koa-Wing, N. W. F. Linton, Z. I. Whinnett, D. C. Lefroy, D. W. Davies, P. B. Lim, N. S. Peters, P. Kanagaratnam and A. M. Varnava (2019). "Prevalence of spontaneous type I ECG pattern, syncope, and other risk markers in sudden cardiac arrest survivors with Brugada syndrome." Pacing Clin Electrophysiol **42**(2): 257-264.

Leong, K. M. W., F. S. Ng, C. Roney, C. Cantwell, M. J. Shun-Shin, N. W. F. Linton, Z. I. Whinnett, D. C. Lefroy, D. W. Davies, S. E. Harding, P. B. Lim, D. Francis, N. S. Peters, A. M. Varnava and P. Kanagaratnam (2018). "Repolarization abnormalities unmasked with exercise in sudden cardiac death survivors with structurally normal hearts." J Cardiovasc Electrophysiol **29**(1): 115-126.

Leong, K. M. W., F. S. Ng, M. J. Shun-Shin, M. Koa-Wing, N. Qureshi, Z. I. Whinnett, N. F. Linton, D. Lefroy, D. P. Francis, S. E. Harding, D. W. Davies, N. S. Peter, P. B. Lim, E. Behr, P. D. Lambiase, A. Varnava and P. Kanagaratnam (2020). "Non-invasive detection of exercise-induced cardiac conduction abnormalities in sudden cardiac death survivors in the inherited cardiac conditions." EP Europace.

Leoni, A. L., B. Gavillet, J. S. Rougier, C. Marionneau, V. Probst, S. Le Scouarnec, J. J. Schott, S. Demolombe, P. Bruneval, C. L. Huang, W. H. Colledge, A. A. Grace, H. Le Marec, A. A. Wilde, P. J. Mohler, D. Escande, H. Abriel and F. Charpentier (2010). "Variable Na(v)1.5 protein expression from the wild-type allele correlates with the penetrance of cardiac conduction disease in the Scn5a(+/-) mouse model." PLoS One **5**(2): e9298.

Levine, M. and M. H. H. Ensom (2001). "Post Hoc Power Analysis: An Idea Whose Time Has Passed?" Pharmacotherapy: The Journal of Human Pharmacology and Drug Therapy **21**(4): 405-409.

Li, G. R., C. P. Lau, A. Ducharme, J. C. Tardif and S. Nattel (2002). "Transmural action potential and ionic current remodeling in ventricles of failing canine hearts." Am J Physiol Heart Circ Physiol **283**(3): H1031-1041.

Li, Z. and Q. Yang (2018). "Systems and synthetic biology approaches in understanding biological oscillators." Quantitative biology (Beijing, China) **6**(1): 1-14.

Link, M. S. (2012). "Commotio cordis: ventricular fibrillation triggered by chest impact-induced abnormalities in repolarization." Circ Arrhythm Electrophysiol **5**(2): 425-432.

Lip, G. Y., R. Nieuwlaat, R. Pisters, D. A. Lane and H. J. Crijns (2010). "Refining clinical risk stratification for predicting stroke and thromboembolism in atrial fibrillation using a novel risk factor-based approach: the euro heart survey on atrial fibrillation." Chest **137**(2): 263-272.

Lyon, A. R., A. Bueno-Orovio, Z. E, A. R, G. V, S. Neubauer, H. Watkins, B. Rodriguez and A. Minchole (2018). "ECG phenotypes in hypertrophic cardiomyopathy caused by distinct mechanisms: apico-basal repolarization gradients versus Purkinje-myocardial coupling abnormalities. Insights from a high-performance simulation study informed by cardiac magnetic resonance." under review with minor corrections at Europace.

MacLeod, K. T., S. B. Marston, P. A. Poole-Wilson, N. J. Severs and P. H. Sugden (2015). Oxford Textbook of Medicine. Cardiac myocytes and the cardiac action potential, Oxford University Press.

Makimoto, H., E. Nakagawa, H. Takaki, Y. Yamada, H. Okamura, T. Noda, K. Satomi, K. Suyama, N. Aihara, T. Kurita, S. Kamakura and W. Shimizu (2010). "Augmented ST-segment elevation during recovery from exercise predicts cardiac events in patients with Brugada syndrome." J Am Coll Cardiol **56**(19): 1576-1584.

Marban, E., S. W. Robinson and W. G. Wier (1986). "Mechanisms of arrhythmogenic delayed and early afterdepolarizations in ferret ventricular muscle." J Clin Invest **78**(5): 1185-1192.

Margey, R., A. Roy, S. Tobin, C. J. O'Keane, C. McGorrian, V. Morris, S. Jennings and J. Galvin (2011). "Sudden cardiac death in 14- to 35-year olds in Ireland from 2005 to 2007: a retrospective registry." Europace **13**(10): 1411-1418.

Marks, A. R. (2013). "Calcium cycling proteins and heart failure: mechanisms and therapeutics." The Journal of clinical investigation **123**(1): 46-52.

Maroco, J., D. Silva, A. Rodrigues, M. Guerreiro, I. Santana and A. de Mendonça (2011). "Data mining methods in the prediction of Dementia: A real-data comparison of the accuracy, sensitivity and specificity of linear discriminant analysis, logistic regression, neural networks, support vector machines, classification trees and random forests." BMC Research Notes **4**(1): 299.

Maron, B. J., S. A. Casey, R. H. Chan, R. F. Garberich, E. J. Rowin and M. S. Maron (2015). "Independent Assessment of the European Society of Cardiology Sudden Death Risk Model for Hypertrophic Cardiomyopathy." Am J Cardiol **116**(5): 757-764.

Maron, B. J., J. M. Gardin, J. M. Flack, S. S. Gidding, T. T. Kurosaki and D. E. Bild (1995). "Prevalence of hypertrophic cardiomyopathy in a general population of young adults. Echocardiographic analysis of 4111 subjects in the CARDIA Study. Coronary Artery Risk Development in (Young) Adults." Circulation **92**(4): 785-789.

Marsiglia, J. D. C. and A. C. Pereira (2014). "Hypertrophic cardiomyopathy: how do mutations lead to disease?" Arquivos brasileiros de cardiologia **102**(3): 295-304.

Mason, C. H. and W. D. Perreault (1991). "Collinearity, Power, and Interpretation of Multiple Regression Analysis." Journal of Marketing Research **28**(3): 268-280.

Masrur, S., S. Memon and P. D. Thompson (2015). "Brugada syndrome, exercise, and exercise testing." Clin Cardiol **38**(5): 323-326.

McKenna, W., J. Deanfield, A. Faruqui, D. England, C. Oakley and J. Goodwin (1981). "Prognosis in hypertrophic cardiomyopathy: Role of age and clinical, electrocardiographic and hemodynamic features." American Journal of Cardiology **47**(3): 532-538.

McKenna, W. J., D. England, Y. L. Doi, J. E. Deanfield, C. Oakley and J. F. Goodwin (1981). "Arrhythmia in hypertrophic cardiomyopathy. I: Influence on prognosis." Br Heart J **46**(2): 168-172.

Mellor, G. J., L. J. Blom, S. A. Groeneveld, B. G. Winkel, B. Ensam, J. Bargehr, B. van Rees, C. Scrocco, I. P. C. Krapels, P. G. A. Volders, J. Tfelt-Hansen, A. D. Krahn, R. J. Hassink and E. R. Behr (2021). "Familial Evaluation in Idiopathic Ventricular Fibrillation: Diagnostic Yield and Significance of J Wave Syndromes." Circ Arrhythm Electrophysiol **14**(3): e009089.

Meregalli, P. G., A. A. M. Wilde and H. L. Tan (2005). "Pathophysiological mechanisms of Brugada syndrome: Depolarization disorder, repolarization disorder, or more?" Cardiovascular Research **67**(3): 367-378.

Mines, G. R. (1913). "On dynamic equilibrium in the heart." J Physiol **46**(4-5): 349-383.

Mitropoulos, A., A. Gumber, H. Crank and M. Klonizakis (2017). "Validation of an Arm Crank Ergometer Test for Use in Sedentary Adults." Journal of sports science & medicine **16**(4): 558-564.

Miura, M., N. Ishide, H. Oda, M. Sakurai, T. Shinozaki and T. Takishima (1993). "Spatial features of calcium transients during early and delayed afterdepolarizations." Am J Physiol **265**(2 Pt 2): H439-444.

Mizusawa, Y. and A. A. Wilde (2012). "Brugada syndrome." Circ Arrhythm Electrophysiol **5**(3): 606-616.

Monserrat, L., P. M. Elliott, J. R. Gimeno, S. Sharma, M. Penas-Lado and W. J. McKenna (2003). "Non-sustained ventricular tachycardia in hypertrophic cardiomyopathy." an independent marker of sudden death risk in young patients **42**(5): 873-879.

Moss, A. J., H. T. Davis, J. DeCamilla and L. W. Bayer (1979). "Ventricular ectopic beats and their relation to sudden and nonsudden cardiac death after myocardial infarction." Circulation **60**(5): 998-1003.

Mukharji, J., R. E. Rude, W. K. Poole, N. Gustafson, L. J. Thomas, Jr., H. W. Strauss, A. S. Jaffe, J. E. Muller, R. Roberts, D. S. Raabe, Jr. and et al. (1984). "Risk factors for sudden death after acute myocardial infarction: two-year follow-up." Am J Cardiol **54**(1): 31-36.

Mustafa, A., A. Rienow, I. Saadi, M. Cools and J. Teller (2018). "Comparing support vector machines with logistic regression for calibrating cellular automata land use change models." European Journal of Remote Sensing **51**(1): 391-401.

Myles, R. C., O. Bernus, F. L. Burton, S. M. Cobbe and G. L. Smith (2010). "Effect of activation sequence on transmural patterns of repolarization and action potential duration in rabbit ventricular myocardium." Am J Physiol Heart Circ Physiol **299**(6): H1812-1822.

Nademanee, K., G. Veerakul, P. Chandanamattha, L. Chaothawee, A. Ariyachaipanich, K. Jirasirirojanakorn, K. Likittanasombat, K. Bhuripanyo and T. Ngarmukos (2011). "Prevention of

ventricular fibrillation episodes in Brugada syndrome by catheter ablation over the anterior right ventricular outflow tract epicardium." Circulation **123**(12): 1270-1279.

Nagase, S., K. F. Kusano, H. Morita, Y. Fujimoto, M. Kakishita, K. Nakamura, T. Emori, H. Matsubara and T. Ohe (2002). "Epicardial electrogram of the right ventricular outflow tract in patients with the Brugada syndrome: using the epicardial lead." J Am Coll Cardiol **39**(12): 1992-1995.

Ng, G. A. (2006). "Treating patients with ventricular ectopic beats." Heart (British Cardiac Society) **92**(11): 1707-1712.

Nordin, C., E. Gilat and R. S. Aronson (1985). "Delayed afterdepolarizations and triggered activity in ventricular muscle from rats with streptozotocin-induced diabetes." Circ Res **57**(1): 28-34.

O'Mahony, C., P. Elliott and W. McKenna (2013). "Sudden cardiac death in hypertrophic cardiomyopathy." Circ Arrhythm Electrophysiol **6**(2): 443-451.

O'Mahony, C., F. Jichi, M. Pavlou, L. Monserrat, A. Anastasakis, C. Rapezzi, E. Biagini, J. R. Gimeno, G. Limongelli, W. J. McKenna, R. Z. Omar, P. M. Elliott and I. Hypertrophic Cardiomyopathy Outcomes (2014). "A novel clinical risk prediction model for sudden cardiac death in hypertrophic cardiomyopathy (HCM risk-SCD)." Eur Heart J **35**(30): 2010-2020.

Olde Nordkamp, L. R., A. S. Vink, A. A. Wilde, F. J. de Lange, J. S. de Jong, W. Wieling, N. van Dijk and H. L. Tan (2015). "Syncope in Brugada syndrome: prevalence, clinical significance, and clues from history taking to distinguish arrhythmic from nonarrhythmic causes." Heart Rhythm **12**(2): 367-375.

Oliphant, T. E. (2007). "Python for Scientific Computing." Computing in Science & Engineering **9**(3): 10-20.

Oliveira, R. S., S. Alonso, F. O. Campos, B. M. Rocha, J. F. Fernandes, T. Kuehne and R. W. dos Santos (2018). "Ectopic beats arise from micro-reentries near infarct regions in simulations of a patient-specific heart model." Scientific Reports **8**(1): 16392.

Oosterhoff, P., L. G. Tereshchenko, M. A. van der Heyden, R. N. Ghanem, B. J. Fetics, R. D. Berger and M. A. Vos (2011). "Short-term variability of repolarization predicts ventricular tachycardia and sudden cardiac death in patients with structural heart disease: a comparison with QT variability index." Heart Rhythm **8**(10): 1584-1590.

Ozaydin, M., K. Moazzami, S. Kalantarian, H. Lee, M. Mansour and J. N. Ruskin (2015). "Long-Term Outcome of Patients With Idiopathic Ventricular Fibrillation: A Meta-Analysis." J Cardiovasc Electrophysiol **26**(10): 1095-1104.

Palazzuoli, A., M. Beltrami, L. Gennari, A. G. Dastidar, R. Nuti, E. McAlindon, G. D. Angelini and C. Bucciarelli-Ducci (2015). "The impact of infarct size on regional and global left ventricular systolic function: a cardiac magnetic resonance imaging study." Int J Cardiovasc Imaging **31**(5): 1037-1044.

Panesar, S. S., R. N. D'Souza, F.-C. Yeh and J. C. Fernandez-Miranda (2018). "Machine learning versus logistic regression methods for 2-year mortality prognostication in a small, heterogeneous glioma database." bioRxiv: 472555.

Pappone, C., J. Brugada, G. Vicedomini, G. Ciconte, F. Manguso, M. Saviano, R. Vitale, A. Cuko, L. Giannelli, Z. Calovic, M. Conti, P. Pozzi, A. Natalizia, S. Crisà, V. Borrelli, R. Brugada, G. Sarquella-Brugada, M. Guazzi, A. Frigiola, L. Menicanti and V. Santinelli (2017). "Electrical Substrate Elimination in 135 Consecutive Patients With Brugada Syndrome." Circ Arrhythm Electrophysiol **10**(5): e005053.

Paratz, E. D., L. Rowsell, D. Zentner, S. Parsons, N. Morgan, T. Thompson, P. James, A. Pflaumer, C. Semsarian, K. Smith, D. Stub and A. La Gerche (2020). "Cardiac arrest and sudden cardiac death registries: a systematic review of global coverage." Open Heart **7**(1): e001195.

Parisi, G. I., R. Kemker, J. L. Part, C. Kanan and S. Wermter (2019). "Continual lifelong learning with neural networks: A review." Neural Networks **113**: 54-71.

Passini, E., A. Minchole, R. Coppini, E. Cerbai, B. Rodriguez, S. Severi and A. Bueno-Orovio (2016). "Mechanisms of pro-arrhythmic abnormalities in ventricular repolarisation and anti-arrhythmic therapies in human hypertrophic cardiomyopathy." J Mol Cell Cardiol **96**: 72-81.

Perelshtein Brezinov, O., R. Klempfner, S. B. Zekry, I. Goldenberg and R. Kuperstein (2017). "Prognostic value of ejection fraction in patients admitted with acute coronary syndrome: A real world study." Medicine (Baltimore) **96**(9): e6226.

Perez-Alday, E. A., K. T. Haq, D. M. German, C. Hamilton, K. Johnson, F. Phan, N. M. Rogovoy, K. Yang, A. Wirth, J. A. Thomas, K. Dalouk, C. Fuss, M. Ferencik, S. Heitner and L. G. Tereshchenko (2020). "Mechanisms of Arrhythmogenicity in Hypertrophic Cardiomyopathy: Insight From Non-invasive Electrocardiographic Imaging." Frontiers in physiology **11**: 344-344.

Pick, A. (1953). "Parasystole." Circulation **8**(2): 243-252.

Pieroni, M., P. Notarstefano, A. Oliva, O. Campuzano, P. Santangeli, M. Coll, M. Nesti, A. Carnevali, A. Fraticelli, A. Iglesias, S. Grassi, R. Brugada and L. Bolognese (2018). "Electroanatomic and Pathologic Right Ventricular Outflow Tract Abnormalities in Patients With Brugada Syndrome." Journal of the American College of Cardiology **72**(22): 2747.

Pochet, N. and J. Suykens (2006). "Support vector machines versus logistic regression: improving prospective performance in clinical decision-making." Ultrasound in Obstetrics and Gynecology: The Official Journal of the International Society of Ultrasound in Obstetrics and Gynecology **27**(6): 607-608.

Pogwizd, S. M. and P. B. Corr (1987). "Reentrant and nonreentrant mechanisms contribute to arrhythmogenesis during early myocardial ischemia: results using three-dimensional mapping." Circulation research **61**(3): 352-371.

Priori, S. G., C. Blomstrom-Lundqvist, A. Mazzanti, N. Blom, M. Borggrefe, J. Camm, P. M. Elliott, D. Fitzsimons, R. Hatala, G. Hindricks, P. Kirchhof, K. Kjeldsen, K. H. Kuck, A. Hernandez-Madrid, N. Nikolaou, T. M. Norekval, C. Spaulding, D. J. Van Veldhuisen and E. S. C. S. D. Group (2015). "2015 ESC Guidelines for the management of patients with ventricular arrhythmias and the prevention of sudden cardiac death: The Task Force for the Management of Patients with Ventricular Arrhythmias and the Prevention of Sudden Cardiac Death of the European Society of Cardiology (ESC). Endorsed by: Association for European Paediatric and Congenital Cardiology (AEPC)." Eur Heart J **36**(41): 2793-2867.

Priori, S. G., M. Gasparini, C. Napolitano, P. Della Bella, A. G. Ottonelli, B. Sassone, U. Giordano, C. Pappone, G. Mascioli, G. Rossetti, R. De Nardis and M. Colombo (2012). "Risk stratification in Brugada syndrome: results of the PRELUDE (PRogrammed ELectrical stimUlation preDictive valuE) registry." J Am Coll Cardiol **59**(1): 37-45.

Priori, S. G., A. A. Wilde, M. Horie, Y. Cho, E. R. Behr, C. Berul, N. Blom, J. Brugada, C. E. Chiang, H. Huikuri, P. Kannankeril, A. Krahn, A. Leenhardt, A. Moss, P. J. Schwartz, W. Shimizu, G. Tomaselli and C. Tracy (2013). "Executive summary: HRS/EHRA/APHRS expert consensus statement on the diagnosis and management of patients with inherited primary arrhythmia syndromes." Heart Rhythm **10**(12): e85-108.

Probst, V., J. B. Gourraud, S. Chatel, J. Mansourati, F. Sacher, D. Babuty, P. Mabo and H. Le Marec (2013). "Comparison between flecainide and ajmaline challenge in Brugada syndrome patients." European Heart Journal **34**(suppl_1).

Probst, V., C. Veltmann, L. Eckardt, P. G. Meregalli, F. Gaita, H. L. Tan, D. Babuty, F. Sacher, C. Giustetto, E. Schulze-Bahr, M. Borggrefe, M. Haissaguerre, P. Mabo, H. Le Marec, C. Wolpert and A. A. Wilde (2010). "Long-term prognosis of patients diagnosed with Brugada syndrome: Results from the FINGER Brugada Syndrome Registry." Circulation **121**(5): 635-643.

Proietti, R., J.-F. Roux, A. Verma, A. Alturki, M. L. Bernier and V. Essebag (2016). "A Historical Perspective on the Role of Functional Lines of Block in the Re-entrant Circuit of Ventricular Tachycardia." Pacing and Clinical Electrophysiology **39**(5): 490-496.

Pruszkowska-Skrzep, P., Z. Kalarus, B. Sredniawa, R. Lenarczyk, O. Kowalski, A. Musialik-Łydka, J. Stabryła-Deska, J. Prokopczuk and A. Sliwińska (2005). "Effectiveness of radiofrequency catheter ablation of right ventricular outflow tract tachycardia using the CARTO system." Kardiol Pol **62**(2): 138-144.

Raatikainen, M. P., D. O. Arnar, K. Zeppenfeld, J. L. Merino, F. Levya, G. Hindriks and K.-H. Kuck (2015). "Statistics on the use of cardiac electronic devices and electrophysiological procedures in the European Society of Cardiology countries: 2014 report from the European Heart Rhythm Association." Ep Europace **17**(suppl_1): i1-i75.

Raju, H., M. Papadakis, M. Govindan, R. Bastiaenen, N. Chandra, A. O'Sullivan, G. Baines, S. Sharma and E. R. Behr (2011). "Low prevalence of risk markers in cases of sudden death due to Brugada syndrome relevance to risk stratification in Brugada syndrome." J Am Coll Cardiol **57**(23): 2340-2345.

Ramanathan, C., R. N. Ghanem, P. Jia, K. Ryu and Y. Rudy (2004). "Noninvasive electrocardiographic imaging for cardiac electrophysiology and arrhythmia." Nat Med **10**(4): 422-428.

Ramanathan, C., P. Jia, R. Ghanem, D. Calvetti and Y. Rudy (2003). "Noninvasive electrocardiographic imaging (ECGI): application of the generalized minimal residual (GMRes) method." Annals of biomedical engineering **31**(8): 981-994.

Rijnierse, M. T., C. P. Allaart and P. Knaapen (2016). "Principles and techniques of imaging in identifying the substrate of ventricular arrhythmia." Journal of nuclear cardiology : official publication of the American Society of Nuclear Cardiology **23**(2): 218-234.

Rizas, K. D., W. Hamm, S. Kääb, G. Schmidt and A. Bauer (2016). "Periodic Repolarisation Dynamics: A Natural Probe of the Ventricular Response to Sympathetic Activation." Arrhythmia & electrophysiology review **5**(1): 31-36.

Roberts, R. and U. Sigwart (2005). "Current concepts of the pathogenesis and treatment of hypertrophic cardiomyopathy." Circulation **112**(2): 293-296.

Robinson, R. B. and S. A. Siegelbaum (2003). "Hyperpolarization-Activated Cation Currents: From Molecules to Physiological Function." Annual Review of Physiology **65**(1): 453-480.

Rolf, S., H.-J. Bruns, T. Wichter, P. Kirchhof, M. Ribbing, K. Wasmer, M. Paul, G. Breithardt, W. Haverkamp and L. Eckardt (2003). "The ajmaline challenge in Brugada syndrome: Diagnostic impact, safety, and recommended protocol." European Heart Journal **24**(12): 1104-1112.

Rosner, B. and R. J. Glynn (2011). "Power and sample size estimation for the clustered wilcoxon test." Biometrics **67**(2): 646-653.

Rudy, Y. and B. D. Lindsay (2015). "Electrocardiographic imaging of heart rhythm disorders: from bench to bedside." Card Electrophysiol Clin **7**(1): 17-35.

Rudy, Y. and B. J. Messinger-Rapport (1988). "The inverse problem in electrocardiography: solutions in terms of epicardial potentials." Crit Rev Biomed Eng **16**(3): 215-268.

Sacher, F., V. Probst, P. Maury, D. Babuty, J. Mansourati, Y. Komatsu, C. Marquie, A. Rosa, A. Diallo, R. Cassagneau, C. Loizeau, R. Martins, M. E. Field, N. Derval, S. Miyazaki, A. Denis, A. Nogami, P. Ritter, J. B. Gourraud, S. Ploux, A. Rollin, A. Zemmoura, D. Lamaison, P. Bordachar, B. Pierre, P. Jais, J. L. Pasquie, M. Hocini, F. Legal, P. Defaye, S. Boveda, Y. Iesaka, P. Mabo and M. Haissaguerre (2013). "Outcome after implantation of a cardioverter-defibrillator in patients with Brugada syndrome: a multicenter study-part 2." Circulation **128**(16): 1739-1747.

Said, M., R. Becerra, J. Palomeque, G. Rinaldi, M. A. Kaetzel, P. L. Diaz-Sylvester, J. A. Copello, J. R. Dedman, C. Mundina-Weilenmann, L. Vittone and A. Mattiazzi (2008). "Increased intracellular Ca2+ and SR Ca2+ load contribute to arrhythmias after acidosis in rat heart. Role of Ca2+/calmodulin-dependent protein kinase II." Am J Physiol Heart Circ Physiol **295**(4): H1669-1683.

Saumarez, R. C., A. J. Camm, A. Panagos, J. S. Gill, J. T. Stewart, M. A. de Belder, I. A. Simpson and W. J. McKenna (1992). "Ventricular fibrillation in hypertrophic cardiomyopathy is associated with increased fractionation of paced right ventricular electrograms." Circulation **86**(2): 467-474.

Saumarez, R. C., M. Pytkowski, M. Sterlinski, J. P. Bourke, J. R. Clague, S. M. Cobbe, D. T. Connelly, M. J. Griffith, P. P. McKeown, K. McLeod, J. M. Morgan, N. Sadoul, L. Chojnowska, C. L. Huang and A. A. Grace (2008). "Paced ventricular electrogram fractionation predicts sudden cardiac death in hypertrophic cardiomyopathy." Eur Heart J **29**(13): 1653-1661.

Savitzky, A. and M. J. E. Golay (1964). "Smoothing and Differentiation of Data by Simplified Least Squares Procedures." Analytical Chemistry **36**(8): 1627-1639.

Schumacher, B., F. H. Gietzen, H. Neuser, J. Schümmelfeder, M. Schneider, S. Kerber, R. Schimpf, C. Wolpert and M. Borggrefe (2005). "Electrophysiological characteristics of septal hypertrophy in

patients with hypertrophic obstructive cardiomyopathy and moderate to severe symptoms." Circulation **112**(14): 2096-2101.

Sen-Chowdhry, S. and W. J. McKenna (2008). "Non-invasive risk stratification in hypertrophic cardiomyopathy: don't throw out the baby with the bathwater." European Heart Journal **29**(13): 1600-1602.

Serinagaoglu Dogrusoz, Y., L. Bear, J. Bergquist, R. Dubois, W. Good, R. MacLeod, A. Rababah and J. Stoks (2019). Effects of Interpolation on the Inverse Problem of Electrocardiography.

Shenasa, M., G. Hindricks, D. J. Callans, J. M. Miller and M. E. Josephson (2019). Cardiac mapping, John Wiley & Sons.

Shimizu, W., T. Ohe, T. Kurita, H. Takaki, N. Aihara, S. Kamakura, M. Matsuhisa and K. Shimomura (1991). "Early afterdepolarizations induced by isoproterenol in patients with congenital long QT syndrome." Circulation **84**(5): 1915-1923.

Shun-Shin, M. J., K. M. W. Leong, F. S. Ng, N. W. F. Linton, Z. I. Whinnett, M. Koa-Wing, N. Qureshi, D. C. Lefroy, S. E. Harding, P. B. Lim, N. S. Peters, D. P. Francis, A. M. Varnava and P. Kanagaratnam (2019). "Ventricular conduction stability test: a method to identify and quantify changes in whole heart activation patterns during physiological stress." EP Europace.

Shun-Shin, M. J., S. L. Zheng, G. D. Cole, J. P. Howard, Z. I. Whinnett and D. P. Francis (2017). "Implantable cardioverter defibrillators for primary prevention of death in left ventricular dysfunction with and without ischaemic heart disease: a meta-analysis of 8567 patients in the 11 trials." Eur Heart J **38**(22): 1738-1746.

Sieira, J., G. Conte, G. Ciconte, G. B. Chierchia, R. Casado-Arroyo, G. Baltogiannis, G. Di Giovanni, Y. Saitoh, J. Julia, G. Mugnai, M. La Meir, F. Wellens, J. Czapla, G. Pappaert, C. de Asmundis and P. Brugada (2017). "A score model to predict risk of events in patients with Brugada Syndrome." Eur Heart J **38**(22): 1756-1763.

Silver, D., J. Schrittwieser, K. Simonyan, I. Antonoglou, A. Huang, A. Guez, T. Hubert, L. Baker, M. Lai, A. Bolton, Y. Chen, T. Lillicrap, F. Hui, L. Sifre, G. van den Driessche, T. Graepel and D. Hassabis (2017). "Mastering the game of Go without human knowledge." Nature **550**(7676): 354-359.

Snyder, J. P. (1997). Flattening the earth: two thousand years of map projections, University of Chicago Press.

Solomon, S. D., S. Zelenkofske, J. J. V. McMurray, P. V. Finn, E. Velazquez, G. Ertl, A. Harsanyi, J. L. Rouleau, A. Maggioni, L. Kober, H. White, F. Van de Werf, K. Pieper, R. M. Califf and M. A. Pfeffer (2005). "Sudden Death in Patients with Myocardial Infarction and Left Ventricular Dysfunction, Heart Failure, or Both." New England Journal of Medicine **352**(25): 2581-2588.

Stambler, B. S., G. Fenelon, R. K. Shepard, H. F. Clemo and C. M. Guiraudon (2003). "Characterization of sustained atrial tachycardia in dogs with rapid ventricular pacing-induced heart failure." J Cardiovasc Electrophysiol **14**(5): 499-507.

Steyerberg, E. W. and Y. Vergouwe (2014). "Towards better clinical prediction models: seven steps for development and an ABCD for validation." European heart journal **35**(29): 1925-1931.

Swoboda, P. P., A. K. McDiarmid, S. P. Page, J. P. Greenwood and S. Plein (2016). "Role of T1 Mapping in Inherited Cardiomyopathies." European cardiology **11**(2): 96-101.

Teare, D. (1958). "ASYMMETRICAL HYPERTROPHY OF THE HEART IN YOUNG ADULTS." British Heart Journal **20**(1): 1-8.

Tian, J., M. F. Smith, G. Ahmad, V. Dilsizian, A. Jimenez and T. Dickfeld (2012). "Integration of 3-dimensional scar models from SPECT to guide ventricular tachycardia ablation." J Nucl Med **53**(6): 894-901.

Tokioka, K., K. F. Kusano, H. Morita, D. Miura, N. Nishii, S. Nagase, K. Nakamura, K. Kohno, H. Ito and T. Ohe (2014). "Electrocardiographic parameters and fatal arrhythmic events in patients with Brugada syndrome: combination of depolarization and repolarization abnormalities." J Am Coll Cardiol **63**(20): 2131-2138.

Uretsky, B. F. and R. G. Sheahan (1997). "Primary prevention of sudden cardiac death in heart failure: will the solution be shocking?" J Am Coll Cardiol **30**(7): 1589-1597.

van Dam, P. M., T. F. Oostendorp, A. C. Linnenbank and A. van Oosterom (2009). "Non-invasive imaging of cardiac activation and recovery." Annals of biomedical engineering **37**(9): 1739-1756.

van Dam, P. M., R. Tung, K. Shivkumar and M. Laks (2013). "Quantitative localization of premature ventricular contractions using myocardial activation ECGI from the standard 12-lead electrocardiogram." Journal of Electrocardiology **46**(6): 574-579.

Van Steenkiste, G., G. van Loon and G. Crevecoeur (2020). "Transfer Learning in ECG Classification from Human to Horse Using a Novel Parallel Neural Network Architecture." Scientific Reports **10**(1): 186.

Varnava, A. (2018). Ajmaline Challenge Guidelines. I. C. H. N. Trust. ICHNT Intranet.

Varnava, A. M., P. M. Elliott, C. Baboonian, F. Davison, M. J. Davies and W. J. McKenna (2001). "Hypertrophic cardiomyopathy: histopathological features of sudden death in cardiac troponin T disease." Circulation **104**(12): 1380-1384.

Vassalle, M. and C. I. Lin (2004). "Calcium overload and cardiac function." J Biomed Sci **11**(5): 542-565.

Veerakul, G. and K. Nademanee (2016). "Will we be able to cure brugada syndrome?" Heart Rhythm **13**(11): 2159-2160.

Verkerk, A. O., M. W. Veldkamp, A. Baartscheer, C. A. Schumacher, C. Klopping, A. C. van Ginneken and J. H. Ravesloot (2001). "Ionic mechanism of delayed afterdepolarizations in ventricular cells isolated from human end-stage failing hearts." Circulation **104**(22): 2728-2733.

Verplancke, T., S. Van Looy, D. Benoit, S. Vansteelandt, P. Depuydt, F. De Turck and J. Decruyenaere (2008). "Support vector machine versus logistic regression modeling for prediction of hospital mortality in critically ill patients with haematological malignancies." BMC Medical Informatics and Decision Making **8**(1): 56.

Vijayakumar, R., J. N. Silva, K. A. Desouza, R. L. Abraham, M. Strom, F. Sacher, G. F. Van Hare, M. Haissaguerre, D. M. Roden and Y. Rudy (2014). "Electrophysiologic substrate in congenital Long QT syndrome: noninvasive mapping with electrocardiographic imaging (ECGI)." Circulation **130**(22): 1936-1943.

Vilcant, V. and R. Zeltser (2020). Treadmill Stress Testing. StatPearls. Treasure Island (FL), StatPearls Publishing

Viskin, S. and B. Belhassen (1990). "Idiopathic ventricular fibrillation." American Heart Journal **120**(3): 661-671.

Viskin, S., R. Rosso, L. Friedensohn, O. Havakuk and A. A. M. Wilde (2015). "Everybody has Brugada syndrome until proven otherwise?" Heart Rhythm **12**(7): 1595-1598.

Visser, M., F. van der Heijden Jeroen, A. Doevendans Pieter, P. Loh, A. Wilde Arthur and J. Hassink Rutger (2016). "Idiopathic Ventricular Fibrillation." Circulation: Arrhythmia and Electrophysiology **9**(5): e003817.

Volpi, A., A. Cavalli, E. Santoro and G. Tognoni (1990). "Incidence and prognosis of secondary ventricular fibrillation in acute myocardial infarction. Evidence for a protective effect of thrombolytic therapy. GISSI Investigators." Circulation **82**(4): 1279-1288.

Vutthikraivit, W., P. Rattanawong, P. Putthapiban, W. Sukhumthammarat, P. Vathesatogkit, T. Ngarmukos and A. Thakkinstian (2018). "Worldwide Prevalence of Brugada Syndrome: A Systematic Review and Meta-Analysis." Acta Cardiologica Sinica **34**(3): 267-277.

Waldmann, V., K. Narayanan, N. Combes, D. Jost, X. Jouven and E. Marijon (2018). "Electrical cardiac injuries: current concepts and management." European Heart Journal **39**(16): 1459-1465.

Walt, S. v. d., S. C. Colbert and G. Varoquaux (2011). "The NumPy Array: A Structure for Efficient Numerical Computation." Computing in Science & Engineering **13**(2): 22-30.

Wang, J., Z. Zhang, Y. Li, Y. Xu, K. Wan and Y. Chen (2019). "Variable and Limited Predictive Value of the European Society of Cardiology Hypertrophic Cardiomyopathy Sudden-Death Risk Model: A Meta-analysis." Canadian Journal of Cardiology **35**(12): 1791-1799.

Wang, N., A. Xie, R. Tjahjono, D. H. Tian, S. Phan, T. D. Yan, P. Bajona and K. Phan (2017). "Implantable cardioverter defibrillator therapy in hypertrophic cardiomyopathy: an updated systematic review and meta-analysis of outcomes and complications." Ann Cardiothorac Surg **6**(4): 298-306.

Watkins, H., W. J. McKenna, L. Thierfelder, H. J. Suk, R. Anan, A. O'Donoghue, P. Spirito, A. Matsumori, C. S. Moravec, J. G. Seidman and et al. (1995). "Mutations in the genes for cardiac troponin T and alpha-tropomyosin in hypertrophic cardiomyopathy." N Engl J Med **332**(16): 1058-1064.

Weiss, J. N., A. Garfinkel, H. S. Karagueuzian, P.-S. Chen and Z. Qu (2010). "Early afterdepolarizations and cardiac arrhythmias." Heart rhythm **7**(12): 1891-1899.

Weng, Z., J. Yao, R. H. Chan, J. He, X. Yang, Y. Zhou and Y. He (2016). "Prognostic Value of LGE-CMR in HCM: A Meta-Analysis." JACC Cardiovasc Imaging **9**(12): 1392-1402.

Wilde, A. A. M., P. G. Postema, J. M. Di Diego, S. Viskin, H. Morita, J. M. Fish and C. Antzelevitch (2010). "The pathophysiological mechanism underlying Brugada syndrome: depolarization versus repolarization." Journal of molecular and cellular cardiology **49**(4): 543-553.

Wilkoff, B. L., L. Fauchier, M. K. Stiles, C. A. Morillo, S. M. Al-Khatib, J. Almendral, L. Aguinaga, R. D. Berger, A. Cuesta, J. P. Daubert, S. Dubner, K. A. Ellenbogen, N. A. Mark Estes, III, G. Fenelon, F. C. Garcia, M. Gasparini, D. E. Haines, J. S. Healey, J. L. Hurtwitz, R. Keegan, C. Kolb, K.-H. Kuck, G. Marinskis, M. Martinelli, M. McGuire, L. G. Molina, K. Okumura, A. Proclemer, A. M. Russo, J. P. Singh, C. D. Swerdlow, W. S. Teo, W. Uribe, S. Viskin, C.-C. Wang and S. Zhang (2016). "2015 HRS/EHRA/APHRS/SOLAECE expert consensus statement on optimal implantable cardioverter-defibrillator programming and testing." Heart Rhythm **13**(2): e50-e86.

Wit, A. and M. Rosen (1986). "The heart and cardiovascular system." New York, NY: Raven Press Publishers: 1449-1490.

Wolpert, C., C. Echternach, C. Veltmann, C. Antzelevitch, G. P. Thomas, S. Spehl, F. Streitner, J. Kuschyk, R. Schimpf, K. K. Haase and M. Borggrefe (2005). "Intravenous drug challenge using flecainide and ajmaline in patients with Brugada syndrome." Heart rhythm **2**(3): 254-260.

Wrobleski, D., C. Houghtaling, M. E. Josephson, J. N. Ruskin and V. Y. Reddy (2003). "Use of electrogram characteristics during sinus rhythm to delineate the endocardial scar in a porcine model of healed myocardial infarction." J Cardiovasc Electrophysiol **14**(5): 524-529.

Wu, J., J. Wu and D. P. Zipes (2002). "Early Afterdepolarizations, U Waves, and Torsades de Pointes." Circulation **105**(6): 675-676.

Wu, K. C. (2017). "Sudden Cardiac Death Substrate Imaged by Magnetic Resonance Imaging: From Investigational Tool to Clinical Applications." Circulation. Cardiovascular imaging **10**(7).

Wyatt, R. F., M. J. Burgess, A. K. Evans, R. L. Lux, J. A. Abildskov and T. Tsutsumi (1981). "Estimation of ventricular transmembrane action potential durations and repolarization times from unipolar electrograms." The American Journal of Cardiology **47**: 488.

Xie, J. T., P. M. Cunningham and C. T. January (1995). "Digoxin-induced delayed afterdepolarizations: biphasic effects of digoxin on action potential duration and the Q-T interval in cardiac Purkinje fibers." Methods Find Exp Clin Pharmacol **17**(2): 113-120.

Xie, Y., E. Grandi, J. L. Puglisi, D. Sato and D. M. Bers (2013). "β-adrenergic stimulation activates early afterdepolarizations transiently via kinetic mismatch of PKA targets." Journal of molecular and cellular cardiology **58**: 153-161.

Xie, Y., D. Sato, A. Garfinkel, Z. Qu and J. N. Weiss (2010). "So little source, so much sink: requirements for afterdepolarizations to propagate in tissue." Biophysical journal **99**(5): 1408-1415.

Yan, G.-X., Y. Wu, T. Liu, J. Wang, R. A. Marinchak and P. R. Kowey (2001). "Phase 2 Early Afterdepolarization as a Trigger of Polymorphic Ventricular Tachycardia in Acquired Long-QT Syndrome." Circulation **103**(23): 2851-2856.

Yan, G. X. and C. Antzelevitch (1999). "Cellular basis for the Brugada syndrome and other mechanisms of arrhythmogenesis associated with ST-segment elevation." Circulation **100**(15): 1660-1666.

Youden, W. J. (1950). "Index for rating diagnostic tests." Cancer **3**(1): 32-35.

Ypey, D. L., W. P. M. van Meerwijk, S. Umar, D. A. Pijnappels, M. J. Schalij and A. van der Laarse (2013). "Depolarization-induced automaticity in rat ventricular cardiomyocytes is based on the gating properties of L-type calcium and slow Kv channels." European Biophysics Journal **42**(4): 241-255.

Yu, H., F. Chang and I. S. Cohen (1993). "Pacemaker current exists in ventricular myocytes." Circulation research **72**(1): 232-236.

Yue, A. M., T. R. Betts, P. R. Roberts and J. M. Morgan (2005). "Global Dynamic Coupling of Activation and Repolarization in the Human Ventricle." Circulation **112**(17): 2592-2601.

Zhang, J., M. Hocini, M. Strom, P. S. Cuculich, D. H. Cooper, F. Sacher, M. Haïssaguerre and Y. Rudy (2017). "The Electrophysiological Substrate of Early Repolarization Syndrome: Noninvasive Mapping in Patients." JACC: Clinical Electrophysiology **3**(8): 894-904.

Zhang, J., F. Sacher, K. Hoffmayer, T. O'Hara, M. Strom, P. Cuculich, J. Silva, D. Cooper, M. Faddis, M. Hocini, M. Haïssaguerre, M. Scheinman and Y. Rudy (2015). "Cardiac electrophysiological substrate underlying the ECG phenotype and electrogram abnormalities in Brugada syndrome patients." Circulation **131**(22): 1950-1959.

Zipes, D. P. and H. J. Wellens (1998). "Sudden cardiac death." Circulation **98**(21): 2334-2351.

Appendix A

Imperial College London

Imperial College Healthcare NHS Trust

Participant information sheet – Brugada syndrome

FIRST-BrS: Feasibility of Improving Risk Stratification in Brugada Syndrome

Thank you for considering our study. We are aiming to test out a new way of measuring the heart's electricity to help people at risk of sudden cardiac death. This leaflet will explain what is involved. Please take time to read the following information carefully and discuss it with others if you wish.

WHAT IS THE PURPOSE OF THE STUDY?

600 young people die every year from Sudden Cardiac Death due to dangerously fast heart beats. By studying both normal and abnormal hearts we are aiming to make a test that can tell if someone is at high risk of having these dangerous beats and give them a life -saving device called an Implantable Cardioverter Defibrillator (ICD). We are also aiming to ensure people at low risk do not receive ICDs as there are risks involved in having one. The study forms part of a PhD project.

WHAT IS BEING TESTED?

The device is called CardioINSIGHT and the test is called Ventricular Conduction Stability (or V -CoS). It centres around a vest of sensors combined with a scan of the heart which, in combination with a special computer programme written by the research team, might be able to tell the difference between people who need a life -saving ICD and those who do not.

WHY HAVE I BEEN CHOSEN?

We are looking for six main groups of people to take part, and you belong to the group of patients with Brugada syndrome who have had a previous cardiac arrest or treatment from your ICD.

The other groups are:

- People with normal hearts who are athletic.
- People with normal hearts who have relatives with Brugada syndrome
- People with atrial fibrillation, an irregular heart beat
- People who have previously had a dangerously fast heart beat due to a heart attack but have since fully recovered
- People who have 'safe' but abnormal heartbeats undergoing treatment.

DO I HAVE TO TAKE PART?

No, it is up to you to decide whether or not to take part. If you do, you can keep this information sheet and will be asked to sign a consent form. You will be free to leave the study at any time without giving a reason. Withdrawing from the study or not choosing to join will not affect the standard of care you receive from the service.

THE PROCESS

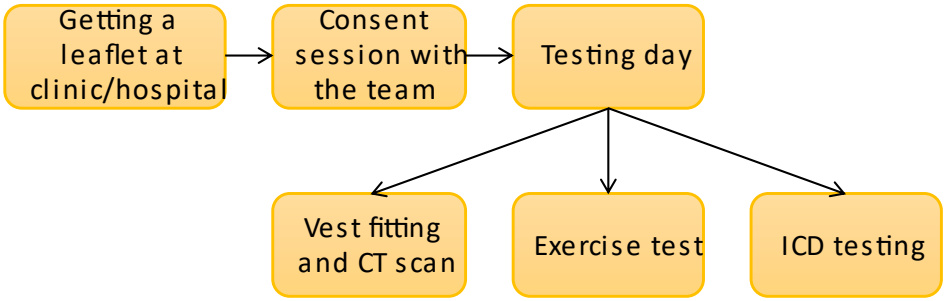

Altogether you will spend less than a whole day in the hospital for the tests. The study is a **"cohort study"**, which means we will test multiple groups of people and attempt to find differences in their results.

Consent session
You'll meet a member of our team who will talk you through the process in detail so you can decide if you want to go ahead. This is a good chance to ask any questions you might have. You will then be given a date for your Testing Day.

Vest fitting and CT scan
The test hinges around a vest of sensors you will wear. To see how this fits with your heart we will also do a CT scan of your chest, which is like a 3D X -ray. This part of the test involves a small dose of radiation.

Exercise test
Next there will be a treadmill exercise test with the vest on. The test starts off on the flat and is like walking progressively faster up a steepening hill. We will ask you to lie down at various points so we can measure the heart's electricity readings. It lasts about 20 minutes and you can stop it at any time.

ICD testing
Only those of you with an implanted device (ICD) will be enrolled to this step. It involves triggering an extra beat in your heart and using the vest to measure the response. This is routinely done during other heart procedures called Electrophysiological Studies. We will be approaching people individually to do this test; the research fellow or nurse will speak to you before the test about this.

WHAT EFFECT MIGHT THIS HAVE ON MY LIFE?

There are no specific lifestyle changes that you will need to make for this study. We cannot promise the study will help you, but the information we get might help improve the treatment of people at risk for sudden cardiac death related conditions.

IS THERE A RISK TO ME?

There is risk in every medical procedure; our process has been designed to minimise risks as much as possible and has been independently scrutinized by an ethics committee to ensure that no unnecessary risks have been taken. The main points are:

- The CT scan – there is a radiation dose associated with this, equivalent to 3 years of background radiation. Combined with the radiation dose from the EP study (below), this raises your chance of cancer by less than 1 in 1000.

- The Exercise test – very rarely there is a risk of your heart reacting badly to this test. It is performed routinely in a place where all the relevant safety professionals are readily available in case of emergency. The risk is similar to the risk taken when walking hard up a steep hill.

- The ICD test – there is a 0.5 to 1.5% risk of complications in this study. The same safety procedures for the Exercise test apply for the ICD test too.

As there is a small radiation dose involved **we will not be allowing people under the age of 18, or pregnant women to take part** . If you are at risk of pregnancy we may ask you to have a pregnancy test to ensure you can take part safely. If you do become pregnant during the course of the study you will have to let us know immediately.

Rarely we may find problems in our diagnostic tests that you were previously unaware of. Amongst other things this might include abnormal heart beats or growths in your lungs. **If we find something that may be worrisome we will let you and your family doctor know so follow up and/or treatment can be organised** . At this point we may have meet you to talk about whether you can carry on with the study.

Sometimes during the course of a research project, new information becomes available about the process that is being studied. If this happens, we will tell you about it and ask you whether you want to continue in the study. If you decide to withdraw, we will make arrangements for your care to continue. If you decide to continue in the study you will be asked to sign an updated consent form.

WHAT IF SOMETHING GOES WRONG?

This is known as an 'adverse event'. **The study takes place within an NHS Trust which has a full complement of medical staff to deal with problems** . All adverse events are reported and recorded. If there are any questions these are normally directed at the Principal Investigator. If the adverse event is very serious it will be reported to the Research Ethics Committee that approved the study.

Imperial College holds Public Liability ("negligent harm") and Clinical Trial ("non -negligent harm") insurance policies which apply to this trial. If you can demonstrate that you experienced harm or injury as a result of your participation in this trial, you will be eligible to claim compensation without having to prove that Imperial College is at fault. If the injury resulted from any procedure which is not part of the trial, Imperial College will not be required to compensate you in this way. Your legal rights to claim compensation for injury where you can prove negligence are not affected.

If you wish to complain about any aspect of the way in which you have been approached or treated during the course of this study, you should ask to speak to the researchers who will do their best to answer your questions. Contact details are at the end of the leaflet.

If you remain unhappy and wish to complain formally, you can do this by contacting the Patient Advisory Liaison Service (PALS). PALS is a confidential NHS service that can provide you with support for any complains or queries you may have. Imperial College's PALS team is contactable on 020 3313 0088 or imperial.pals@nhs.net.

WHAT ABOUT CONFIDENTIALITY?

If you consent to take part in the research any of your medical records may be inspected by the groups sponsoring the research for purposes of analysing the results. They may also be looked at by people from the organising bodies and from regulatory authorities to check that the study is being carried out correctly. Sometimes the information learned from your test is used in the future by other universities, hospitals and companies performing research to help find ways to treat people with a heart conditions. Your name, however, will not be disclosed outside the hospital/GP surgery – the information will all be anonymous.

WHAT HAPPENS NEXT?

The information will be analysed to help understand the way in which the vest could detect differences between people at risk of sudden death, and those not at risk. Altogether we expect that the study will take 3 years, although individually you will only spend about half a day with us.

During the study we will attempt to fully reimburse you for relevant expenses, and will pass on information to your family doctor to help guide your care. For patients from outside the M25 we will provide a maximum of £50 for travel, or £15 from within the M25. Receipts must be provided and these arrangements are subject to changes.

WHAT HAPPENS WHEN THE STUDY STOPS?

We will analyse the information gathered and publish our findings. No identifiable information will be released about you to the public, and we will make any results from the study available to you, the participants. You will then return to your normal follow up schedule if you are a patient in a clinic.

WHO IS ORGANISING AND FUNDING THE RESEARCH?

The study is funded by The Daniel Bagshaw Trust, a charity promoting research into the early diagnosis of cardiac risk in the young and the improvement of treatment methods for sudden cardiac arrest. The Principal Investigators are Dr Prapa Kanagaratnam and Dr Amanda Varnava, consultant cardiologists. The device is provided by Medtronic, a manufacturer of medical equipment.

This study has been given ethical approval by Fulham Research Ethics committee.

HOW DO I SIGN UP?

If you're about to have your clinic appointment, tell the person you're about to have it with. If you've taken this sheet home to think about it further and you've decided to you'd like to join us, contact:

Dr Ji-Jian Chow
First-brs@imperial.ac.uk subject: JOIN FIRST-BrS
020 3313 6758
07774 178478

If you need to contact anyone regarding the study once you are enrolled please do so by email or phone as above. If you have a medical question not related to the study, please contact your GP.

Thanks for considering our study! We think this could give us new information to help us in the ongoing research into dangerously fast heart beats and reducing the number of people who die from these conditions.

Appendix B

Imperial College Healthcare NHS
NHS Trust

PATIENT INFORMATION SHEET - SITES EXTERNAL TO IMPERIAL COLLEGE

Version 2.0, 30/09/2017

You are being invited to take part in a study. Before you decide, it is important for you to understand why the study is being done and what it will involve. Please take the time to read the following information carefully. Ask us if there is anything that is not clear or if you would like more information.

Title- **P**REDICTING **R**ISK USING **E**CVUE: **D**ETECTION OF ACTIVATION CHANGES DURING PHYSIOLOGICAL STRESS THAT **I**NDICATE A **C**RI**T**ICAL SUBSTRATE FOR **V**ENTRICULAR **F**IBRILLATION **(PREDICT-VF)**

Chief Investigator- Dr Prapa Kanagaratnam

1) Invitation and brief summary

You have been invited to participate in this study because your cardiologist has diagnosed you with a cardiac condition that can cause fast heart rhythms. These conditions are often inherited, but the manner in which our genetic information results in fast heart rhythms is not known. Often we have to perform invasive tests which involve passing catheters into the heart to diagnose the type of rhythm disturbance and whether it is dangerous or not. Unfortunately, during these tests we cannot mimic the conditions under which these fast heart rhythms start and this compromises their reliability.

In this study, we will be trying to understand whether it is possible to predict if a person is going to get fast heart rhythms using tests that do not involve passing catheters into the heart. We will use a novel vest which can detect the electrical conduction of the heart, and by exposing the study subject to typical situations which can trigger rhythm disturbances such as exercise and relaxation, we hope to understand the differences between people that develop heart rhythms and those that do not.

2) What procedures or tests will this study involve?

The study will involve you wearing a novel vest which sticks to the skin and looks like a tank top and can be worn all day. It has 256 electrodes which measure the electrical impulses from the heart. You will have a CT scan with low x-ray exposure which produces a 3D image of the heart. This will take approximately 30 seconds. The electrical information from the vest and the 3D images from the scan are combined to enable us to work out how fast and the direction in which electricity spreads around the heart.

We will then aim to mimic the situations that can trigger these fast heart rhythms whilst information is collected with the vest. You will run on a treadmill whilst we collect information from the vest. The treadmill test would last anywhere between 5 to 20 minutes depending on your level of fitness.

After your clinical study is completed we will spend a few minutes trying to mimic the various scenarios which can cause rhythm disturbances, and the doctor taking your consent will explain these to you in more detail.

In summary, the **additional investigations** you may undergo by participating in this study are:

i) Wearing a vest and undergoing a CT scan of your chest

ii) An exercise treadmill test

3) What are the possible benefits of taking part in the study?

Whilst the study will not alter the current management of your condition, your participation and contribution will provide better insight and understanding of your heart condition which could be used in the future to guide management.

4) What are the possible disadvantages of taking part?

There is a small amount of radiation exposure from the CT scan, which carries a very low risk of inducing cancer.

There is also the possibility of discovering health related findings during the course of our tests. We will inform and discuss these findings with you and advise you accordingly.

5) Am I able to participate if I have a device? (e.g. defibrillator or pacemaker)

Yes, and it is safe to do so. The aforementioned tests have all been carried out safely in individuals with devices.

6) What is the purpose of the study?

The purpose of this study is to find out why certain people with a heart condition are more vulnerable to dangerous heart rhythms.

7) Why have I been chosen?

You have been invited to take part because you have a heart condition that is associated with rhythm problems. We would like to do the additional tests using the vest in people undergoing procedures in order to compare how information from the vest relates to the information taken directly from the heart.

8) Who will be excluded from the study?

We will not include people who have heart conditions that do not cause rhythm disturbance. We will not include people who cannot perform exercise tests. Women who are pregnant or not using highly effective contraception will not be able to participate.

9) Do I have to take part?

It is up to you to decide whether or not to take part. If you decide to take part you will be asked to sign a consent form. If you decide to take part you are still free to withdraw at anytime without giving a reason. A decision to withdraw at anytime, or a decision not to take part, will not affect your care in any way.

10) What do I have to do?

We will aim to have all your investigations performed on the same day, and you will receive a letter detailing the date of your attendance for these. Reimbursement for travel costs can be discussed with us if you are situated outside of greater London.

11) **What will happen to me if I take part**?

i) On the morning of the study, you will be in the cardiac day ward to have an ECG taken.

ii) The vest will then be fitted followed by a CT scan of the chest.

iii) You will then be taken to the cardiac investigations department to have your treadmill test.

iv) We will collect electrical information from the vest during the clinical study. We will also perform some manoeuvres that mimic the situations that cause rhythm disturbances. The specific test will be explained at the time of your consent.

12) What are the risks and side effects of all the procedures and tests?

Exercise Testing

Risks or adverse effects of these physiological tests are low. These include:-

i) New or worsening heart rhythm disturbance
ii) Low blood pressure
iii) Palpitations due to fast or slow heart rates

ECGi Vest

During the fitting of the equipment you will undergo a CT scan. This is a special type of X-ray test and involves radiation. The amount of radiation is very low – equivalent to about 6 months of the natural radiation someone receives during their normal lives.

High levels of radiation can cause cancer; therefore we always use as little as possible. The CT is performed by someone professionally trained in using 'as low as reasonably possible' dose of radiation.

In addition to these safety measures, we still warn people that there may be a very small increased risk of cancer over the course of your lifetime – about 1 in 3333.

Overall, the additional risks of taking part in the study are low. During these procedures, there will be a full complement of staff present that is fully trained to deal with medical emergencies.

13) What if new information becomes available?

Sometimes during the course of a research project, new information becomes available which may affect the research or your clinical care. If this occurs, we will inform you and discuss with you whether you wish to continue with the study.

If you decide to withdraw from the study, your research doctor will make arrangements for your care to continue. If you decide to continue in the study you will be asked to sign an updated consent form.

Also, on receiving new information your research doctor might consider to be in your best interests to withdraw from the study. Your doctor will explain the reasons and arrange for your care to continue.

14) What if something goes wrong?

Imperial College London holds insurance policies which apply to this study. If you experience serious and enduring harm or injury as a result of taking part in this study, you may be eligible to claim compensation without having to prove that Imperial College is at fault. This does not affect your legal rights to seek compensation.

If you are harmed due to someone's negligence, then you may have grounds for a legal action. Regardless of this, if you wish to complain, or have any concerns about any aspect of the way you have been treated during the course of this study then you should immediately inform the Investigator (Insert name and contact details). The normal National Health Service complaints mechanisms are also available to you. If you are still not satisfied with the response, you may contact the Imperial AHSC Joint Research Compliance Office.

15) Will my taking part in the study be kept confidential?

The information coming out of the study may be shared with other centres or commercial entities to help improve present and future research. These may include NHS Trusts, external universities and commercial entities involved in this field of study. All information which is collected about you during

the course of the research will be kept strictly confidential. Any information about you which leaves the hospital will have your name and address removed so that you cannot be recognised from it.

We will be asking for your agreement for us to inform you GP of your participation in this trial.

16) What will happen to the results of the research study?

The results of this study should be available in 3 years. We aim to publish these results in a leading medical journal. You will not be identified in any publications. We will be able to let you know about the results at the end of the study.

17) Who is organising and funding the research?

Imperial College London is the sponsor and is providing funding for the research which is being done as part of a PhD.

18) Contact for further information

Your first point of contact is **Dr Ji-Jian Chow**, Research Fellow who will provide you his contact details should you decide to participate. You can also contact the Arrhythmia Specialist Nurses via switchboard at 02083831000. Alternatively, please contact Dr Prapa Kanagaratnam, Consultant Cardiologist at 02033123783.

In an emergency situation, you should call 999 for an ambulance.

Thank you for reading this information leaflet. Please feel free to contact us if you require further information or clarification.

Please keep this copy of the information sheet and signed consent form.

Appendix C

Imperial College Healthcare NHS Trust

Sponsor: Imperial College London
Centre Number : Hammersmith Hospital
Study Number :
Patient Identification Number for this study:

CONSENT FORM

Title of Project: **Feasibility of Improving Risk Stratification in Brugada Syndrome**

Simplified Title: **FIRST-BrS**

Name of Researchers: Dr J Chow, Dr K Leong, Professor P Kanagaratnam, Dr A Varnava.
Imperial College Healthcare NHS Trust

		Please initial box
1.	I confirm that I have read and understand the information sheet dated 13/02/2018 (Version 4.1) for the above study and have had the opportunity to ask questions.	
2.	I understand that my participation is voluntary and that I am free to withdraw at any time, without giving any reason, without my medical care or legal rights being affected. If I cannot consent any more I will be withdrawn from the study, but my information may be kept for completion of the research.	
3.	I understand that sections of any of my medical notes may be looked at by the researchers with Imperial College London or by regulatory authorities where it is relevant to my taking part in research. I give permission for these individuals to have access to my records.	
4.	I understand that data collected during this study may be shared with third parties for future research purposes. These may include NHS Trusts, external universities and commercial entities involved in this field of study.	
5.	I give permission for the researchers to inform my GP of my participation in this study.	
6.	I agree to wear the ECGi vest, perform a treadmill test and have a CT scan.	
7.	I agree to take part in Non-Invasive Programmed Stimulation.	
8.	I agree to take part in the above study.	

Name of Patient	Signature	Date
Name of Person taking consent (if different from researcher)	Signature	Date
Name of Investigator	Signature	Date

1 for patient; 1 for researcher; 1 to be kept with hospital notes

Appendix D

EcVUE™ CARDIAC MAPPING SYSTEM
SIZE SELECTION AND APPLICATION REFERENCE GUIDE

Sensor Array Multi-Electrode Mapping Vest

Vest Sizing Chart

Please use the sizing chart to select the size using the ratio of the patient's height and weight.

Additional Sizing Considerations:

- Circumference of abdomen at navel
- Circumference of chest (widest point below the underarms)
- Breadth of shoulders

If one area of the body appears disproportionately larger in comparison to the rest (e.g., large abdomen), it is recommended the vest be sized up.

	lbs	105	110	115	120	125	130	135	140	145	150	155	160	165	170	175	180	185	190	195	200	205	210	215	220	225	230	235	240	245	250
	kg	48	50	52	54	57	59	61	64	66	68	70	73	75	77	80	82	84	86	89	91	93	95	98	100	102	105	107	109	111	114
58 in	147 cm	1	1	1	3	3	2	2	2	2	2	2	2	2	2	4	3	3	3	3	3	3	3	3	3						
59 in	150 cm	1	1	1	3	3	2	2	2	2	2	2	2	2	2	3	3	3	3	3	3	3	3	3	3						
60 in	152 cm	1	1	1	3	3	3	2	2	2	2	2	2	2	2	2	3	3	3	3	3	3	3	3	3						
61 in	155 cm	1	1	1	1	3	3	2	2	2	2	2	2	2	2	2	3	3	3	3	3	3	3	3	3	4					
62 in	157 cm	1	1	1	1	3	3	3	2	2	2	2	2	2	2	2	2	3	3	3	3	3	3	3	3	4					
63 in	160 cm	1	1	1	1	1	3	3	2	2	2	2	2	2	2	2	2	2	3	3	3	3	3	3	3	4	4	4			
64 in	162 cm	1	1	1	1	1	3	3	2	2	2	2	2	2	2	2	2	2	3	3	3	3	3	3	3	4	4	4	4		
65 in	165 cm	1	1	1	1	1	3	3	3	2	2	2	2	2	2	2	2	2	2	3	3	3	3	3	3	4	4	4	4		
66 in	167 cm	1	1	1	1	1	1	3	3	2	2	2	2	2	2	2	2	2	2	3	3	3	3	3	3	4	4	4	4	4	
67 in	170 cm	1	1	1	1	1	1	3	3	3	2	2	2	2	2	2	2	2	2	2	3	3	3	3	3	4	4	4	4	4	4
68 in	173 cm		1	1	1	1	1	1	3	3	2	2	2	2	2	2	2	2	2	2	3	3	3	3	3	4	4	4	4	4	4
69 in	175 cm			1	1	1	1	1	3	3	3	2	2	2	2	2	2	2	2	2	2	3	3	3	3	4	4	4	4	4	4
70 in	178 cm				1	1	1	1	3	3	3	2	2	2	2	2	2	2	2	2	2	2	3	3	3	4	4	4	4	4	4
71 in	180 cm				1	1	1	1	3	3	3	2	2	2	2	2	2	2	2	2	2	2	3	3	3	4	4	4	4	4	4
72 in	183 cm					1	1	1	3	3	3	3	2	2	2	2	2	2	2	2	2	2	3	3	3	4	4	4	4	4	4
73 in	185 cm					1	1	1	3	3	3	3	2	2	2	2	2	2	2	2	2	2	3	3	3	4	4	4	4	4	4
74 in	188 cm					1	1	1	3	3	3	3	3	2	2	2	2	2	2	2	2	2	3	3	3	4	4	4	4	4	4
75 in	190 cm								1	1	3	3	3	2	2	2	2	2	2	2	2	2	3	3	3	4	4	4	4	4	4
76 in	193 cm											3	3	3	2	2	2	2	2	2	2	2	3	3	3	4	4	4	4	4	4

1 2 3 4

Per the IFU, the above sizing chart utilizes the ratio of the patient's height (in/cm)/weight (lb/kg) X 100 to select the appropriate vest for the patient.

Medtronic

1 Shave patient's torso from neck to umbilicus.

2 Clean patient with a product that is:

- Either a liquid or a wipe
- Non-abrasive
- Hypoallergenic
- Non-staining
- Non-alcoholic

NOTE: If an organic solvent is used on patient, allow to dry for at least 1 minute prior to applying vest

3 Apply **front left** panel of vest. Medial end of clavicle should be between electrodes 65 and 66.

NOTE: Apply front panels with breasts in their natural lying position.

4 Apply **front right** panel of vest. Should be staggered slightly higher and fit like a puzzle with the front left panel.

NOTE: Apply front panels with breasts in their natural lying position.

5 Tape front panels together.

6 Sit patient up and apply back panel so electrode 192 is level with the point where the neck meets the shoulders.

7 Tape shoulders and left and right side panels.

8 If planning to record patient prior to CT, connect ECG patches to ground reference cable and apply patches to patient as indicated in IFU. Connect signal cables to vest panels.

Medtronic
710 Medtronic Parkway
Minneapolis, MN 55432-5604
USA
Tel: 763.514.4000
Fax: 763.514.4879

medtronic.com

cardioinsightservice@medtronic.com
Toll-free: 1.800.328.2518
(24-hour technical support for physicians and medical professionals)

Medtronic

Appendix E

Which risk prediction? Quick survey

Dear colleague,

We're interested to know what you personally think about risk stratification in the ICCs using Brugada syndrome and Hypertrophic cardiomyopathy as examples. Please take a minute to indicate your views using the questions below:

Brugada syndrome

1. Do you risk stratify BrS patients by [circle one per question]…
    a. Spontaneous Type 1 pattern and syncope?
        i. Yes
        ii. No
        iii. Not heard of it
    b. Siera-Brugada risk score (EHJ 2017)?
        i. Yes
        ii. No
        iii. Not heard of it
    c. Shanghai score (2016 for diagnosis, used for risk strat in JACC 2018)?
        i. Yes
        ii. No
        iii. Not heard of it
    d. Other [write comment overleaf]

2. How likely are you to perform invasive EPS on BrS patients with [mark a cross on the line]…
    a. Spontaneous Type 1 pattern with syncope?

        Least likely----------Most likely
    b. Spontaneous Type 1 pattern without syncope?

        Least likely----------Most likely
    c. Concealed Type 1 pattern with syncope?

        Least likely----------Most likely

d. Concealed Type 1 pattern without syncope?

Least likely----------Most likely

3. If invasive EPS is performed, do you routinely perform sinus node testing?
    a. Yes
    b. No

4. At my centre, we perform EPS on _____ % of our patients [write an estimate]

Hypertrophic Cardiomyopathy

1. Which HCM risk stratification system do you use?
    a. 2003 ACC/ESC guidelines
        i. Yes
        ii. No
        iii. Not heard of it
    b. 2011 ACCF/AHA guidelines
        i. Yes
        ii. No
        iii. Not heard of it
    c. 2014 ESC risk calculator
        i. Yes
        ii. No
        iii. Not heard of it
    d. Other [please write comments below]

2. Out of the risk stratification systems do you have a favourite/ one that takes priority?
    a. 2003 ACC/ESC
    b. 2011 ACCF/AHA
    c. 2014 ESC

3. Any comments on why?

Comments